

# An Estimate of the Rate Constants and Arrhenius Parameters for H-Atom Abstraction from $\text{Bu}_3\text{SnH}$ by the 2,2-Dimethylvinyl Radical in PhMe. Kinetic Evidence for an Entirely Free Radical Mechanism for the O-Directed Hydrostannation of Alkynols with Stannanes and $\text{Et}_3\text{B}/\text{O}_2$

Hamish A. Watson,<sup>a</sup> K. Lawrence E. Hale,<sup>a</sup> John M. Marron,<sup>a</sup>  
Soraya Manaviazar,<sup>a</sup> Alistair J. Fielding,\*<sup>b</sup> and Karl J. Hale\*<sup>a,c</sup>

<sup>a</sup>*The School of Chemistry & Chemical Engineering,  
Queen's University Belfast,  
Stranmillis Road, Belfast BT9 5AG,  
Northern Ireland, United Kingdom*

<sup>b</sup>*The School of Pharmacy and Biomolecular Sciences,  
Liverpool John Moores University,  
Byrom Street, Liverpool L3 3AF,  
United Kingdom.*

<sup>c</sup>*Current Address: Halazar Pharma Ltd, Edgware, Middlesex HA8 7RB, UK.*  
Emails for correspondence: [k.hale120@btinternet.com](mailto:k.hale120@btinternet.com)  
[A.J.Fielding@lju.ac.uk](mailto:A.J.Fielding@lju.ac.uk)

**Electronic Supplementary Information  
(171 Pages Inclusive of Cover Pages)**

## Index

- Page 5      **Part A. Experimental Section**
- Page 6      **Part 1.** An Estimate of the  $k_{\text{H-atom}}$  Abstraction Values for the 2,2-Dimethylvinyl Radical **6** from  $\text{Bu}_3\text{SnH}$  in PhMe Between 273 and 353K, and Estimates of the  $k_{\text{ring-opening}}$  and Arrhenius Parameters for the Cyclopropane Ring-Opening of the  $\alpha$ -Cyclopropyl- $\beta$ -Tri-*n*-Butylstannylvinyl Radical **2a** in Pentane and PhMe
- Page 7      **1.1** The Averaged Ratios of **4a:5a** Obtained from the O-Directed Hydrostannation of **1** with  $\text{Bu}_3\text{SnH}/\text{cat. Et}_3\text{B}$  as Determined by 600.13 MHz  $^1\text{H}$  NMR Spectroscopy of the Crude Concentrated Hydrostannation Reaction Mixtures in  $\text{CDCl}_3$
- Page 8      **1.2** Use of the Arrhenius Log A,  $E_a$  and  $k_{\text{H-atom abstraction Bu}_3\text{SnH}}$  Data Derived for the 2,2-Dimethylvinyl Radical (**6**) in Pentane to Calibrate the *In Situ*-Generated Stannylvinyl Radical (*Z*)-**2a** in Pentane and Provide Estimates for the  $k_{\text{H-atom abstraction Bu}_3\text{SnH}}$  Rate Constants of **6** and (*Z*)-**2a** at in Pentane at 293 and 298 K
- Page 13     **1.3** Estimation of the Rate Constants for H-Atom Abstraction ( $k_{\text{H-atom abstraction Bu}_3\text{SnH}}$ ) for the 2,2-Dimethylvinyl Radical (**6**) in PhMe and the Accompanying Arrhenius Parameter Determinations
- Page 18     **1.4** Estimation of the  $k_{\text{ring-opening}}$  Rate Constants and Arrhenius Parameters for the Cyclopropane Ring-Opening of the Tri-*n*-Butylstannylvinyl Radical **2a** in PhMe From The Averaged **4a:5a** Ratios in PhMe
- Page 23     **1.5** Our Mechanistic Interpretation of The Arrhenius Parameters Obtained for the **2a**→**4a** Conversion: Support for An Entirely Free Radical E<sub>H</sub>1 Mechanism For Cyclopropane Ring-Opening

- Page 24 **1.6** The Arrhenius Parameters Obtained for the **2a**→**4a** Conversion in PhMe Do Not Support Stannyvinyl Cation Involvement in the Mechanism of the Cyclopropane Ring-Opening of **2a**
- Page 36 **Part 2.** An Estimate of the  $k_{\text{ring-opening}}$  of the Cyclopropane Ring in the Tri-*n*-Butylstannyvinyl Radical **13** in PhMe at Different Temperatures and the Arrhenius Parameters Derived Therefrom
- Page 37 **2.1** The Experimentally Determined Average Ratios of **15:16** Obtained from the O-Directed Hydrostannation of **12**
- Page 39 **2.2** The  $k_{\text{ring-opening}}$  and Arrhenius Data Obtained for Stannyvinyl Radical **13** and Our Mechanistic Interpretation of That Data
- Page 45 **2.3** References
- Page 47 **Part 3.** Product Ratio Comparisons for the O-Directed Free Radical Hydrostannation of Alkynol **1** with Ph<sub>3</sub>SnH in PhMe
- Page 48 **3.1** The Experimentally Determined Average Ratios of **4b:5b** Obtained from the O-Directed Hydrostannation of **1**
- Page 49 **Part B.** The 600.13 MHz <sup>1</sup>H NMR and 150.90 MHz <sup>13</sup>C NMR Spectra of the Tributylstannyvinyltin **5a** and Tributylstannyallene **4a** in CDCl<sub>3</sub>
- Page 57 **Part C.** The 600.13 MHz <sup>1</sup>H NMR Ratio Determinations For the Tributylstannyallene **4a** and Tributylstannyvinyltin **5a** in CDCl<sub>3</sub>
- Page 92 **Part D.** The 600.13 MHz <sup>1</sup>H NMR and 150.90 MHz <sup>13</sup>C NMR Spectra of the Triphenylstannyvinyltin **5b** and Triphenylstannyallene **4b** in CDCl<sub>3</sub>
- Page 103 **Part E.** The 600.13 MHz <sup>1</sup>H NMR Ratio Determinations For the Triphenylstannyallene **4b** and Triphenylstannyvinyltin **5b** in CDCl<sub>3</sub>

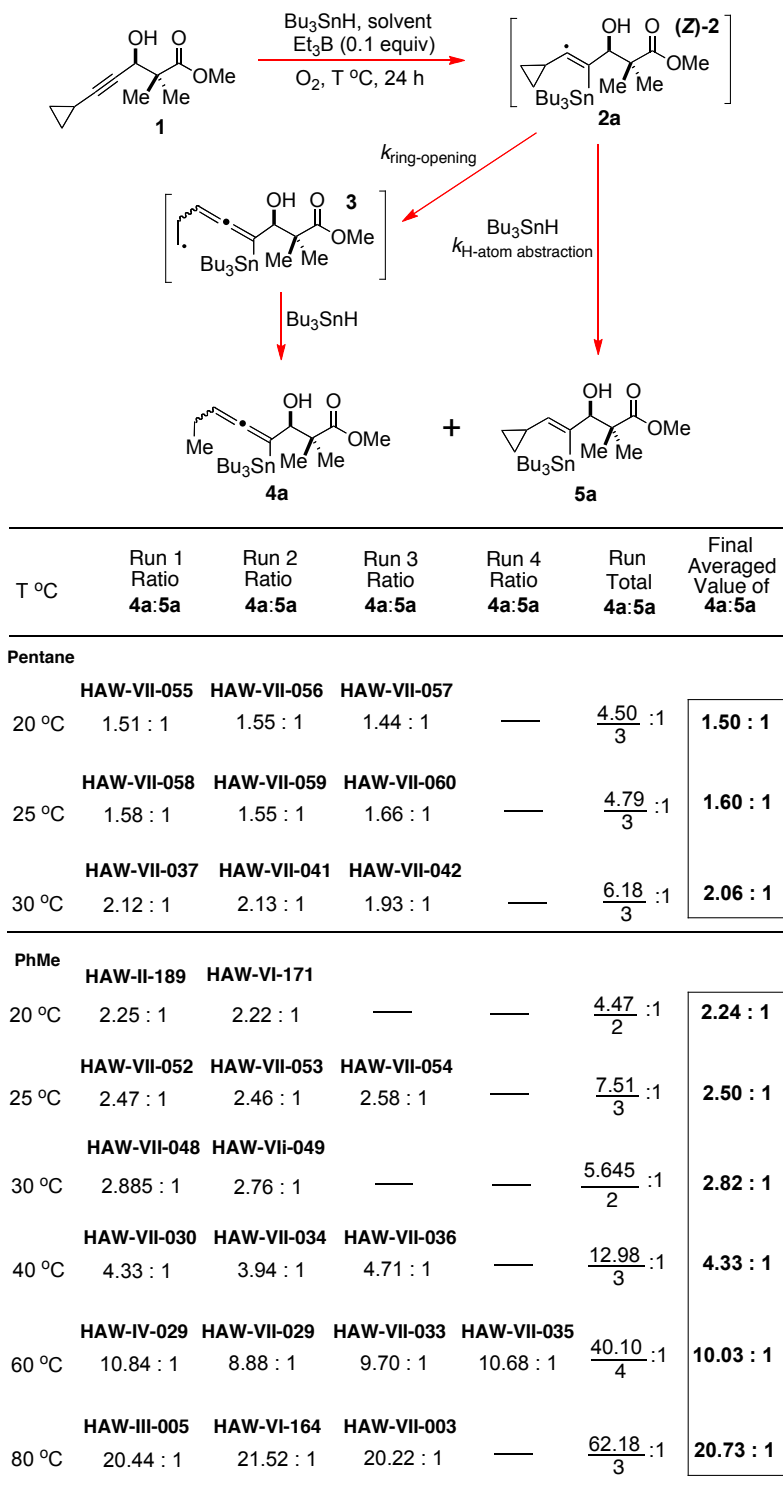
Page 121 **Part F.** The 600.13 MHz  $^1\text{H}$  NMR and 150.90 MHz  $^{13}\text{C}$  NMR Spectra of the Cyclopropylpropargylic Alcohol **12** and the Tributylstannylallene **15** in  $\text{CDCl}_3$

Page 154 **Part G.** The 600.13 MHz  $^1\text{H}$  NMR Ratio Determinations For the Tributylstannylallene **15** and Tributylstannylvinyltin **16** in  $\text{CDCl}_3$  Over the 313 K-353 K Temperature Range

## **Part A. Experimental Section**

**Part 1. An Estimate of the  $k_{\text{H-atom}}$  Abstraction Values  
for the 2,2-Dimethylvinyl Radical 6 from  $\text{Bu}_3\text{SnH}$  in  
PhMe Between 273 and 353K, and Estimates of the  
 $k_{\text{ring-opening}}$  and Arrhenius Parameters for the  
Cyclopropane Ring-Opening of the  $\alpha$ -Cyclopropyl- $\beta$ -  
Tri-*n*-Butylstannylvinyl Radical 2a in Pentane and  
PhMe**

**1.1 The Averaged Ratios of 4a:5a Obtained from the O-Directed Hydrostannation of 1 with Bu<sub>3</sub>SnH/cat. Et<sub>3</sub>B as Determined by 600.13 MHz <sup>1</sup>H NMR Spectroscopy of the Crude Concentrated Hydrostannation Reaction Mixtures in CDCl<sub>3</sub>**



**1.2 Use of the Arrhenius Log A, E<sub>a</sub> and k<sub>H-atom abstraction Bu<sub>3</sub>SnH</sub> Data Derived for the 2,2-Dimethylvinyl Radical (**6**) in Pentane to Calibrate the *In Situ*-Generated Stannylvinyl Radical (**Z**)-**2a** in Pentane and Provide Estimates for the k<sub>H-atom abstraction Bu<sub>3</sub>SnH</sub> Rate Constants of **6** and (**Z**)-**2a** in Pentane at 293 and 298 K**

In the Supporting Information of their paper, Ingold and coworkers reported<sup>7</sup> that in pentane the 2,2-dimethylvinyl radical **6** abstracted the reactive H-atom of Bu<sub>3</sub>SnH with a  $k = 2.96 \times 10^8 \text{ mol}^{-1} \text{ s}^{-1}$  at 298 K. Ingold *et al.* also reported a log A of 9.67 for this process,<sup>7</sup> and an  $E_a = +1.624 \pm 0.407 \text{ kcal mol}^{-1}$ . After multiplication of  $1.624 \times 4184 \text{ J}$  and including their errors, an  $E_a = +6794.816 \text{ J mol}^{-1} \pm 1702.888 \text{ J mol}^{-1}$  was recorded.

The availability of this data allowed us to calculate the theoretical  $k_{\text{H-atom abstraction}}$  values for the radical **6** from Bu<sub>3</sub>SnH at 293 K and 303 K in pentane respectively, and using these values to calibrate the reaction of **2a** with Bu<sub>3</sub>SnH thereafter allowed us to deduce the  $k_{\text{ring-opening}}$  values for the stannylvinyl radical (**Z**)-**2a** (R = Bu) in pentane at these two temperatures, as well as at 298 K.

Those theoretical  $k_{\text{H-atom abstraction}}$  calculations that we performed utilised the logarithmic form of the Arrhenius equation  $k = Ae^{-E_a/RT}$  where:

$$\log k = \log A - \frac{E_a}{2.303RT}$$

where  $R$  = Gas Constant (8.314) and  $T$  = Absolute Temperature in K  
and  $A$  = the Frequency or Pre-Exponential Factor

Thus, at 20 °C (293 K), the calculated  $k_{\text{H-atom abstraction}}$  rate constant for **6** from Bu<sub>3</sub>SnH in pentane was deduced using Ingold's reported log A = 9.67 and his  $E_a = 6794.816 \text{ J mol}^{-1}$  (1.624 kcal mol<sup>-1</sup>):

$$\log k_{\text{H-atom abstraction 293 K}} = 9.67 - \frac{6794.816}{2.303 \times 8.314 \times 293}$$

$$\log k_{\text{H-atom abstraction 293 K}} = 9.67 - \frac{6794.816}{5610.1126}$$

$$\log k_{\text{H-atom abstraction 293 K}} = 9.67 - 1.211173 = 8.458827$$

$$\therefore k_{\text{H-atom abstraction 293 K}} = 10^{8.458827} = 2.87625 \times 10^8 \text{ mol}^{-1} \text{ s}^{-1}$$

Likewise, the  $k_{\text{H-atom abstraction Bu}_3\text{SnH}}$  rate constant for **6** at 30 °C (303 K) was calculated from:

$$\log k_{\text{H-atom abstraction 303 K}} = 9.67 - \frac{6794.816}{2.303 \times 8.314 \times 303}$$

$$\log k_{\text{H-atom abstraction 303 K}} = 9.67 - \frac{6794.816}{5801.5840}$$

$$\log k_{\text{H-atom abstraction 303 K}} = 9.67 - 1.1712 = 8.4988$$

$$\therefore k_{\text{H-atom abstraction 303 K}} = 10^{8.4988} = 3.153552 \times 10^8 \text{ mol}^{-1} \text{ s}^{-1}$$

Although the experimentally determined  $k_{\text{H-atom abstraction Bu}_3\text{SnH}}$  quoted by Ingold *et al.*<sup>6</sup> for **6** at 25 °C (298 K) was  $2.96 \times 10^8 \text{ mol}^{-1} \text{ s}^{-1}$ , such a  $k$  value would in actual fact require an Arrhenius energy of activation of  $E_a = 1.6347146 \text{ kcal mol}^{-1}$  ( $6839.646 \text{ J mol}^{-1}$ ) to arrive at this figure (see below).

Importantly though, this  $E_a$  is only 0.01 kcal mol<sup>-1</sup> different from the general mean value of  $E_a = +1.624 \pm 0.407 \text{ kcal mol}^{-1}$  ( $+6794.816 \text{ J mol}^{-1} \pm 1702.888 \text{ J mol}^{-1}$ ) that was reported in the SI of Ingold's paper,<sup>7</sup> and Ingold's team did claim a  $\pm 25\%$  level of error in the  $E_a$  they were reporting.<sup>7</sup>

The two calculations provided below have utilised the above  $E_a$  value ( $6839.646 \text{ J mol}^{-1}$ ) and Ingold's  $E_a = 6794.816 \text{ J mol}^{-1}$  to confirm this fact. They further show the veracity of our overall method of calculation for the two 273 K and 303 K  $k_{\text{H-atom abstraction Bu}_3\text{SnH}}$  values in pentane, and that our method of calculation is totally correct. Thus:

$$\text{For } E_a = 1.6347146 \text{ kcal mol}^{-1} \times 4184 = 6839.646 \text{ J mol}^{-1}$$

$$\log k_{\text{H-atom abstraction 298 K}} = 9.67 - \frac{6839.646}{2.303 \times 8.314 \times 298}$$

$$\log k_{\text{H-atom abstraction 298 K}} = 9.67 - \frac{6839.646}{5705.848316}$$

$$\log k_{\text{H-atom abstraction 298 K}} = 9.67 - 1.198708 = 8.471292$$

$$\therefore k_{\text{H-atom abstraction 298 K}} = 10^{8.471292} = 2.9600 \times 10^8 \text{ mol}^{-1} \text{ s}^{-1}$$

$$= 2.96 \times 10^8 \text{ mol}^{-1} \text{ s}^{-1}$$

$$\text{For } E_a = 1.624 \text{ kcal mol}^{-1} \times 4184 = 6794.816 \text{ J mol}^{-1}$$

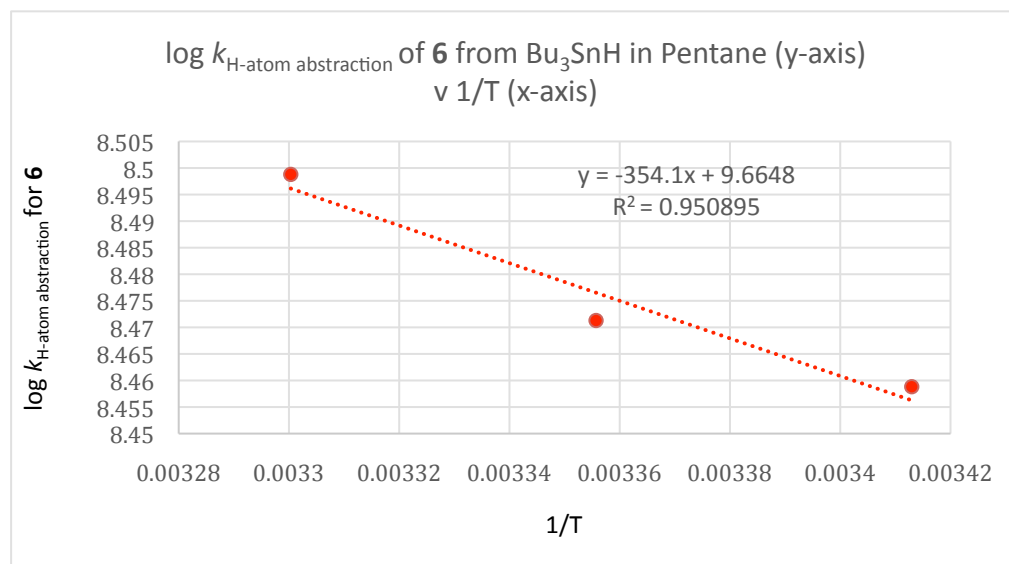
$$\log k_{\text{H-atom abstraction}} \text{ at } 298 \text{ K} = 9.67 - \frac{6794.816}{2.303 \times 8.314 \times 298}$$

$$\log k_{\text{H-atom abstraction}} \text{ at } 298 \text{ K} = 9.67 - \frac{6794.816}{5705.848316}$$

$$\log k_{\text{H-atom abstraction}} \text{ at } 298 \text{ K} = 9.67 - 1.1908512 = 8.4791488$$

$$\therefore k_{\text{H-atom abstraction}} \text{ at } 298 \text{ K} = 10^{8.4791488} = 3.014 \times 10^8 \text{ mol}^{-1} \text{ s}^{-1}$$

When the two *calculated*  $\log k_{\text{H-atom abstraction}}$  6 from  $\text{Bu}_3\text{SnH}$  in pentane values at 293 K and 303 K (*calculated* using Ingold's  $E_a = 6794.816 \text{ J mol}^{-1} = 1.624 \text{ kcal mol}^{-1}$  data) were merged with Ingold's experimentally derived  $k$  value for 6 of  $2.96 \times 10^8 \text{ mol}^{-1} \text{ sec}^{-1}$  at 298 K,<sup>7</sup> the following three  $\log k_{\text{H-atom abstraction}}$  6 values emerged i.e. 8.458827; 8.471292; and 8.4988, and when these three resulting  $\log k_{\text{H-atom abstraction}}$  6 values were plotted against the following  $1/T$  values (i.e.  $1/293 \text{ K} = 0.003413$ ;  $1/298 \text{ K} = 0.003356$ ; and  $1/303 \text{ K} = 0.0033$ ) in Arrhenius format, the following Excel plot was obtained (see below). It consisted of a straight line plot that had a negative slope and an  $R^2$  value of 0.950895 i.e. there was just a 5% deviation in the plotted points, with a 95% data fit when Ingold's experimental 298 K  $k_{\text{H-atom abstraction}}$  value was included in the plot. This exercise was done solely to check the veracity of our two newly calculated  $k$  values for 6 when merged with his experimentally-derived  $k$  value, and as can be seen, the results are excellent ( $\log A = 9.6648$ ).<sup>7</sup>



With this task duly completed, the aforementioned  $k_{\text{H-atom abstraction Bu}_3\text{SnH}}$  values for **6** in pentane were used to calibrate the stannylvinyl radical **2a** ( $\text{R} = \text{Bu}$ ) in pentane, to allow the rate constants for the cyclopropane ring-opening ( $k_{\text{ring-opening}}$ ) event to be estimated for **2a** ( $\text{R} = \text{Bu}$ ) at these three reaction temperatures. The latter data was secured at constant excess tin hydride concentration (0.2 M), by running 3 separate competition experiments at the temperatures of 293, 298 and 303 K, where the final ratio of allenyltin:vinyltin products **4a:5a** was established by 600.13 MHz  $^1\text{H}$  NMR spectroscopy of the crude concentrated reaction mixtures in  $\text{CDCl}_3$ . The following equation of Baines,<sup>13</sup> Newcomb,<sup>14</sup> and Crich<sup>15</sup> was used to determine the  $k_{\text{ring-opening}}$  values:

$$\frac{[\text{Vinyltin}]}{[\text{Allenyltin}]} = [(\text{R})_3\text{SnH}] \times \frac{k_{\text{H-atom abstraction}}}{k_{\text{ring-opening}}} \quad (\text{Eqn 1})$$

which rearranges to Eqn 2:

$$k_{\text{ring-opening}} = [(\text{R})_3\text{SnH}] \times k_{\text{H-atom abstraction}} \times \frac{[\text{Allenyltin}]}{[\text{Vinyltin}]} \quad (\text{Eqn 2})$$

**At 20 °C (293 K),** from 3 independent reaction runs, the average ratio of **4a:5a** ( $\text{R} = \text{Bu}$ ) was 1.50:1.

This allowed a  $k_{\text{ring-opening 2a in pentane}_{293\text{ K}}} = [0.2] \times 2.88 \times 10^8 \times 1.50/1 = 8.64 \times 10^7 \text{ s}^{-1}$  to be established, and a  $\log k_{\text{ring-opening 2a in pentane}_{293\text{ K}}} = 7.936513742$ .

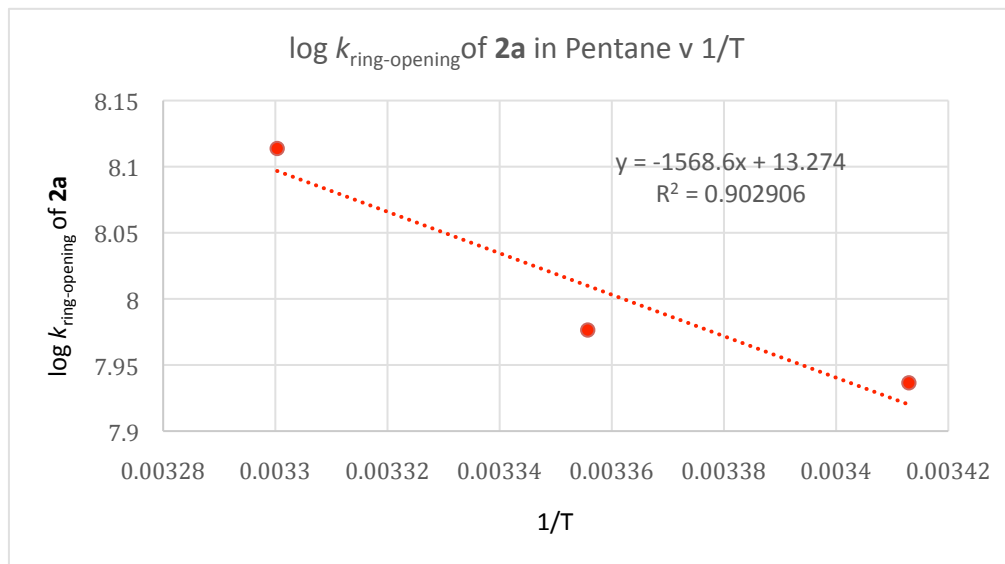
**At 25 °C (298 K),** from 3 independent reaction runs, the average ratio of **4a:5a** ( $\text{R} = \text{Bu}$ ) was 1.60:1.

This led to a  $k_{\text{ring-opening 2a in pentane}_{298\text{ K}}} = [0.2] \times 2.96 \times 10^8 \times 1.60/1 = 9.472 \times 10^7 \text{ s}^{-1}$  which, in turn, gave a  $\log k_{\text{ring-opening 2a in pentane}_{298\text{ K}}} = 7.976441689$ .

**At 30 °C (303 K),** from 3 independent reaction runs, the average ratio of **4a:5a** ( $\text{R} = \text{Bu}$ ) was 2.06:1

Accordingly, a  $k_{\text{ring-opening 2a in pentane}_{303\text{ K}}} = [0.2] \times 3.154 \times 10^8 \times 2.06/1 = 1.299448 \times 10^8$  which gave rise to a  $\log k_{\text{ring-opening 2a in pentane}_{303\text{ K}}} = 8.1137589$ .

An Excel Arrhenius plot of these values of  $\log k_{\text{ring-opening 2a}}$  in pentane v  $1/T$  (i.e.  $1/293 \text{ K} = 0.003413$ ;  $1/298 \text{ K} = 0.003356$ ; and  $1/303 \text{ K} = 0.0033$ ), employing the least-squares regression method, gave a straight-line output whose intercept provided the  $\log A$  of the reaction, which was 13.274 (see below). The latter value enabled a Pre-Exponential or Frequency Factor  $A$  of  $1.88 \times 10^{13} \text{ s}^{-1}$  to be deduced for the ring-opening process, which was consistent with an entirely free radical  $E_{\text{H}}1$  ring-cleavage occurring within **2a** to give **3a**. The slope of the plot was -1568.6, while its  $R^2 = 0.902906$ . Such a net deviation confirmed that our data had given a reasonable fit of the averaged experimentally-derived **4a:5a** ratio determinations made. The deviation observed included the 5% deviation already present in Ingold's  $k$  calibrating data (see the earlier plot), and the 5% data point deviation in our own reaction run data. Most importantly though, the high magnitude of the  $\log A$  (13.274) obtained for this ring-opening was unmistakeable, and it was a number that was sufficiently reliable to allow it to be confidently asserted that an entirely free radical, scissive,  $E_{\text{H}}1$  ring-opening was occurring in **2a** in pentane to give **3a**.



The Arrhenius energy of activation for this cyclopropane radical ring-opening event was deduced from the expression  $E_a = -(slope) \times 2.303R$ , which, for the ring-opening of the stannylyvinyl radical **2a** ( $R = \text{Bu}$ ) in pentane led to an  $E_a$  of  $+7.18 \text{ kcal mol}^{-1}$  being calculated. Thus:

$$E_a = -(-1568.6) \times 2.303 \times 8.314 = +30034.207 \text{ J mol}^{-1} = +30.034 \text{ kJ mol}^{-1}, \text{ but to obtain the corresponding } E_a \text{ in units of } \text{kcal mol}^{-1}, \text{ this figure was divided by } 4.184, \text{ which gave an } E_a = 30.034/4.184 = +7.18 \text{ kcal mol}^{-1}.$$

### **1.3 Estimation of the Rate Constants for H-Atom Abstraction ( $k_{\text{H-atom abstraction Bu}_3\text{SnH}}$ ) for the 2,2-Dimethylvinyl Radical (**6**) in PhMe and the Accompanying Arrhenius Parameter Determinations**

The temperature dependent  $k_{\text{H-atom abstraction Bu}_3\text{SnH}}$  data for the 2,2-dimethylvinyl radical **6** from  $\text{Bu}_3\text{SnH}$  in PhMe was experimentally derived in the following way.

Free radical hydrostannation reactions were conducted on the alkynol **1** with  $\text{Bu}_3\text{SnH}/\text{cat. Et}_3\text{B}$  in PhMe over a 20-30 °C (293-303 K) temperature range, in an analogous manner to the way in which these reactions were run in pentane, and the averaged product ratios of **4a:5a** for 2-3 reaction runs were determined by 600.13 MHz  $^1\text{H}$  NMR spectroscopy of the concentrated crude reaction mixtures in  $\text{CDCl}_3$ . The differences in the **4a:5a** product ratios, in pentane and PhMe, were then compared with respect to the allenyltin **4a** ( $\text{R} = \text{Bu}$ ) component. This allowed us to estimate the differing rates of H-atom abstraction by **(Z)-2a** to give **5a** over the 293-303 K temperature range examined. It transpired that, within this narrow temperature window, the rate of H-atom abstraction of **(Z)-2a** from  $\text{Bu}_3\text{SnH}$  was approximately 1.47 x slower in PhMe than in pentane, where a larger quantity of **5a** was formed. As a result of this slower rate of H-atom abstraction by **(Z)-2a** in PhMe, more cyclopropane ring-opening product **4a** was formed in PhMe than in pentane.

The precise reduction in the rate of  $\text{Bu}_3\text{SnH}$  H-atom abstraction in PhMe was estimated by dividing the relative ratios of **4a** formed in the two reaction solvents at the temperature under investigation. Thus, at 293 K the **4a** ratio difference was  $2.24/1.5 = 1.493$ ; at 298 K it was  $2.50/1.60 = 1.56$ ; and at 303K it was  $2.82/2.06 = 1.37$ . The average sum of these net reductions in the rate of H-atom abstraction in PhMe was thus  $4.423/3 = 1.47$ . Accordingly, we reduced the  $k_{\text{H-atom abstraction Bu}_3\text{SnH}}^{\text{pentane}}$  values that we had obtained in pentane by a factor of 1.47. This gave rise to the following new reduced  $k_{\text{H-atom abstraction Bu}_3\text{SnH}}^{\text{PhMe}}$  estimates for the rate of H-atom abstraction from the  $\text{Bu}_3\text{SnH}$  by the 2,2-dimethylvinyl radical **6** and **2a** in PhMe.

$$k_{\text{H-atom abstraction Bu}_3\text{SnH by 6/2a PhMe } 293 \text{ K}} = \frac{2.88 \times 10^8 \text{ mol}^{-1} \text{ s}^{-1}}{1.47} = 1.959184 \times 10^8 \text{ mol}^{-1} \text{ s}^{-1}$$

$$k_{\text{H-atom abstraction Bu}_3\text{SnH by 6/2a PhMe } 298 \text{ K}} = \frac{2.96 \times 10^8 \text{ mol}^{-1} \text{ s}^{-1}}{1.47} = 2.013605 \times 10^8 \text{ mol}^{-1} \text{ s}^{-1}$$

$$k_{\text{H-atom abstraction Bu}_3\text{SnH by 6/2a PhMe } 303 \text{ K}} = \frac{3.154 \times 10^8 \text{ mol}^{-1} \text{ s}^{-1}}{1.47} = 2.145578 \times 10^8 \text{ mol}^{-1} \text{ s}^{-1}$$

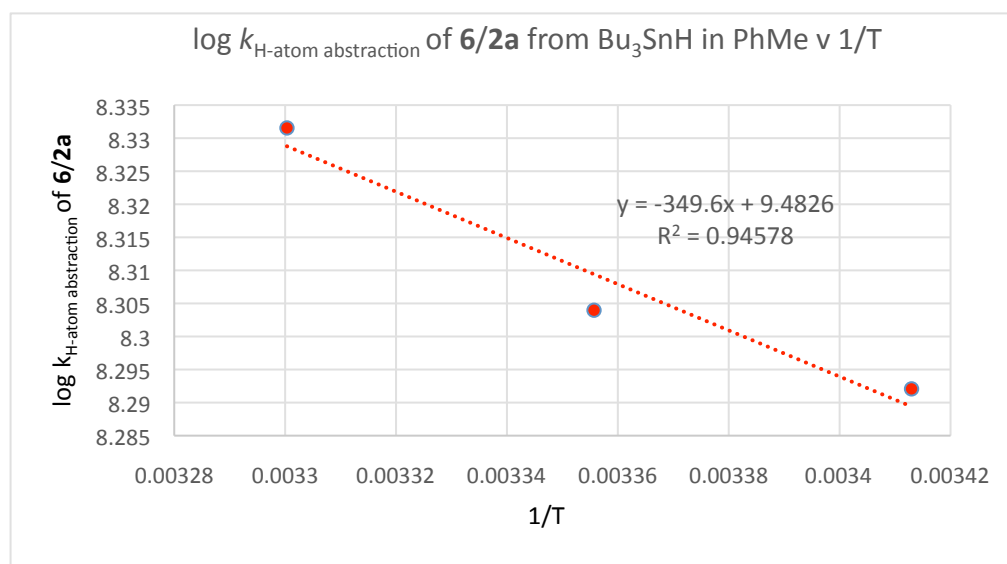
These estimates, in turn, gave rise to the following  $\log k_{\text{H-atom abstraction Bu}_3\text{SnH 6/2a}}$  values in PhMe:

$$\log k_{\text{H-atom abstraction 6/2a PhMe } 293 \text{ K}} = 8.292075$$

$$\log k_{\text{H-atom abstraction 8/2a PhMe } 298 \text{ K}} = 8.303974$$

$$\log k_{\text{H-atom abstraction 6/2a PhMe } 303 \text{ K}} = 8.331544$$

When these three estimated  $\log k_{\text{H-atom abstraction Bu}_3\text{SnH}}$  values for **6/2a** ( $R = Bu$ ) in PhMe were plotted against the following  $1/T$  values (i.e.  $1/293 \text{ K} = 0.003413$ ;  $1/298 \text{ K} = 0.003356$ ; and  $1/303 \text{ K} = 0.0033$ ) in classical Arrhenius format, the following Excel plot was obtained via the least-squares regression method:



Significantly, this plot yielded a  $\log A = 9.4826$  (Frequency Factor  $A = 3.04 \times 10^9 \text{ s}^{-1}$ ) and had a slope = -349.6 and an  $R^2$  value of 0.94578, for seven experimentally determined **4a:5a** ratio measurements in PhMe. The fact that the  $R^2$  value was 94.58% confirmed that the experimental data fit was good.

From that slope, an  $E_a = -(-349.6) \times 2.303 \times 8.314 = +6693.84 \text{ J mol}^{-1}$  or  $+6.69384 \text{ kJ mol}^{-1}$  was deduced, which translated into an  $E_a$  of  $+1.59879 \text{ kcal mol}^{-1}$ , following multiplication by 0.238846 (i.e.  $+6.69384 \text{ kJ mol}^{-1} \times 0.238846 = E_a = +1.59879 \text{ kcal mol}^{-1}$  or  $1.6 \text{ kcal mol}^{-1}$ ). The close match of these Arrhenius parameters with the Ingold data for **6** and  $\text{Bu}_3\text{SnH}$  in pentane clearly corroborated the validity of our experimentally-derived Arrhenius plot for **6 (2a)** and  $\text{Bu}_3\text{SnH}$  in PhMe and its integrity.

From these new, experimentally-determined, Arrhenius parameters for **6** in PhMe ( $\log A = 9.4826$  and  $E_a = 6693.84 \text{ J mol}^{-1}$ ) derived from this averaged Arrhenius plot, the following five additional new  $k_{\text{H-atom abstraction Bu}_3\text{SnH PhMe}}$  values were calculated. This allowed the entire 313-353 K temperature range to be fully calibrated and covered for **6**, which was to serve as the  $k_{\text{H-atom abstraction Bu}_3\text{SnH PhMe}}$  calibrant for **2a** ( $R = \text{Bu}$ ) and later **13**.

**At 313K:** For  $E_a = 6693.84 \text{ J mol}^{-1}$

$$\log k_{\text{H-atom abstraction PhMe } 313 \text{ K}} = 9.4826 - \frac{6693.84}{2.303 \times 8.314 \times 313}$$

$$\log k_{\text{H-atom abstraction PhMe } 313 \text{ K}} = 9.4826 - \frac{6693.84}{5993.055}$$

$$\log k_{\text{H-atom abstraction PhMe } 313 \text{ K}} = 9.4826 - 1.1169 = 8.3657$$

$$\therefore k_{\text{H-atom abstraction PhMe } 313 \text{ K}} = 10^{8.3657} = 2.321133 \times 10^8 \text{ mol}^{-1} \text{ s}^{-1}$$

**At 323K:** For  $E_a = 6693.84 \text{ J mol}^{-1}$

$$\log k_{\text{H-atom abstraction PhMe}} = 9.4826 - \frac{6693.84}{2.303 \times 8.314 \times 323}$$

$$\log k_{\text{H-atom abstraction PhMe}} = 9.4826 - \frac{6693.84}{6184.5269}$$

$$\log k_{\text{H-atom abstraction PhMe}} = 9.4826 - 1.082353 = 8.4002$$

$$\therefore k_{\text{H-atom abstraction PhMe}} = 10^{8.4002} = 2.513043 \times 10^8 \text{ mol}^{-1} \text{ s}^{-1}$$

**At 333K:** For  $E_a = 6693.84 \text{ J mol}^{-1}$

$$\log k_{\text{H-atom abstraction PhMe}} = 9.4826 - \frac{6693.84}{2.303 \times 8.314 \times 333}$$

$$\log k_{\text{H-atom abstraction PhMe}} = 9.4826 - \frac{6693.84}{6375.9983}$$

$$\log k_{\text{H-atom abstraction PhMe}} = 9.4826 - 1.04985 = 8.43275$$

$$\therefore k_{\text{H-atom abstraction PhMe}} = 10^{8.43275} = 2.708631 \times 10^8 \text{ mol}^{-1} \text{ s}^{-1}$$

**At 343K:** For  $E_a = 6693.84 \text{ J mol}^{-1}$

$$\log k_{\text{H-atom abstraction PhMe}} = 9.4826 - \frac{6693.84}{2.303 \times 8.314 \times 343}$$

$$\log k_{\text{H-atom abstraction PhMe}} = 9.4826 - \frac{6693.84}{6567.470}$$

$$\log k_{\text{H-atom abstraction PhMe}} = 9.4826 - 1.01924 = 8.46336$$

$$\therefore k_{\text{H-atom abstraction PhMe}} = 10^{8.46336} = 2.90643 \times 10^8 \text{ mol}^{-1} \text{ s}^{-1}$$

**At 353K:** For  $E_a = 6693.84 \text{ J mol}^{-1}$

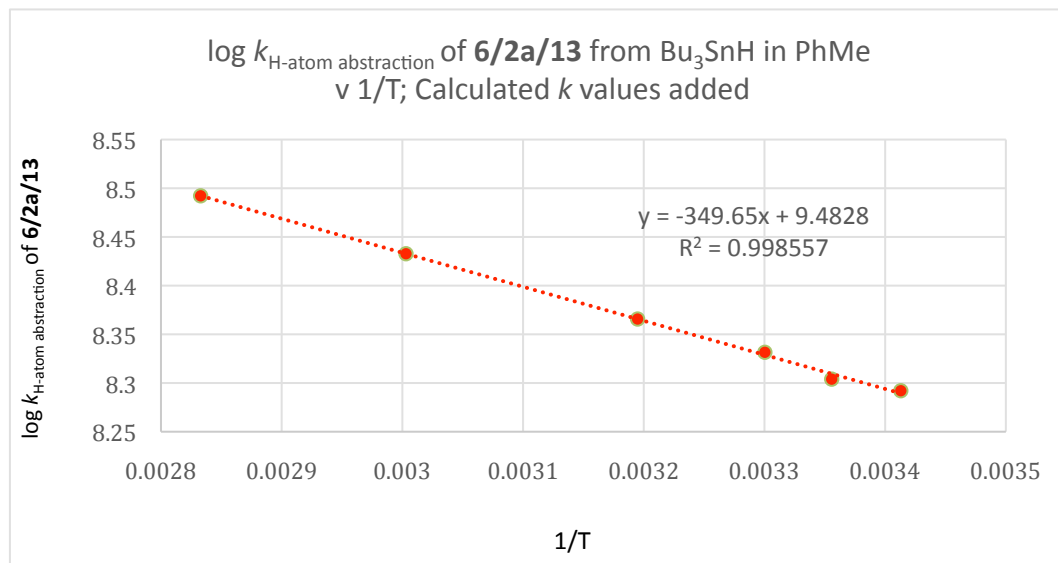
$$\log k_{\text{H-atom abstraction PhMe}} = 9.4826 - \frac{6693.84}{2.303 \times 8.314 \times 353}$$

$$\log k_{\text{H-atom abstraction PhMe}} = 9.4826 - \frac{6693.84}{6758.941}$$

$$\log k_{\text{H-atom abstraction PhMe}} = 9.4826 - 0.990368 = 8.49223$$

$$\therefore k_{\text{H-atom abstraction PhMe}} = 10^{8.49223} = 3.106204 \times 10^8 \text{ mol}^{-1} \text{ s}^{-1}$$

With respect to the radical **6** (and the calibrated radicals **2a** and **13**), the calculated  $\log k_{\text{H-atom}}$  abstraction  $\text{Bu}_3\text{SnH}$  values at 313K, 333K and 353 K were added to a new Arrhenius plot, alongside the 293 K, 298 K and 303 K  $\log k_{\text{H-atom}}$  abstraction  $\text{Bu}_3\text{SnH}$  data, to check their numerical integrity. The output is shown below:



The fact that this Arrhenius plot now had an  $R^2 = 0.998557$  indicated a near perfect fit of the data.

It used the following  $1/T$  and  $\log k_{\text{H-atom}}$  abstraction  $\text{Bu}_3\text{SnH}$  PhMe values:

$$1/293 \text{ K} = 0.003412969.$$

$$\log k_{\text{H-atom}} \text{ abstraction } 293\text{K} = 8.292075.$$

$$1/298 \text{ K} = 0.003355704698.$$

$$\log k_{\text{H-atom}} \text{ abstraction } 298\text{K} = 8.303974.$$

$$1/303 \text{ K} = 0.00330033.$$

$$\log k_{\text{H-atom}} \text{ abstraction } 303\text{K} = 8.331544.$$

$$1/313 \text{ K} = 0.003194888.$$

$$\log k_{\text{H-atom}} \text{ abstraction } 313\text{K} = 8.3657.$$

$$1/333 \text{ K} = 0.003003.$$

$$\log k_{\text{H-atom}} \text{ abstraction } 333\text{K} = 8.43275.$$

$$1/353 \text{ K} = 0.0028328611.$$

$$\log k_{\text{H-atom}} \text{ abstraction } 353\text{K} = 8.49223.$$

**1.4 Estimation of the  $k_{\text{ring-opening}}$  Rate Constants and Arrhenius Parameters for the Cyclopropane Ring-Opening of the Tri-*n*-Butylstannylvinyl Radical **2a** in PhMe From The Averaged **4a:5a** Ratios in PhMe**

With this mix of calculated and experimentally-derived  $k_{\text{H-atom abstraction}} \text{Bu}_3\text{SnH}$  PhMe values in hand for **6** and **2a** ( $\text{R} = \text{Bu}$ ) in PhMe, as well as the newly experimentally-derived **4a:5a** ( $\text{R} = \text{Bu}$ ) ratios, the following  $k_{\text{ring-opening 2a}}$  values were determined in PhMe at each specified temperature. As was the case with the pentane reaction runs, all product ratios were derived from reaction runs that were performed at a 0.2 M [Bu<sub>3</sub>SnH]. The  $k_{\text{ring-opening 2a PhMe}}$  values were again calculated using equation 2:

$$k_{\text{ring-opening}} = [(R)_3\text{SnH}] \times k_{\text{H-atom abstraction}} \times \frac{[\text{Allenyltin}]}{[\text{Vinyltin}]} \quad (\text{Eqn 2})$$

These calculations are collated below:

$$\text{At 293 K: } k_{\text{ring-opening 2a PhMe 293 K}} = [0.2] \times 1.959184 \times 10^8 \times 2.24/1 = 8.7771443 \times 10^7 \text{ s}^{-1}.$$

$$\text{At 298 K: } k_{\text{ring-opening 2a PhMe 298 K}} = [0.2] \times 2.013605 \times 10^8 \times 2.5/1 = 1.0068025 \times 10^8 \text{ s}^{-1}.$$

$$\text{At 303 K: } k_{\text{ring-opening 2a PhMe 303 K}} = [0.2] \times 2.145578 \times 10^8 \times 2.82/1 = 1.210106 \times 10^8 \text{ s}^{-1}.$$

$$\text{At 313 K: } k_{\text{ring-opening 2a PhMe 313 K}} = [0.2] \times 2.321133 \times 10^8 \times 4.33/1 = 2.0101011 \times 10^8 \text{ s}^{-1}.$$

$$\text{At 333 K: } k_{\text{ring-opening 2a PhMe 333 K}} = [0.2] \times 2.708631 \times 10^8 \times 10.03/1 = 5.4335138 \times 10^8 \text{ s}^{-1}.$$

$$\text{At 353 K: } k_{\text{ring-opening 2a PhMe 353 K}} = [0.2] \times 3.106204 \times 10^8 \times 20.73/1 = 1.2878322 \times 10^9 \text{ s}^{-1}.$$

The 1/T and log  $k_{\text{ring-opening 2a PhMe}}$  values that were used in the subsequent Arrhenius plot are listed below:

$$1/293 \text{ K} = 0.003412969. \quad \log k_{\text{ring-opening 2a PhMe 293 K}} = \log 8.7771443 \times 10^7 \text{ s}^{-1} = 7.943353.$$

$$1/298 \text{ K} = 0.003355704698. \quad \log k_{\text{ring-opening 2a PhMe 298 K}} = \log 1.0068025 \times 10^8 \text{ s}^{-1} = 8.002944.$$

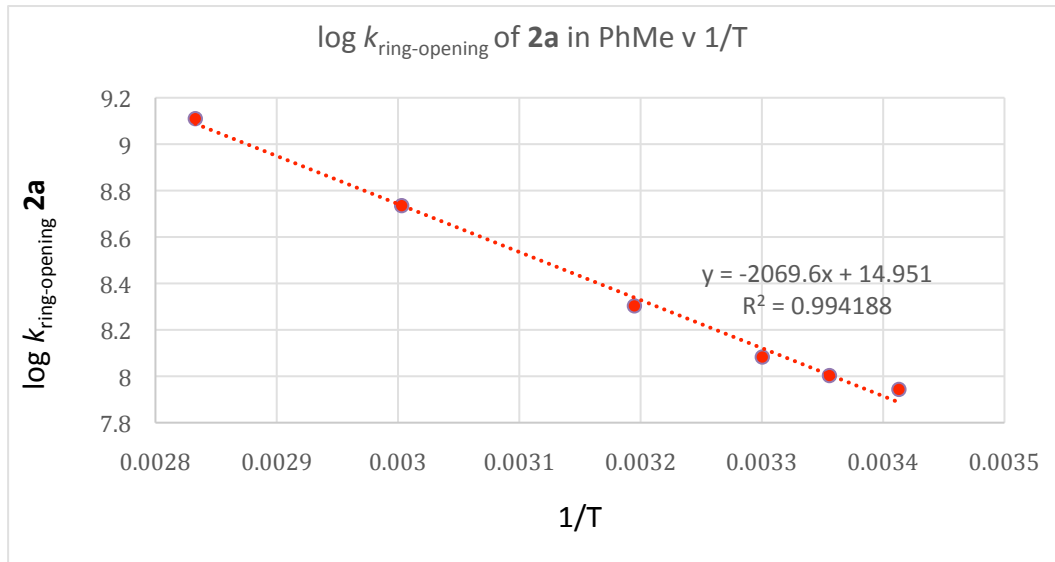
$$1/303 \text{ K} = 0.00330033. \quad \log k_{\text{ring-opening 2a PhMe 303 K}} = \log 1.210106 \times 10^8 \text{ s}^{-1} = 8.08282341.$$

$$1/313 \text{ K} = 0.003194888. \quad \log k_{\text{ring-opening 2a PhMe 313 K}} = \log 2.0101011 \times 10^8 \text{ s}^{-1} = 8.3032179.$$

$$1/333 \text{ K} = 0.003003. \quad \log k_{\text{ring-opening 2a PhMe 333 K}} = \log 5.4335138 \times 10^8 \text{ s}^{-1} = 8.735080.$$

$$1/353 \text{ K} = 0.0028328611. \quad \log k_{\text{ring-opening 2a PhMe 353 K}} = \log 1.2878322 \times 10^9 \text{ s}^{-1} = 9.109859.$$

That Arrhenius plot is shown below in Excel, and gave rise to the following Arrhenius expression for the ring-opening of radical **2a**:  $\log k_{\text{ring-opening 2a}} = 14.951 - 9.47/2.303RT$ .



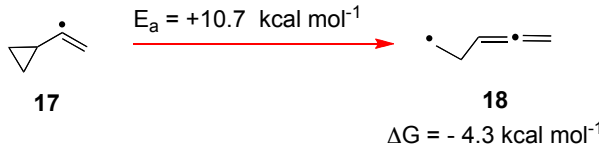
Clearly, now that there were 6 experimental data points included in this Arrhenius Plot, from 17 independent reaction runs, a great improvement was seen in the overall  $R^2$  score ( $R^2 = 0.994188$ ), which lent considerable weight and confidence to the experimental accuracy of the experimental data that was deduced.

Our calculation of the  $E_a$  for the ring-opening of **2a** to give **3a** is presented below. It used the slope of -2069.6 derived from the above Arrhenius plot to deduce the final calculated figure for the  $E_a$  of the ring-opening of **2a**.

$$\begin{aligned}\therefore E_a \text{ ring-opening } \mathbf{2a} &= -(-2069.6) \times 2.303 \times 8.314 \text{ J mol}^{-1} \\ \therefore E_a \text{ ring-opening } \mathbf{2a} &= 39626.925 \text{ J mol}^{-1} = 39.6269 \text{ kJ mol}^{-1} \\ \therefore E_a \text{ ring-opening } \mathbf{2a} &= \frac{39.6269 \text{ kJ mol}^{-1}}{4.184} = +9.47 \text{ kcal mol}^{-1}\end{aligned}$$

This  $E_a$  of  $+9.47 \text{ kcal mol}^{-1}$  for the ring-opening of **2a** showed a reasonably good level of agreement with Guo's theoretical value<sup>22</sup> for the mechanistically analogous  $E_{\text{H1}}$  ring-opening of the  $\alpha$ -

cyclopropylvinyl radical **17**, if one also considers that the  $\text{Bu}_3\text{Sn}$ -substituent will almost certainly be hyperconjugatively stabilising **2a** while also accelerating the actual ring-opening event itself.



J. Shi, M. Zhang, Y. Fu, L. Liu, Q.-X. Guo *Tetrahedron* **2007**, *63*, 12681.

Our  $\Delta S^\ddagger_{333 \text{ K}}$  calculation for the **2a**  $\rightarrow$  **3a** conversion is also shown overleaf for comparison. It used two methods of calculation: the Avery  $\Delta S^\ddagger$  equation<sup>2a</sup> and variants of the Bennett  $\Delta S^\ddagger$  equation.<sup>28</sup>

The origin of Avery's  $\Delta S^\ddagger$  equation<sup>2a</sup> is shown below for ease of understanding (see p 67 of ref 2a):

Using statistical thermodynamics, Wynne-Evans and Eyring<sup>26</sup> have shown that the rate constant  $k_r$  is related to the Boltzmann Constant  $k_{\text{Boltzmann}}$ , Planck's Constant  $h$ , the reaction temperature  $T$ , and the standard free energy of activation ( $-\Delta G^\ddagger$ ) by the following form of the Arrhenius Equation:

$$k_r = \frac{k_{\text{Boltzmann}} T}{h} \exp\left(\frac{-\Delta G^\ddagger}{RT}\right)$$

If we now incorporate  $\Delta G = \Delta H - T\Delta S$  into this expression, it follows that:

$$k_r = \frac{k_{\text{Boltzmann}} T}{h} \exp\left(n + \frac{\Delta S^\ddagger}{R}\right) \exp\left(\frac{-\Delta H^\ddagger}{RT}\right)$$

Since the enthalpy of activation ( $\Delta H^\ddagger$ ) is related to the activation energy ( $E_a$ ) by  $\Delta H = E_a - nRT$ , where  $n$  (the molecularity) = 1 for all unimolecular or liquid phase reactions, it follows that:

$$k_r = \frac{k_{\text{Boltzmann}} T}{h} \exp\left(n + \frac{\Delta S^\ddagger}{R}\right) \exp\left(\frac{E_a}{RT}\right) \quad \begin{aligned} h &= 6.62 \times 10^{-34} \text{ mol}^{-1} \text{ Planck's Constant} \\ R &= 8.314 \text{ J K}^{-1} \text{ mol}^{-1} \text{ Gas Constant} \\ n &= \text{Molecularity of Reaction} \\ k_{\text{Boltzmann}} &= 1.38 \times 10^{-23} \text{ J K}^{-1} \end{aligned}$$

In this expression,

$$\frac{k_{\text{Boltzmann}} T}{h} \exp\left(n + \frac{\Delta S^\ddagger}{R}\right) = A = \text{Pre-Exponential or Frequency Factor}$$

The A factor gives a measure of the number of successful molecular collisions with the correct orientation and energy to react. and thereby give rise to the product(s).

So, from a knowledge of the reaction temperature and the A factor, one can work out the entropy of activation ( $\Delta S^\ddagger$ ). Assuming  $n = 1$  (for a unimolecular reaction), and taking natural logarithms, allows further equation simplification to:

$$\ln A = \ln \frac{k_{\text{Boltzmann}} T}{h} + 1 + \frac{\Delta S^\ddagger}{R}$$

Further conversion of the natural logarithm terms in this equation into  $\log_{10}$  values requires multiplication by a factor of 2.303, and further rearrangement thereafter gives Avery's equation,<sup>2a</sup> (page 67) since he is the chemist who popularised it.:

$$\Delta S^\ddagger = R \left[ 2.303 \log A - 2.303 \log \frac{k_{\text{Boltzmann}} T}{h} - 1 \right] \quad \text{Avery's equation for } \Delta S^\ddagger \text{ for unimolecular reactions}$$

Taking the log A of 14.951 derived from the intercept of our above Arrhenius plot of the  $\log k_{\text{ring-opening}}$  of **2a** in PhMe vs 1/T (for our **2a**→**3a** conversion), and using it in Avery's  $\Delta S^\ddagger$  equation (which, most importantly, takes into account the effect of reaction molecularity),<sup>2a</sup> we arrived at the final  $\Delta S^\ddagger_{333\text{ K}}$  value shown below after insertion of the relevant numerical values into that equation.

$$\Delta S^\ddagger_{333\text{K}} = 8.314 \left[ (2.303 \times 14.951) - 2.303 \log \left( \frac{1.38 \times 10^{-23} \times 333}{6.626 \times 10^{-34}} \right) - 1 \right] \text{ J K}^{-1} \text{ mol}^{-1}$$

$$\Delta S^\ddagger_{333\text{K}} = 8.314 \left[ (34.4322) - 2.303 \log (6.935406 \times 10^{12}) - 1 \right] \text{ J K}^{-1} \text{ mol}^{-1}$$

$$\Delta S^\ddagger_{333\text{K}} = 8.314 \left[ (34.4322) - 2.303 (12.84107) - 1 \right] \text{ J K}^{-1} \text{ mol}^{-1}$$

$$\Delta S^\ddagger_{333\text{K}} = 8.314 \left[ (34.4322) - 29.5730 - 1 \right] \text{ J K}^{-1} \text{ mol}^{-1}$$

$$\Delta S^\ddagger_{333\text{K}} = 8.314 \left[ (34.4322) - 30.5730 \right] \text{ J K}^{-1} \text{ mol}^{-1}$$

$$\Delta S^\ddagger_{333\text{K}} = 8.314 [ +3.8592 ] \text{ J K}^{-1} \text{ mol}^{-1}$$

$$\Delta S^\ddagger_{333\text{K}} = +32.085 \text{ J K}^{-1} \text{ mol}^{-1}$$

$$\therefore \boxed{\Delta S^\ddagger_{333\text{K}} = \frac{+32.085 \text{ J K}^{-1} \text{ mol}^{-1}}{4.184} = +7.67 \text{ e.u.} = +7.67 \text{ cal K}^{-1} \text{ mol}^{-1}}$$

However, in order to check the overall veracity of our  $\Delta S^\ddagger_{333\text{ K}}$  determination, we also used Anslyn and Dougherty's simplified variant<sup>27</sup> of Bunnett's long-established  $\Delta S^\ddagger$  equation<sup>28</sup> to confirm the general magnitude of the  $\Delta S^\ddagger_{333\text{ K}}$  value we had derived for the **2a**→**3a** conversion via the Avery equation.<sup>2a</sup>

Although not specified by Anslyn and Dougherty in their book,<sup>27</sup> their simplified variant of Bunnett's much earlier  $\Delta S^\ddagger$  equation<sup>28</sup> produces an output that is in entropy units (i.e. 1 e.u. = 1 cal  $\text{K}^{-1} \text{ mol}^{-1}$ ). It was formulated entirely analogously to Alder, Baker and Brown's earlier simplified 1971  $\Delta S^\ddagger$  e.u. equation for a 298 K determination, which had  $\Delta S^\ddagger_{298\text{ K}} = 4.576 (\log A - 13.23)$ .<sup>29</sup> The  $\Delta S^\ddagger$  values that emerge from these two equations thus require multiplication by a factor of 4.184 to convert them into the more familiar  $\text{J K}^{-1} \text{ mol}^{-1}$  unit of quantification that one typically sees for  $\Delta S^\ddagger$  values reported in the literature.

We ourselves have formulated our own simplified variant of the Bunnett  $\Delta S^\ddagger$  equation<sup>28</sup> shown below on the left, which does the  $J\ K^{-1}\ mol^{-1}$   $\Delta S^\ddagger$  calculation directly.

Significantly, both of these simplified  $\Delta S^\ddagger$  equations work very well indeed for providing this key Arrhenius parameter for both **unimolecular** and **bimolecular** reactions (in the liquid phase), without all of the complex calculations that the Avery equation and its variants require.

The **2a**→**3a**  $\Delta S^\ddagger_{333\ K}$  calculations where we used our own and Anslyn-Dougherty's  $\Delta S^\ddagger$  equations are shown below. They give identical results:

The $\Delta S^\ddagger$ Equation in Units of $J\ K^{-1}\ mol^{-1}$	Bunnett's $\Delta S^\ddagger$ Equation in Entropy Units
$\Delta S^\ddagger_{Temp\ K} = 2.303R \left[ \log A - \log \left( \frac{e k_{Boltzmann}}{h_{Planck}} \right) - \log T \right] J\ K^{-1}\ mol^{-1}$ <p style="text-align: center;"><math>e</math> = Euler's Constant = 2.7182818 or  <math display="block">\Delta S^\ddagger_{Temp\ K} = 19.147 \left[ \log A - 10.753 - \log T \right] J\ K^{-1}\ mol^{-1}</math> <span style="float: right;">This work</span></p>	$\Delta S^\ddagger_{Temp\ K} = 4.576 \left[ \log k - \log \left( \frac{e k_{Boltzmann}}{h_{Planck}} \right) - \log T + \frac{E^\ddagger}{4.576T} \right]$ <p style="text-align: center;">where <math>\log k = \log A - \log \frac{E^\ddagger}{4.576T}</math> and <math>e</math> = Euler's Constant or  <math display="block">\Delta S^\ddagger_{Temp\ K} = 4.576 \left[ \log A - 10.753 - \log T \right] cal\ K^{-1}\ mol^{-1}</math> or e.u.  <span style="float: right;">Anslyn-Dougherty</span></p>

#### 2a → 3a $\Delta S^\ddagger_{333\ K}$ Calculations

$$\begin{aligned}\Delta S^\ddagger_{333\ K} &= 19.147 [14.951 - 10.753 - 2.522] J\ K^{-1}\ mol^{-1} \\ \Delta S^\ddagger_{333\ K} &= 19.147 [14.951 - 13.275] J\ K^{-1}\ mol^{-1} \\ \Delta S^\ddagger_{333\ K} &= 19.147 [1.676] J\ K^{-1}\ mol^{-1} \\ \Delta S^\ddagger_{333\ K} &= + 32.09 J\ K^{-1}\ mol^{-1}\end{aligned}$$

#### 2a → 3a $\Delta S^\ddagger_{333\ K}$ Calculations

$$\begin{aligned}\Delta S^\ddagger_{333\ K} &= 4.576 [14.951 - 10.753 - 2.522] cal\ K^{-1}\ mol^{-1}$$
 or e.u.  

$$\Delta S^\ddagger_{333\ K} = 4.576 [1.676] cal\ K^{-1}\ mol^{-1}$$
 or e.u.  

$$\Delta S^\ddagger_{333\ K} = + 7.669 cal\ K^{-1}\ mol^{-1}$$
 or e.u. × 4.184  

$$\Delta S^\ddagger_{333\ K} = + 32.09 J\ K^{-1}\ mol^{-1}$$

Significantly, the  $\Delta S^\ddagger$  values so obtained matched up perfectly well with the  $\Delta S^\ddagger_{333\ K}$  value that we had derived using Avery's equation.<sup>2a</sup> This agreement thus confirmed that our method was sound.

Finally, the enthalpy of activation  $\Delta H^\ddagger$  and the free energy of activation  $\Delta G^\ddagger$  for the unimolecular ring-opening of **2a** were also calculated from the experimentally-derived data in the following way:

$$\begin{aligned}\Delta H^\ddagger &= E_a - nRT \therefore \Delta H^\ddagger = 39.6269 - \frac{1 \times 8.314 \times 333}{1000} \text{ kJ mol}^{-1} \\ \Delta H^\ddagger &= 39.6269 - 2.77 = 36.86 \text{ kJ mol}^{-1} = +8.8 \text{ kcal mol}^{-1}\end{aligned}$$

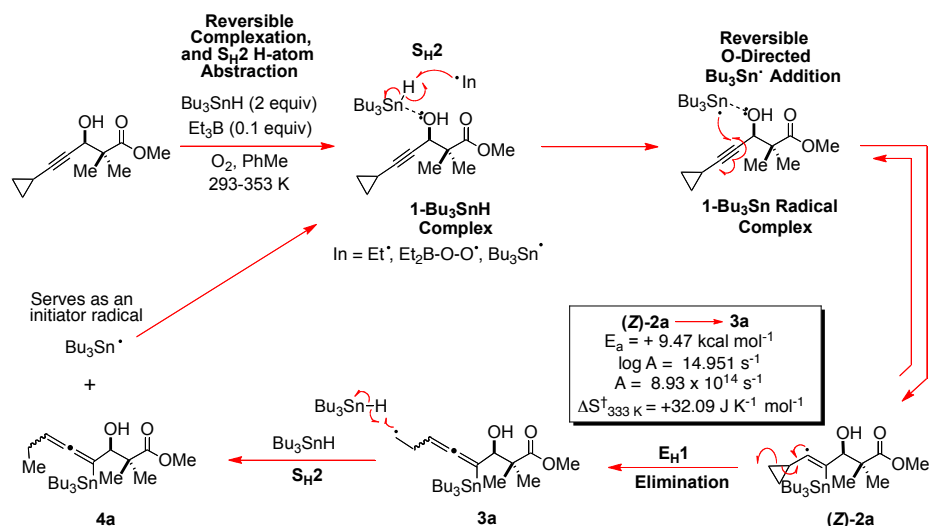
$$\text{Since } \Delta G^\ddagger = \Delta H^\ddagger - T\Delta S^\ddagger \therefore \Delta G^\ddagger = 36.86 - \frac{333 \times 32.09}{1000} \text{ kJ mol}^{-1}$$

$$\therefore \Delta G^\ddagger = 36.86 - 10.69 = 26.17 \text{ kJ mol}^{-1} = +6.25 \text{ kcal mol}^{-1}$$

## 1.5 Our Mechanistic Interpretation of The Arrhenius Parameters Obtained for the $2\text{a} \rightarrow 4\text{a}$ Conversion: Support for An Entirely Free Radical $E_{\text{H}}1$ Mechanism For Cyclopropane Ring-Opening

Clearly the large positive log A value of 14.951 that is seen here for the ring-opening of **2a** in PhMe at 333 K, and its accompanying  $\Delta S^{\ddagger}_{333\text{ K}}$  of +32.09 J K<sup>-1</sup> mol<sup>-1</sup> (+7.67 e.u.) only satisfactorily align with a single molecular entity (**2a**) entering the rate-determining step (r.d.s), and it undergoing homolytic cyclopropane ring-cleavage as shown in Scheme 4. The log A of 14.951 that was observed lies well within the range that one would normally see for cyclopropane radical homolyses,<sup>2b</sup> which typically give log A values of 13.29-16.11.<sup>20</sup> The fact that our log A sits right in the middle of this range of values possibly reflects some of the rotational freedom that is lost when the new C=C double bond forms in the r.d.s. Nonetheless, its high magnitude does strongly point to this being a unimolecular ring-opening event that is proceeding via a “very loose”, but still cyclic, solvent-stabilised radicaloid activated complex, in which partial homolytic bond cleavage and partial radicaloid bond formation are both at advanced stages by the mid-point of the reaction.

Once formed, the activated complex can then either revert to **2a** or eventually undergo full  $E_{\text{H}}1$  homolytic ring-cleavage to produce the stannyl homoallenyl radical **3a** (Scheme 4),<sup>3b,c</sup> with **3a** then going on to H-atom abstract from the Bu<sub>3</sub>SnH by the S<sub>H2</sub> pathway shown, to finally produce **4a**. A key component of this mechanistic scheme is **2a** itself arising from a reversible O-directed stannyl radical addition to the alkyne carbon that is  $\alpha$ - to the propargylic alcohol group.<sup>3,17-19</sup>

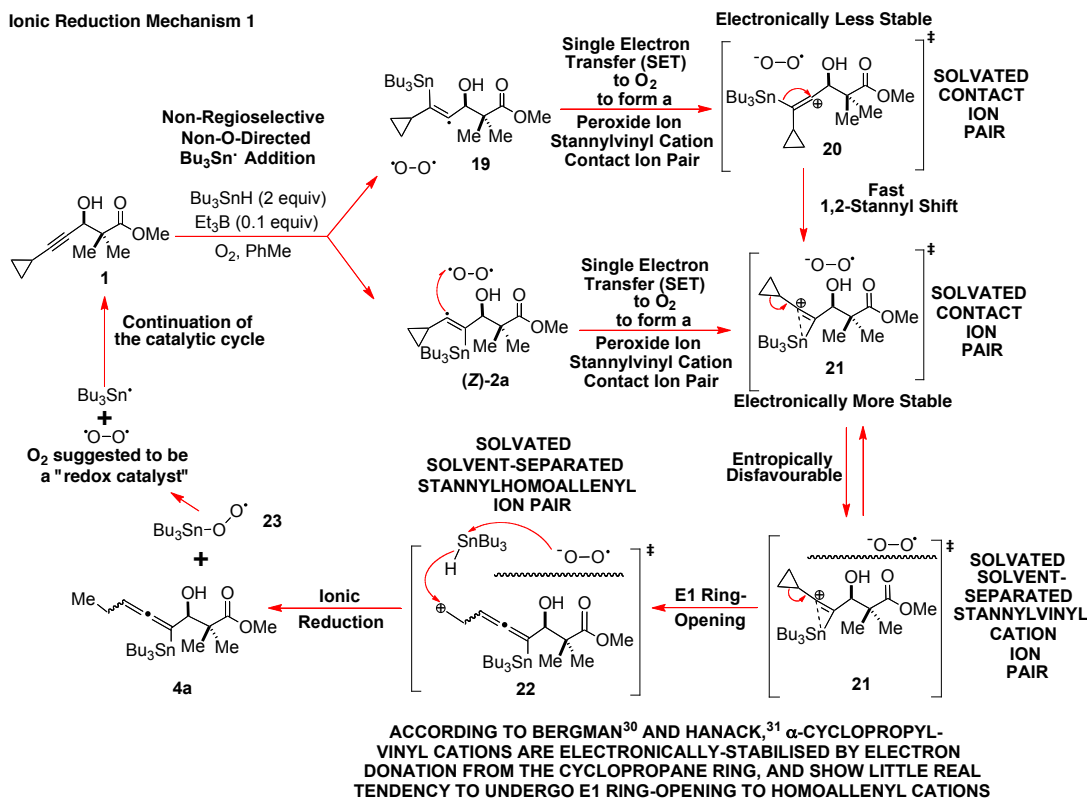


**Scheme 4.** The sequential O-directed stannyl radical addition/ $E_{\text{H}}1/\text{S}_{\text{H}2}$  mechanistic pathway that most satisfactorily rationalises the formation of **4a** from **3a** and **2a** in the non-polar PhMe solvent.

## 1.6 The Arrhenius Parameters Obtained for the 2a→4a Conversion in PhMe Do Not Support

### Stannylvinyl Cation Involvement in the Mechanism of the Cyclopropane Ring-Opening of 2a

The high log A of 14.951 observed for the ring cleavage of **2a** in PhMe over the temperature range 293–353K is at great odds with the stannylvinyl cationic mechanistic hypothesis that was recently put forward for alkyne hydrostannation,<sup>6a–6d</sup> and further propagated by two recent reviews,<sup>6e,f</sup> despite prior contradicting reports.<sup>3,4a</sup> In the stannylvinyl cationic mechanistic theory,<sup>6</sup> a fast “outer sphere” single electron transfer (SET) oxidation event is proposed to occur involving the stannylvinyl radical and O<sub>2</sub>. In the present instance, this would ultimately afford the solvent-separated solvated stannylvinyl cation ion pair **21**, which would subsequently undergo cyclopropane ring cleavage, *either* by the polar unimolecular mechanism of Scheme 5, where Bu<sub>3</sub>SnH reduction of the carbocation **22** would occur (**Ionic Reduction Mechanism 1**) (see below) *or* by the direct bimolecular Bu<sub>3</sub>SnH reduction mechanism shown in Scheme 6 (**Ionic Reduction Mechanism 2**) (see page 33).



**Scheme 5.** The *untenable* “outer sphere” SET/stannylvinyl cation reduction mechanism<sup>6a–d</sup> as applied to the alkynol **1** with Bu<sub>3</sub>SnH/Et<sub>3</sub>B/O<sub>2</sub> (**Ionic Reduction Mechanism 1**). It can be *ruled out* on the basis of the log A data reported here, our prior stannylvinyl radical EPR spectroscopy,<sup>3d</sup> and by our unsuccessful cation capture studies when **1** was hydrostannated in THF:H<sub>2</sub>O (4:1).<sup>3b,c</sup>

**Background.** In the stannylvinyl cation mechanistic theory of alkyne hydrostannation with tin hydrides and radical initiators,<sup>6</sup> it is postulated<sup>6a-d</sup> that a **non-coordinatively controlled, non-regioselective**, addition of a tin radical occurs at either alkyne carbon of propargylically-oxygenated dialkyl acetylene substrates. As applied to **1**, this would require that a mixture of the stannylvinyl radicals **19** and **2a** is formed (Scheme 5), which would then engage in a fast “outer sphere” single electron transfer (SET) with O<sub>2</sub>, to initially provide the solvent-caged contact ion pairs **20** and **21**. To arrive at **4a**, the theory<sup>6</sup> then demands that the less inductively stable of these two solvated stannylvinyl cation ion pairs, **20**, will undergo a fast, 1,2-tributylstannyll shift to produce the solvent-caged contact ion pair **21** *virtually exclusively*, which would then solvatively separate into its constituent ions, before engaging in cationic reduction either by the two-step **Ionic Reduction Mechanism 1** of Scheme 5, or by the one-step **Ionic Reduction Mechanism 2** of Scheme 6 (see page 33 of this SI).

**Ionic Reduction Mechanism 1.** Given that Sherrod and Bergman,<sup>30</sup> and Hanack<sup>31</sup> have both noted that  $\alpha$ -cyclopropylvinyl cations generated from 1-cyclopropyl-1-iodoalkenes do not willingly undergo cyclopropane ring-opening under solvolytic conditions, one can reasonably assume that the transition of **21** into **22** would be rate-determining, if the **Ionic Reduction Mechanism 1** of Scheme 5 prevailed.

If one accepts this key tenet, then in the **non-polar** solvent **PhMe**, one would expect a cationic unimolecular ring-opening of this sort to be associated with significant solvent electrostriction, and a massive loss in translational entropy, as the solvated contact ion pair **21** attempted to transit into the activated reaction complex that would produce **22**.

In such a mechanism, a solvent-induced dissociation of the peroxide anion away from the newly formed stannylvinyl cation of **21** would almost certainly be a requirement, to unmask the strong positive charge on the vinylic carbon, needed for the key fissive ring-opening event to effectively proceed.

However, given the very low dielectric constant of PhMe ( $\epsilon = 2.38$ ), it is hard to imagine how such a solvent could ever bring about such an effective charge separation, or solvatively stabilise the developing activated complex needed to induce cyclopropane ring-opening to give **22**. Rather, a polar activated complex of this sort would initially repel PhMe.

In fact, if initial electroneutrality already prevailed within the solvated contact ion pair form of **21** in PhMe, there would have to be significant solvent intercalation and massive bulk solvent reorganisation, to enable a full charge separation of that ion pair to occur. Only then could a stannylvinyl cation of sufficient electrophilicity be unmasked, to allow the requisite activated complex to satisfactorily form to enable the cyclopropane ring-opening to proceed (Scheme 5).

In our considered opinion, such a solvent-induced ionic charge separation would simply not be feasible in non-polar PhMe, due to the extremely strong attractive forces that would exist between the two oppositely charged ions in that solvent, as estimated by Coulomb's Law.

According to Kreevoy<sup>32</sup> and Dill,<sup>33</sup> the electric field/force lines of two oppositely charged ions always penetrate very deeply into non-polar reaction solvents of low dielectric constant; much more so than they ever do in solvents of high dielectric constant like H<sub>2</sub>O ( $\epsilon = 78.54$ ). Indeed in PhMe, the electric field associated with two oppositely charged ions is so enormous that it would likely extend over a distance of some 210 Å (21 nm); the so-called Bjerrum length,<sup>33-35</sup> which corresponds to the distance at which the Coulombic energy of attraction of one mole of ion pairs is equal to the thermal energy  $RT$  required to separate them.<sup>33</sup>

**How the Attractive Electrostatic Interaction Energy ( $F$ ) Between Two Oppositely Charged Ions is Affected by the Solvent Medium and the Bjerrum Length ( $L_{Bjerrum}$ )**

$$L_{Bjerrum} = \frac{k_e e^2 N_{Avogadro}}{\epsilon_{\text{Medium}} RT}$$

Thus, for PhMe ( $\epsilon_{\text{Medium}} = 2.38$ ) at a T = 333 K

$$L_{Bjerrum \text{ PhMe}} = \frac{1.386 \times 10^{-4} \text{ J m mol}^{-1}}{2.38 \times 8.314 \text{ J mol}^{-1} \text{ K}^{-1} \times 333 \text{ K}}$$

$$L_{Bjerrum \text{ PhMe}} = \frac{1.386 \times 10^{-4} \text{ J m mol}^{-1}}{6589.178 \text{ J mol}^{-1}} = 210.3 \text{ \AA}$$

where

$k_e$  = the Coulomb or Electric Force Constant =  $1/4\pi\epsilon_0$

$e = q_1 = q_2 = e$  = charge on an electron =  $-1.6 \times 10^{-19} \text{ C}$

$N_{Avogadro}$  = Avogadro's Number =  $6.02214 \times 10^{23}$

$\epsilon_{\text{Medium}}$  = Medium Dielectric Constant

$R$  = Gas Constant =  $8.314 \text{ J mol}^{-1} \text{ K}^{-1}$

$T$  = Temperature in K and

$$k_e e^2 N_{Avogadro} = \frac{e^2 N_{Avogadro}}{4\pi\epsilon_0} = 1.386 \times 10^{-4} \text{ J m mol}^{-1}$$

where

$\epsilon_0 = 8.85 \times 10^{-12} \text{ C}^2 \text{ J}^{-1} \text{ m}^{-1}$  = the permittivity of a vacuum

$4\pi = 12.568$

Since the Electrostatic Interaction Energy  $F = \frac{L_{Bjerrum}}{r} \times RT$  where  $r$  is the ion separation distance, it follows that for two oppositely charged ions separated by 2.81 Å in PhMe, the Electrostatic Interaction Energy  $F = 49.52 \text{ kcal mol}^{-1}$  and  $F = 46.39 \text{ kcal mol}^{-1}$  when they are separated by 3.0 Å

$$F_{333 \text{ K}} = \frac{210.3 \text{ \AA}}{2.81 \text{ \AA}} \times 8.314 \text{ J mol}^{-1} \text{ K}^{-1} \times 333 \text{ K} = \frac{207.2 \text{ kJ mol}^{-1}}{4.184} = 49.52 \text{ kcal mol}^{-1}$$

$$F_{333 \text{ K}} = \frac{210.3 \text{ \AA}}{3.0 \text{ \AA}} \times 8.314 \text{ J mol}^{-1} \text{ K}^{-1} \times 333 \text{ K} = \frac{194.1 \text{ kJ mol}^{-1}}{4.184} = 46.39 \text{ kcal mol}^{-1}$$

It further transpires that the Coulombic energy of attraction  $F$  between two oppositely charged ions in an ion pair depends upon the distance between them, and would be of the order of +50.6 kcal mol<sup>-1</sup> if they were only 2.75 Å apart in PhMe at 333 K. This value does, however, change to +49.52 kcal mol<sup>-1</sup> at 2.81 Å separation and *ca.* +46.39 kcal mol<sup>-1</sup> at a 3.0 Å separation. Given that such high energies of attraction will always exist at such short ion separations in non-polar PhMe, it seems most unlikely that any solvent-mediated ion pair separation would ever be achievable in this solvent at such a temperature, unless the SET event involved long-range electron tunnelling; evidence for which has not been provided by the stannylvinyl cation-originating team,<sup>6</sup> in their published mechanistic work. Moreover, while we recognise that  $F$  calculations of this sort do *rather simplistically* treat the ions of an ion pair as rigid hard spheres, even so, they do give a very good idea of the separation energy  $F$  and the overall energy input needed to bring about a complete ion dissociation in PhMe, notwithstanding such calculations ignoring dipole-dipole, dipole-quadrupole, and quadrupole-quadrupole type interactions.

Interestingly enough, the +50.6 kcal mol<sup>-1</sup> energy input that we have calculated would be necessary to bring about a full ion separation of a typical contact ion pair in PhMe at 333 K, from an initial inter ion distance of 2.75 Å, accords very well with Alabugin's polarisable continuum model (PCM)-based calculation<sup>17a</sup> for the energy input ( $\Delta E = +50.5$  kcal mol<sup>-1</sup>) required for trimethylstannylvinyl radical electron transfer to O<sub>2</sub> in PhMe at 110 °C, with accompanying formation of a separated solvated trimethylstannylvinyl cation superoxide anion ion pair.

Significantly, Alabugin's computational calculations<sup>17a</sup> confirmed that the energy input needed to induce formation of such a solvent separated ion pair would be far too high to allow that type of entity to ever readily form at temperatures of between 60 and 110 °C in PhMe, and the fact that our own  $F$  calculations have shown that a similar energy input would be needed to effect a contact ion pair ion separation in PhMe again indicates that the latter process would be equally energetically unfeasible in the **21** system.

It is also important to point out that any ion pairs, generated in a non-polar solvent medium like PhMe, would almost certainly cause considerable polarisation of the solvent in all of those regions of the solvent that became subject to their respective electric fields during ion separation. The resulting ion pair/solvent dipolar forces would then rapidly disperse through the bulk medium, to

greatly restrict the random movements of all those solvent molecules that fell within the zones of those electric fields, which, given the huge 210 Å Bjerrum length<sup>33</sup> of two oppositely charged ions in PhMe, would likely be a great many in number. This effect would also be multi-directional in its nature due to the random movement of the putative ion pairs and reagent diffusion.

One of the main manifestations of this would obviously be a very severe restriction of the mobility of all solvent molecules in the immediate vicinity of any putative developing charged activated complexes derived from **21** *en route* to **22** (a process known as electrostriction). Such charge development and solvent shell immobilisation would almost certainly NOT be associated with a high log A value, nor a strongly positive  $\Delta S^\ddagger$  but, instead, with a much lower log A, and a large negative  $\Delta S^\ddagger$ .<sup>2a,32</sup>

It will thus be appreciated that the strongly positive  $\Delta S^\ddagger_{333\text{ K}}$  of +32.09 J K<sup>-1</sup> mol<sup>-1</sup> (+7.67 e.u.) that we have seen in the overall **2a**→**4a** transition *in PhMe* is NOT what one would normally expect to see for a genuinely cationic reaction pathway in which the rate-determining step was the unimolecular heterolytic ring-cleavage of solvent separated **21** to give **22**.

To illustrate this point still further, we draw very specific attention to the fact that most S<sub>N</sub>1 reactions generally have large **negative** entropies of activation associated with them when organic solvents are the main or exclusive reaction medium, notwithstanding entropically-favourable unimolecular bond-heterolysis occurring. This is due, primarily, to the substantial solvent reordering that is always required to achieve heterolysis in pure organic solvents,<sup>32</sup> or even aqueous binary organic solvent mixtures, when H<sub>2</sub>O is present as only the minor solvent component.

Additionally, many pure, low polarity, organic solvents like PhMe or benzene do not have the ability to form multiple H-bonds, to favourably dissipate negative anionic charge through complexation, which further hampers their ability to mediate ion pair formation and ion separation.

Thus, Fainberg and Winstein<sup>36</sup> found that *t*-BuCl underwent hydrolysis in 3:2 EtOH: H<sub>2</sub>O with a  $\Delta S^\ddagger$  of -15.5 J K<sup>-1</sup> mol<sup>-1</sup> (-3.7 e.u.), and they noted that this  $\Delta S^\ddagger$  value decreased to -27.6 J K<sup>-1</sup> mol<sup>-1</sup> (-6.6

e.u.) as the EtOH constituency increased to 4:1 EtOH:H<sub>2</sub>O. Hughes and Cooper<sup>37</sup> likewise observed a log A of 11.89 at 25 °C in 4:1 EtOH: H<sub>2</sub>O, which translated into a  $\Delta S^\ddagger$  of -25.6 J K<sup>-1</sup> mol<sup>-1</sup> (-6.12 e.u.) for this heterolysis, which is in broad agreement with the Fainberg-Winstein  $\Delta S^\ddagger$  determination that was reported subsequently.<sup>36</sup> These recorded values of  $\Delta S^\ddagger$  are despite the  $L_{\text{Bjerrum}}$  of two oppositely charged ions being just 15.66 Å in 4:1 EtOH:H<sub>2</sub>O (w/w) ( $\epsilon = 35.72$  at 298 K) and the  $F$  value being approximately +3.3 kcal mol<sup>-1</sup> at 2.81 Å ion separation, which emphasises that it is not just electrostatic attractions and Field Effects that are dominating the magnitudes of the  $\Delta S^\ddagger$  values of reactions that involve the formation of ion pairs. In entirely analogous fashion, the S<sub>N</sub>1 hydrolysis of *t*-BuCl in 3:2 dioxane:H<sub>2</sub>O was associated with a substantial negative  $\Delta S^\ddagger$  of -29.29 J K<sup>-1</sup> mol<sup>-1</sup> (-7.0 e.u.).<sup>36</sup> It will thus be appreciated that for S<sub>N</sub>1 reactions in binary solvent mixtures, and less polar solvents with large molecular masses, the processes of polar bond heterolysis are generally associated with much greater degrees of solvent reorientation and entropy loss, whenever those activated reaction complexes are attempting to form.

Only when neat 100% H<sub>2</sub>O was used for the *t*-BuCl hydrolysis performed at 25 °C did Fainberg and Weinstein<sup>36</sup> observe that it reacted with a large positive  $\Delta S^\ddagger$  of +51.04 J K<sup>-1</sup> mol<sup>-1</sup> (+12.2 e.u.).

This ability of H<sub>2</sub>O to essentially non-electrostrictively surround and stabilise a polar activated complex that is transitioning into an intimate ion pair is unique, for it allows for much more facile charge separation in the developing ion pair transition state, which can now become considerably looser and more entropically-free (and product-like) as measured by the large positive overall  $\Delta S^\ddagger$ .

Another way of thinking about such reactions is as follows. Whenever pure H<sub>2</sub>O is employed as the reaction solvent for the S<sub>N</sub>1 solvolysis of a *tert*-alkyl halide, due to its very high dielectric constant ( $\epsilon = 78.54$ ), this lowers the Bjerrum length between the two newly emerging oppositely charged ions to just 7.12 Å at 298 K, which means that the Coulombic energy of attraction  $F$  between the two ions is now a mere +1.5 kcal mol<sup>-1</sup> when those ions are just 2.81 Å apart, which is negligible. Such a weak attractive interaction is relatively easy to thermally disrupt. This contrasts very profoundly, however, with the Coulombic energy of attraction  $F$  that exists between two such oppositely charged ions in PhMe at 3 Å separation, where the  $F$  can now be estimated to be approximately +46.39 kcal mol<sup>-1</sup> at 333 K; a value so large that it effectively prohibits facile ion separation from ever occurring in that solvent at that temperature.

In essence, because of the very high dielectric constant of H<sub>2</sub>O ( $\epsilon = 78.54$ ), when it solvates a nascent activated complex of a *tert*-alkyl halide that is separating into two oppositely charged ions, the super-efficient solvation that occurs serves to completely ablate the huge Coulombic attractive forces that would otherwise confound and prohibit heterolytic bond fission in a much lower dielectric solvent such as PhMe.

This greatly enhanced ability of H<sub>2</sub>O to more effectively solvate and promote the transition of a neutral dipolar molecule into the loose polar activated complex needed to undergo full heterolysis is thus not associated with the severe electrostriction that is often seen in organic solvents, or the binary solvent mixtures in which they predominate, and this property helps to explain the huge positive increase in the  $\Delta S^\ddagger$  that was seen by Fainberg and Winstein<sup>36</sup> during the hydrolysis of *t*-BuCl in 100% H<sub>2</sub>O.

Basically, pure organic solvents and aqueous organic solvent mixtures always have much lower dielectric constants than pure H<sub>2</sub>O itself, and this inevitably increases the Bjerrum lengths<sup>33-35</sup> that are associated with any developing activated complexes that are attempting to transit into ion pairs in those solvent media. This, in turn, leads to greatly increased solvent electrostriction and significantly decreased solvent movement<sup>34</sup> in the vicinity of the polar activated complex itself, as well as far beyond it. Such factors thus serve to make reactions that involve ion separation far harder to achieve in low polarity solvents. This is why solvolyses of tertiary alkyl halides are typically associated with substantive negative  $\Delta S^\ddagger$  values in solvents that are primarily organic in their nature, but these are not the sole factors that determine outcome (*vide infra*).

In full agreement with these observations, Moelwyn-Hughes and Biordi<sup>38</sup> recorded a negative  $\Delta S^\ddagger$  of -15.73 J K<sup>-1</sup> mol<sup>-1</sup> (-3.76 e.u.) for the solvolysis of *t*-BuCl in neat dry MeOH ( $\epsilon = 32.7$ ) at 25 °C, while Fainberg and Winstein<sup>36</sup> recorded a  $\Delta S^\ddagger$  of -3.1 e.u. (-12.97 J K<sup>-1</sup> mol<sup>-1</sup>) for this same solvolysis in MeOH. Cowie and coworkers<sup>39</sup> also found that *t*-BuBr underwent hydrolysis in 70% Me<sub>2</sub>CO:30% H<sub>2</sub>O with a  $\Delta S^\ddagger$  of -42.68 J K<sup>-1</sup> mol<sup>-1</sup> (-10.2 e.u.) at 50 °C. Acetone has an  $\epsilon = 21$ .

Analogously, Sherrod and Bergman<sup>30</sup> observed a large negative  $\Delta S^\ddagger$  of between -88.70 and -83.68 J K<sup>-1</sup> mol<sup>-1</sup> (-21.2 and -20.0 e.u.) for the high temperature S<sub>N</sub>1 solvolysis of 1-cyclopropyl-1-iodoethylene with 1 equiv of Et<sub>3</sub>N in MeOH, which proceeds via an  $\alpha$ -cyclopropyl-vinyl cation.

The key point being made here is that, typically, the formation of solvated charged contact ion pairs, or solvent-separated ion pairs, is highly entropically disfavoured in solvents of low-polarity such as PhMe, due to the huge field effects and flux lines that inevitably arise, which require massive solvent reorganisation to occur, which inevitably translates into large negative  $\Delta S^\ddagger$  values being seen for most such reactions, and accompanying log A values that fall well below 13.

A similar entropically unfavourable solvent reorganisation would almost certainly be required for any cyclopropane ring-opening event that involved the solvated contact ion pair **21** *in non-polar PhMe*. It would thus be extremely unlikely that such an electronically-destabilised activated ring-opening complex would ever willingly form from the electroneutral solvated contact ion pair **21** in that solvent. We also doubt that any of the solvent separated ion pairs **21** or **22** would ever readily form in the mechanistic pathway to **4a** from the stannylyvinyl radical **2a**.

In our view, the log A of 14.951 that was recorded for the ring-opening of stannylyvinyl radical **2a** in PhMe at 333 K, and its accompanying  $\Delta S^\ddagger$  of +32.09 J K<sup>-1</sup> mol<sup>-1</sup> (+7.67 e.u.), are totally incompatible with **Ionic Reduction Mechanism 1** (Scheme 5) being the source of **4a**. Nor does this log A support the idea that a stannylyvinyl cation-containing ion pair<sup>6</sup> more generally is forming in the non-polar solvent PhMe under our O-directed free radical hydrostannation conditions,<sup>3</sup> contrary to the experimentally unsupported assertions of those who advance the stannylyvinyl cationic theory.<sup>6</sup>

*It is a log A value that only mechanistically aligns with the “electrically neutral”, unimolecular, homolytic ring cleavage process shown in Scheme 4 being the r.d.s for this reaction in PhMe.*<sup>3b,c</sup>

In this very connection, we must highlight here how we have hitherto been unable to trap the putative primary stannylyhomoallenyl cation of the hypothesised contact ion pair **22** with H<sub>2</sub>O,<sup>3b,c</sup> to obtain the corresponding primary alcohol, and we have been equally unsuccessful at trapping the stannylyvinyl cations<sup>6</sup> of the putative ion pairs **20** and **21** with H<sub>2</sub>O, notwithstanding Sherrod and Bergman having readily intercepted such  $\alpha$ -cyclopropyl-stabilised vinyl cations with H<sub>2</sub>O with great ease; these workers having secured  $\alpha$ -cyclopropyl ketones in good yield from such efforts.<sup>30</sup> The fact that Velgraki and Stratakis<sup>40</sup> have also successfully trapped gold-stabilised  $\alpha$ -cyclopropylvinyl cations in 4:1 THF:H<sub>2</sub>O mixtures at rt, further substantiates our claim that **21** and **22** cannot be

intermediates in the pathway where **2a** is converted into **4a**, as would be claimed by proponents of the stannylvinyl cation alkyne hydrostannation theory.<sup>6</sup>

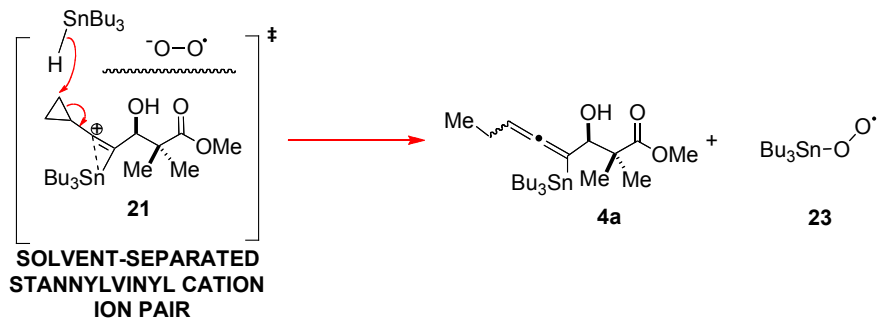
Of great relevance here is the fact that Bergman<sup>30</sup> and Hanack<sup>31</sup> have each independently proposed that the positive charge in secondary  $\alpha$ -cyclopropyl-vinyl cations is very strongly hyperconjugatively stabilised by electron-donation from the cyclopropane ring into the empty carbocation *p*-orbital; provided that this orbital is aligned *syn*- with respect to the two proximal C-C bonds of the cyclopropane ring. This cation-stabilisation effect would thus strongly disfavour spontaneous cyclopropane ring-opening, due to the ring-opened primary carbocation of the new ion pair not enjoying such excellent charge stabilisation, nor any activated complex *en route* to it.

Finally, whenever PhMe or C<sub>6</sub>H<sub>6</sub> have been used as the solvents for any of these O-directed alkyne hydrostannations, never has any product of electrophilic aromatic substitution of the aromatic solvent been encountered.<sup>3</sup> One would surely see such a product if a putative stannylvinyl cation<sup>6</sup> was indeed a genuine intermediate. Naturally this casts further doubt on the stannylvinyl cation mechanistic theory for alkyne hydrostannation<sup>6</sup> under the cat. Et<sub>3</sub>B/O<sub>2</sub>-initiated conditions.

On account of these collective outcomes, **Ionic Reduction Mechanism 1** can effectively be ruled out as playing any role in the transition of **2a**→**4a**.

**Ionic Reduction Mechanism 2.** The alternative **Ionic Reduction Mechanism 2** (Scheme 6) can equally well be discounted for explaining how the **2a**→**4a** conversion proceeds. This is because such a bimolecular “associative” “S<sub>N</sub>2”-type ionic reduction of the stannylvinyl cation in **21** would lead to a considerable loss in translational entropy during the key “rate-determining” reductive ring-cleavage step. In fact, a bimolecular r.d.s of this sort would typically be associated with a much lower log A of 5-11, and a strongly negative entropy of activation<sup>2</sup> due to the massive decrease in translational entropy that would inevitably accompany formation of the solvated, charged, bimolecular activated complex in PhMe, and the strict requirements for correct orbital overlap and alignment to form the partial bonds of the activated reaction complex that would lead to stannyllallene **4a**.

**Ionic Reduction Mechanism 2**

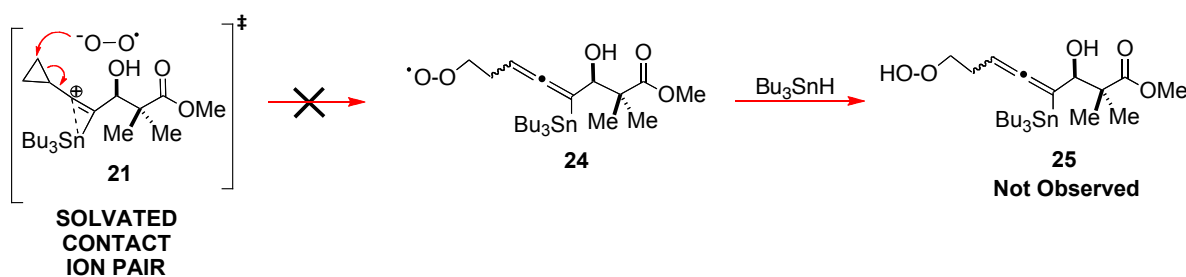


**Scheme 6. Ionic Reduction Mechanism 2**, proceeding via **21** (solvent-separated), would be incompatible with the high log A value of 14.951 observed for the conversion of **2a** into **4a**, due to the highly associative bimolecular nature of the solvated activated complex that would need to form, the requisite tin-stabilisation of the cation, and the substantial solvent reorganisation that would likely be required to separate the initially formed electroneutral contact ion pair into the solvent-separated charged ion pair needed to initiate such an S<sub>N</sub>2-type ionic reduction event. Like **Ionic Reduction Mechanism 1**, **Ionic Reduction Mechanism 2**<sup>6</sup> can effectively be ruled out and considered mechanistically unviable<sup>6</sup> on the basis of the log A and the positive ΔS<sup>‡</sup> data<sup>2</sup> at hand.

Entropically unfavourable, solvent-mediated, contact ion pair separation of electrically neutral **21** would also likely be a key requirement for the aforementioned **Ionic Reduction Mechanism 2** to proceed in non-polar PhMe. Clearly, such an electrostrictive charge separation would be a necessity to unmask the full positive charge on the vinylic cation component of **21** to facilitate the aforementioned “S<sub>N</sub>2” ionic reduction event. Like the concerted bimolecular reduction itself, such electrostrictive behaviour would once more be associated with a large negative ΔS<sup>‡</sup> in PhMe. On these grounds, this mechanistic thesis can equally well be rejected.

**Further Comments.** It is also difficult to imagine how any charged contact ion-pair such as **21** would not immediately self-react to some significant degree in PhMe to give **24** and thereafter **25** (Scheme 7), given the fact that the newly created superoxide anion would be negatively charged and far more nucleophilic than its neutral tri-n-butylin hydride counterpart. The fact also that it would be sitting right at the heart of the solvated ion pair cage of **21** would seemingly mandate this.

Moreover, primary alkyl hydroperoxides are readily synthesised by direct S<sub>N</sub>2 displacement of alkyl bromides with 2 equiv of aq. H<sub>2</sub>O<sub>2</sub> in the presence of CF<sub>3</sub>CO<sub>2</sub>Ag, and they are not unduly unstable under neutral conditions, having previously been prepared and isolated by Davies and Roberts.<sup>41</sup> Yet, there was no sign of any hydroperoxide products such as **25** (or derivatives thereof) in the hydrostannation of **1** in PhMe (Scheme 7).



**Scheme 7.** Hydroperoxide products such as **25** were never seen in our free radical hydrostannations of **1**. If **Ionic Reduction Mechanism 2** was genuinely operative, one might see such products co-formed.

The presence of a nucleophilic hydroxy within the cationic component of ion pair **21** would provide yet another pathway for self-reaction, if such an ionic intermediate<sup>6</sup> was indeed genuinely forming in PhMe. Again, however, we saw no evidence for the formation of ether-type products in our hydrostannation of **1**, which further argues against the intermediacy of a stannylvinyl cation<sup>6</sup> in these O-directed dialkylacetylene free radical hydrostannations.<sup>3,4,17-19</sup>

Therefore, on the basis of us investigating this mechanistic problem in a manifold way,<sup>28a</sup> using a wide variety of experimental techniques, we have been able to firmly rule out the existence of stannylvinyl cations<sup>6</sup> in alkyne hydrostannation reactions mediated by tin hydrides under the cat. Et<sub>3</sub>B/O<sub>2</sub> (or AIBN) initiated conditions, in both PhMe and in other solvents that include THF/H<sub>2</sub>O.<sup>3</sup>

Some of those aforementioned experimental techniques have included EPR spectroscopy<sup>3d</sup> to characterise the triphenylstannylvinyl radicals of some of these O-directed dialkyl acetylene free radical hydrostannation reactions with Ph<sub>3</sub>SnH/cat. Et<sub>3</sub>B in PhMe. The fact that the shortest timescale of EPR spectroscopy is of the order of microseconds, yet we have been able to routinely observe triphenylstannylvinyl radicals for prolonged periods at temperatures of between -50 °C

and -10 °C in the presence of O<sub>2</sub>,<sup>3d</sup> only helps to further confirm that the hypothesised<sup>6</sup> single electron transfer event involving O<sub>2</sub> ***is NOT occurring*** as stated in the various iterations of the stannylvinyl cation mechanistic theory that have so far appeared.<sup>6</sup>

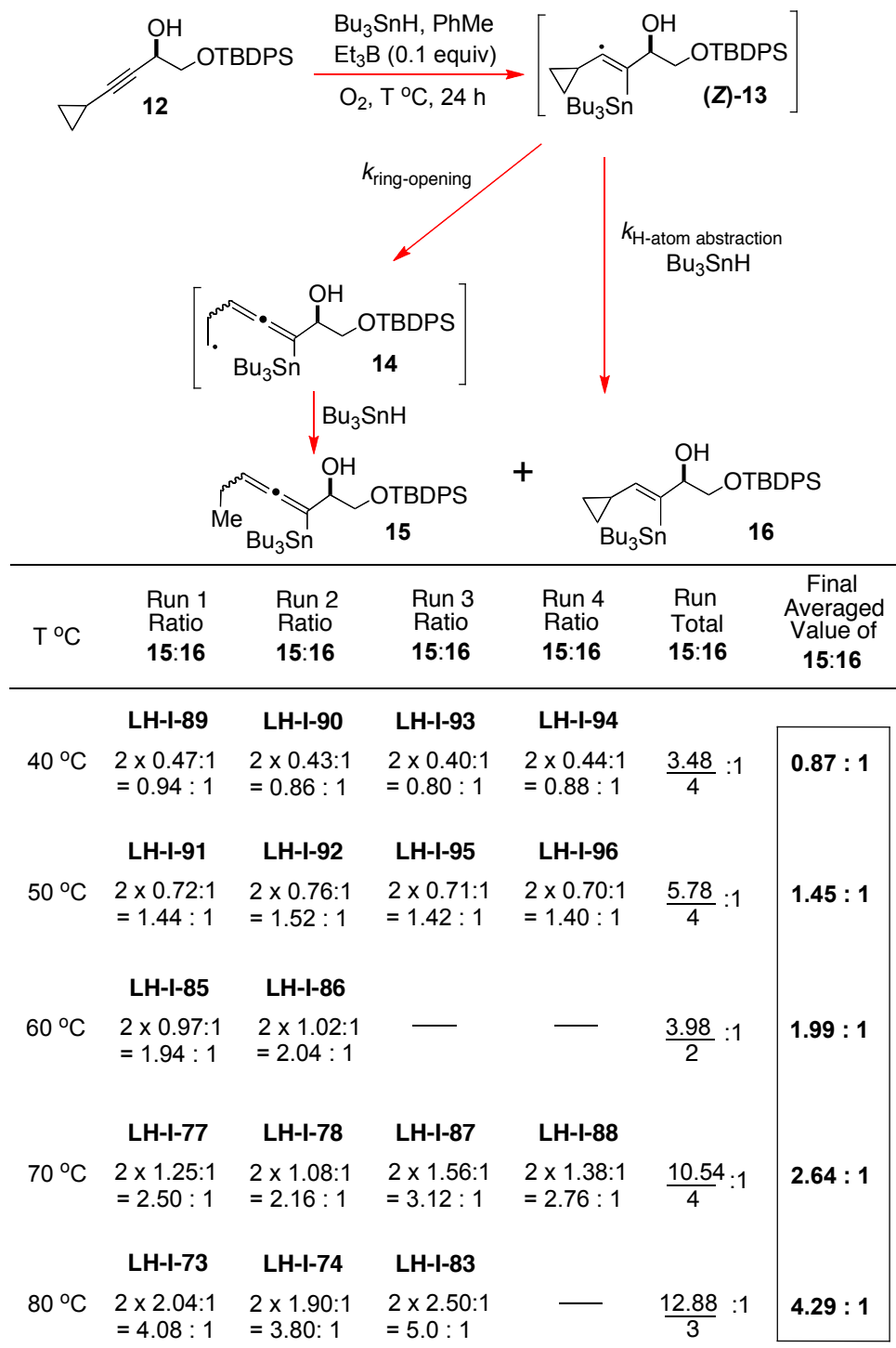
The above EPR work<sup>3d</sup> has also unambiguously confirmed that it is “O-directed” triphenylstannylvinyl radicals that are primarily being formed in these reactions and, this very fact, has allowed us to confidently ***restate*** that this process is indeed predominantly O-directed<sup>3a,17-19,42</sup> under the standard, reasonably concentrated, experimental reaction conditions that we<sup>3</sup> and others<sup>6,16-19,42</sup> typically use to run such free radical hydrostannation reactions. This counters other experimentally-unsupported proposals,<sup>6,16</sup> *which have not seemingly taken into account the changing regiochemistry<sup>3</sup> that is observed in these tin radical additions as the stannane concentration changes, which clearly rules out exclusive electronic regiocontrol in such propargylically-oxygenated dialkyl acetylene systems at higher stannane concentrations.*

In fact, it almost goes without saying that high stannane concentrations will promote intermolecular O-Sn coordination<sup>3a,17-19</sup> in these hydrostannations, but we will restate this here for the record. For this very reason, we strongly advise that all such processes are always generally conducted at higher stannane concentrations, within the limits of experimental expediency of course.

Finally, Alabugin and his team<sup>17,42</sup> have gone to great lengths to provide very strong and convincing computational support for such a propargyloxy O-Sn radical coordination event beneficially occurring, in their recent NBO calculations and modelling of these O-directed alkyne free radical hydrostannation reactions. They have also shown that such O-coordinated Sn radicals generally always prefer to add to the  $\alpha$ -alkyne carbon, due to this mode of addition giving rise to a significantly lower energy stannylvinyl free radical.<sup>17,41</sup> This powerfully elegant and insightful work by Alabugin and his team<sup>17,42</sup> warrants special commendation, for it has controverted many incorrect mechanistic ideas associated with the stannylvinyl cation theory,<sup>6a-d</sup> and it has very strongly supported not just our own 2005 experimental contributions to the O-directed disubstituted acetylene free radical hydrostannation area,<sup>3,4</sup> but also those excellent experimental contributions from the Alabugin laboratory themselves.<sup>17,42</sup> It has additionally confirmed the earlier O-directed assertions of the Taddei/Nativi<sup>18</sup> and Geilen/Willem<sup>19</sup> laboratories beforehand.

**Part 2. An Estimate of the  $k_{\text{ring-opening}}$  of the  
Cyclopropane Ring in the Tri-*n*-Butylstannylvinyl  
Radical 13 in PhMe at Different Temperatures and  
the Arrhenius Parameters Derived Therefrom**

**2.1 The Experimentally Determined Average Ratios of 15:16 Obtained from the O-Directed Hydrostannation of 12**



The ratios of **15:16** were numerically determined by  $^1\text{H}$  NMR spectroscopy of the crude concentrated reaction mixture in  $\text{CDCl}_3$ . The latter determination involved a comparison of the numerical integral of the olefinic resonance at  $\delta$  5.55 ppm for the vinyltin product **16** with the corresponding integral for one of the two allenyltin diastereomers of **15**. Specifically, the allenyltin **15** gave rise to two separate allenic proton signals at  $\delta$  4.77 and 4.71 ppm, which were attributable to the two geometric isomers that always formed non-stereoselectively as a 1:1 mixture. The allenic resonance at  $\delta$  4.71 ppm was the one that was typically used to make these ratio comparisons, since this signal was typically unobsured by impurities. However, in some instances, where there was an obvious overlapping impurity, it was found necessary to perform the integration on the  $\delta$  4.77 pm triplet of doublets in order to obtain an accurate quantifying integral value. In either case, it was always necessary to multiply the numerically measured integral for the  $\delta$  4.71 or 4.77 ppm resonance by a factor of 2, to obtain the real ratio of **15:16** formed in each reaction run at the specified temperature. The ratios of **15:16** were then averaged at those specific temperatures (eg. at 40 °C), and it is these averaged ratios that have been used for the various  $k_{\text{ring-opening}}$  determinations shown below for the conversion of **13** into **14** and thence **15** at the various temperatures studied. While at higher temperatures above 70 °C there is an increased ±16-18% variation in the ratios obtained, relative to the averaged ratio, when these reactions are run below 70 °C, the deviations in ratio are much lower and correspond to an overall measurement error that is approximately ± 2.5-8% which, in both cases, is perfectly reasonable for a thermally mediated radical reaction. In fact, variable kinetics are often a hallmark of free radical reactions and such variations are thus to be expected.

## 2.2 The $k_{\text{ring-opening}}$ and Arrhenius Data Obtained for Stannylvinyl Radical 13 and Our Mechanistic Interpretation of That Data

As already indicated:

$$k_{\text{ring-opening}} = [(R)_3SnH] \times k_{\text{H-atom abstraction}} \times \frac{[\text{Allenyltin}]}{[\text{Vinyltin}]} \quad (\text{Eqn 2})$$

Consequentially, using equation 2 and the above averaged ratios of **15:16** obtained at 0.2 M [Bu<sub>3</sub>SnH] in PhMe, the following  $k_{\text{ring-opening}}$  constants and their log  $k_{\text{ring-opening}}$  values were determined for **13** at each temperature specified:

At 313 K:  $k_{\text{ring-opening 13, 313 K}} = [0.2] \times 2.32 \times 10^8 \times 0.87/1 = 4.0368 \times 10^7 \text{ s}^{-1}$ .

At 323 K:  $k_{\text{ring-opening 13, 323 K}} = [0.2] \times 2.51 \times 10^8 \times 1.45/1 = 7.2790 \times 10^7 \text{ s}^{-1}$ .

At 333 K:  $k_{\text{ring-opening 13, 333 K}} = [0.2] \times 2.71 \times 10^8 \times 1.99/1 = 1.07858 \times 10^8 \text{ s}^{-1}$ .

At 343 K:  $k_{\text{ring-opening 13, 343 K}} = [0.2] \times 2.906 \times 10^8 \times 2.64/1 = 1.53437 \times 10^8 \text{ s}^{-1}$ .

At 353 K:  $k_{\text{ring-opening 13, 353 K}} = [0.2] \times 3.106 \times 10^8 \times 4.29/1 = 2.66495 \times 10^8 \text{ s}^{-1}$ .

The corresponding 1/T values that were used in the same Arrhenius plot are as follows:

$$1/313 \text{ K} = 0.003194888. \quad \log k_{\text{ring-opening 13, 313 K}} = 7.60604.$$

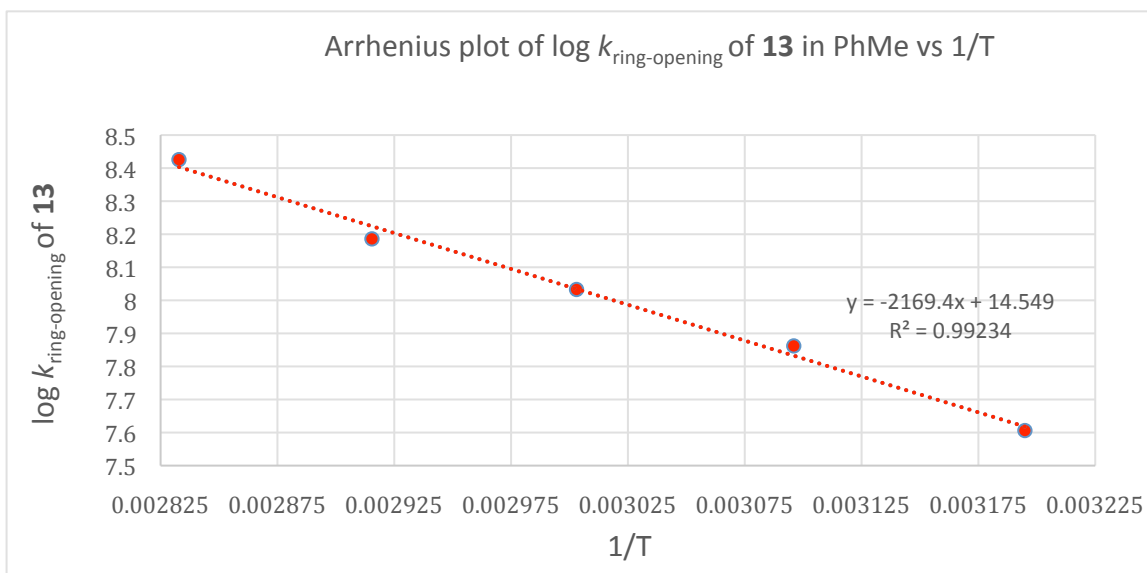
$$1/323 \text{ K} = 0.003096. \quad \log k_{\text{ring-opening 13, 323 K}} = 7.862072.$$

$$1/333 \text{ K} = 0.003003. \quad \log k_{\text{ring-opening 13, 333 K}} = 8.03285.$$

$$1/343 \text{ K} = 0.002915. \quad \log k_{\text{ring-opening 13, 343 K}} = 8.185930.$$

$$1/353 \text{ K} = 0.0028328611. \quad \log k_{\text{ring-opening 13, 353 K}} = 8.425688.$$

The aforementioned  $\log k_{\text{ring-opening}} \text{ of } \mathbf{13}$  values between 313-353 °K were then graphically displayed in the form of an Arrhenius plot ( $\log k_{\text{ring-opening}}$  of **13** v  $1/T$ ) in Excel; this plot is shown below. Importantly, its intercept furnished a  $\log A$  of 14.549, which confirmed an  $E_H1$  radical-induced ring-opening mechanism was again operating. The aforementioned Arrhenius plot also had a slope of -2169.4 and an  $r^2 = 0.99234$ , which indicated a 99.2% quality of data fit.



From that slope, the  $E_a$  was calculated to be  $41537.809 \text{ J mol}^{-1}$  or  $+9.921 \text{ kcal mol}^{-1}$  (i.e.  $9.92 \text{ kcal mol}^{-1}$ ). That  $E_a$  calculation is set out below to show our method.

$$\begin{aligned} \text{From the slope: } E_a \text{ ring-opening } \mathbf{13} &= -(-2169.4) \times 2.303 \times 8.314 \text{ J mol}^{-1} \\ \therefore E_a \text{ ring-opening } \mathbf{13} &= 41537.810 \text{ J mol}^{-1} = 41.5378 \text{ kJ mol}^{-1} \\ \therefore E_a \text{ ring-opening } \mathbf{13} &= 41.5378 \text{ kJ mol}^{-1} (x 0.238846) = +9.921 \text{ kcal mol}^{-1} \end{aligned}$$

This value compares very favourably with the experimentally-derived, two temperature point,  $E_a$  of  $+10.35 \text{ kcal mol}^{-1}$  deduced for the cyclopropane ring-opening of **13** using the logarithmic form ( $\log_{10}$ ) of the Arrhenius equation<sup>2a (page 53)</sup> shown below:

$$\log \frac{[k_2]}{[k_1]} = \frac{E_a}{2.303R} \left[ \frac{T_2 - T_1}{T_1 T_2} \right]$$

which for the  $k_{\text{ring-opening}}$  at 313 and 353 K gives

$$\log \left( \frac{2.66 \times 10^8}{4.04 \times 10^7} \right) = \frac{E_a}{2.303 \times 8.314} \left( \frac{353 - 313}{313 \times 353} \right)$$

which reduces to

$$\log (6.58416) = \frac{E_a}{2.303 \times 8.314} \left( \frac{40}{110489} \right)$$

$$\text{or } 0.81850 = \frac{E_a}{2.303 \times 8.314} \left( \frac{40}{110489} \right)$$

which rearranges to

$$E_a = \frac{0.8185004 \times 2.303 \times 8.314 \times 110489}{40} \text{ J mol}^{-1}$$

$$= +43.289 \text{ kJ mol}^{-1}$$

which when divided by 4.184

gives an  $E_{a \text{ ring-opening}}$  for **13** = +10.35 kcal mol<sup>-1</sup>

This used just two experimentally-determined  $k_{\text{ring-opening}}$  values for **13** at 313 and 353 °K in PhMe to arrive at this calculated value, which is quite close in magnitude to Guo's  $E_{a \text{ ring-opening}}$  **13** of +10.7 kcal mol<sup>-1</sup> shown in Scheme 3 of our main paper.

However, given that our Arrhenius plot had used the five averaged  $k_{\text{ring-opening}}$  of **13** in PhMe data points v 1/T and it had an  $r^2$  value of 0.99224, this value must be considered the more reliable of the two for the determination of the  $E_{a \text{ ring-opening}}$  **13**.

Nonetheless, the close level of agreement between the two  $E_a$  values is most reassuring, notwithstanding the 2 experimental data point calculation being +0.43 kcal mol<sup>-1</sup> higher in magnitude than the  $E_a = +9.92$  kcal mol<sup>-1</sup> figure. Given the much greater degree of accuracy of the  $E_{a \text{ ring-opening}}$  **13** = +9.92 kcal mol<sup>-1</sup> value, we suggest that this is the  $E_a$  value that should be adopted in all future  $k_{\text{ring-opening}}$  calculations involving **13** at different temperatures, and that it be used alongside our experimentally determined log A value of 14.549 in the following Arrhenius expression:  $\log k_{\text{ring-opening}} \text{ } \mathbf{13} = 14.549 - 9.92/2.303RT$ .

With regard to this  $\log A$  of 14.549, it resulted in a  $\Delta S^\ddagger_{333\text{ K}} = +24.39 \text{ J K}^{-1} \text{ mol}^{-1}$  (+5.83 e.u.) being estimated for the ring-opening of **13** at the mean reaction temperature of 333 K (60 °C). This was calculated as follows via the Avery equation<sup>2a</sup> (page 67 of Avery's book):

$$\Delta S^\ddagger_{333\text{ K}} = 8.314 \left[ (2.303 \times 14.549) - 2.303 \log \left( \frac{1.38 \times 10^{-23} \times 333}{6.626 \times 10^{-34}} \right) - 1 \right] \text{ J K}^{-1} \text{ mol}^{-1}$$

$$\Delta S^\ddagger_{333\text{ K}} = 8.314 [33.5063 - 2.303 \log (6.935406 \times 10^{12}) - 1] \text{ J K}^{-1} \text{ mol}^{-1}$$

$$\Delta S^\ddagger_{333\text{ K}} = 8.314 [33.5063 - 2.303 (12.84107) - 1] \text{ J K}^{-1} \text{ mol}^{-1}$$

$$\Delta S^\ddagger_{333\text{ K}} = 8.314 [33.5063 - 29.5730 - 1] \text{ J K}^{-1} \text{ mol}^{-1}$$

$$\Delta S^\ddagger_{333\text{ K}} = 8.314 [33.5063 - 30.5730] \text{ J K}^{-1} \text{ mol}^{-1}$$

$$\Delta S^\ddagger_{333\text{ K}} = 8.314 [+2.933] \text{ J K}^{-1} \text{ mol}^{-1}$$

$$\Delta S^\ddagger_{333\text{ K}} = +24.388 \text{ J K}^{-1} \text{ mol}^{-1}$$

$$\therefore \Delta S^\ddagger_{333\text{ K}} = \frac{+24.388 \text{ J K}^{-1} \text{ mol}^{-1}}{4.184} = +5.83 \text{ e.u.} = +5.83 \text{ cal K}^{-1} \text{ mol}^{-1}$$

It was also reconfirmed by calculation using the Hale and Anslyn/Dougherty<sup>27</sup> simplified  $\Delta S^\ddagger$  equations. Thus:

$$\Delta S^\ddagger_{333\text{ K}} = 19.147 [14.549 - 10.753 - 2.522] \text{ J K}^{-1} \text{ mol}^{-1}$$

$$\Delta S^\ddagger_{333\text{ K}} = 19.147 [1.274] \text{ J K}^{-1} \text{ mol}^{-1}$$

$$\Delta S^\ddagger_{333\text{ K}} = +24.39 \text{ J K}^{-1} \text{ mol}^{-1}$$

$$\Delta S^\ddagger_{333\text{ K}} = 4.576 [14.549 - 10.753 - 2.522] \text{ cal K}^{-1} \text{ mol}^{-1}$$

or e.u.

$$\Delta S^\ddagger_{333\text{ K}} = 4.576 [1.274] \text{ cal K}^{-1} \text{ mol}^{-1}$$

or e.u.

$$\Delta S^\ddagger_{333\text{ K}} = +5.830 \text{ cal K}^{-1} \text{ mol}^{-1}$$

or e.u.  $\times 4.184$

$$\Delta S^\ddagger_{333\text{ K}} = +24.39 \text{ J K}^{-1} \text{ mol}^{-1}$$

Clearly, the high positive magnitude of this  $\Delta S^\ddagger$  value once more confirmed that a non-associative, unimolecular, fissive E<sub>H</sub>1 ring-opening was mechanistically operating in the transition of **13** into the activated complex that ultimately resulted in radical **14** (and thence **15**). This value further reflected the substantial bond-loosening and increase in entropy that was occurring in the activated complex as it was being formed, when compared with its precursor radical **13**. Of course, this activated complex had the choice of either reverting back to **13**, or ultimately eliminatively

transiting into the ring-opened homoallenyl radical **14**, which then could irreversibly H-atom abstract from the stannane via the S<sub>H</sub>2 mechanistic pathway to give **15**. The fact that the frequency factor A of this unimolecular ring-opening of **13** to give **14** is  $3.54 \times 10^{14} \text{ s}^{-1}$ , confirms that a substantial number of these activated complexes have sufficient translational energy to automatically transit into **14** at the mean reaction temperature of 333 K, once the inherent energy barrier has been overcome, and this establishes that this unimolecular process is strongly entropically favourable and has a product-like transition state. A log A = 14.549 most definitely does not align with an associative bimolecular ionic reductive ring-opening of a stannylyvinyl cation intermediate, as would be advocated by some.<sup>6</sup> This log A value is slightly lower than that seen for the **2a**→**3a** transition, possibly because of the greater loss in overall rotational freedom/entropy encountered in going from **13**→**14**. This might be due to **13** having greater rotational freedom at the very outset. However, most importantly, the large positive  $\Delta S^\ddagger_{333 \text{ K}}$  of  $+24.39 \text{ J K}^{-1} \text{ mol}^{-1}$  ( $+5.83 \text{ e.u.}$ ) most definitely rules out a bimolecular ionic reductive ring cleavage of a putative  $\alpha$ -cyclopropyl- $\beta$ -tributylstannylyvinyl cation<sup>6</sup> as having produced **15**, since bimolecular reactions always have negative  $\Delta S^\ddagger$  values.<sup>2</sup> The large positive  $\Delta S^\ddagger_{333 \text{ K}}$  observed also confirmed that little in the way of solvent immobilisation or electrostriction had occurred, which further ruled out a stannylyvinyl cation origin for **15** from the radical **2a**, as would be advocated by some.<sup>6</sup>

From the  $E_a$  of  $41537.809 \text{ J mol}^{-1}$  or  $+9.92 \text{ kcal mol}^{-1}$  that was calculated for the ring-opening of **13** to give **14**, we have been able to estimate a free energy of activation  $\Delta G^\ddagger_{333 \text{ K}}$  for this radical ring opening event in PhMe. This calculation is shown below:

$$\Delta H^\ddagger = E_a - nRT \therefore \Delta H^\ddagger = 41.53781 - \frac{1 \times 8.314 \times 333}{1000} \text{ kJ mol}^{-1}$$

$$\Delta H^\ddagger = 41.53781 - 2.77 = 38.77 \text{ kJ mol}^{-1} = +9.26 \text{ kcal mol}^{-1}$$

$$\text{Since } \Delta G^\ddagger = \Delta H^\ddagger - T\Delta S^\ddagger \therefore \Delta G^\ddagger = 38.77 - \frac{333 \times 24.39}{1000} \text{ kJ mol}^{-1}$$

$$\therefore \Delta G^\ddagger = 38.77 - 8.12 = 30.65 \text{ kJ mol}^{-1} = +7.32 \text{ kcal mol}^{-1}$$

The composite  $\Delta G^\ddagger$  value that we have determined here now puts a numerical figure on the fundamental energy input needed to bring about formation of the activated complex for the unimolecular radical ring-opening of the more rotationally free radical **13** to give **14**, and the relative contributions that the  $\Delta H^\ddagger$  and  $T\Delta S^\ddagger$  terms make to that overall  $\Delta G^\ddagger$ , as **13** transits into the

activated complex that produces **14**. Although endergonic at +7.32 kcal mol<sup>-1</sup>, this experimentally derived value of  $\Delta G^\ddagger_{333\text{ K}}$  is well below the immense Coulombic energy of attraction ( $F = +46.39$  kcal mol<sup>-1</sup>) that would be needed to separate the hypothetical stannylvinyl cation-superoxide anion pair<sup>6</sup> by 3 Å in PhMe, assuming that the hypothetical stannylvinyl cationic theory of reference 6 was invoked to be operating in this instance. Obviously, given the huge  $\Delta G^\ddagger$  input that would be required to effect such an ion pair separation in the non-polar solvent, PhMe, it cannot possibly be proceeding by such a mechanism. In fact, PhMe would only serve to destabilise any developing polar transition state that could bring about cyclopropane bond fission into a stannylhomoadenyl cation, or which involved a direct S<sub>N</sub>2 ionic reduction of a stannylvinyl cation to give **15**. Energetically therefore, one can state with high confidence that such an experimentally determined  $\Delta G^\ddagger$  value of +7.32 kcal mol<sup>-1</sup> is really only compatible with the much lower energy, radical-induced, β-scissive eliminative pathway giving rise to **15** from **13** (see Scheme 2/Table 2). A homolytic ring-opening of **13** to give **14** also more satisfactorily aligns with the Guo calculations of Scheme 3,<sup>22</sup> and all of the other experimental data that has so far been gathered to date in this area, *which collectively supports an exclusively free radical mechanism for these dialkyl acetylene O-directed hydrostannation reactions<sup>43</sup> with both cat. Et<sub>3</sub>B/O<sub>2</sub> and AIBN initiators.<sup>3</sup>*

### 2.3 References

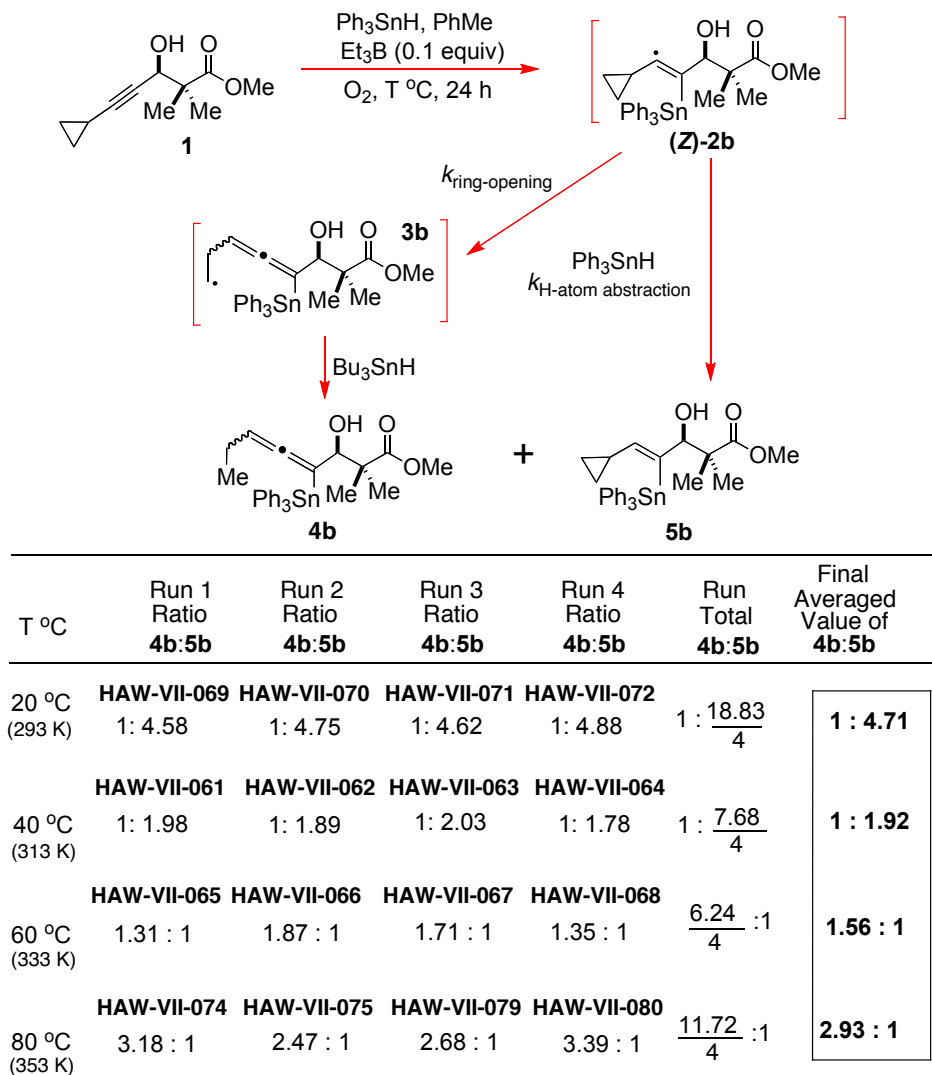
26. W. F. K. Wynne-Jones and H. Eyring, *J. Chem. Phys.*, 1935, **3**, 492.
27. E. V. Anslyn and D. A. Dougherty, *Modern Physical Organic Chemistry*, University Science, Sausalito, CA, 2006, pp. 368.
28. (a) J. F. Bunnett, Chapter VI, The Interpretation of Rate Data, *Technique of Organic Chemistry, Vol. VIII, Part I, Ed. A. Weissberger, Investigation of Rates and Mechanisms of Reactions, Part I*, Eds S. L. Friess, E. S. Lewis, and A. Weissberger, 2<sup>nd</sup> Edn, 1963, 177. (b) See also Jerry March's book for the much more widespread publication of the Bunnett  $\Delta S^\ddagger$  equation with due attribution to Bunnett, who made a major contribution to physical organic chemistry with his initial simplifying rearrangement of the original Eyring-Wynne-Jones-Polanyi equation to give the  $\Delta S^\ddagger$  equation shown. See: J. March, *Advanced Organic Chemistry. Reactions, Mechanism and Structure*, 4<sup>th</sup> Edn. John Wiley & Sons, 1992, pp 225.
29. R. W. Alder, R. Baker, and J. M. Brown, *Mechanism in Organic Chemistry*, John Wiley & Sons, 1971, Chapter 1, Mechanism and Reactivity, pp 1-77 (see page 5 for their  $\Delta S^\ddagger$  equation).
30. (a) S. A. Sherrod, R. G. Bergman, *J. Am. Chem. Soc.*, 1971, **93**, 1925. (b) S. A. Sherrod, R. G. Bergman, *J. Am. Chem. Soc.*, 1969, **91**, 2115.
31. (a) M. Hanack, T. Bassler, *J. Am. Chem. Soc.*, 1969, **91**, 2117. (b) For detailed review on cyclopropyl-stabilized vinyl cations, which discusses the special stability of  $\alpha$ -cyclopropylvinyl cations, see: M. Hanack, *Acc. Chem. Res.*, 1976, **9**, 364.
32. M. M. Kreevoy, Chapter XXIII, Thermodynamics and Reaction Mechanism, *Technique of Organic Chemistry, Vol. VIII, Part II, Ed. A. Weissberger, Investigation of Rates and Mechanisms of Reactions, Part II*, Eds S. L. Friess, E. S. Lewis, and A. Weissberger, 2<sup>nd</sup> Edn, 1963, 1361.
33. K. A. Dill, S. Bromberg and D. Stigter Chapter 20, Coulomb's Law of Electrostatic Forces in *Molecular Driving Forces*, 2<sup>nd</sup> Edn, K. A. Dill and S. Bromberg, Garland Science, Taylor and Francis Group, New York, 2010.
34. (a) N. Bjerrum, *Kgl. Danske Videnskab. Selskab, Math-fys. Medd.*, 1926, **7**, no 9, 1-48 (in German). (b) For an English Language version of the Introductory Survey of this paper, pages 1-17, see: Neils Bjerrum, *Selected Papers*, Chairman of Editorial Committee, Neils Bohr, Einar Munksgaard, Copenhagen, 1949. See page 108 of the PDF of this book at:  
[https://www.royalacademy.dk/Publications/Low/1686\\_Bjerrum,%20Niels.pdf](https://www.royalacademy.dk/Publications/Low/1686_Bjerrum,%20Niels.pdf).

Accessed: 19 June, 2024.

35. R. Moritz, G. Zardalidis, H.-J. Butt, M. Wagner, K. Mullen, and G. Houdas, *Macromolecules*, 2014, **47**, 191.
36. S. Winstein and A. H. Fainberg, *J. Am. Chem. Soc.*, 1957, **79**, 5937.
37. K. A. Cooper and E. D. Hughes, *J. Chem. Soc.*, 1937, 1183.
38. J. Biordi and E. A. Moelwyn-Hughes, *J. Chem. Soc.*, 1962, 4291.
39. G. R. Cowie, H. J. M. Fitches, and G. Kohnstam, *J. Chem. Soc.*, 1963, 1585.
40. G. Velegraki and M. Stratakis, *J. Org. Chem.*, 2013, **78**, 8880.
41. P. G. Cookson, A. G. Davies, and B. P. Roberts, *J. C. S. Chem. Comm.*, 1976, 1022.
42. (a) C. Hu, J. Mena, and I. V. Alabugin, *Nat. Rev. Chem.*, 2023, **7**, 405. (b) A. M. Hughes, G. does Passos Gomes, and I. V. Alabugin, *J. Org. Chem.*, 2019, **84**, 1853.
43. For an excellent new 2024 review on alkyne hydrometallation with Group IV metal hydrides, see the following Book Chapter by: T. Wiesner and M. Haas in *Reference Module in Chemistry, Molecular Sciences and Chemical Engineering*, Elsevier, 2024: <https://doi.org/10.1016/B978-0-323-96025-0.00125-3> (b) For McLaughlan and Roberts' recent highly regiocontrolled PtCl<sub>2</sub>/XPhos-catalysed hydrostannation of terminal aryl acetylenes and propargylic alcohols, see: D. D. Roberts and M. G. McLaughlin, *Adv. Synth. Catal.*, 2023, **365**, 1602. (c) For McLaughlin's recent application of the PtCl<sub>2</sub>/XPhos/Et<sub>3</sub>SiH-catalyst system to the highly regiocontrolled hydroboration of terminal alkyl, aryl and heteroaryl acetylenes with HBPin, see: K. L. E. Hale, D. D. Roberts and M. G. McLaughlin, *Eur. J. Org. Chem.*, 2025, e202401355.

**Part 3. Product Ratio Comparisons For the O-Directed  
Free Radical Hydrostannation of Alkynol 1 with  
 $\text{Ph}_3\text{SnH}$  in PhMe**

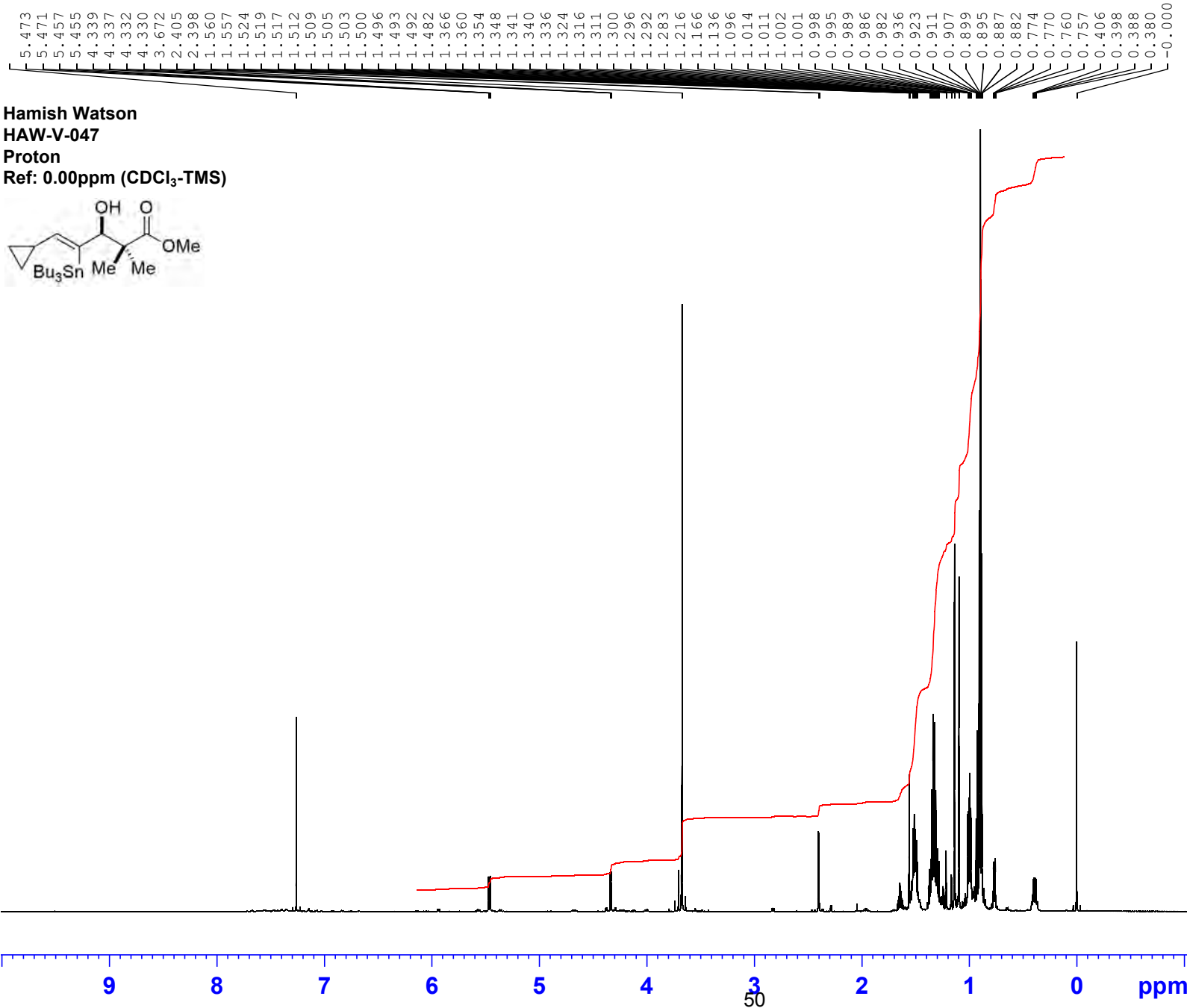
### 3.1 The Experimentally Determined Average Ratios of **4b**:**5b** Obtained from the O-Directed Hydrostannation of **1**



At 20  $^{\circ}\text{C}$  (293 K), from 4 independent reaction runs, the averaged ratio of **4b**:**5b** ( $\text{R} = \text{Ph}$ ) was 1:4.71.

Assuming that the  $k_{\text{H-atom abstraction Ph}_3\text{SnH}}$  value for **2b** is approximately 6.95 faster than the  $k_{\text{H-atom abstraction}}$  for **2a** from  $\text{Bu}_3\text{SnH}$ , this allows one to calculate a tentative  $k_{\text{H-atom abstraction Ph}_3\text{SnH}}$  value for **2b** as  $1.36 \times 10^9 \text{ mol}^{-1} \text{ s}^{-1}$  which, in turn, allows a tentative  $k_{\text{ring-opening}}$  for **2b** in  $\text{PhMe}$  293 K of  $[0.2] \times 1.36 \times 10^9 \times 1/4.71 = 5.77 \times 10^7 \text{ s}^{-1}$  to be estimated.

**Part B. The 600.13 MHz  $^1\text{H}$  NMR and 150.90 MHz  $^{13}\text{C}$  NMR  
Spectra of the Tributylstannylvinyltin 5a and  
Tributylstannylallene 4a in  $\text{CDCl}_3$**



  
**BRUKER**  
 Current Data Parameters  
 NAME HAW-V-Bu<sub>3</sub>Sn\_Probe-(2)\_new  
 EXPNO 10  
 PROCNO 1

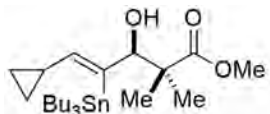
5.560  
 5.557  
 5.555  
 5.473  
 5.471  
 5.457  
 5.455  
 5.438  
 5.373  
 5.371  
 5.368  
 5.367  
 5.356  
 5.355  
 5.352  
 5.350

**Hamish Watson**

HAW-V-047

Proton

Ref: 0.00ppm (CDCl<sub>3</sub>-TMS)



4.381  
 4.374  
 4.372  
 4.339  
 4.337  
 4.332  
 4.330  
 4.297  
 4.295  
 4.293  
 4.288

3.672



Current Data Parameters  
 NAME HAW-V-Bu<sub>3</sub>Sn\_Probe-(2)\_new  
 EXPNO 10  
 PROCNO 1

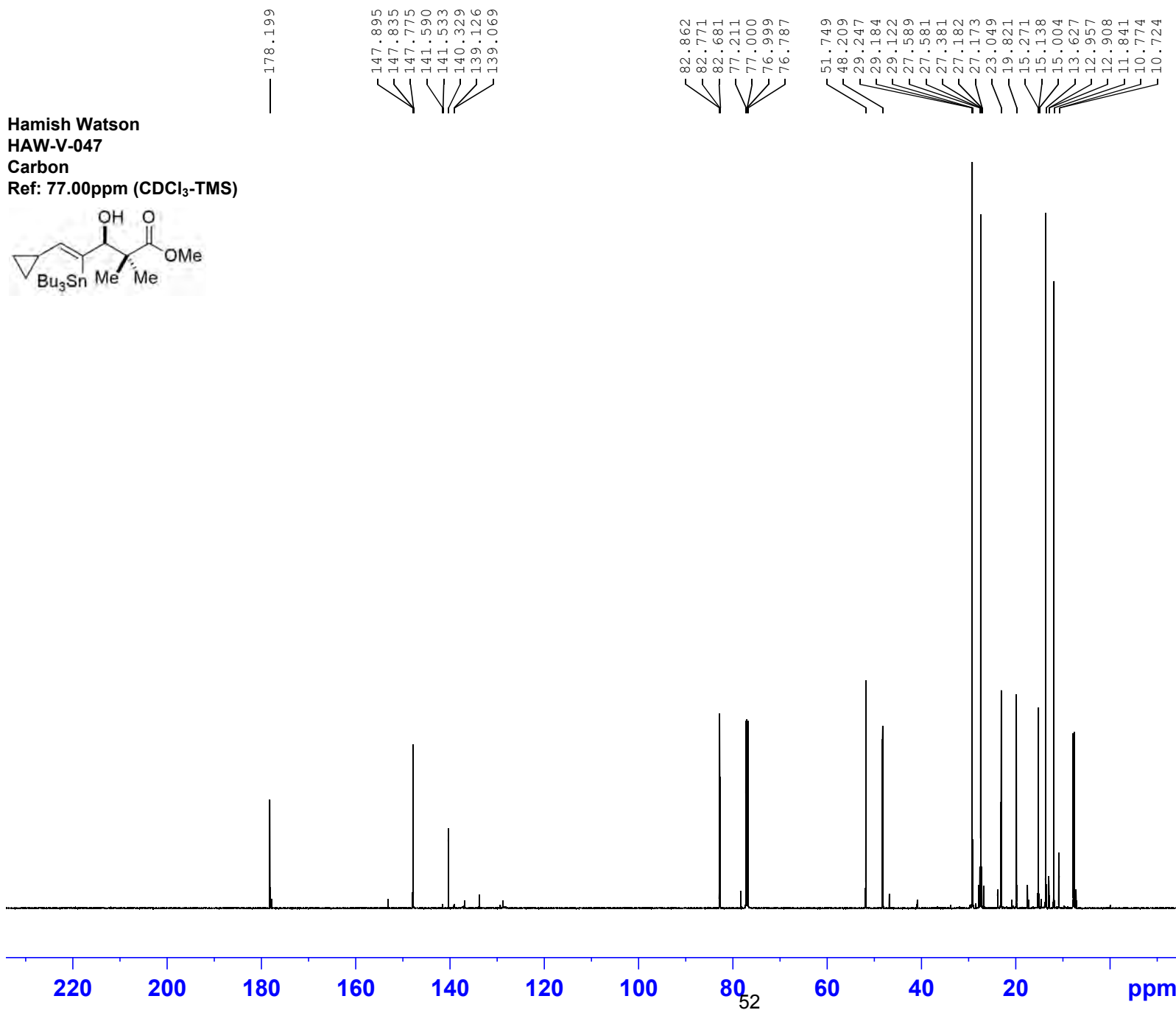
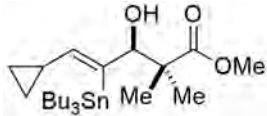
F2 - Acquisition Parameters  
 Date\_ 20181202  
 Time\_ 15.04  
 INSTRUM spect  
 PROBHD 5 mm PABBO BB/  
 PULPROG zg30  
 TD 180286  
 SOLVENT CDCl<sub>3</sub>  
 NS 64  
 DS 0  
 SWH 18028.846 Hz  
 FIDRES 0.100001 Hz  
 AQ 4.9999318 sec  
 RG 97.5  
 DW 27.733 usec  
 DE 7.60 usec  
 TE 300.0 K  
 D1 0.1000000 sec  
 TDO 1

===== CHANNEL f1 ======  
 SFO1 600.1337060 MHz  
 NUC1 1H  
 P1 10.00 usec  
 PLW1 26.60000038 W

F2 - Processing parameters  
 SI 262144  
 SF 600.1300142 MHz  
 WDW EM  
 SSB 0  
 LB 0.10 Hz  
 GB 0  
 PC 1.00

5.6 5.5 5.4 5.3 5.2 5.1 5.0 4.9 4.8 4.7 4.6 4.5 4.4 4.3 4.2 4.1 4.0 3.9 3.8 3.7 ppm

Hamish Watson  
HAW-V-047  
Carbon  
Ref: 77.00ppm (CDCl<sub>3</sub>-TMS)



**BRUKER**

Current Data Parameters  
NAME HAW-V-Bu<sub>3</sub>Sn\_Probe-(2)\_new  
EXPNO 21  
PROCNO 1

F2 - Acquisition Parameters  
Date\_ 20181203  
Time\_ 10.53  
INSTRUM spect  
PROBHD 5 mm PABBO BB/  
PULPROG zgpg30  
TD 119044  
SOLVENT CDCl<sub>3</sub>  
NS 1024  
DS 4  
SWH 37500.000 Hz  
FIDRES 0.315010 Hz  
AQ 1.5872533 sec  
RG 186.92  
DW 13.333 usec  
DE 7.73 usec  
TE 300.0 K  
D1 1.00000000 sec  
D11 0.03000000 sec  
TD0 1

===== CHANNEL f1 ======  
SFO1 150.9194058 MHz  
NUC1 <sup>13</sup>C  
P1 11.80 usec  
PLW1 85.00000000 W

===== CHANNEL f2 ======  
SFO2 600.1324005 MHz  
NUC2 <sup>1</sup>H  
CPDPGR[2] waltz64  
PCPD2 80.00 usec  
PLW2 27.00000000 W  
PLW12 0.43891999 W  
PLW13 0.28090999 W

F2 - Processing parameters  
SI 131072  
SF 150.9028142 MHz  
WDW EM  
SSB 0  
LB 1.00 Hz  
GB 0  
PC 1.40



Current Data Parameters  
NAME HAW-V-Bu<sub>3</sub>Sn\_Probe-(2)\_new  
EXPNO 22  
PROCNO 1

F2 - Acquisition Parameters  
Date\_ 20181203  
Time 11.05  
INSTRUM spect  
PROBHD 5 mm PABBO BB/  
PULPROG deptsp135.b  
TD 119044  
SOLVENT CDCl<sub>3</sub>  
NS 256  
DS 4  
SWH 35714.285 Hz  
FIDRES 0.300009 Hz  
AQ 1.6666160 sec  
RG 186.92  
DW 14.000 usec  
DE 7.44 usec  
TE 300.0 K  
CNST2 145.0000000  
D1 1.00000000 sec  
D2 0.00344828 sec  
D12 0.00002000 sec  
TDO 1

===== CHANNEL f1 =====  
SFO1 150.9178962 MHz  
NUC1 <sup>13</sup>C  
P1 11.80 usec  
P13 2000.00 usec  
PLW0 0 W  
PLW1 85.000000000 W  
SPNAM[5] Crp60comp.4  
SPOAL5 0.500  
SPOFFS5 0 Hz  
SPW5 18.08300018 W

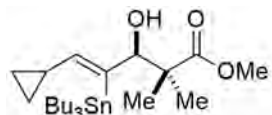
===== CHANNEL f2 =====  
SFO2 600.1324005 MHz  
NUC2 <sup>1</sup>H  
CPDPRG[2] waltz64  
P3 10.20 usec  
P4 20.40 usec  
PCPD2 80.00 usec  
PLW2 27.000000000 W  
PLW12 0.43891999 W

F2 - Processing parameters  
SI 131072  
SF 150.9028142 MHz  
WDW EM  
SSB 0 1.00 Hz  
LB 0  
GB 0  
PC 1.40

Hamish Watson  
HAW-V-047

Dept135

Ref: 77.00ppm (CDCl<sub>3</sub>-TMS)



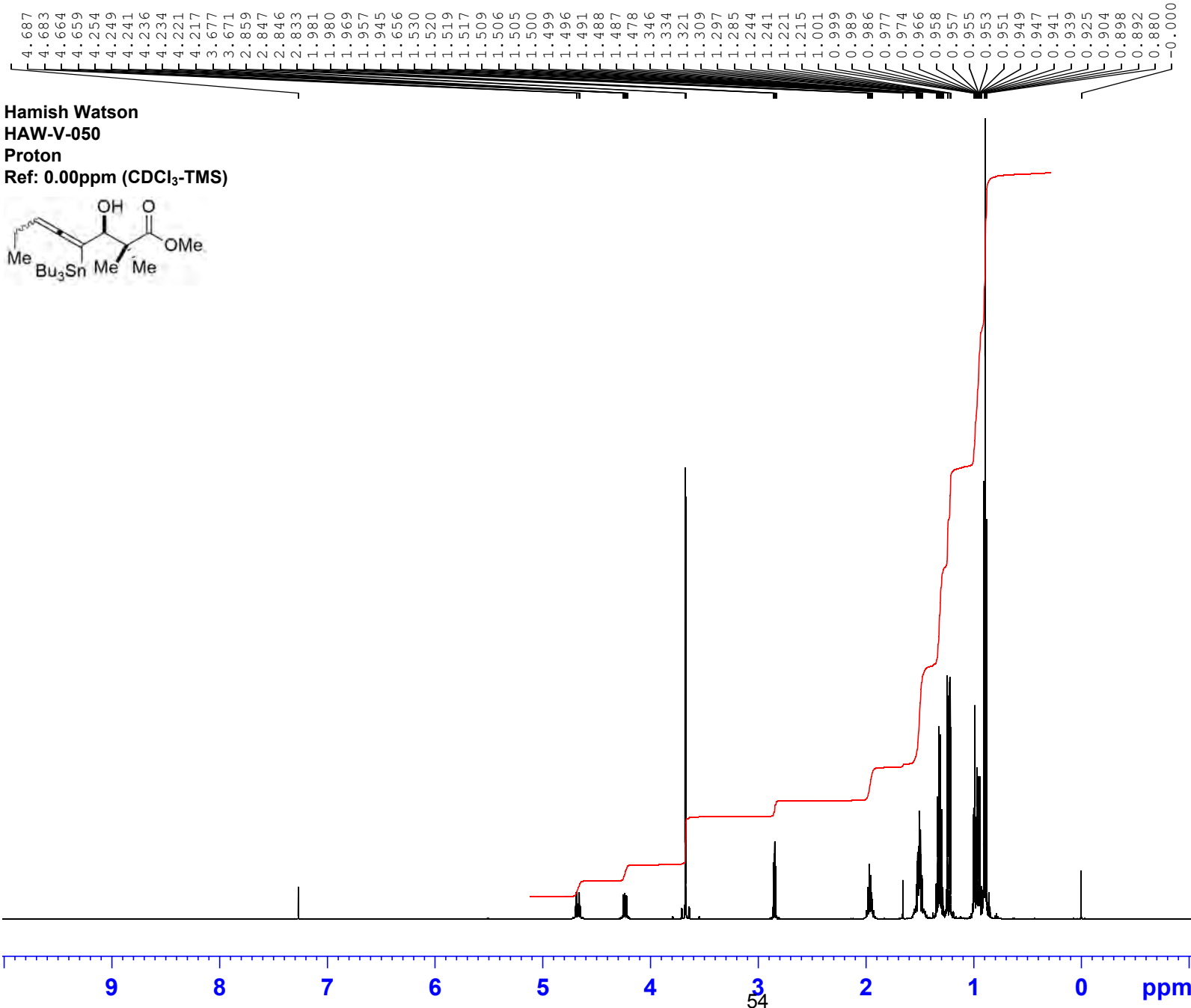
147.836

82.771

51.750

29.188  
27.385  
23.050  
19.820  
15.139  
13.628  
11.840  
7.768  
7.563

200 180 160 140 120 100 80 60 53 40 20 0 ppm

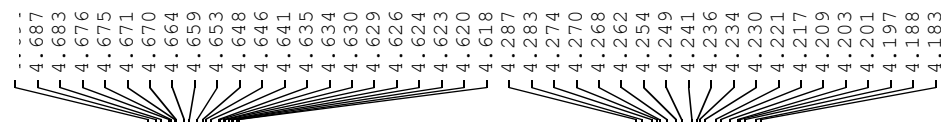


Current Data Parameters  
 NAME HAW-V-Bu3Sn\_Probe-(1)  
 EXPNO 10  
 PROCNO 1

F2 - Acquisition Parameters  
 Date 20181130  
 Time 4.32  
 INSTRUM spect  
 PROBHD 5 mm PABBO BB/  
 PULPROG zg30  
 TD 180286  
 SOLVENT CDCl<sub>3</sub>  
 NS 64  
 DS 0  
 SWH 18028.846 Hz  
 FIDRES 0.100001 Hz  
 AQ 4.9999318 sec  
 RG 22.13  
 DW 27.733 usec  
 DE 7.60 usec  
 TE 300.0 K  
 D1 0.10000000 sec  
 TDO 1

===== CHANNEL f1 ======  
 SFO1 600.1337060 MHz  
 NUC1 1H  
 P1 10.00 usec  
 PLW1 26.60000038 W

F2 - Processing parameters  
 SI 262144  
 SF 600.1300100 MHz  
 WDW EM  
 SSB 0  
 LB 0.10 Hz  
 GB 0  
 PC 1.00

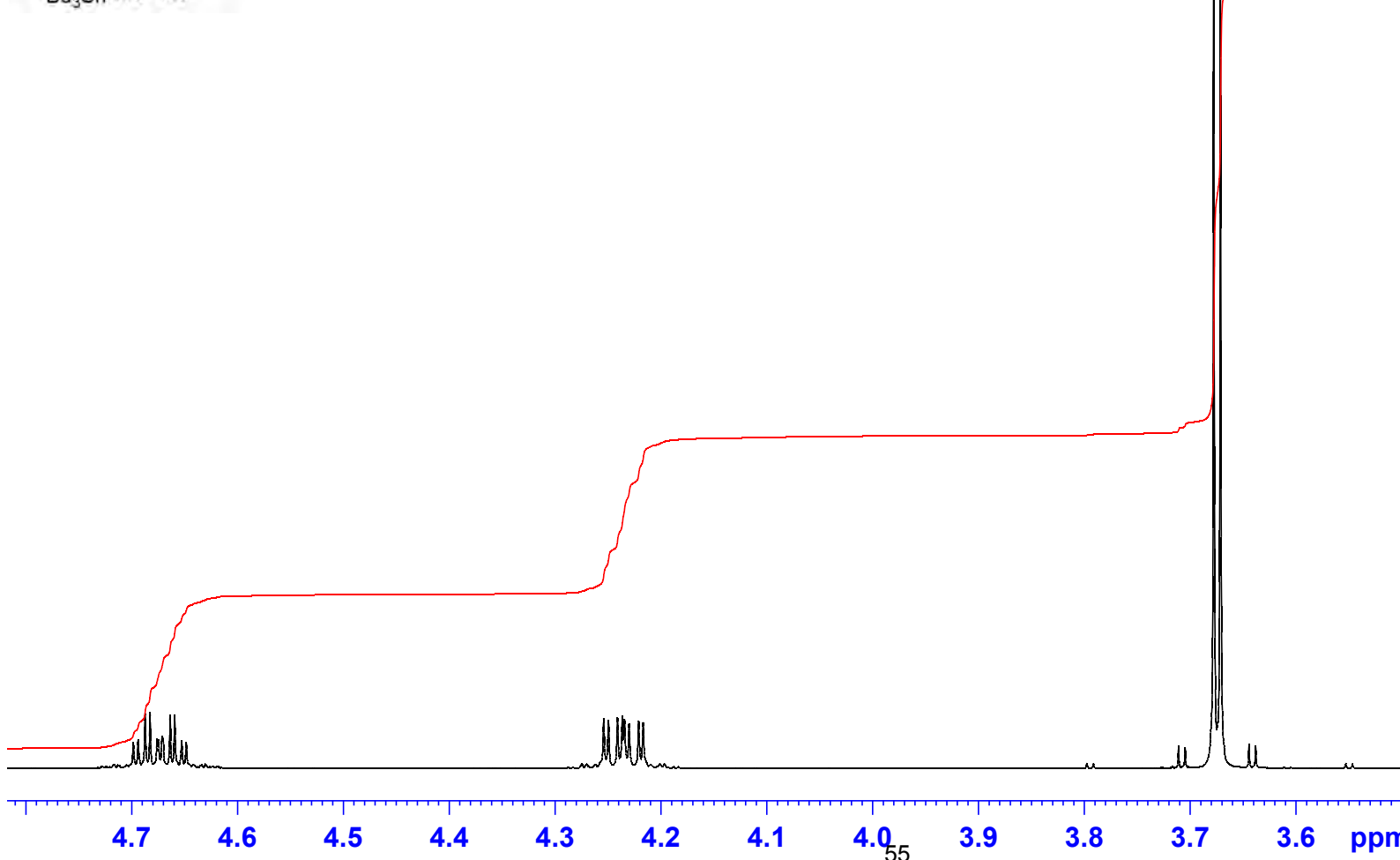
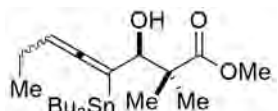


Hamish Watson

HAW-V-050

Proton

Ref: 0.00ppm (CDCl<sub>3</sub>-TMS)

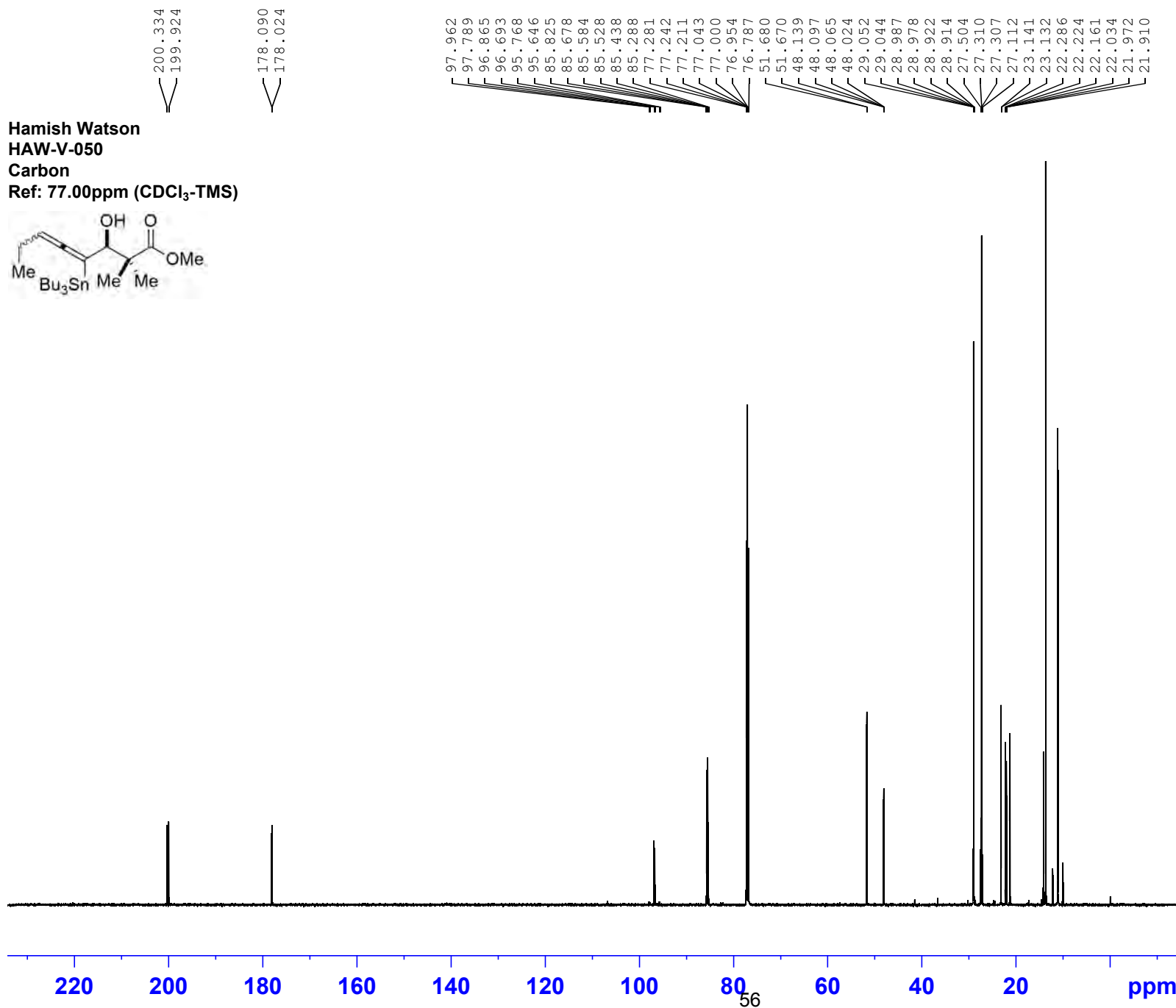


Current Data Parameters  
NAME HAW-V-Bu3Sn\_Probe-(1)  
EXPNO 10  
PROCNO 1

F2 - Acquisition Parameters  
Date 20181130  
Time 4.32  
INSTRUM spect  
PROBHD 5 mm PABBO BB/  
PULPROG zg30  
TD 180286  
SOLVENT CDCl3  
NS 64  
DS 0  
SWH 18028.846 Hz  
FIDRES 0.100001 Hz  
AQ 4.9999318 sec  
RG 22.13  
DW 27.733 usec  
DE 7.60 usec  
TE 300.0 K  
D1 0.10000000 sec  
TD0 1

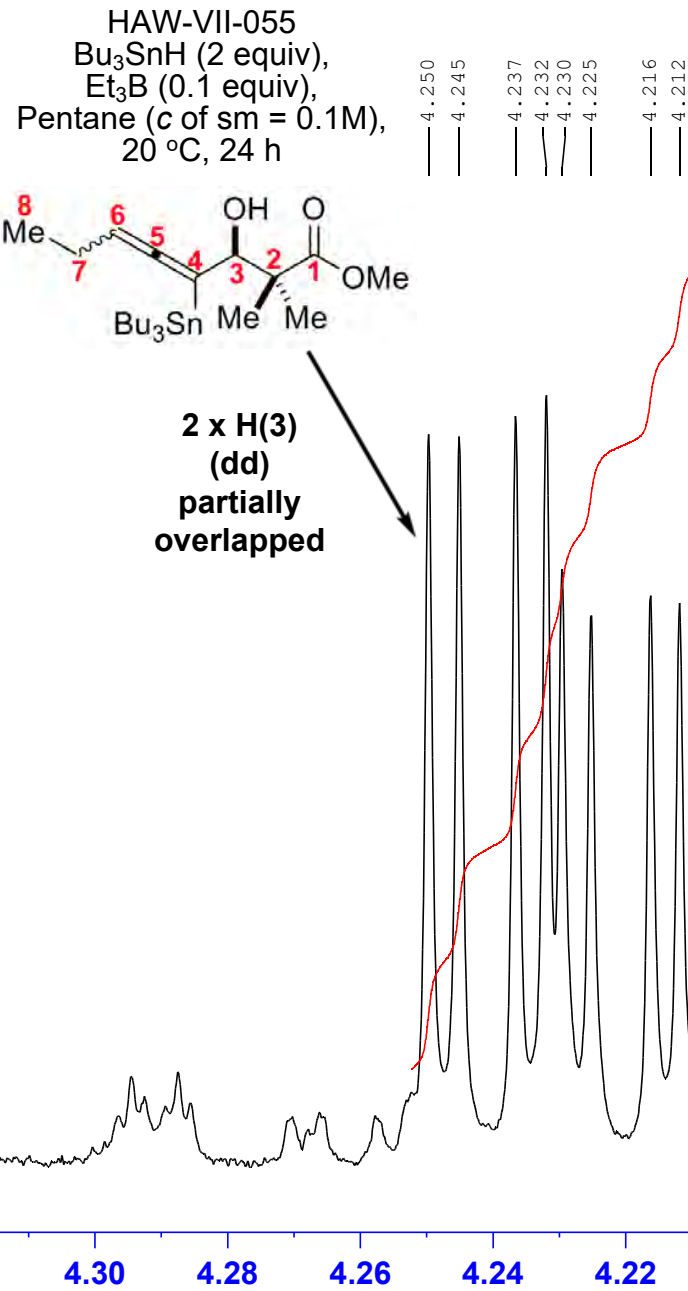
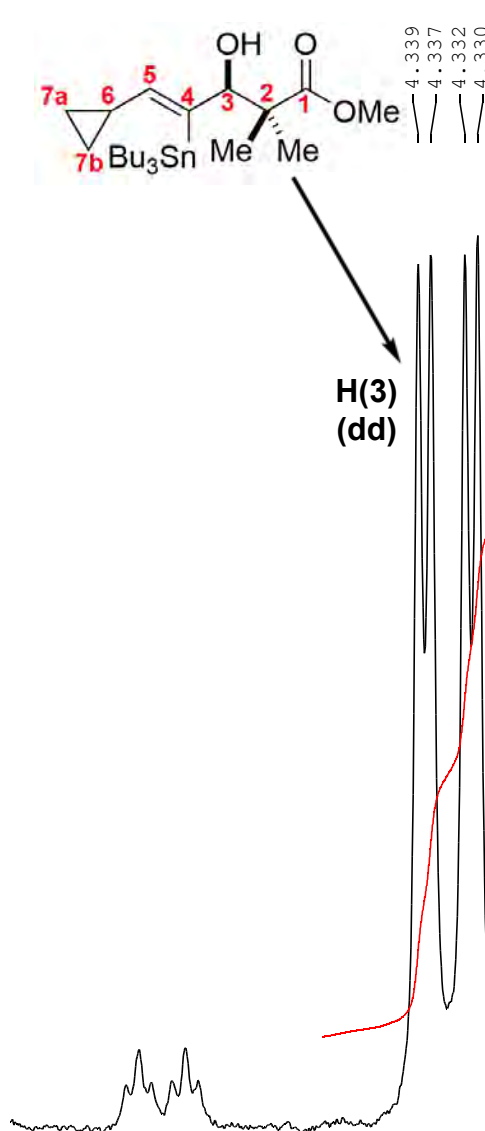
===== CHANNEL f1 =====  
SFO1 600.1337060 MHz  
NUC1 1H  
P1 10.00 usec  
PLW1 26.60000038 W

F2 - Processing parameters  
SI 262144  
SF 600.1300100 MHz  
WDW EM  
SSB 0  
LB 0.10 Hz  
GB 0  
PC 1.00



Current Data Parameters  
 NAME HAW-V-Bu3Sn\_Probe-(1)  
 EXPNO 11  
 PROCNO 1

**Part C. The 600.13 MHz  $^1\text{H}$  NMR Ratio Determinations For  
the Tributylstannylallene 4a and Tributylstannylvinyltin 5a  
in  $\text{CDCl}_3$**

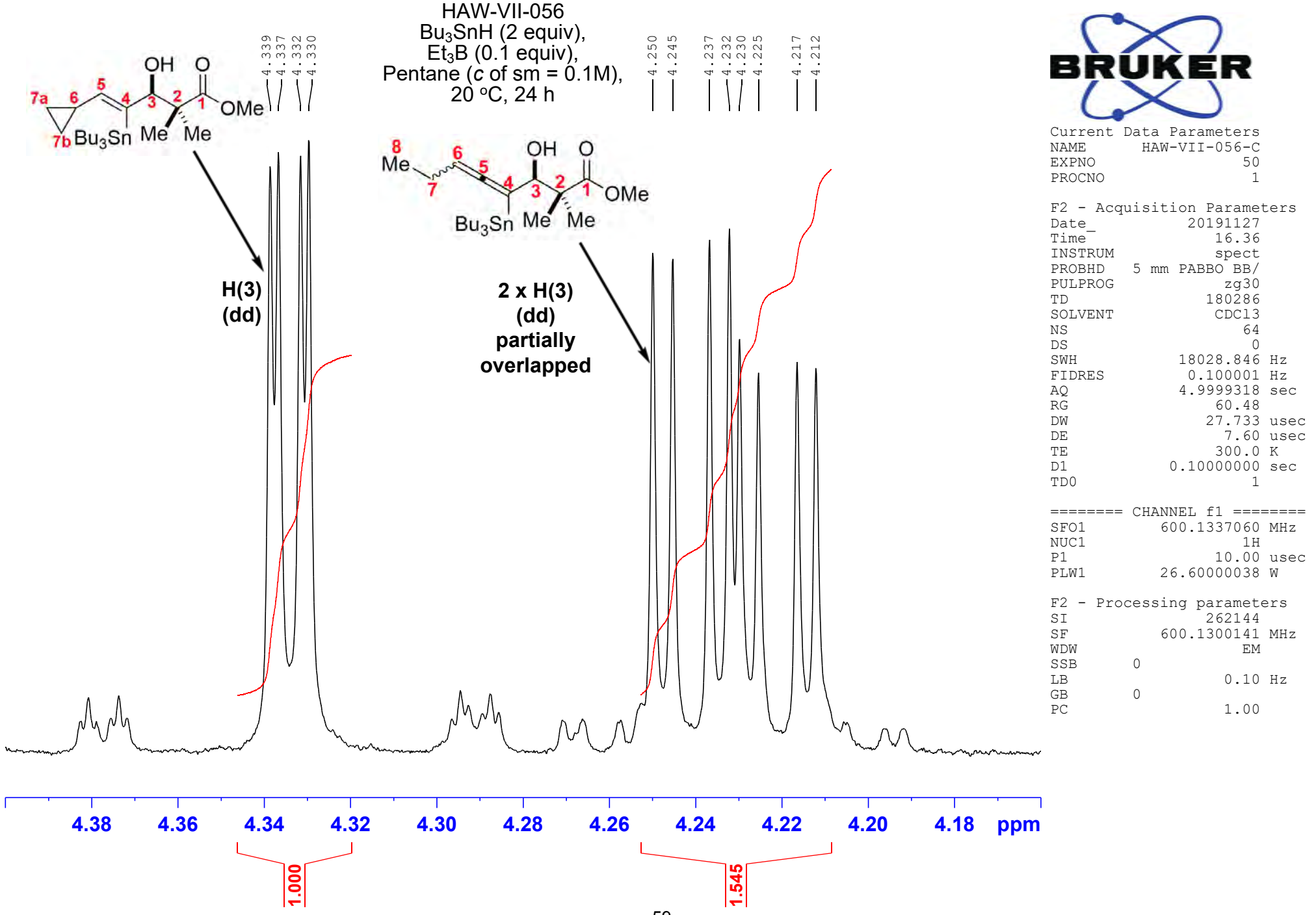


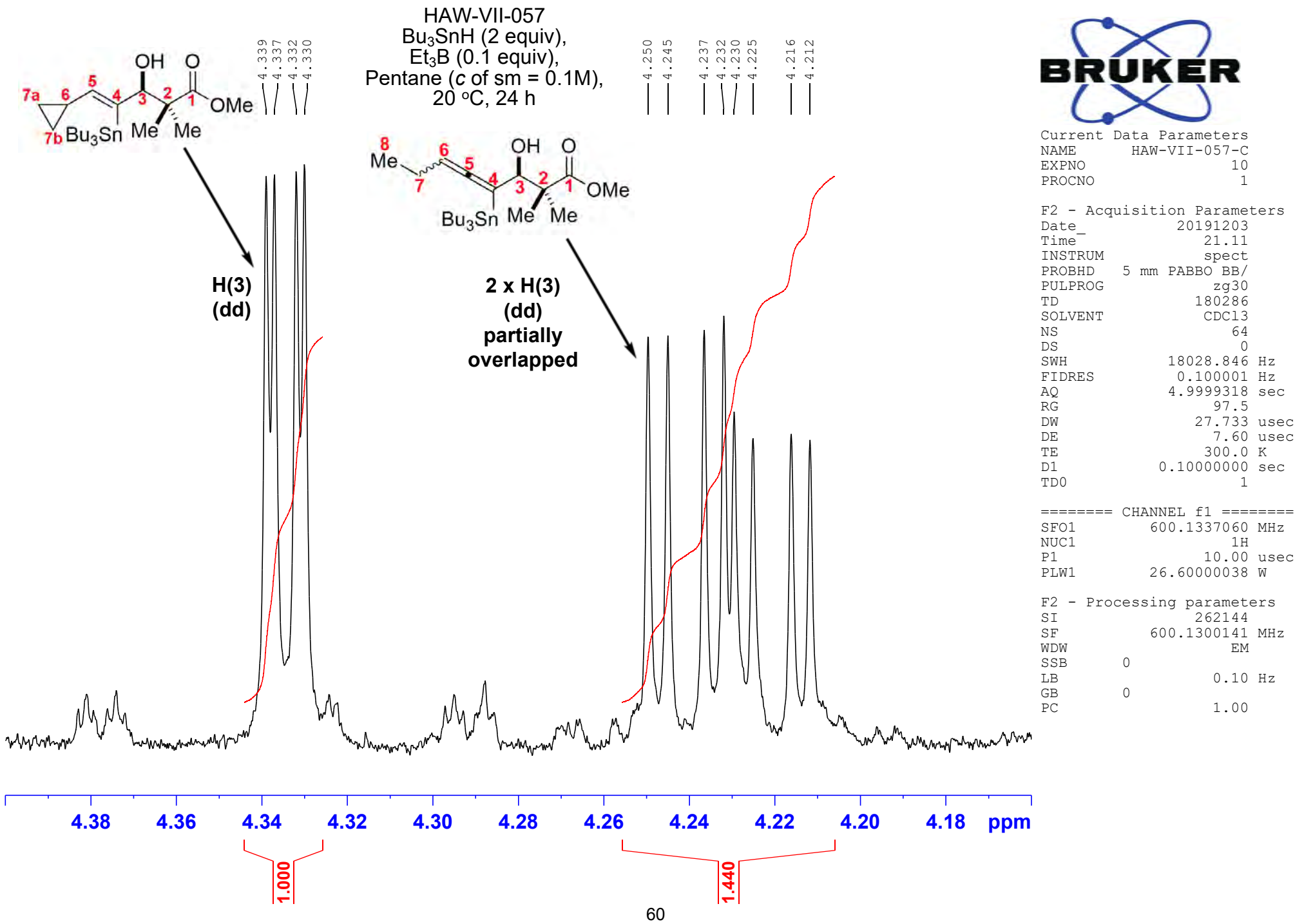
Current Data Parameters  
 NAME HAW-VII-055-C  
 EXPNO 40  
 PROCNO 1

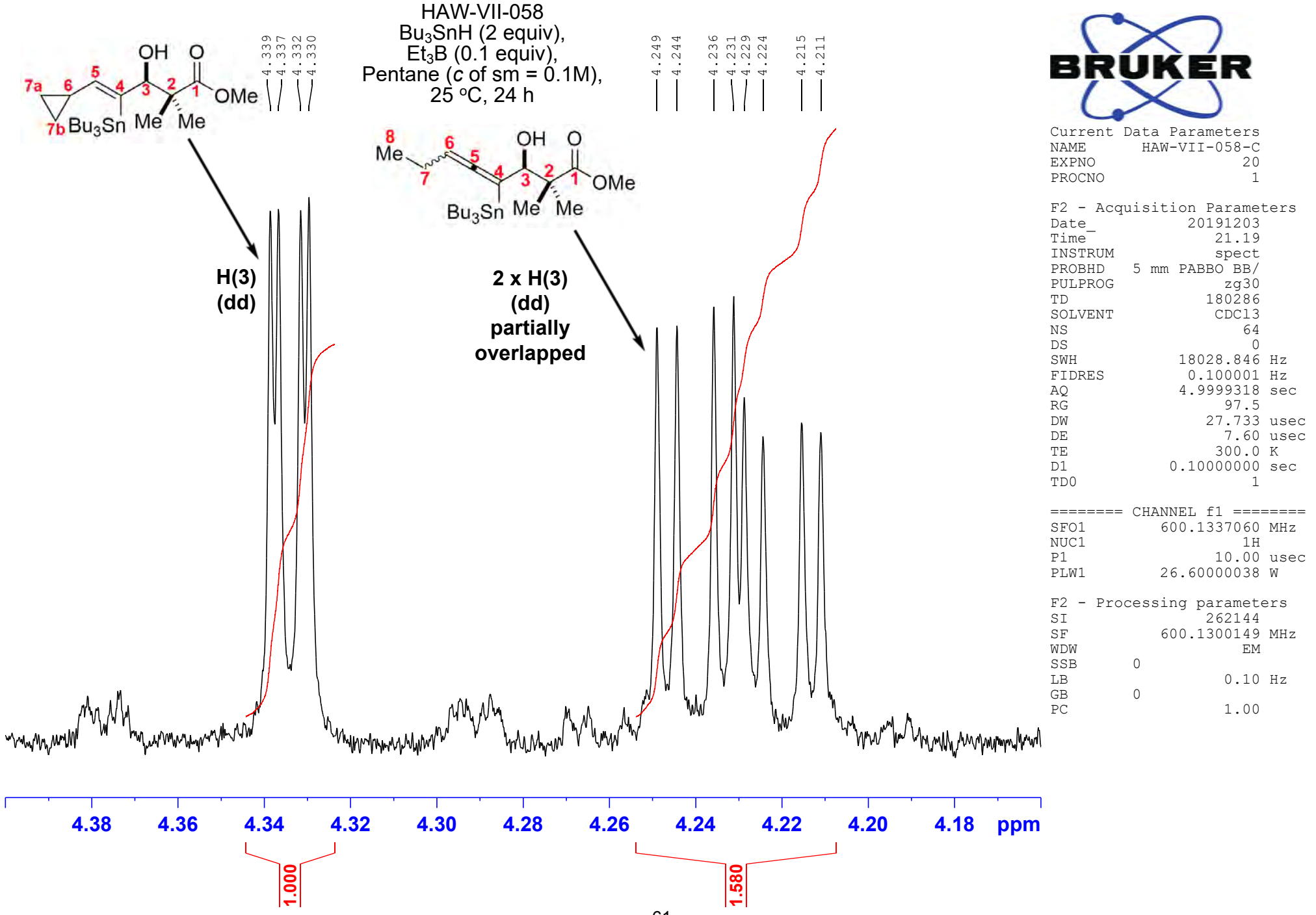
F2 - Acquisition Parameters  
 Date 20191127  
 Time 16.27  
 INSTRUM spect  
 PROBHD 5 mm PABBO BB/  
 PULPROG zg30  
 TD 180286  
 SOLVENT CDCl<sub>3</sub>  
 NS 64  
 DS 0  
 SWH 18028.846 Hz  
 FIDRES 0.100001 Hz  
 AQ 4.9999318 sec  
 RG 97.5  
 DW 27.733 usec  
 DE 7.60 usec  
 TE 300.0 K  
 D1 0.10000000 sec  
 TD0 1

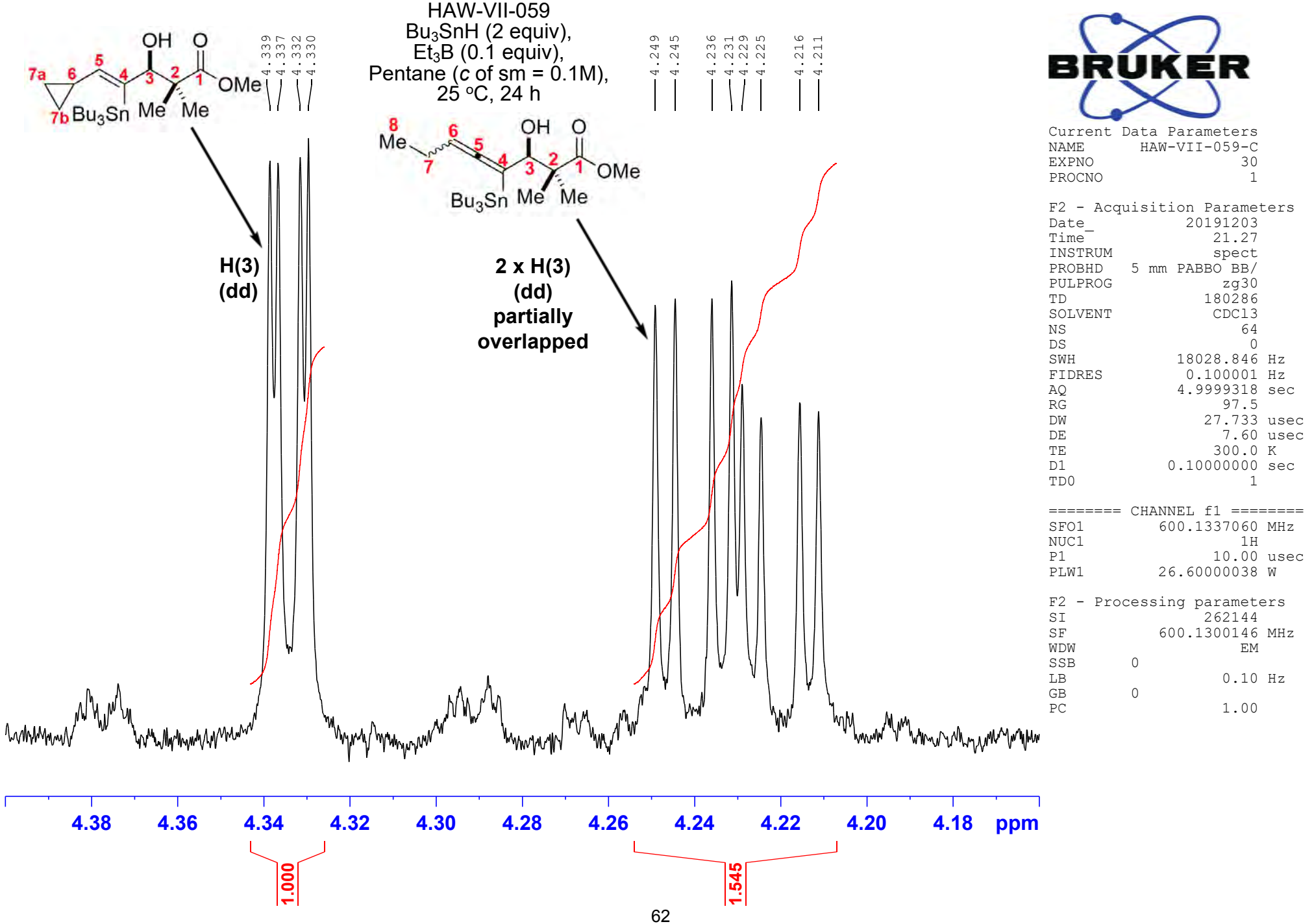
===== CHANNEL f1 =====  
 SFO1 600.1337060 MHz  
 NUC1 1H  
 P1 10.00 usec  
 PLW1 26.60000038 W

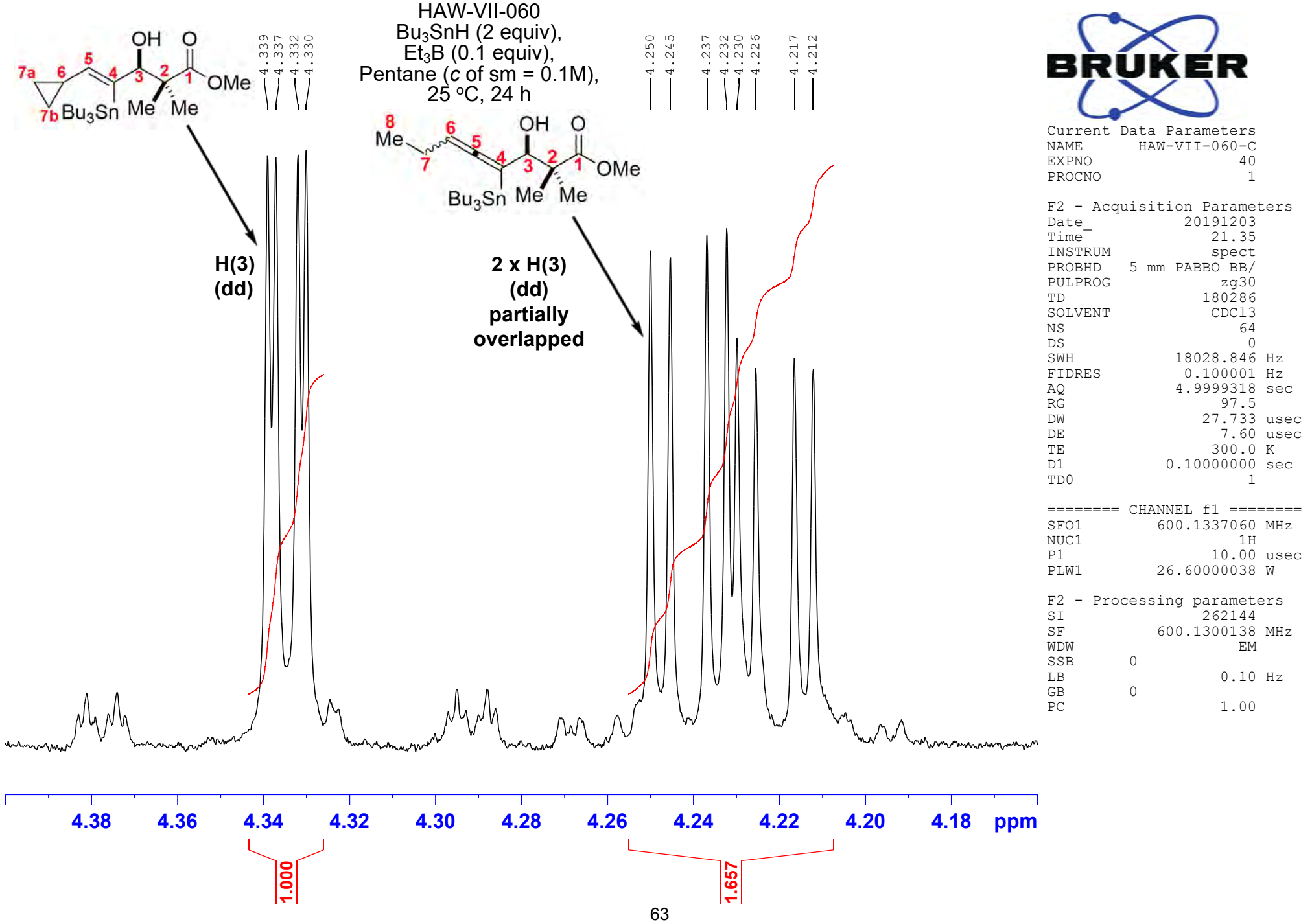
F2 - Processing parameters  
 SI 262144  
 SF 600.1300142 MHz  
 WDW EM  
 SSB 0  
 LB 0.10 Hz  
 GB 0  
 PC 1.00





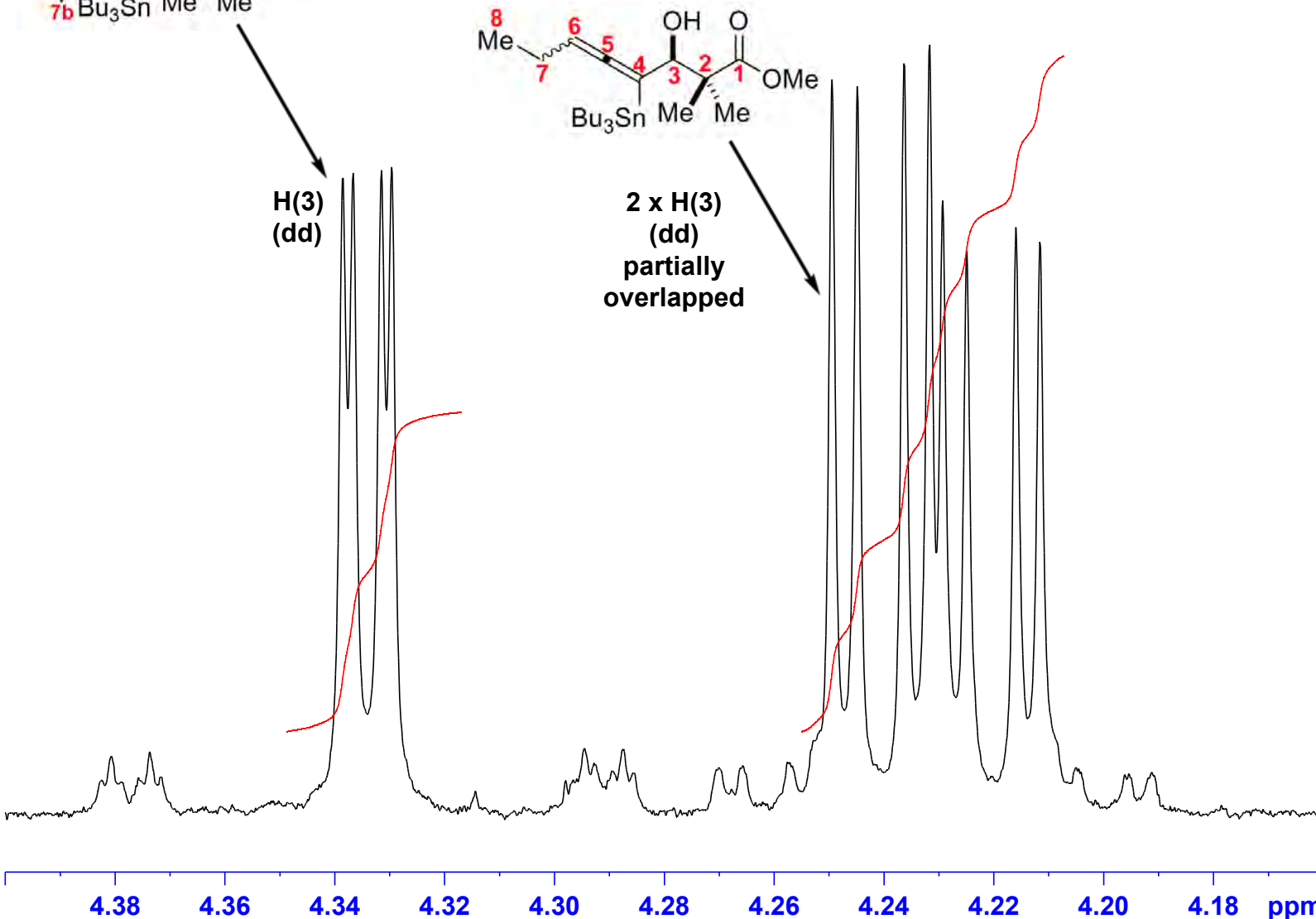








HAW-VII-037  
 $\text{Bu}_3\text{SnH}$  (2 equiv),  
 $\text{Et}_3\text{B}$  (0.1 equiv),  
Pentane ( $c$  of sm = 0.1M),  
30 °C, 24 h

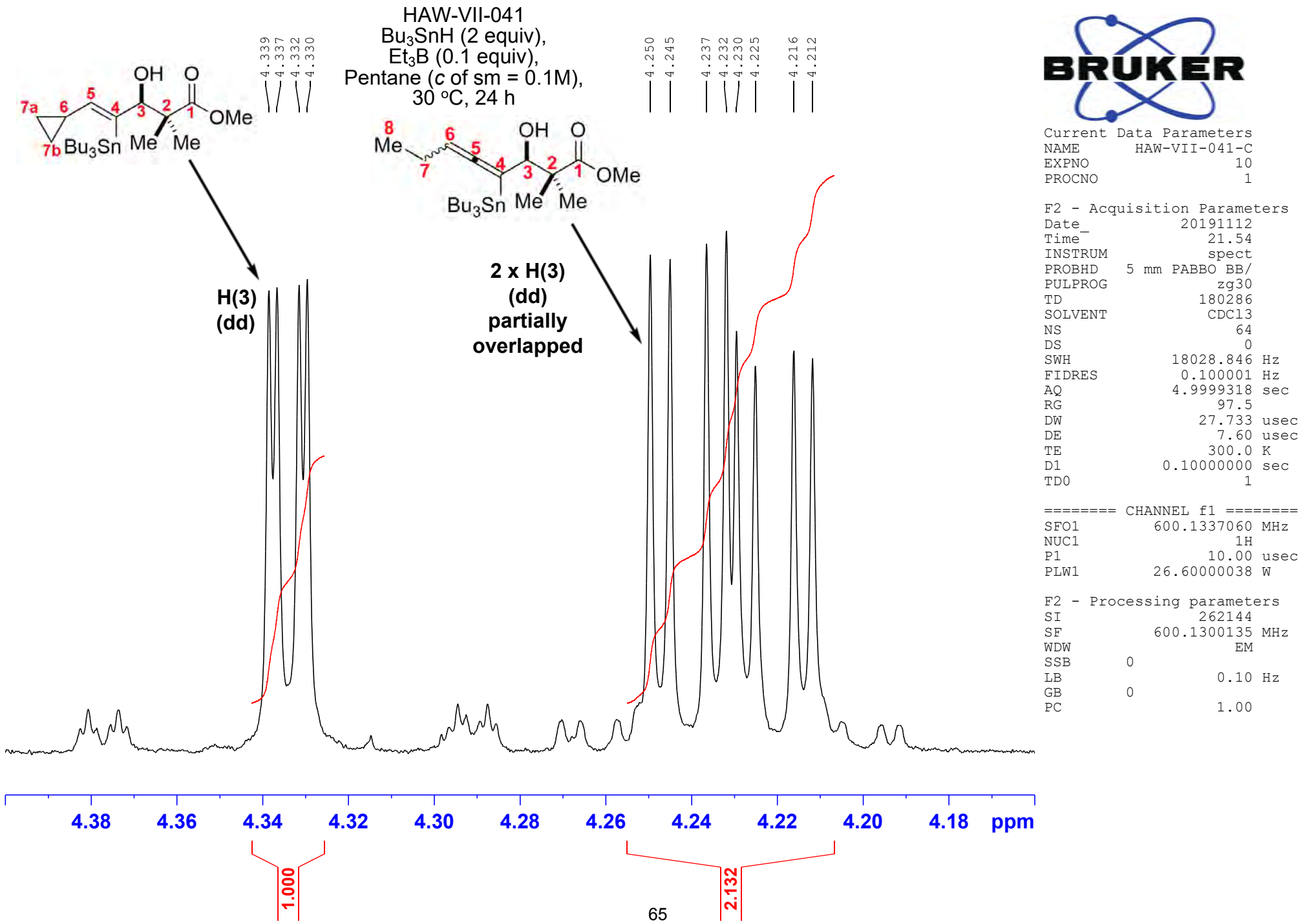


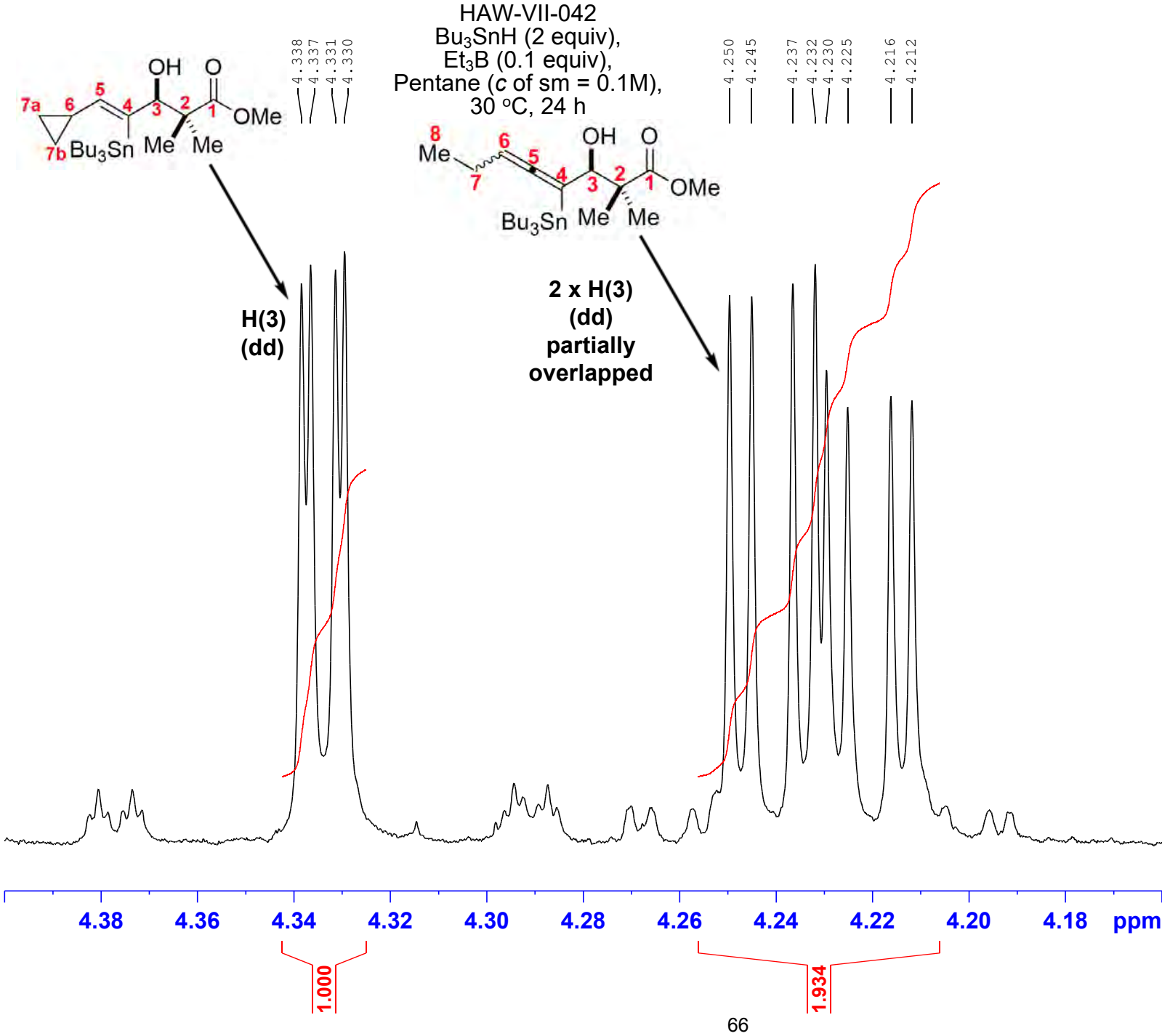
Current Data Parameters  
NAME HAW-VII-037-C  
EXPNO 10  
PROCNO 1

F2 - Acquisition Parameters  
Date 20191108  
Time 15.35  
INSTRUM spect  
PROBHD 5 mm PABBO BB/  
PULPROG zg30  
TD 180286  
SOLVENT CDCl<sub>3</sub>  
NS 64  
DS 0  
SWH 18028.846 Hz  
FIDRES 0.10001 Hz  
AQ 4.9999318 sec  
RG 97.5  
DW 27.733 usec  
DE 7.60 usec  
TE 300.0 K  
D1 0.10000000 sec  
TD0 1

===== CHANNEL f1 =====  
SFO1 600.1337060 MHz  
NUC1 1H  
P1 10.00 usec  
PLW1 26.60000038 W

F2 - Processing parameters  
SI 262144  
SF 600.1300136 MHz  
WDW EM  
SSB 0  
LB 0.10 Hz  
GB 0  
PC 1.00



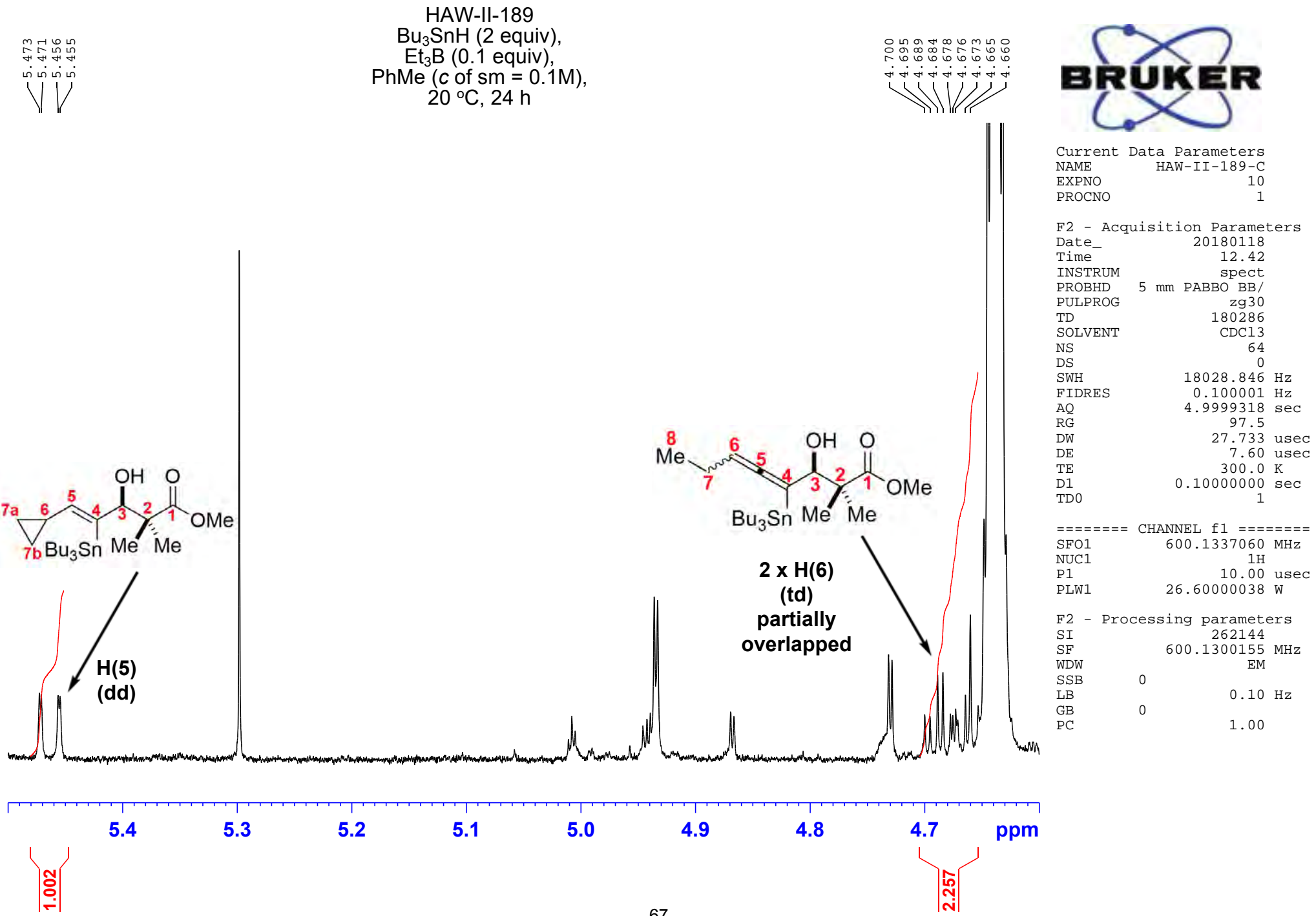


Current Data Parameters  
 NAME HAW-VII-042-C  
 EXPNO 10  
 PROCNO 1

F2 - Acquisition Parameters  
 Date 20191112  
 Time 22.05  
 INSTRUM spect  
 PROBHD 5 mm PABBO BB/  
 PULPROG zg30  
 TD 180286  
 SOLVENT CDCl3  
 NS 64  
 DS 0  
 SWH 18028.846 Hz  
 FIDRES 0.100001 Hz  
 AQ 4.9999318 sec  
 RG 68  
 DW 27.733 usec  
 DE 7.60 usec  
 TE 300.0 K  
 D1 0.10000000 sec  
 TD0 1

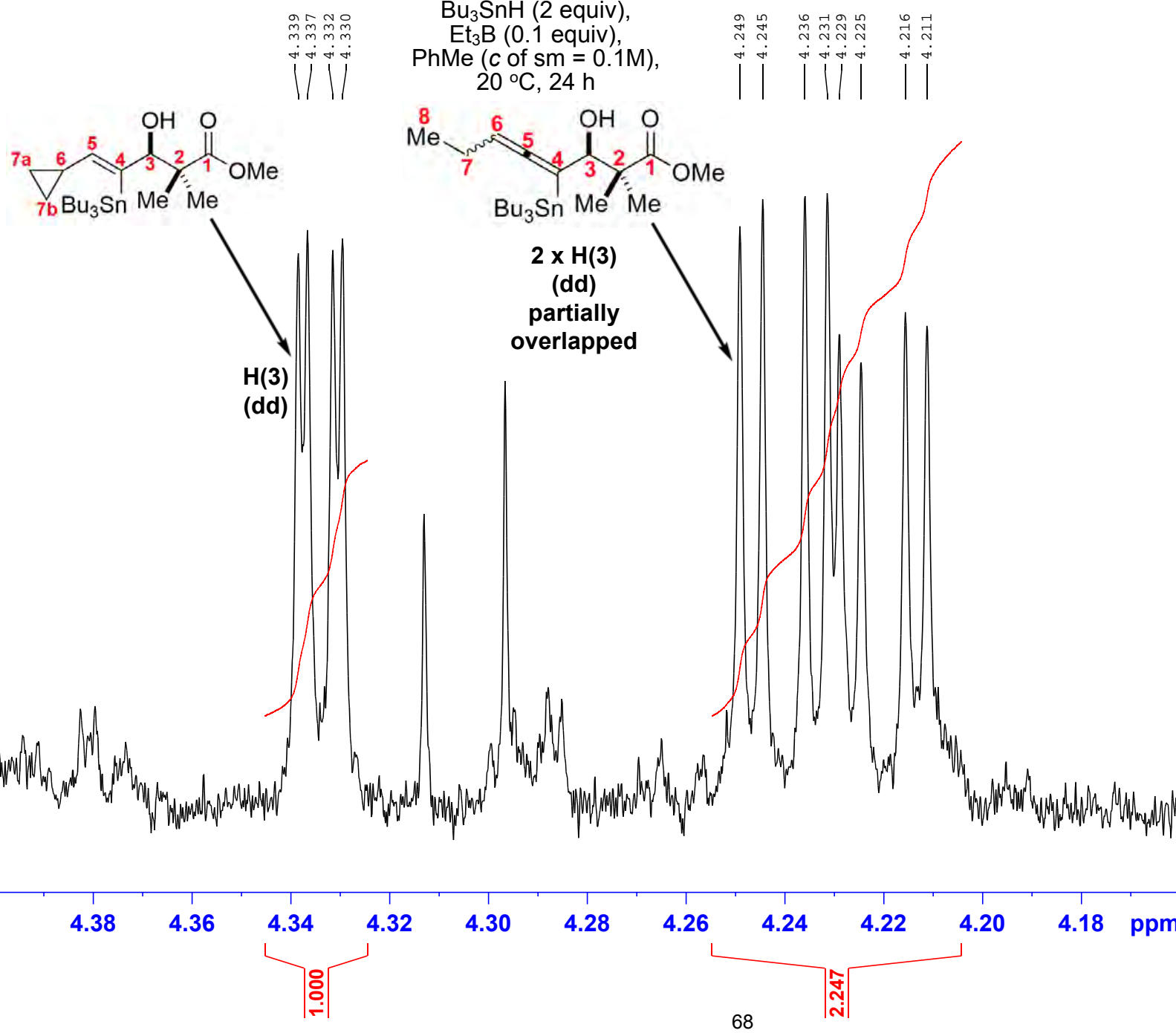
===== CHANNEL f1 ======  
 SFO1 600.1337060 MHz  
 NUC1 1H  
 P1 10.00 usec  
 PLW1 26.60000038 W

F2 - Processing parameters  
 SI 262144  
 SF 600.1300134 MHz  
 WDW EM  
 SSB 0  
 LB 0.10 Hz  
 GB 0  
 PC 1.00





HAW-II-189  
 $\text{Bu}_3\text{SnH}$  (2 equiv),  
 $\text{Et}_3\text{B}$  (0.1 equiv),  
 $\text{PhMe}$  ( $c$  of sm = 0.1M),  
20 °C, 24 h

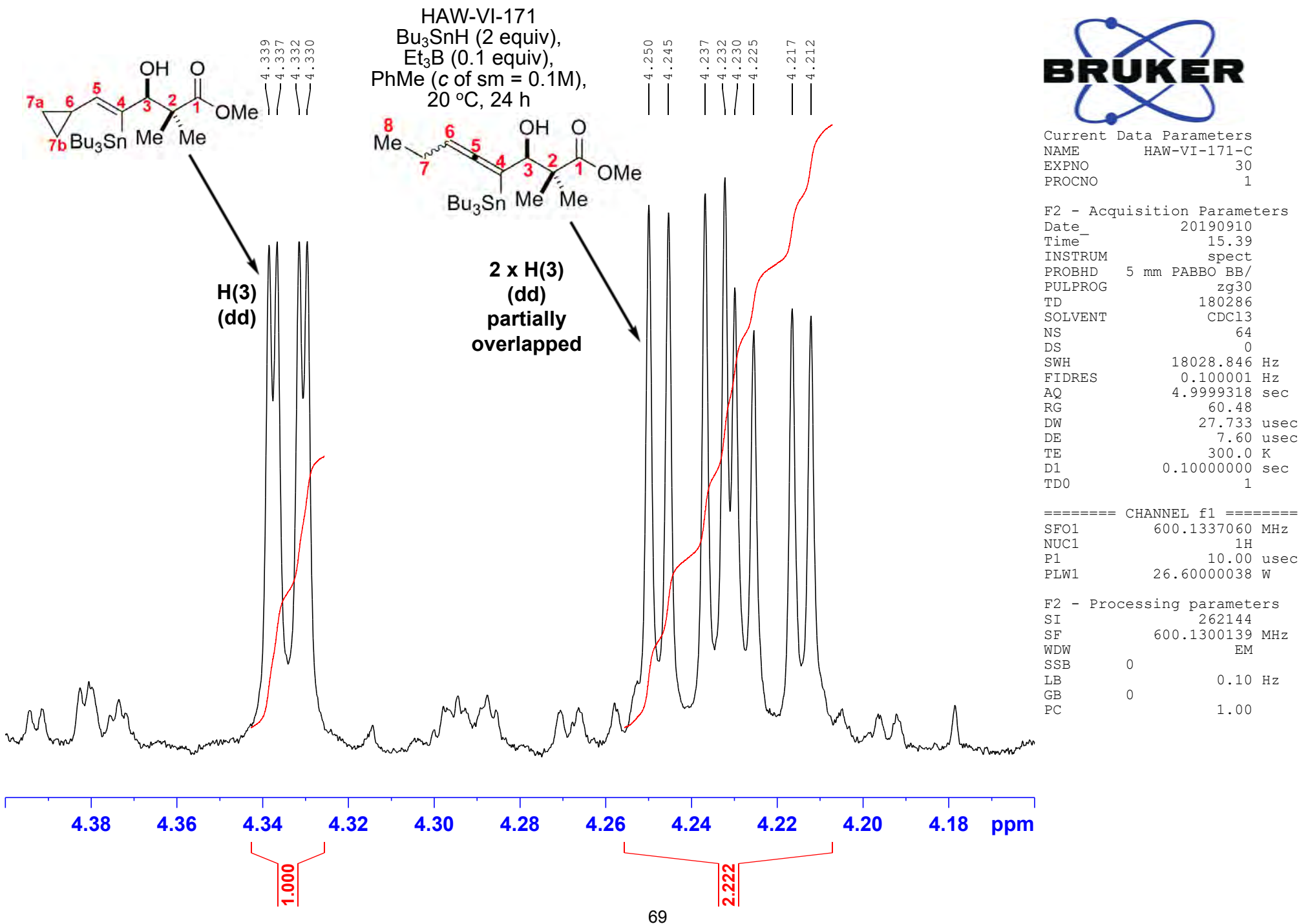


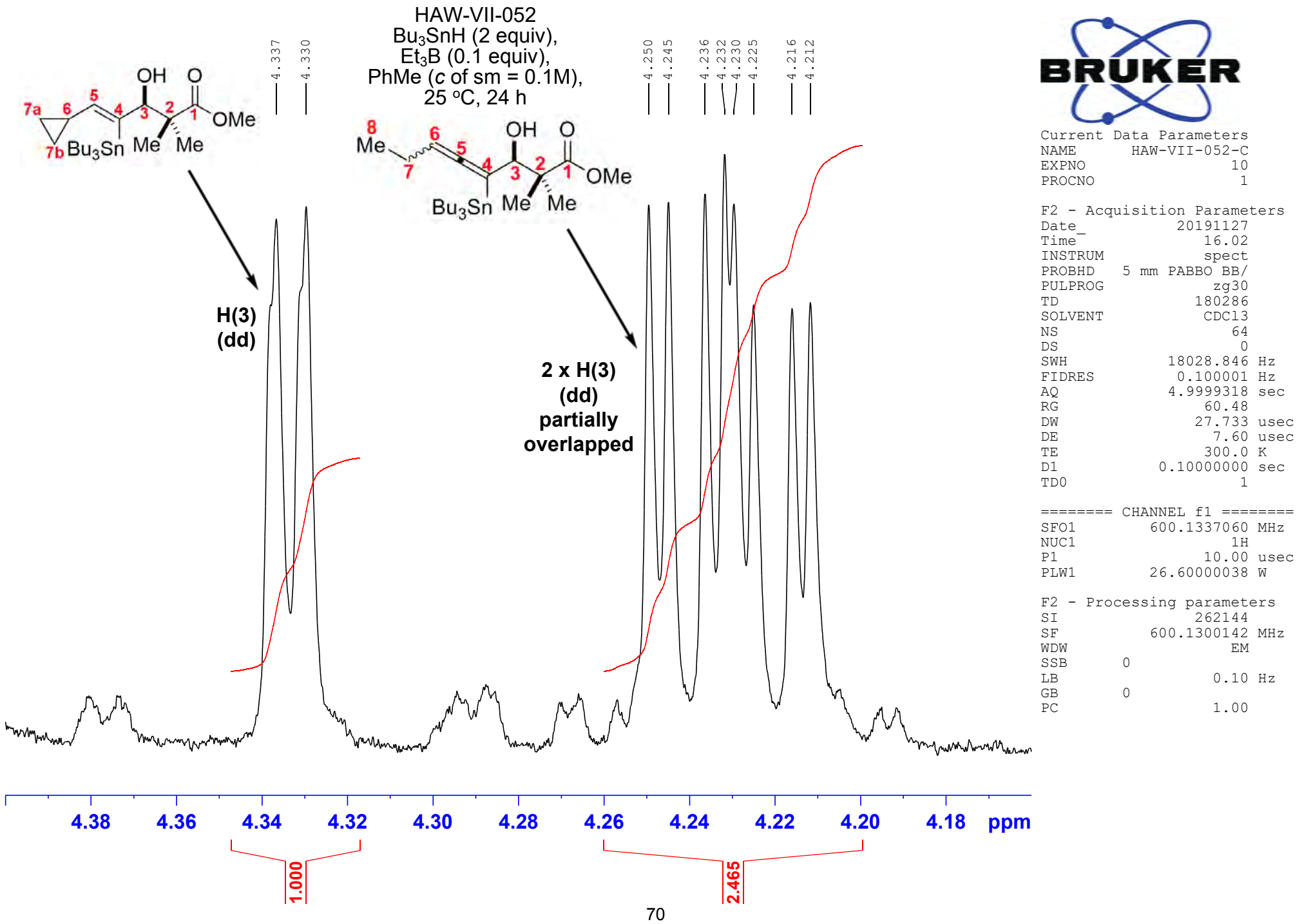
Current Data Parameters  
NAME HAW-II-189-C  
EXPNO 10  
PROCNO 1

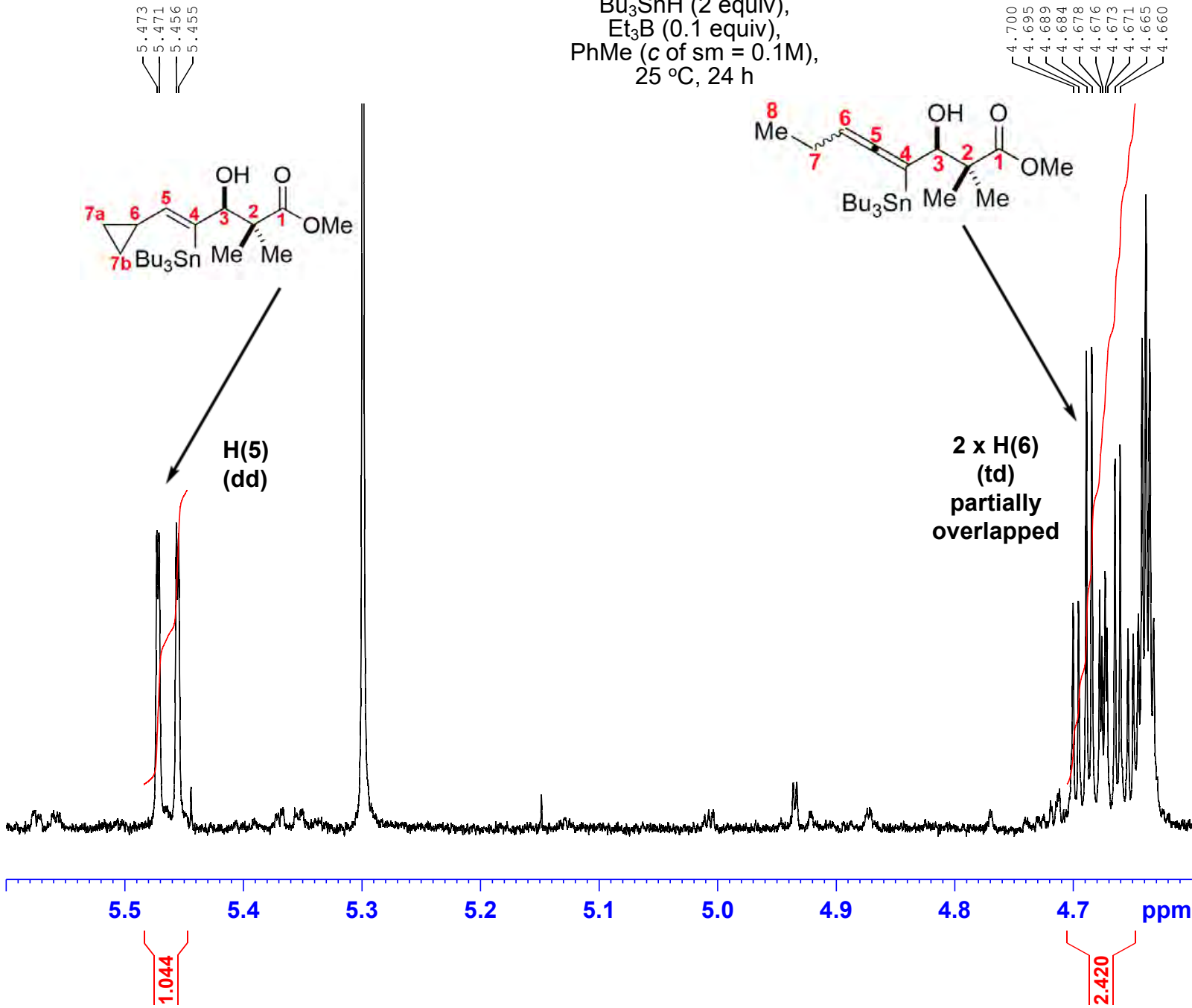
F2 - Acquisition Parameters  
Date 20180118  
Time 12.42  
INSTRUM spect  
PROBHD 5 mm PABBO BB/  
PULPROG zg30  
TD 180286  
SOLVENT CDCl3  
NS 64  
DS 0  
SWH 18028.846 Hz  
FIDRES 0.100001 Hz  
AQ 4.9999318 sec  
RG 97.5  
DW 27.733 usec  
DE 7.60 usec  
TE 300.0 K  
D1 0.10000000 sec  
TD0 1

===== CHANNEL f1 =====  
SFO1 600.1337060 MHz  
NUC1 1H  
P1 10.00 usec  
PLW1 26.60000038 W

F2 - Processing parameters  
SI 262144  
SF 600.1300155 MHz  
WDW EM  
SSB 0  
LB 0.10 Hz  
GB 0  
PC 1.00





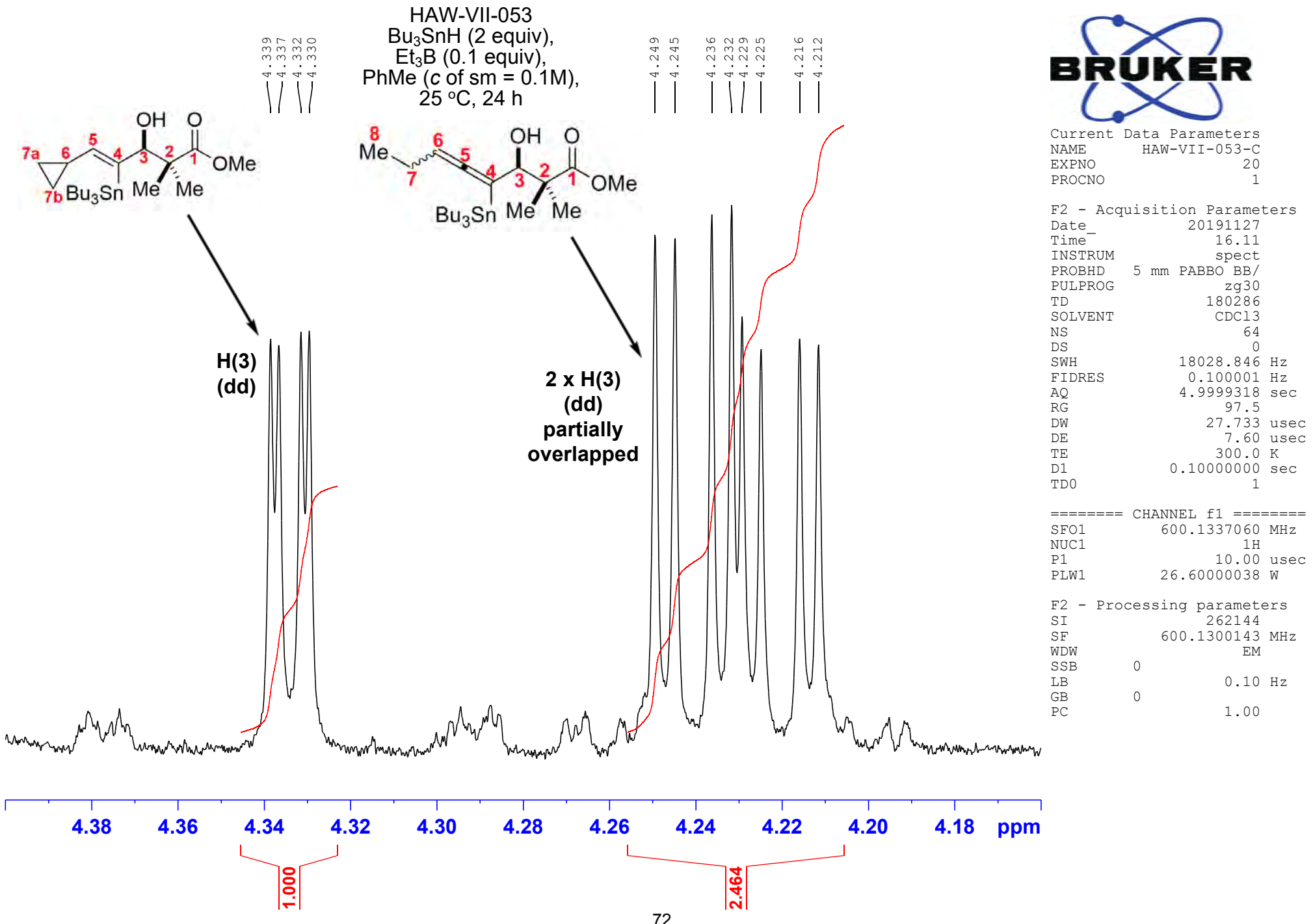


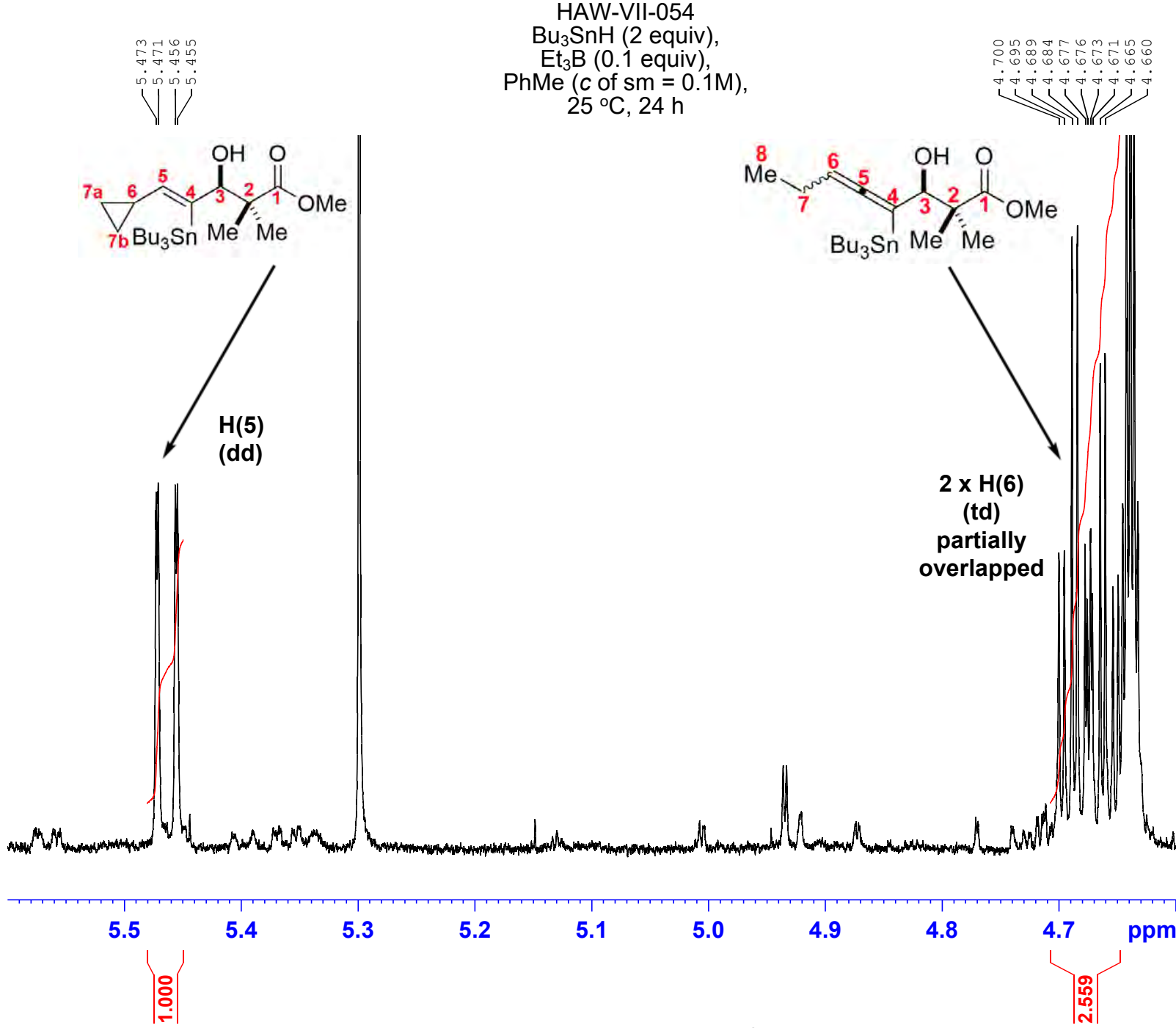
Current Data Parameters  
NAME HAW-VII-053-C  
EXPNO 20  
PROCNO 1

F2 - Acquisition Parameters  
Date 20191127  
Time 16.11  
INSTRUM spect  
PROBHD 5 mm PABBO BB/  
PULPROG zg30  
TD 180286  
SOLVENT CDCl3  
NS 64  
DS 0  
SWH 18028.846 Hz  
FIDRES 0.100001 Hz  
AQ 4.9999318 sec  
RG 97.5  
DW 27.733 usec  
DE 7.60 usec  
TE 300.0 K  
D1 0.10000000 sec  
TD0 1

===== CHANNEL f1 =====  
SFO1 600.1337060 MHz  
NUC1 1H  
P1 10.00 usec  
PLW1 26.60000038 W

F2 - Processing parameters  
SI 262144  
SF 600.1300143 MHz  
WDW EM  
SSB 0  
LB 0.10 Hz  
GB 0  
PC 1.00





Current Data Parameters  
NAME HAW-VII-054-C  
EXPNO 30  
PROCNO 1

F2 - Acquisition Parameters  
Date 20191127  
Time 16.19  
INSTRUM spect  
PROBHD 5 mm PABBO BB/  
PULPROG zg30  
TD 180286  
SOLVENT CDCl3  
NS 64  
DS 0  
SWH 18028.846 Hz  
FIDRES 0.100001 Hz  
AQ 4.9999318 sec  
RG 97.5  
DW 27.733 usec  
DE 7.60 usec  
TE 300.0 K  
D1 0.10000000 sec  
TD0 1

===== CHANNEL f1 =====  
SFO1 600.1337060 MHz  
NUC1 1H  
P1 10.00 usec  
PLW1 26.60000038 W

F2 - Processing parameters  
SI 262144  
SF 600.1300142 MHz  
WDW EM  
SSB 0  
LB 0.10 Hz  
GB 0  
PC 1.00

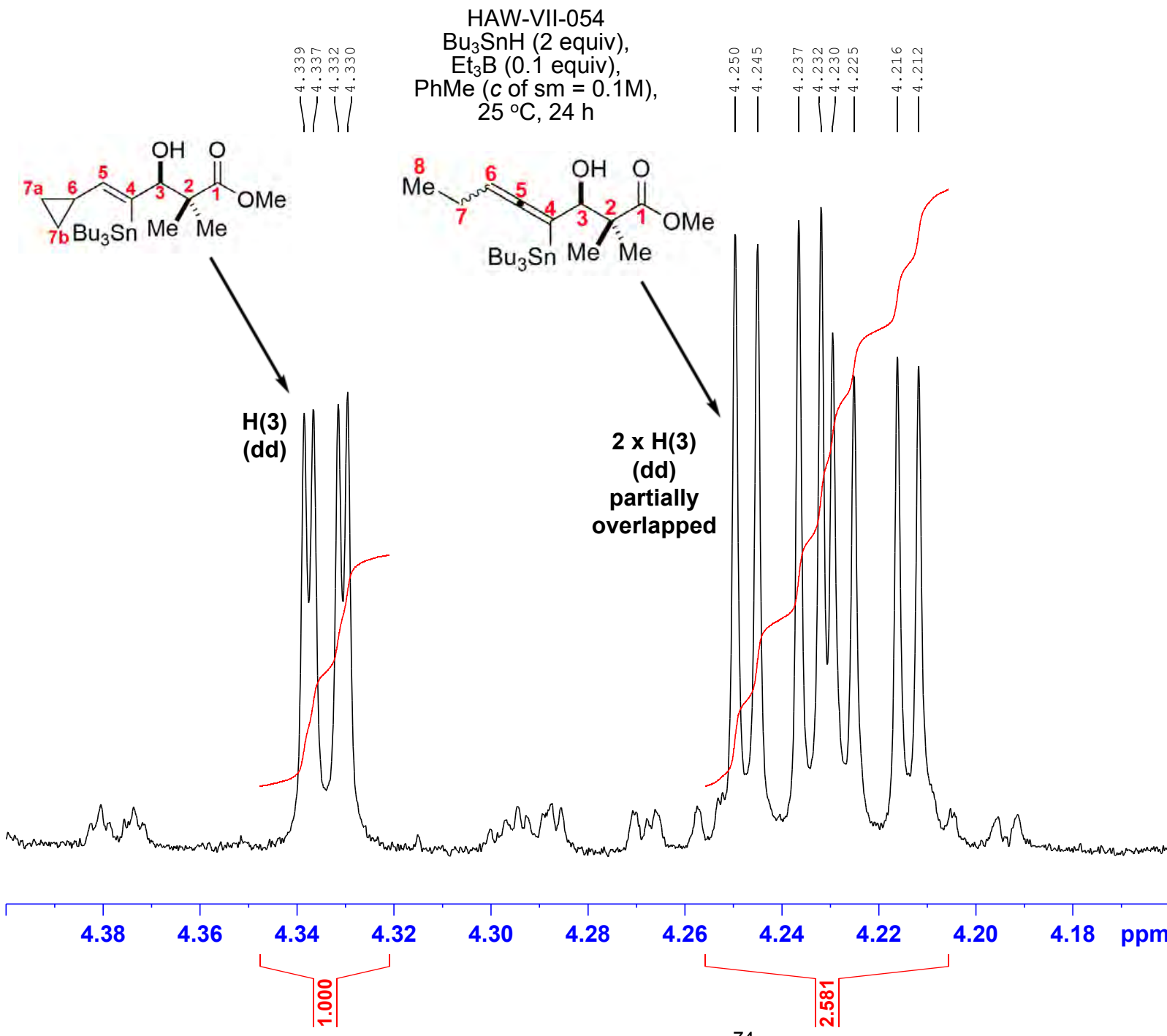


Current Data Parameters  
 NAME HAW-VII-054-C  
 EXPNO 30  
 PROCNO 1

F2 - Acquisition Parameters  
 Date 20191127  
 Time 16.19  
 INSTRUM spect  
 PROBHD 5 mm PABBO BB/  
 PULPROG zg30  
 TD 180286  
 SOLVENT CDCl3  
 NS 64  
 DS 0  
 SWH 18028.846 Hz  
 FIDRES 0.100001 Hz  
 AQ 4.9999318 sec  
 RG 97.5  
 DW 27.733 usec  
 DE 7.60 usec  
 TE 300.0 K  
 D1 0.10000000 sec  
 TD0 1

===== CHANNEL f1 =====  
 SFO1 600.1337060 MHz  
 NUC1 1H  
 P1 10.00 usec  
 PLW1 26.60000038 W

F2 - Processing parameters  
 SI 262144  
 SF 600.1300142 MHz  
 WDW EM  
 SSB 0  
 LB 0.10 Hz  
 GB 0  
 PC 1.00



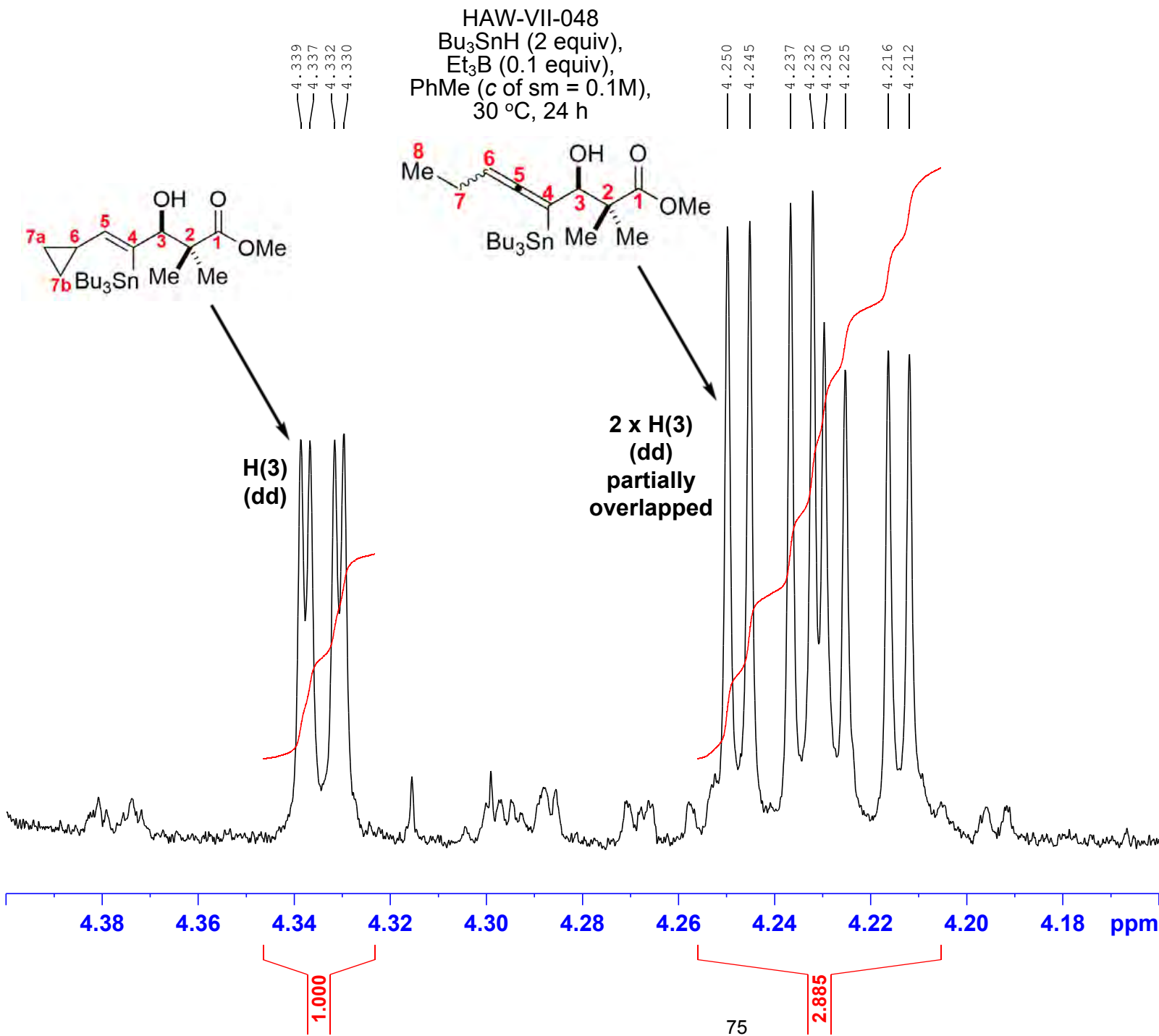


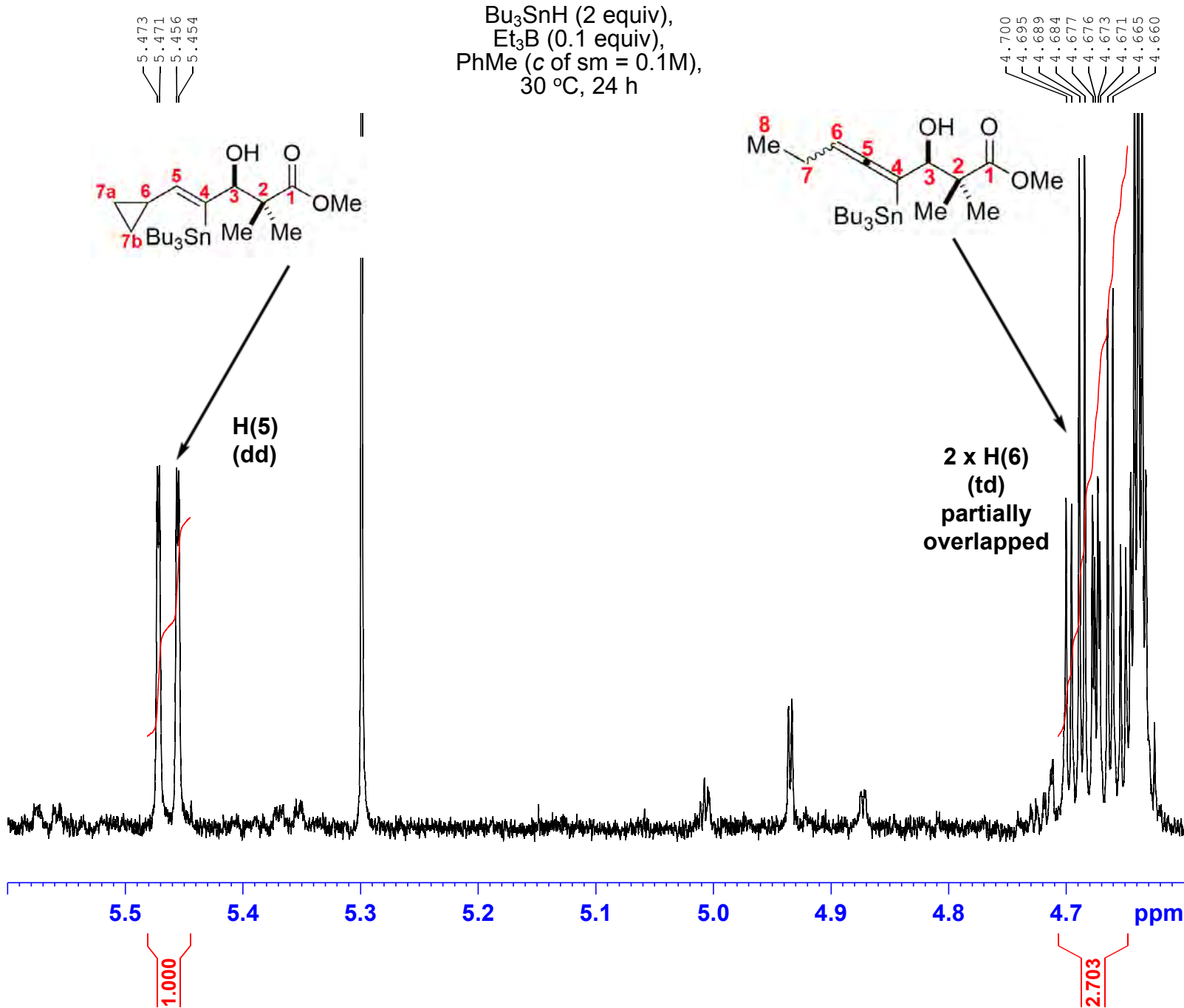
Current Data Parameters  
 NAME HAW-VII-048-C  
 EXPNO 10  
 PROCNO 1

F2 - Acquisition Parameters  
 Date 20191114  
 Time 23.03  
 INSTRUM spect  
 PROBHD 5 mm PABBO BB/  
 PULPROG zg30  
 TD 180286  
 SOLVENT CDCl3  
 NS 64  
 DS 0  
 SWH 18028.846 Hz  
 FIDRES 0.100001 Hz  
 AQ 4.9999318 sec  
 RG 97.5  
 DW 27.733 usec  
 DE 7.60 usec  
 TE 300.0 K  
 D1 0.10000000 sec  
 TD0 1

===== CHANNEL f1 =====  
 SFO1 600.1337060 MHz  
 NUC1 1H  
 P1 10.00 usec  
 PLW1 26.60000038 W

F2 - Processing parameters  
 SI 262144  
 SF 600.1300131 MHz  
 WDW EM  
 SSB 0  
 LB 0.10 Hz  
 GB 0  
 PC 1.00





Current Data Parameters  
NAME HAW-VII-049-C  
EXPNO 20  
PROCNO 1

F2 - Acquisition Parameters  
Date 20191114  
Time 23.14  
INSTRUM spect  
PROBHD 5 mm PABBO BB/  
PULPROG zg30  
TD 180286  
SOLVENT CDCl3  
NS 64  
DS 0  
SWH 18028.846 Hz  
FIDRES 0.100001 Hz  
AQ 4.9999318 sec  
RG 97.5  
DW 27.733 usec  
DE 7.60 usec  
TE 300.0 K  
D1 0.10000000 sec  
TD0 1

===== CHANNEL f1 =====  
SFO1 600.1337060 MHz  
NUC1 1H  
P1 10.00 usec  
PLW1 26.60000038 W

F2 - Processing parameters  
SI 262144  
SF 600.1300134 MHz  
WDW EM  
SSB 0  
LB 0.10 Hz  
GB 0  
PC 1.00

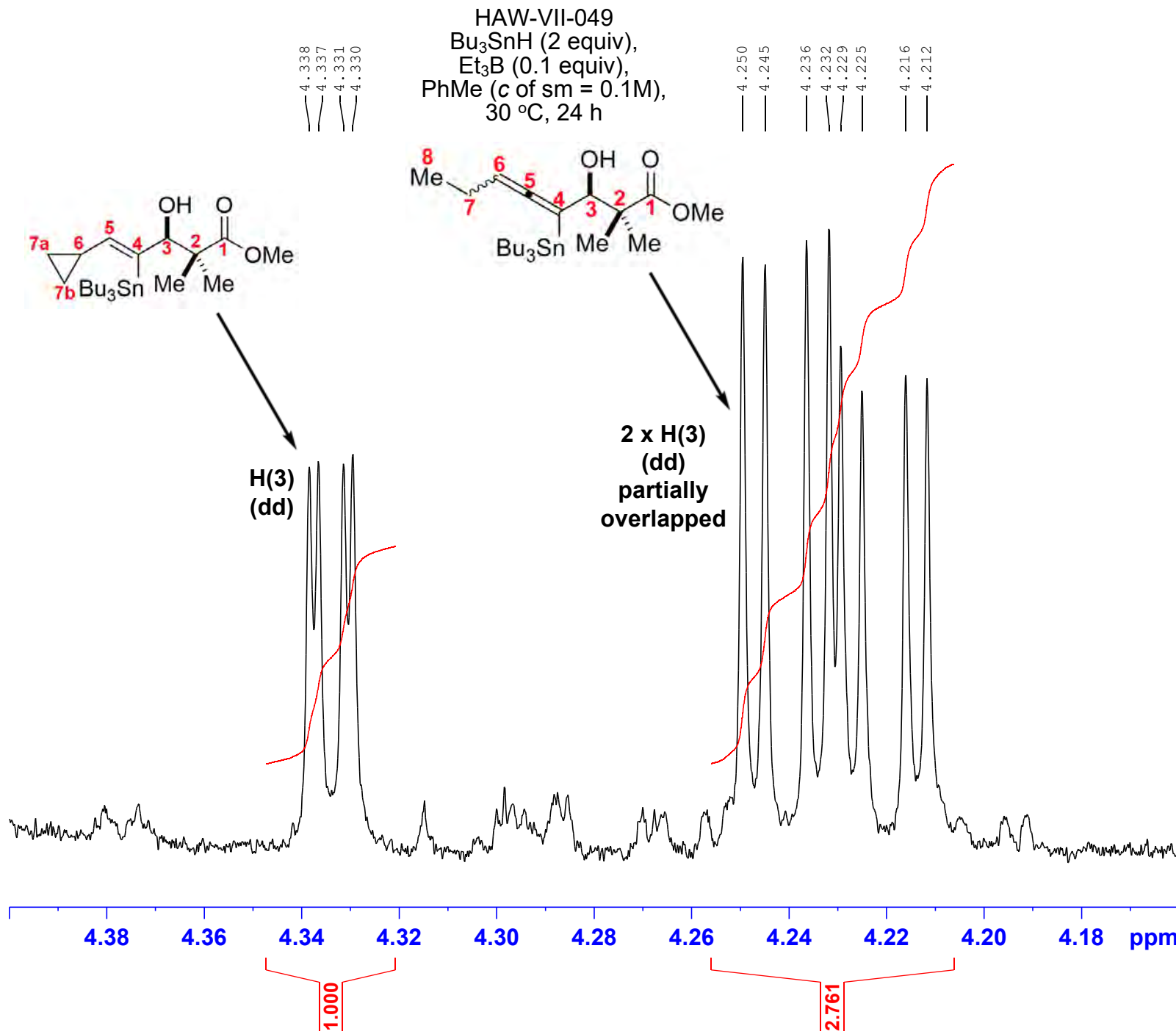


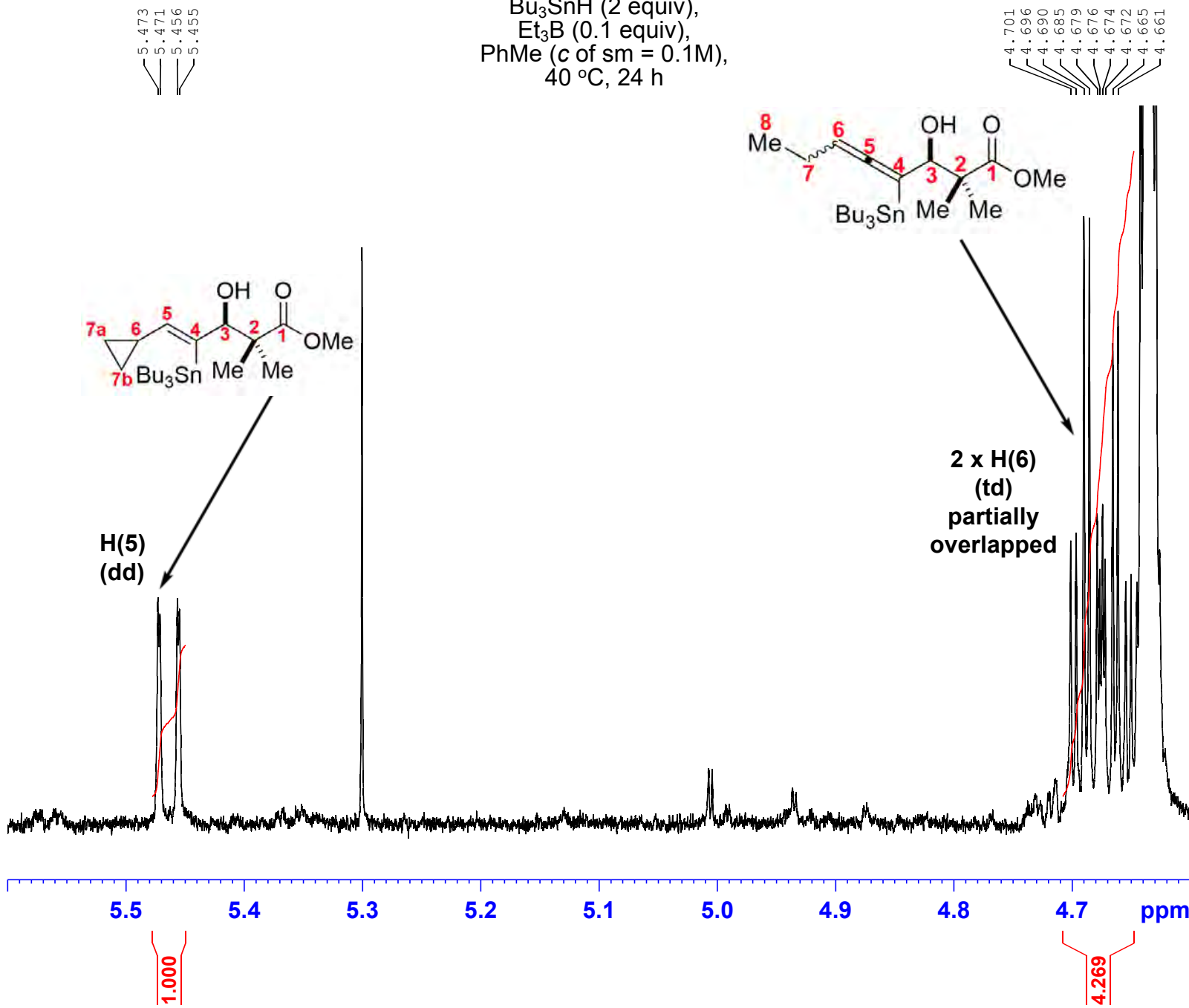
Current Data Parameters  
 NAME HAW-VII-049-C  
 EXPNO 20  
 PROCNO 1

F2 - Acquisition Parameters  
 Date 20191114  
 Time 23.14  
 INSTRUM spect  
 PROBHD 5 mm PABBO BB/  
 PULPROG zg30  
 TD 180286  
 SOLVENT CDCl3  
 NS 64  
 DS 0  
 SWH 18028.846 Hz  
 FIDRES 0.100001 Hz  
 AQ 4.9999318 sec  
 RG 97.5  
 DW 27.733 usec  
 DE 7.60 usec  
 TE 300.0 K  
 D1 0.10000000 sec  
 TD0 1

===== CHANNEL f1 =====  
 SFO1 600.1337060 MHz  
 NUC1 1H  
 P1 10.00 usec  
 PLW1 26.60000038 W

F2 - Processing parameters  
 SI 262144  
 SF 600.1300134 MHz  
 WDW EM  
 SSB 0  
 LB 0.10 Hz  
 GB 0  
 PC 1.00





Current Data Parameters  
NAME HAW-VII-030-C  
EXPNO 10  
PROCNO 1

F2 - Acquisition Parameters  
Date 20191031  
Time 15.11  
INSTRUM spect  
PROBHD 5 mm PABBO BB/  
PULPROG zg30  
TD 180286  
SOLVENT CDCl3  
NS 64  
DS 0  
SWH 18028.846 Hz  
FIDRES 0.100001 Hz  
AQ 4.9999318 sec  
RG 97.5  
DW 27.733 usec  
DE 7.60 usec  
TE 298.0 K  
D1 0.10000000 sec  
TD0 1

===== CHANNEL f1 =====  
SFO1 600.1337060 MHz  
NUC1 1H  
P1 10.00 usec  
PLW1 26.60000038 W

F2 - Processing parameters  
SI 262144  
SF 600.1300137 MHz  
WDW EM  
SSB 0  
LB 0.10 Hz  
GB 0  
PC 1.00

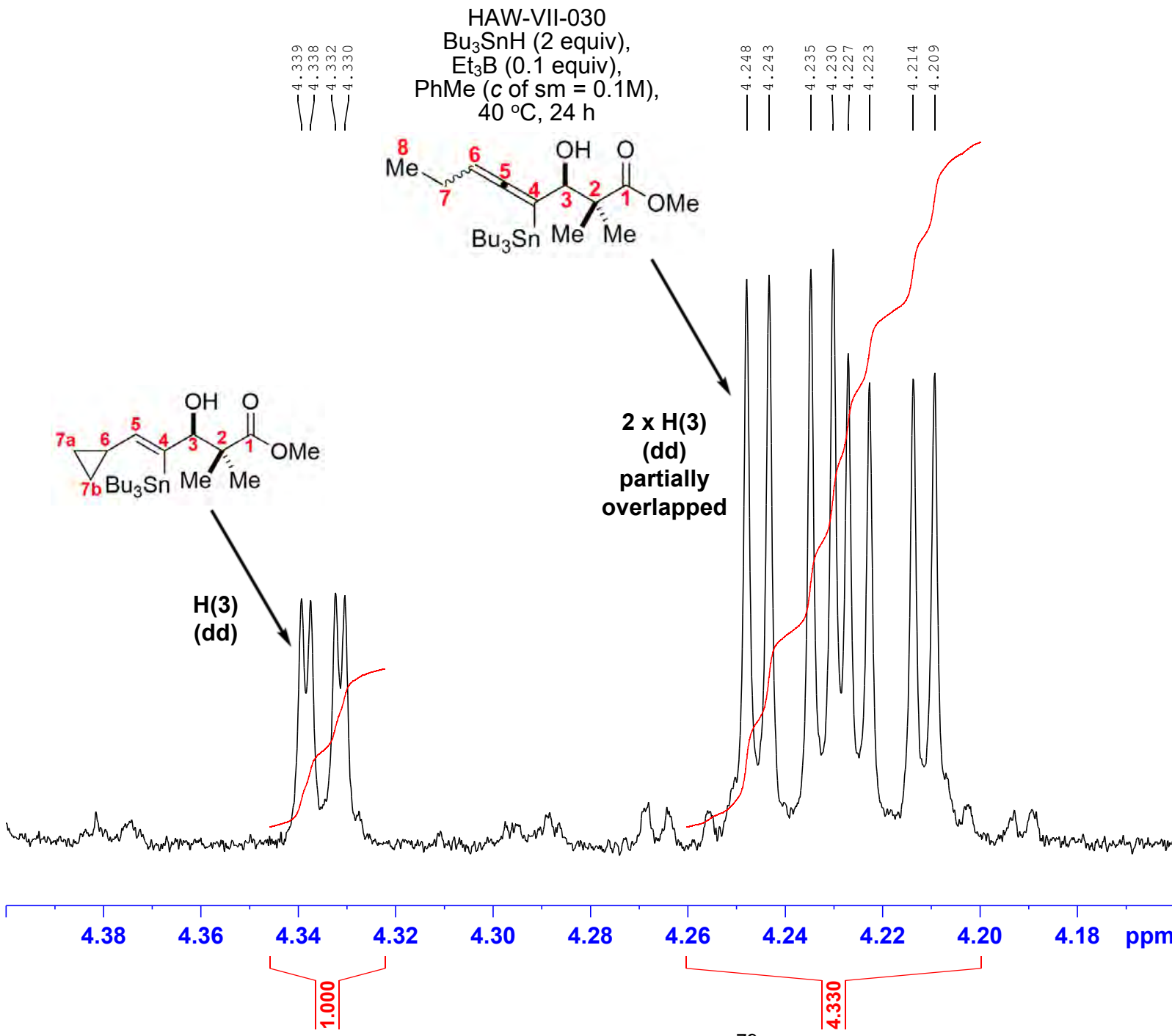


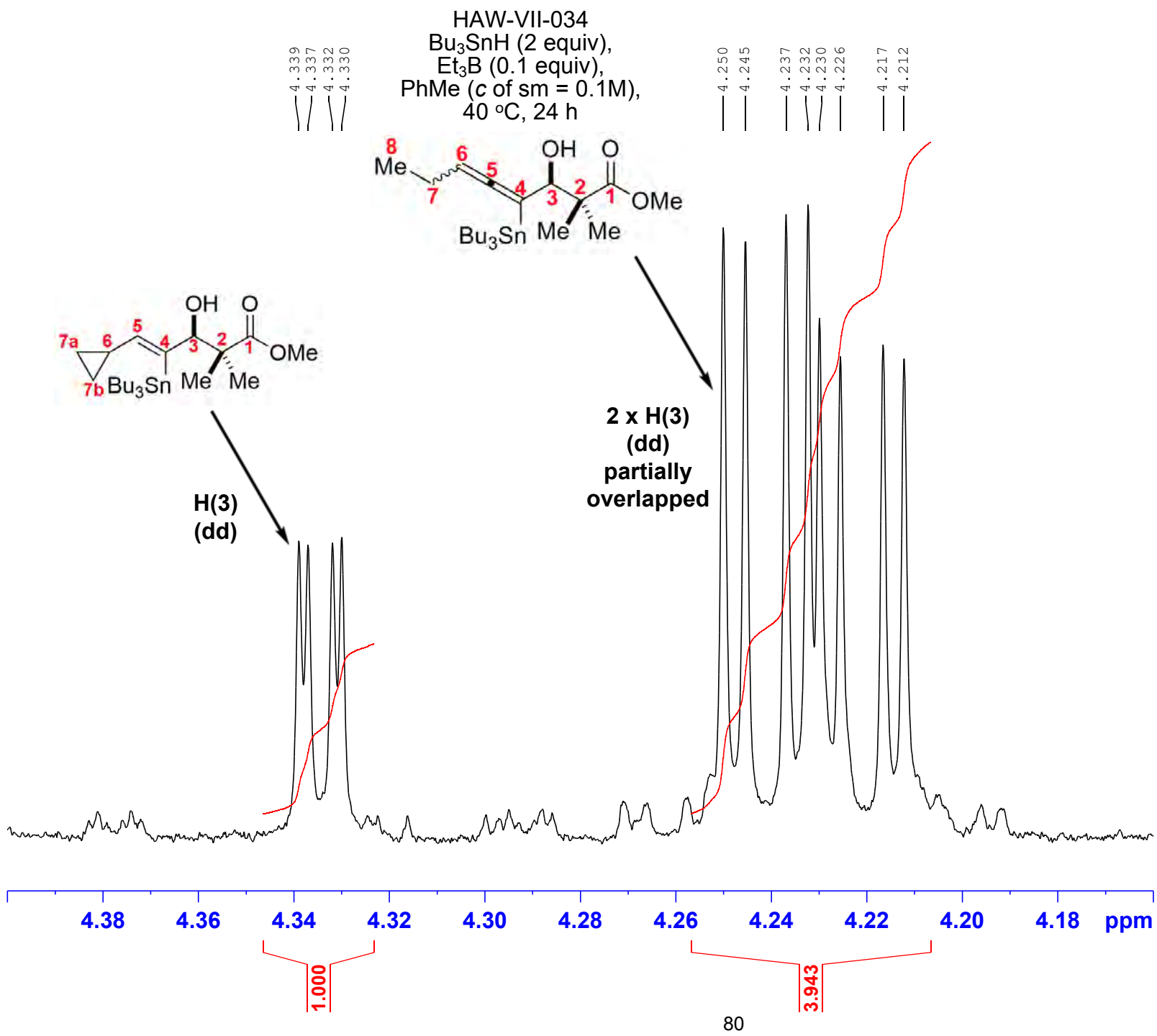
Current Data Parameters  
 NAME HAW-VII-030-C  
 EXPNO 10  
 PROCNO 1

F2 - Acquisition Parameters  
 Date 20191031  
 Time 15.11  
 INSTRUM spect  
 PROBHD 5 mm PABBO BB/  
 PULPROG zg30  
 TD 180286  
 SOLVENT CDCl3  
 NS 64  
 DS 0  
 SWH 18028.846 Hz  
 FIDRES 0.100001 Hz  
 AQ 4.9999318 sec  
 RG 97.5  
 DW 27.733 usec  
 DE 7.60 usec  
 TE 298.0 K  
 D1 0.10000000 sec  
 TD0 1

===== CHANNEL f1 =====  
 SFO1 600.1337060 MHz  
 NUC1 1H  
 P1 10.00 usec  
 PLW1 26.60000038 W

F2 - Processing parameters  
 SI 262144  
 SF 600.1300137 MHz  
 WDW EM  
 SSB 0  
 LB 0.10 Hz  
 GB 0  
 PC 1.00







Current Data Parameters  
NAME HAW-VII-034-C  
EXPNO 10  
PROCNO 1

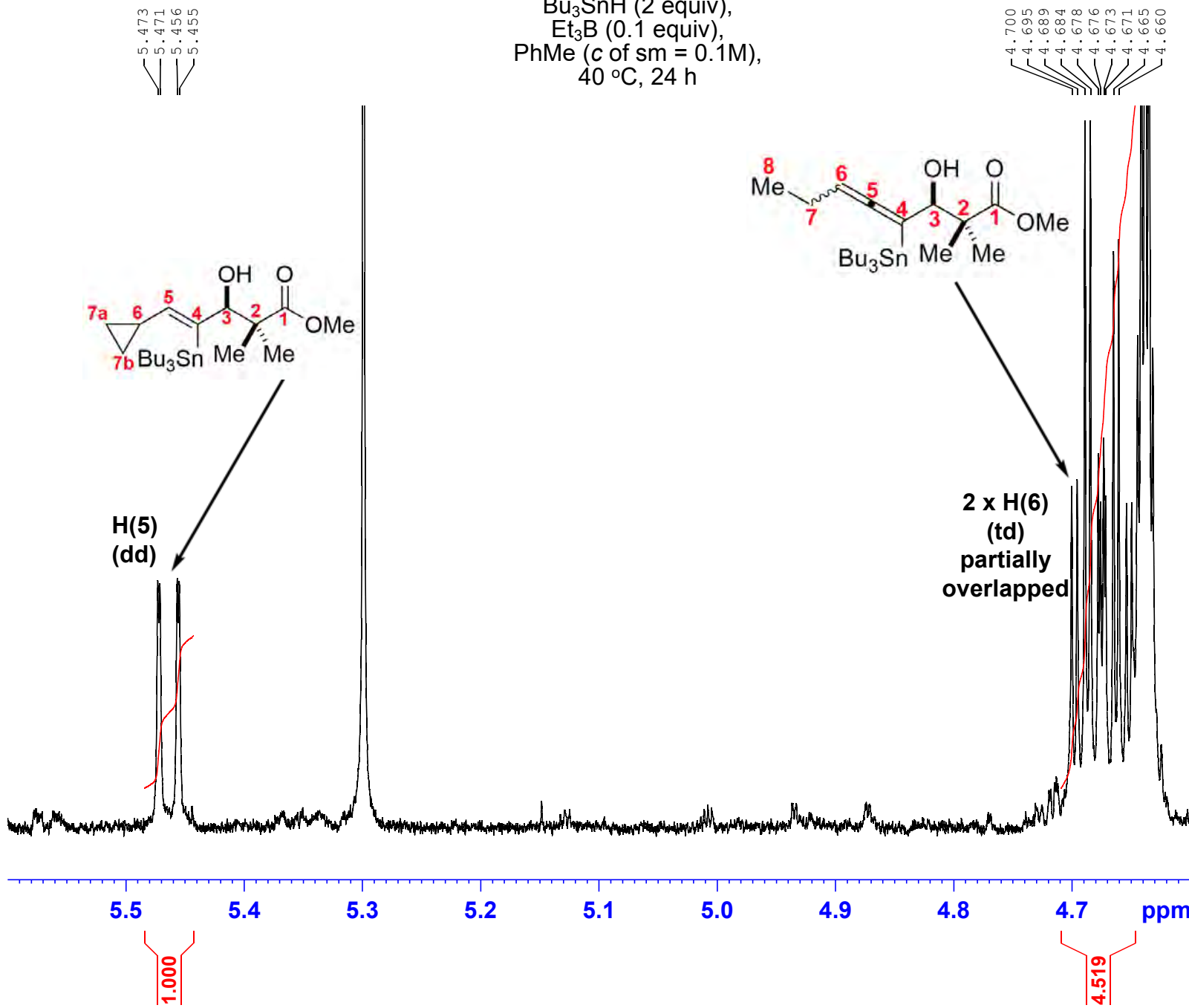
```

F2 - Acquisition Parameters
Date_           20191105
Time_          16.58
INSTRUM       spect
PROBHD      5 mm PABBO BB/
PULPROG     zg30
TD           180286
SOLVENT      CDC13
NS            64
DS             0
SWH          18028.846 Hz
FIDRES      0.100001 Hz
AQ           4.9999318 sec
RG            97.5
DW           27.733 usec
DE            7.60 usec
TE            300.0 K
D1          0.1000000 sec
TD0             1

```

===== CHANNEL f1 =====  
SFO1 600.1337060 MHz  
NUC1 1H  
P1 10.00 usec  
PLW1 26.60000038 W

F2 - Processing parameters  
SI 262144  
SF 600.1300129 MHz  
WDW EM  
SSB 0  
LB 0.10 Hz  
GB 0  
RG 1.00

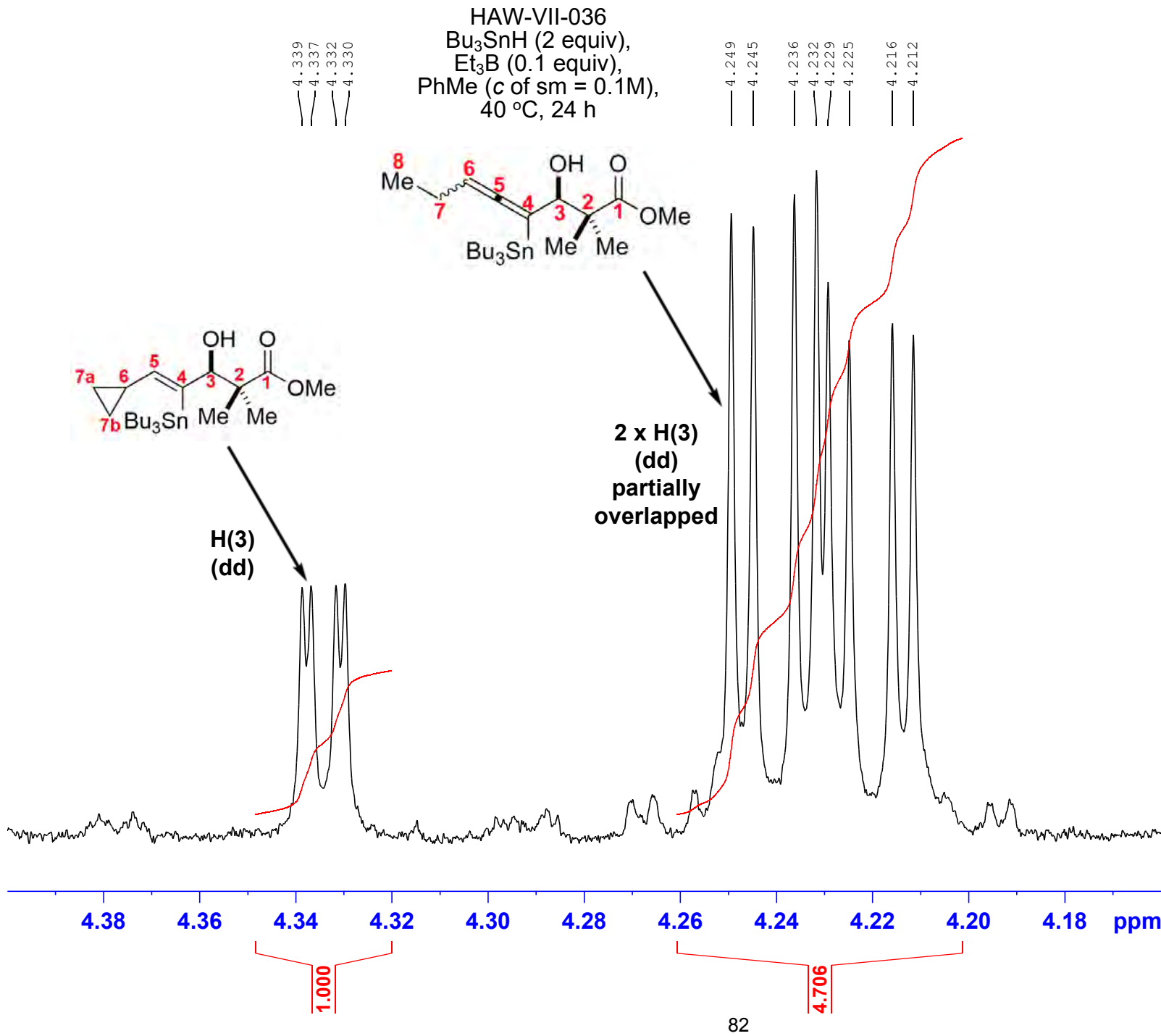


Current Data Parameters  
NAME HAW-VII-036-C  
EXPNO 20  
PROCNO 1

F2 - Acquisition Parameters  
Date 20191107  
Time 20.29  
INSTRUM spect  
PROBHD 5 mm PABBO BB/  
PULPROG zg30  
TD 180286  
SOLVENT CDCl3  
NS 64  
DS 0  
SWH 18028.846 Hz  
FIDRES 0.100001 Hz  
AQ 4.9999318 sec  
RG 97.5  
DW 27.733 usec  
DE 7.60 usec  
TE 300.0 K  
D1 0.10000000 sec  
TD0 1

===== CHANNEL f1 =====  
SFO1 600.1337060 MHz  
NUC1 1H  
P1 10.00 usec  
PLW1 26.60000038 W

F2 - Processing parameters  
SI 262144  
SF 600.1300136 MHz  
WDW EM  
SSB 0  
LB 0.10 Hz  
GB 0  
PC 1.00



Current Data Parameters  
NAME HAW-VII-036-C  
EXPNO 20  
PROCNO 1

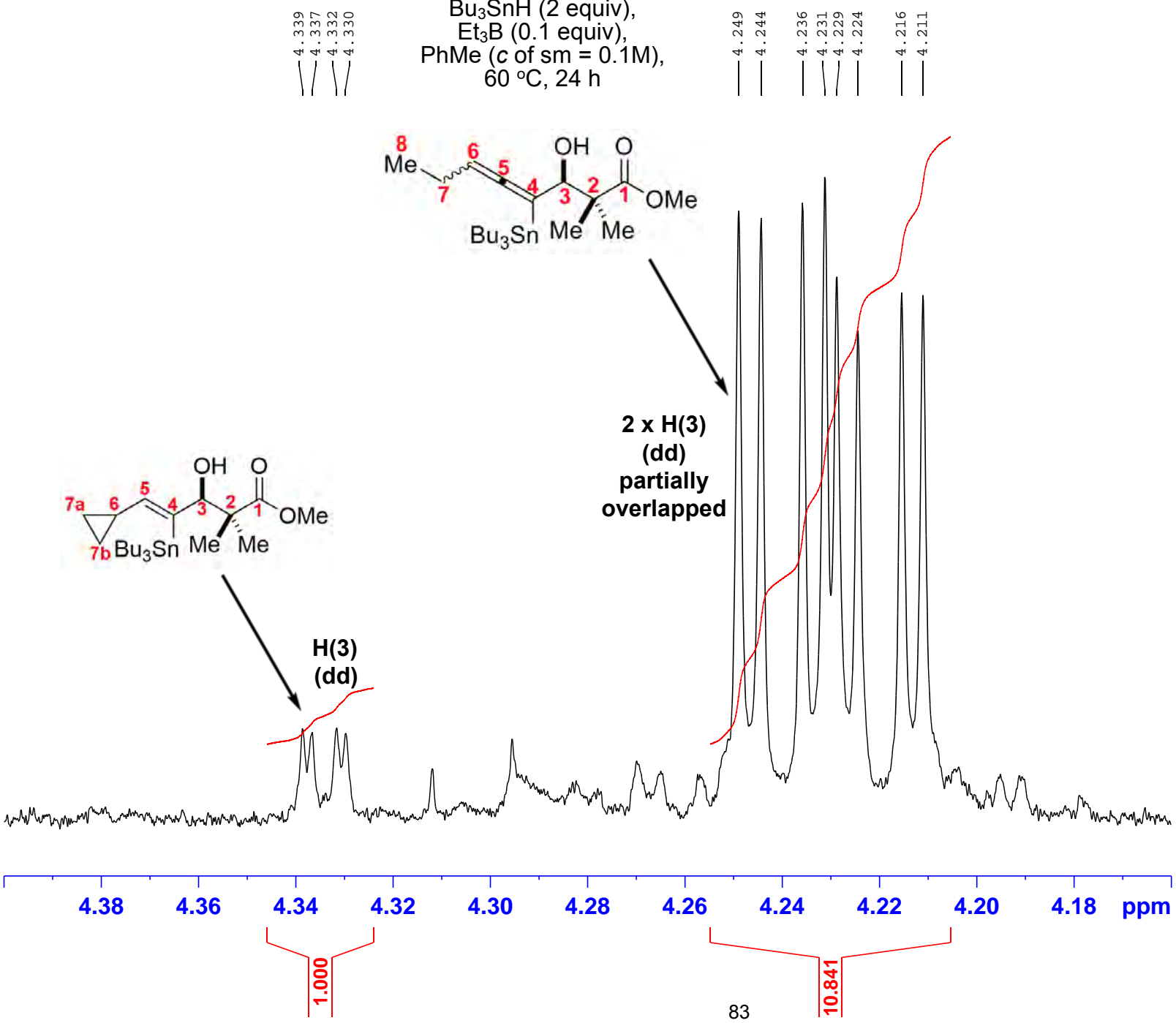
F2 - Acquisition Parameters  
Date 20191107  
Time 20.29  
INSTRUM spect  
PROBHD 5 mm PABBO BB/  
PULPROG zg30  
TD 180286  
SOLVENT CDCl3  
NS 64  
DS 0  
SWH 18028.846 Hz  
FIDRES 0.100001 Hz  
AQ 4.9999318 sec  
RG 97.5  
DW 27.733 usec  
DE 7.60 usec  
TE 300.0 K  
D1 0.10000000 sec  
TD0 1

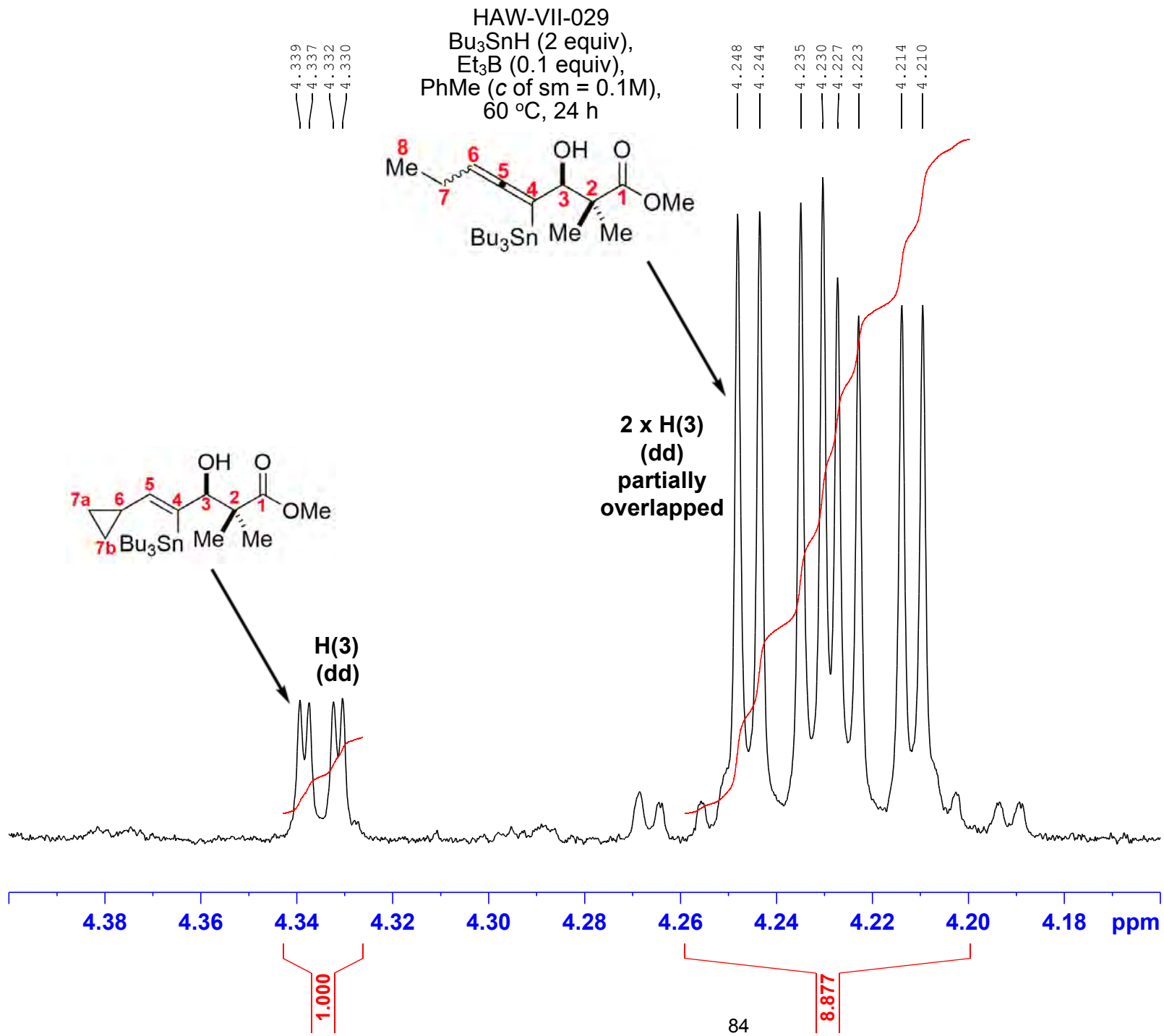
===== CHANNEL f1 =====  
SFO1 600.1337060 MHz  
NUC1 1H  
P1 10.00 usec  
PLW1 26.60000038 W

F2 - Processing parameters  
SI 262144  
SF 600.1300136 MHz  
WDW EM  
SSB 0  
LB 0.10 Hz  
GB 0  
PC 1.00



HAW-IV-029  
 $\text{Bu}_3\text{SnH}$  (2 equiv),  
 $\text{Et}_3\text{B}$  (0.1 equiv),  
 $\text{PhMe}$  ( $c$  of sm = 0.1M),  
60 °C, 24 h





Current Data Parameters  
NAME HAW-VII-029-C  
EXPNO 10  
PROCNO 1

```

F2 - Acquisition Parameters
Date_           20191031
Time_          15.03
INSTRUM       spect
PROBHD      5 mm PABBO BB/
PULPROG        zg30
TD              180286
SOLVENT        CDC13
NS                  64
DS                  0
SWH            18028.846 Hz
FIDRES        0.100001 Hz
AQ            4.9999318 sec
RG                 97.5
DW             27.733 used
DE                 7.60 used
TE                 298.0 K
D1            0.10000000 sec
TD0                      1

```

===== CHANNEL f1 =====  
SFO1 600.1337060 MHz  
NUC1 1H  
P1 10.00 usec  
PLW1 26.60000038 W

F2 - Processing parameters  
SI 262144  
SF 600.1300137 MHz  
WDW EM  
SSB 0  
LB 0.10 Hz  
GB 0  
PC 1.00

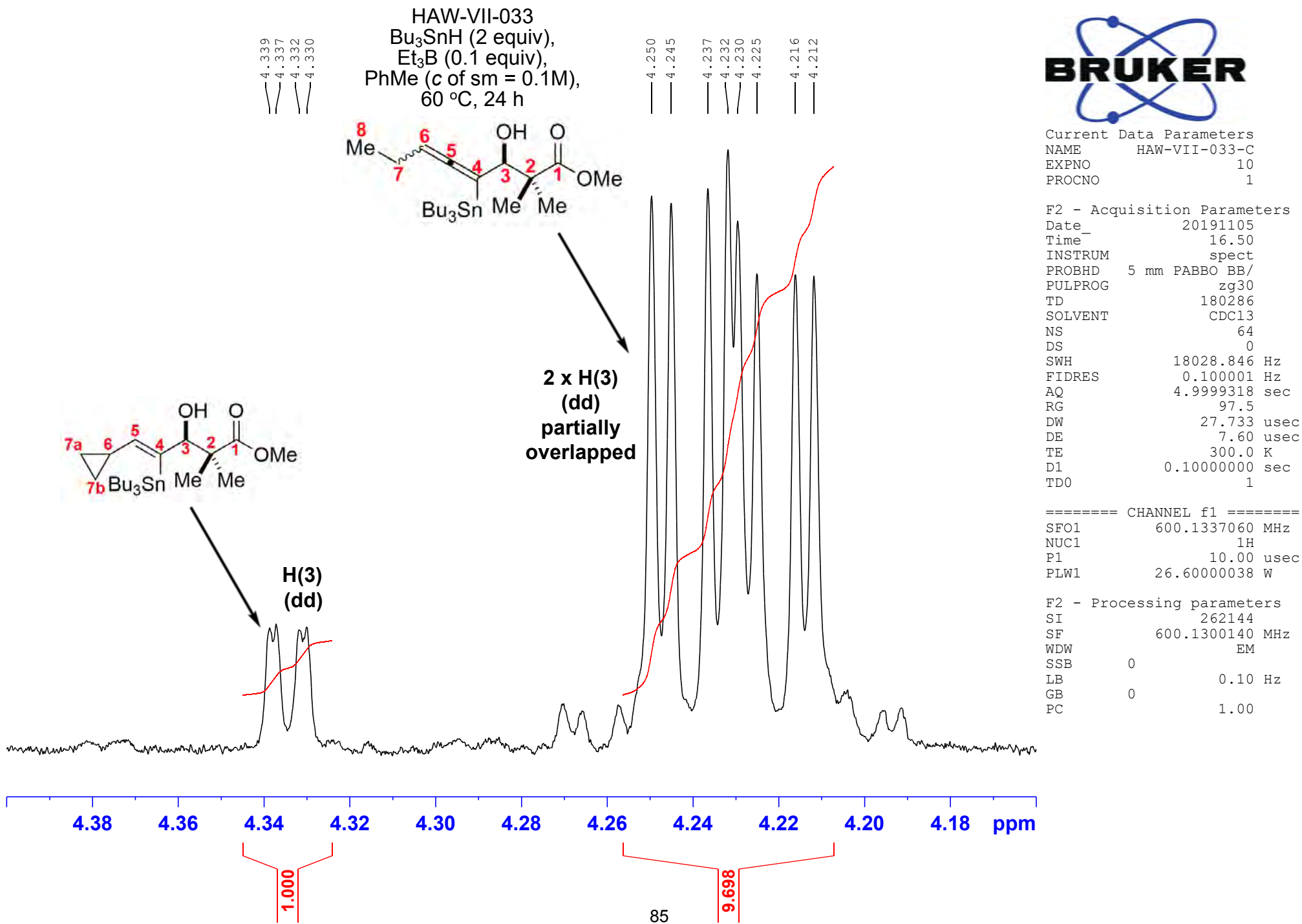


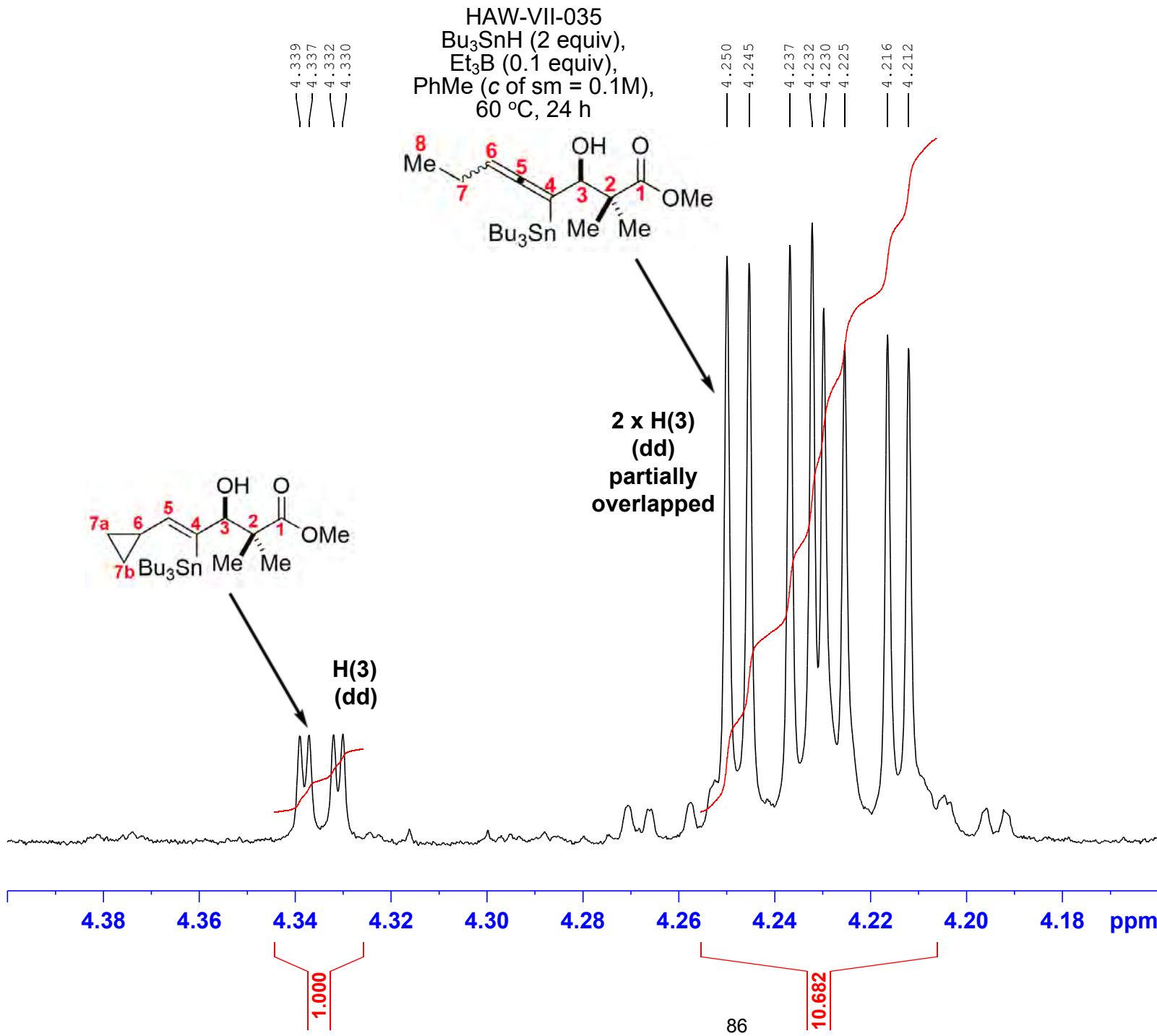
Current Data Parameters  
 NAME HAW-VII-033-C  
 EXPNO 10  
 PROCNO 1

F2 - Acquisition Parameters  
 Date 20191105  
 Time 16.50  
 INSTRUM spect  
 PROBHD 5 mm PABBO BB/  
 PULPROG zg30  
 TD 180286  
 SOLVENT CDCl3  
 NS 64  
 DS 0  
 SWH 18028.846 Hz  
 FIDRES 0.100001 Hz  
 AQ 4.9999318 sec  
 RG 97.5  
 DW 27.733 usec  
 DE 7.60 usec  
 TE 300.0 K  
 D1 0.10000000 sec  
 TD0 1

===== CHANNEL f1 =====  
 SFO1 600.1337060 MHz  
 NUC1 1H  
 P1 10.00 usec  
 PLW1 26.60000038 W

F2 - Processing parameters  
 SI 262144  
 SF 600.1300140 MHz  
 WDW EM  
 SSB 0  
 LB 0.10 Hz  
 GB 0  
 PC 1.00





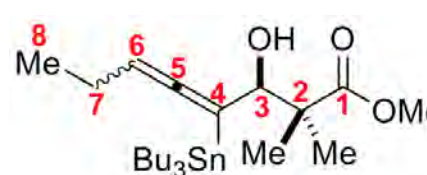
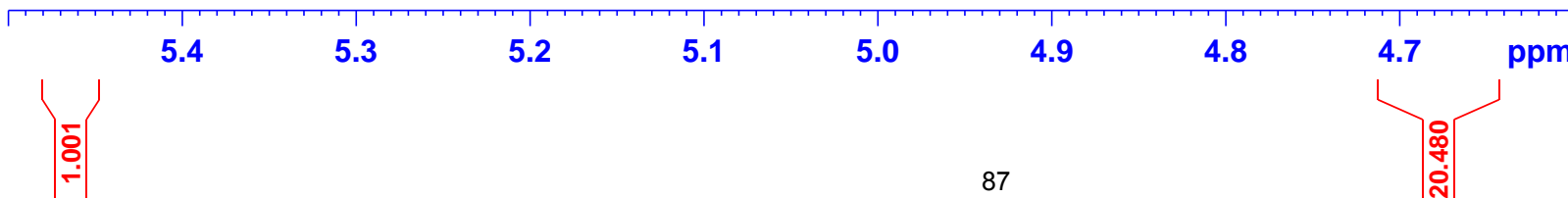
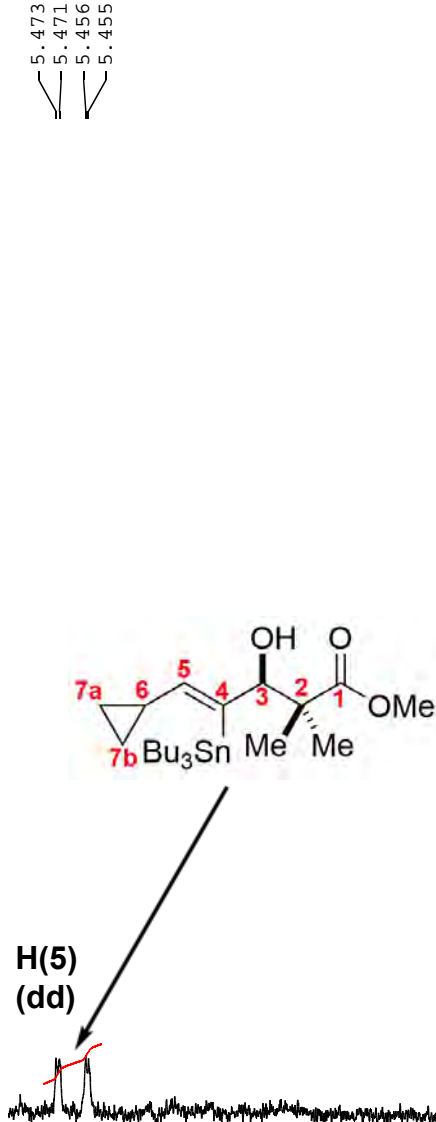
Current Data Parameters  
NAME HAW-VII-035-C  
EXPNO 20  
PROCNO 1

F2 - Acquisition Parameters  
Date 20191108  
Time 9.32  
INSTRUM spect  
PROBHD 5 mm PABBO BB/  
PULPROG zg30  
TD 180286  
SOLVENT CDCl3  
NS 64  
DS 0  
SWH 18028.846 Hz  
FIDRES 0.100001 Hz  
AQ 4.9999318 sec  
RG 97.5  
DW 27.733 usec  
DE 7.60 usec  
TE 300.0 K  
D1 0.10000000 sec  
TD0 1

===== CHANNEL f1 =====  
SFO1 600.1337060 MHz  
NUC1 1H  
P1 10.00 usec  
PLW1 26.60000038 W

F2 - Processing parameters  
SI 262144  
SF 600.1300131 MHz  
WDW EM  
SSB 0  
LB 0.10 Hz  
GB 0  
PC 1.00

HAW-III-005  
 Bu<sub>3</sub>SnH (2 equiv),  
 Et<sub>3</sub>B (0.1 equiv),  
 PhMe (c of sm = 0.1M),  
 80 °C, 24 h



**2 x H(6)  
(td)  
partially  
overlapped**

4.702  
4.698  
4.691  
4.686  
4.680  
4.677  
4.675  
4.673  
4.666  
4.662  
4.655

Current Data Parameters  
NAME HAW-III-005-C  
EXPNO 10  
PROCNO 1

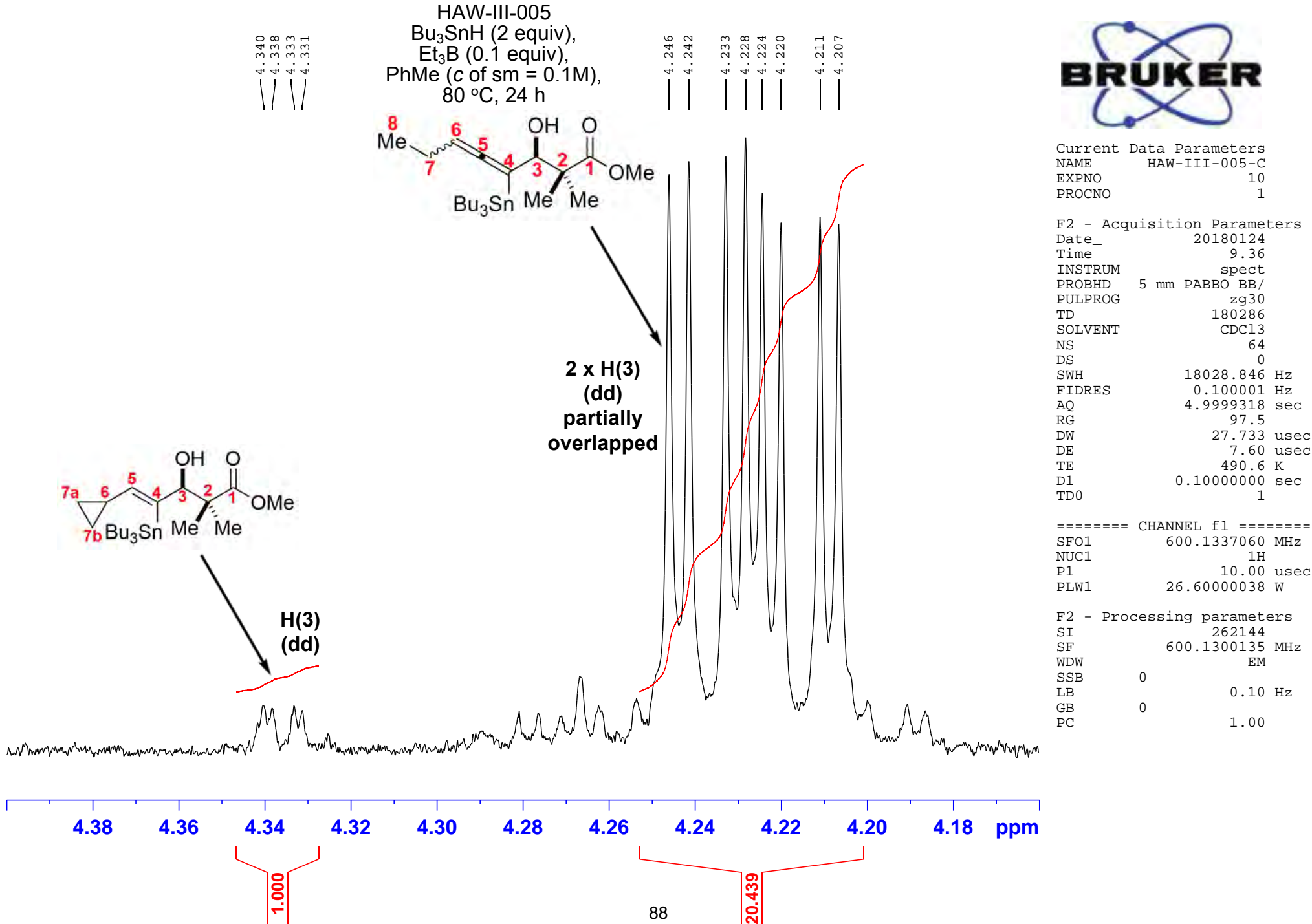
```

F2 - Acquisition Parameters
Date_          20180124
Time           9.36
INSTRUM       spect
PROBHD        5 mm PABBO BB/
PULPROG       zg30
TD            180286
SOLVENT        CDCl3
NS             64
DS              0
SWH           18028.846 Hz
FIDRES        0.100001 Hz
AQ            4.9999318 sec
RG             97.5
DW            27.733 usec
DE             7.60 usec
TE             490.6 K
D1           0.10000000 sec
TD0                  1

```

```
===== CHANNEL f1 ======  
SFO1      600.1337060 MHz  
NUC1          1H  
P1           10.00 usec  
PLW1      26.60000038 W
```

F2 - Processing parameters  
SI 262144  
SF 600.1300135 MHz  
WDW EM  
SSB 0  
LB 0.10 Hz  
GB 0  
PC 1.00



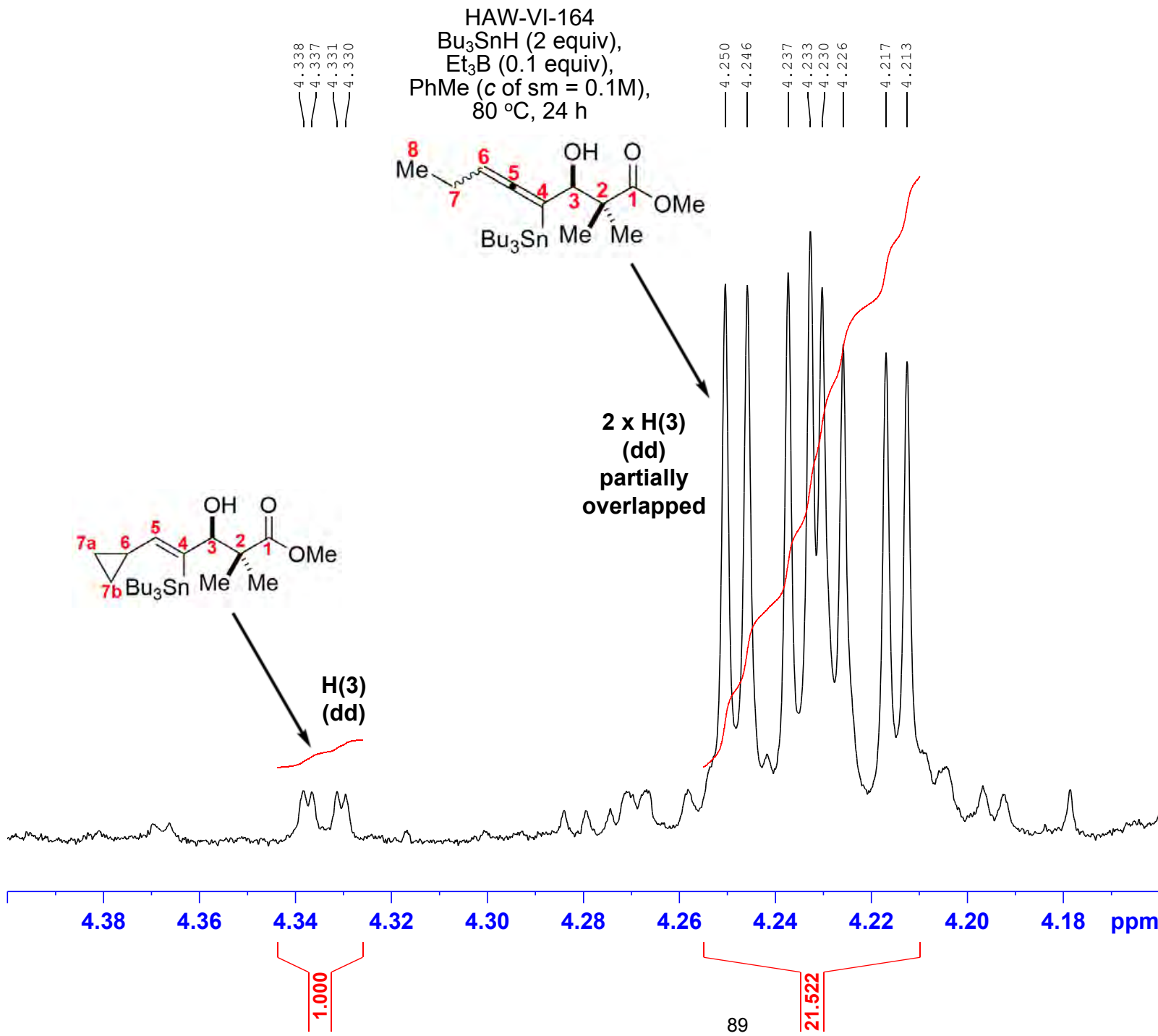


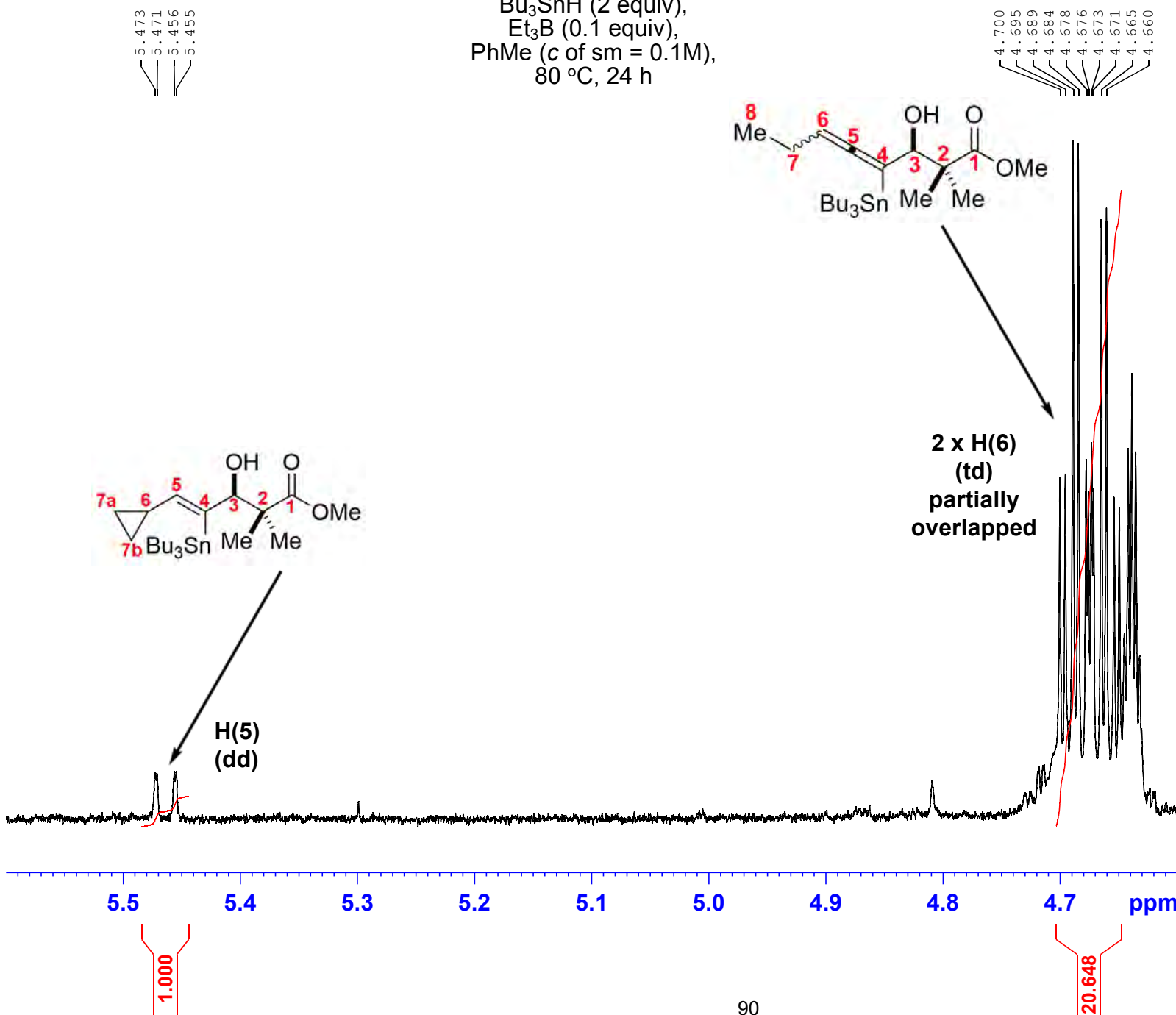
Current Data Parameters  
 NAME HAW-VI-164-C  
 EXPNO 20  
 PROCNO 1

F2 - Acquisition Parameters  
 Date 20190905  
 Time 16.08  
 INSTRUM spect  
 PROBHD 5 mm PABBO BB/  
 PULPROG zg30  
 TD 180286  
 SOLVENT CDCl3  
 NS 64  
 DS 0  
 SWH 18028.846 Hz  
 FIDRES 0.100001 Hz  
 AQ 4.9999318 sec  
 RG 97.5  
 DW 27.733 usec  
 DE 7.60 usec  
 TE 300.0 K  
 D1 0.10000000 sec  
 TD0 1

===== CHANNEL f1 =====  
 SFO1 600.1337060 MHz  
 NUC1 1H  
 P1 10.00 usec  
 PLW1 26.60000038 W

F2 - Processing parameters  
 SI 262144  
 SF 600.1300137 MHz  
 WDW EM  
 SSB 0  
 LB 0  
 GB 0.10 Hz  
 PC 1.00





Current Data Parameters  
NAME HAW-VII-003-C  
EXPNO 10  
PROCNO 1

F2 - Acquisition Parameters  
Date 20190927  
Time 15.18  
INSTRUM spect  
PROBHD 5 mm PABBO BB/  
PULPROG zg30  
TD 180286  
SOLVENT CDCl3  
NS 64  
DS 0  
SWH 18028.846 Hz  
FIDRES 0.100001 Hz  
AQ 4.9999318 sec  
RG 97.5  
DW 27.733 usec  
DE 7.60 usec  
TE 300.0 K  
D1 0.10000000 sec  
TD0 1

===== CHANNEL f1 =====  
SFO1 600.1337060 MHz  
NUC1 1H  
P1 10.00 usec  
PLW1 26.60000038 W

F2 - Processing parameters  
SI 262144  
SF 600.1300147 MHz  
WDW EM  
SSB 0  
LB 0.10 Hz  
GB 0  
PC 1.00

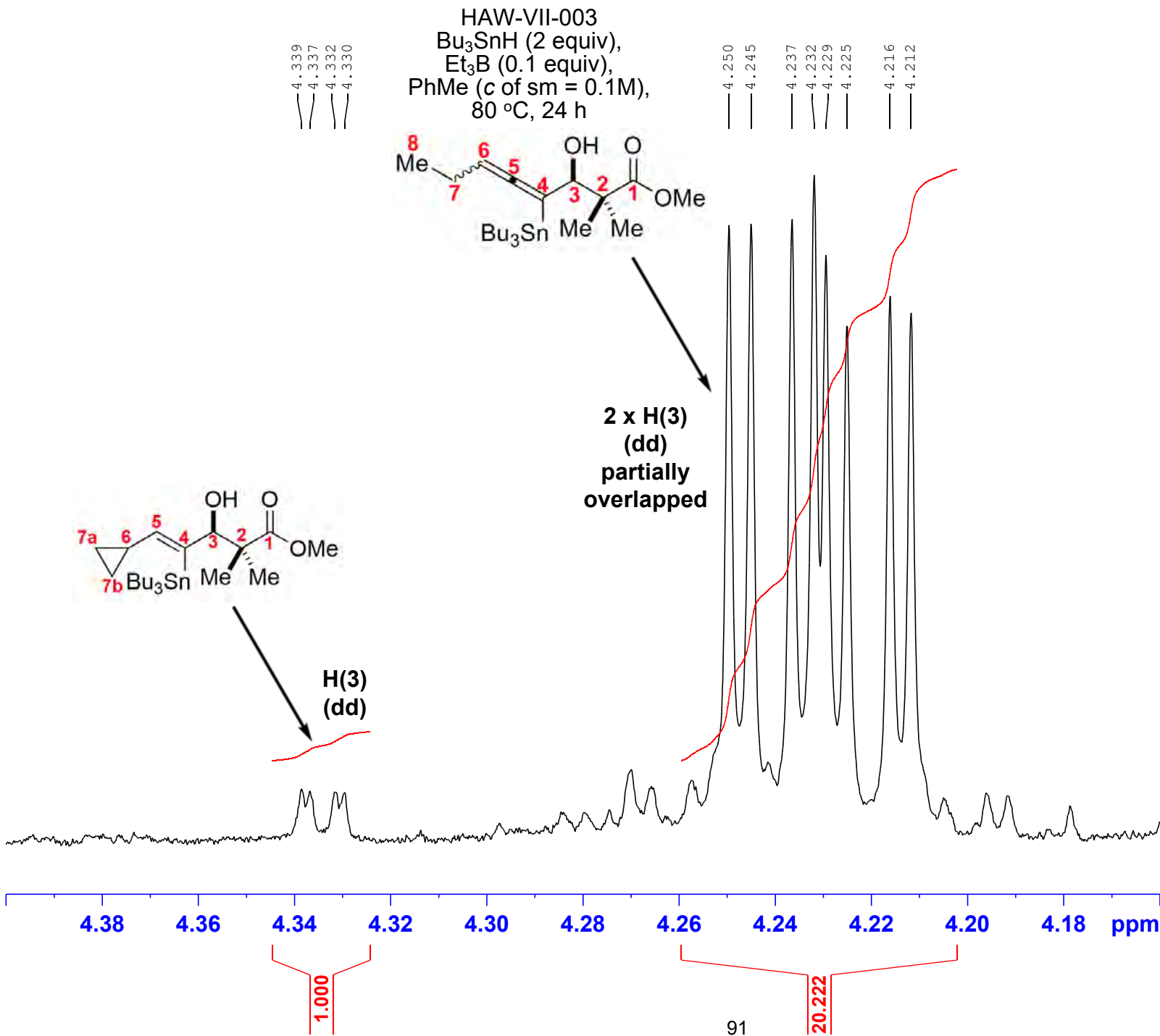


Current Data Parameters  
 NAME HAW-VII-003-C  
 EXPNO 10  
 PROCNO 1

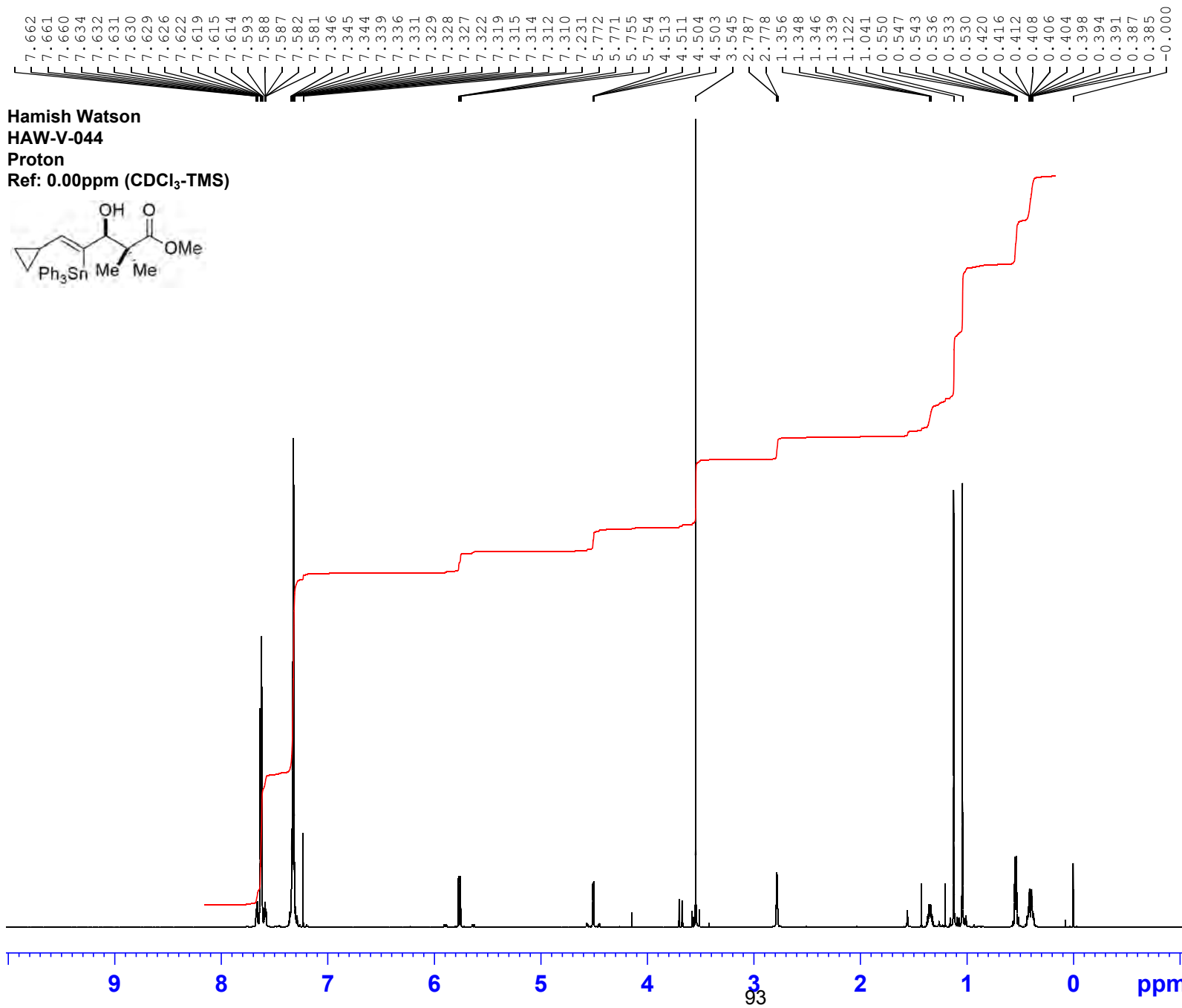
F2 - Acquisition Parameters  
 Date 20190927  
 Time 15.18  
 INSTRUM spect  
 PROBHD 5 mm PABBO BB/  
 PULPROG zg30  
 TD 180286  
 SOLVENT CDCl3  
 NS 64  
 DS 0  
 SWH 18028.846 Hz  
 FIDRES 0.100001 Hz  
 AQ 4.9999318 sec  
 RG 97.5  
 DW 27.733 usec  
 DE 7.60 usec  
 TE 300.0 K  
 D1 0.10000000 sec  
 TD0 1

===== CHANNEL f1 =====  
 SFO1 600.1337060 MHz  
 NUC1 1H  
 P1 10.00 usec  
 PLW1 26.60000038 W

F2 - Processing parameters  
 SI 262144  
 SF 600.1300147 MHz  
 WDW EM  
 SSB 0  
 LB 0.10 Hz  
 GB 0  
 PC 1.00



**Part D. The 600.13 MHz  $^1\text{H}$  NMR and 150.90 MHz  $^{13}\text{C}$  NMR Spectra of the Triphenylstannylvinyltin 5b and Triphenylstannylallene 4b in  $\text{CDCl}_3$**

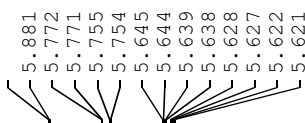


Current Data Parameters  
 NAME HAW-V-Ph3Sn\_Probe-(2)  
 EXPNO 20  
 PROCNO 1

F2 - Acquisition Parameters  
 Date 20181127  
 Time 17.26  
 INSTRUM spect  
 PROBHD 5 mm PABBO BB/  
 PULPROG zg30  
 TD 180286  
 SOLVENT CDCl<sub>3</sub>  
 NS 64  
 DS 0  
 SWH 18028.846 Hz  
 FIDRES 0.100001 Hz  
 AQ 4.9999318 sec  
 RG 34.91  
 DW 27.733 usec  
 DE 7.60 usec  
 TE 300.0 K  
 D1 0.10000000 sec  
 TDO 1

===== CHANNEL f1 ======  
 SF01 600.1337060 MHz  
 NUC1 1H  
 P1 10.00 usec  
 PLW1 26.60000038 W

F2 - Processing parameters  
 SI 262144  
 SF 600.1300317 MHz  
 WDW EM  
 SSB 0  
 LB 0.10 Hz  
 GB 0  
 PC 1.00

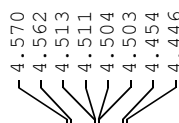
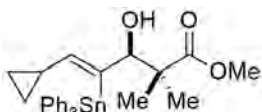


**Hamish Watson**

**HAW-V-044**

**Proton**

**Ref: 0.00ppm (CDCl<sub>3</sub>-TMS)**

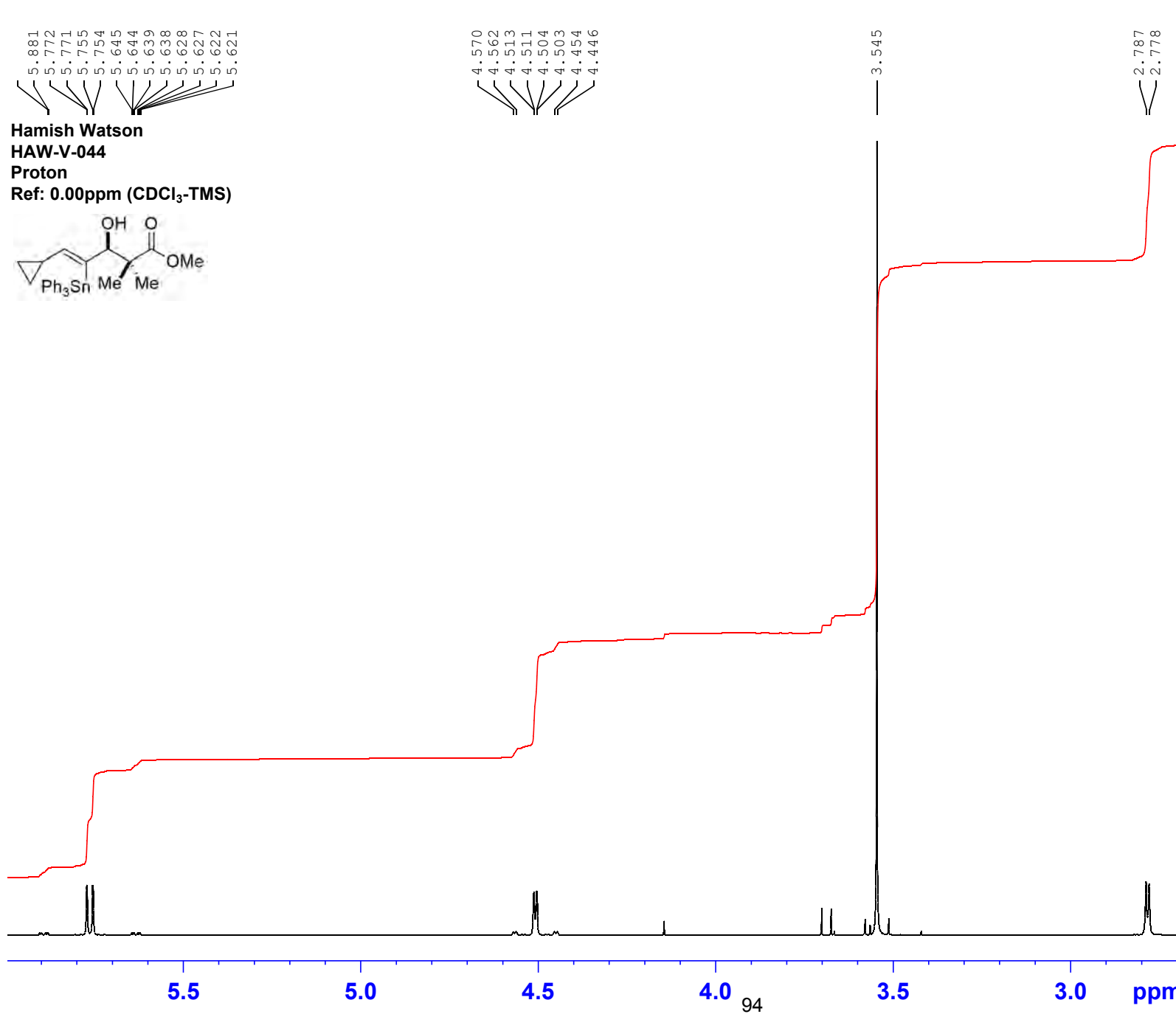


**Hamish Watson**

**HAW-V-044**

**Proton**

**Ref: 0.00ppm (CDCl<sub>3</sub>-TMS)**



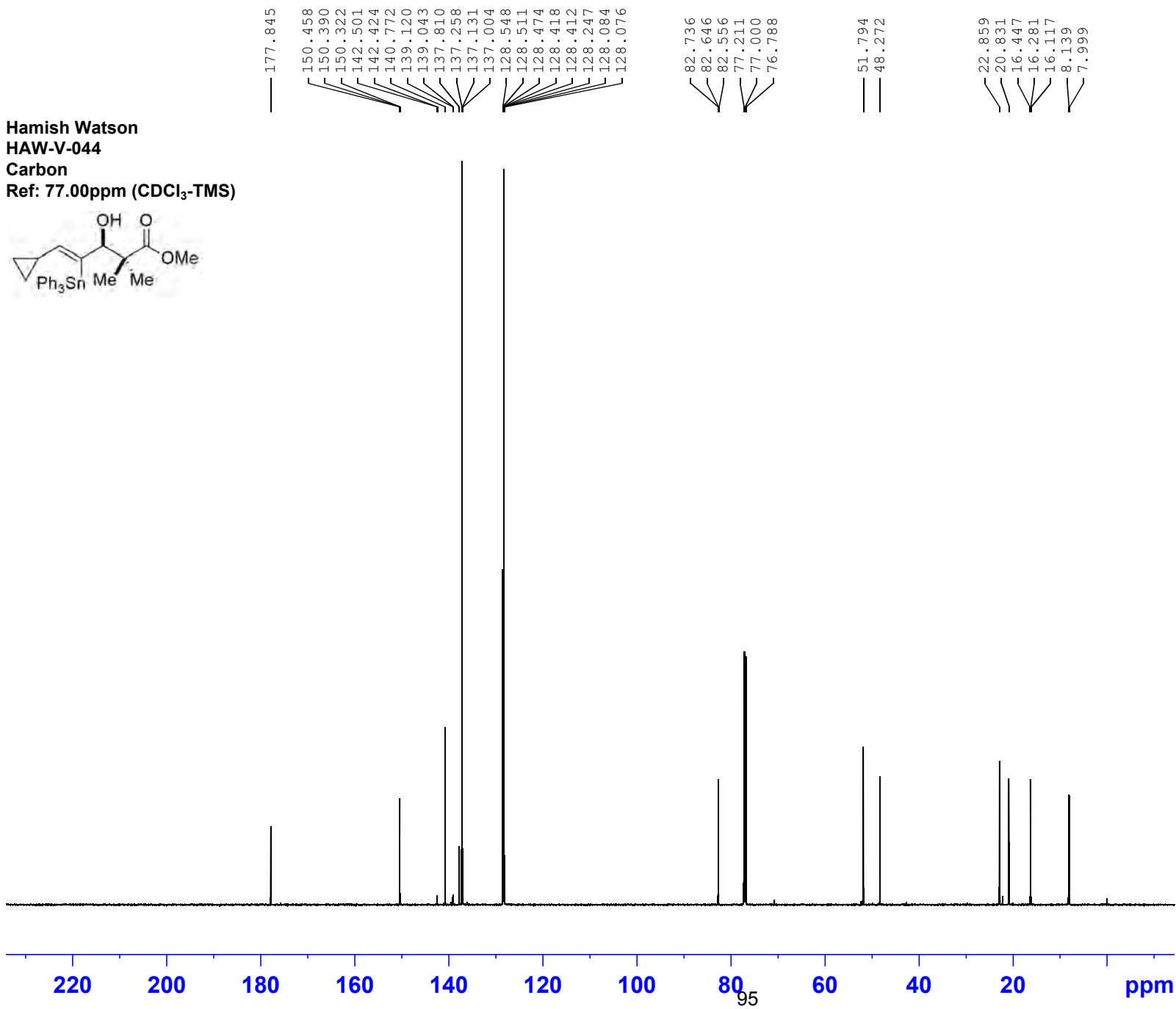
Current Data Parameters  
NAME HAW-V-Ph3Sn\_Probe-(2)  
EXPNO 20  
PROCNO 1

F2 - Acquisition Parameters  
Date 20181127  
Time 17.26  
INSTRUM spect  
PROBHD 5 mm PABBO BB/  
PULPROG zg30  
TD 180286  
SOLVENT CDCl3  
NS 64  
DS 0  
SWH 18028.846 Hz  
FIDRES 0.100001 Hz  
AQ 4.9999318 sec  
RG 34.91  
DW 27.733 usec  
DE 7.60 usec  
TE 300.0 K  
D1 0.10000000 sec  
TD0 1

===== CHANNEL f1 ======

SFO1 600.1337060 MHz  
NUC1 1H  
P1 10.00 usec  
PLW1 26.60000038 W

F2 - Processing parameters  
SI 262144  
SF 600.1300317 MHz  
WDW EM  
SSB 0  
LB 0.10 Hz  
GB 0  
PC 1.00



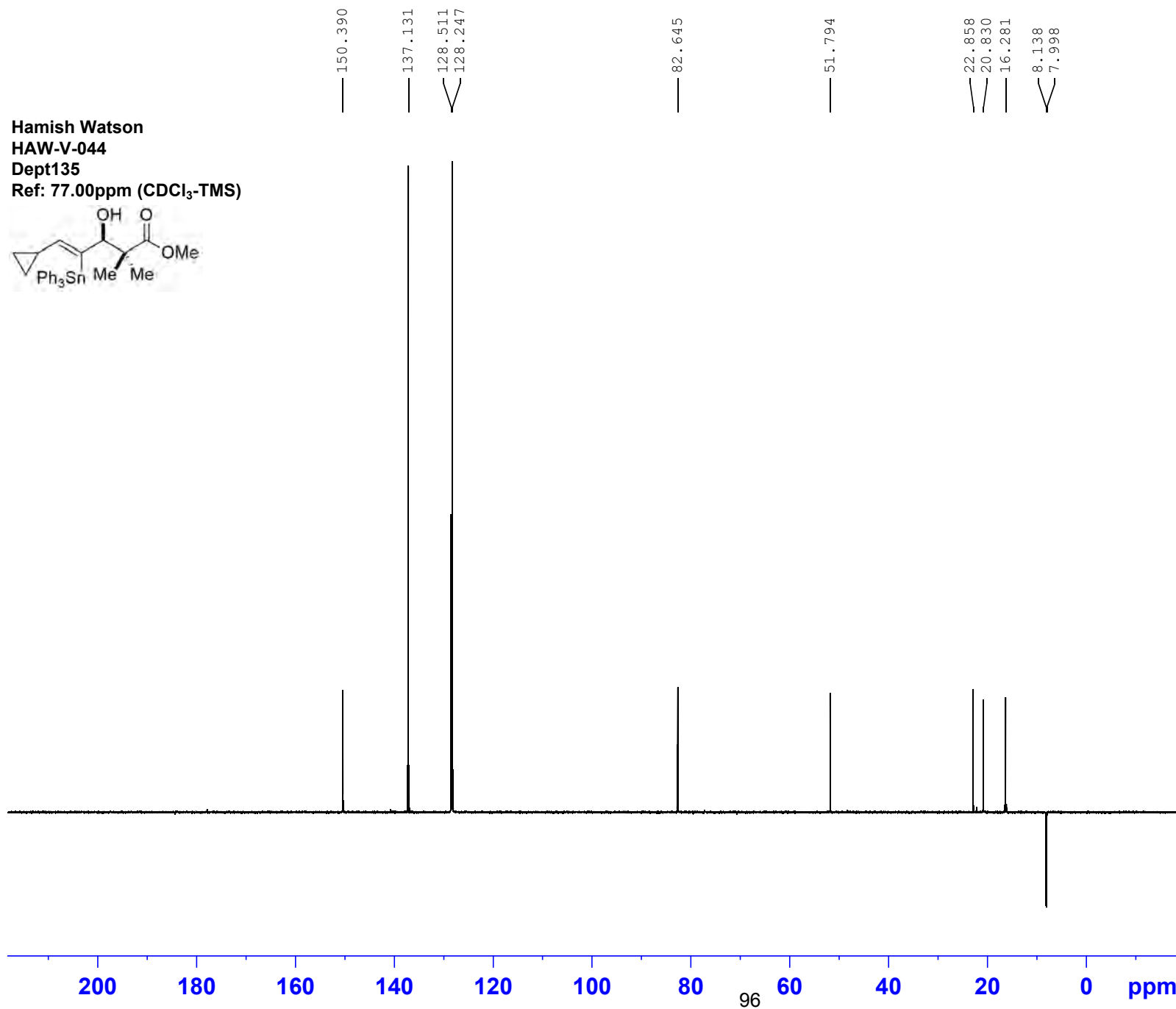
**Current Data Parameters**  
**NAME HAW-V-Ph3Sn\_Probe-(2)**  
**EXPNO 21**  
**PROCNO 1**

**F2 - Acquisition Parameters**  
**Date 20181127**  
**Time 18.12**  
**INSTRUM spect**  
**PROBHD 5 mm PABBO BB/**  
**PULPROG zpg30**  
**TD 119044**  
**SOLVENT CDCl<sub>3</sub>**  
**NS 1024**  
**DS 4**  
**SWH 37500.000 Hz**  
**FIDRES 0.315010 Hz**  
**AQ 1.5872533 sec**  
**RG 186.92**  
**DW 13.333 usec**  
**DE 7.73 usec**  
**TE 300.0 K**  
**D1 1.00000000 sec**  
**D11 0.03000000 sec**  
**TD0 1**

**===== CHANNEL f1 =====**  
**SFO1 150.9194058 MHz**  
**NUC1 <sup>13</sup>C**  
**P1 11.80 usec**  
**PLW1 85.00000000 W**

**===== CHANNEL f2 =====**  
**SFO2 600.1324005 MHz**  
**NUC2 <sup>1</sup>H**  
**CPDPRG[2] waltz64**  
**PCPD2 80.00 usec**  
**PLW2 27.00000000 W**  
**PLW12 0.43891999 W**  
**PLW13 0.28090999 W**

**F2 - Processing parameters**  
**SI 131072**  
**SF 150.9028187 MHz**  
**WDW EM**  
**SSB 0**  
**LB 1.00 Hz**  
**GB 0**  
**PC 1.40**



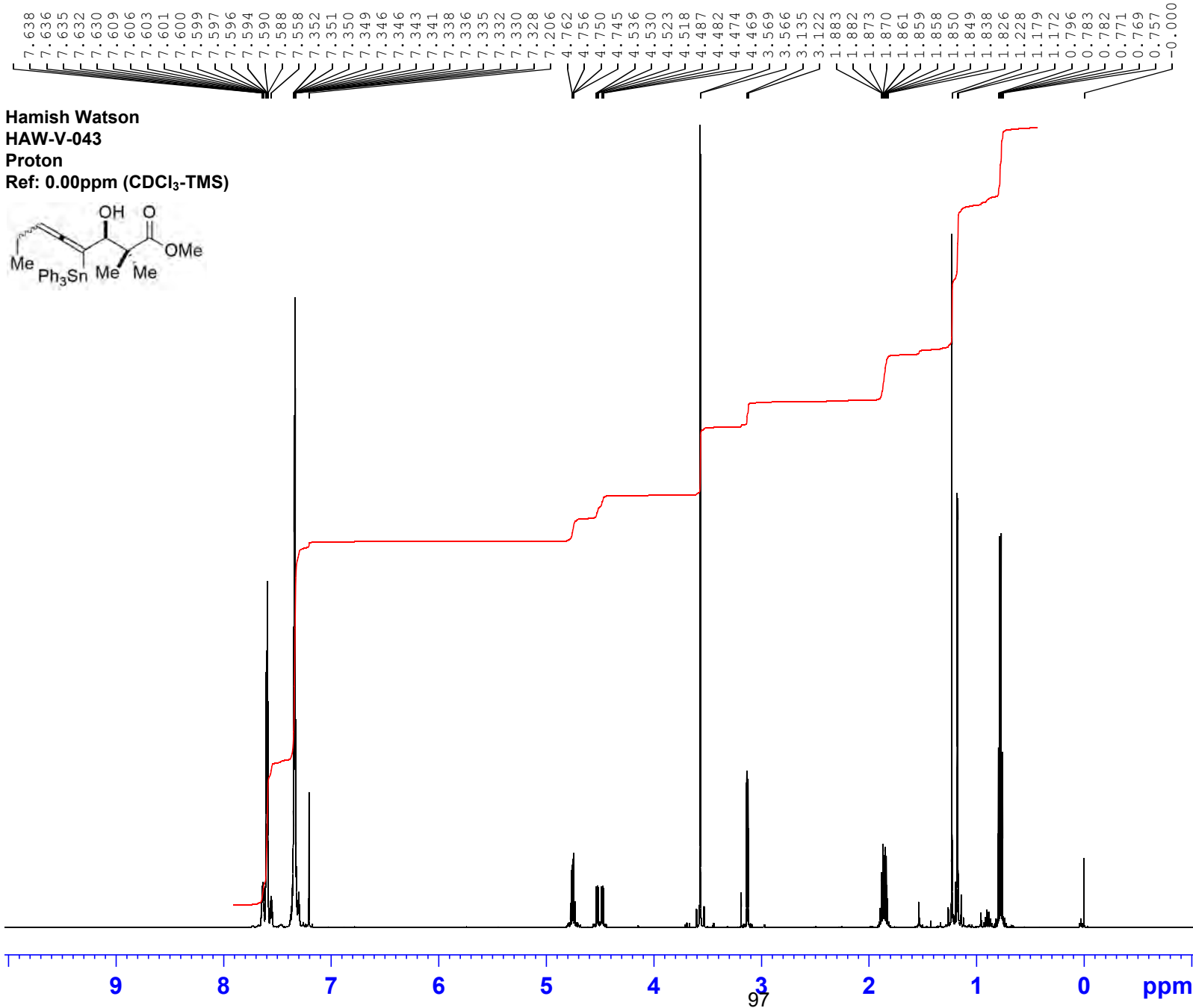
Current Data Parameters  
 NAME HAW-V-Ph3Sn\_Probe-(2)  
 EXPNO 22  
 PROCNO 1

F2 - Acquisition Parameters  
 Date 20181127  
 Time 22.27  
 INSTRUM spect  
 PROBHD 5 mm PABBO BB/  
 PULPROG deptsp135.b  
 TD 119044  
 SOLVENT CDCl<sub>3</sub>  
 NS 256  
 DS 4  
 SWH 35714.285 Hz  
 FIDRES 0.300009 Hz  
 AQ 1.6666160 sec  
 RG 186.92  
 DW 14.000 usec  
 DE 7.44 usec  
 TE 300.0 K  
 CNST2 145.0000000  
 D1 1.0000000 sec  
 D2 0.00344828 sec  
 D12 0.00002000 sec  
 TDO 1

===== CHANNEL f1 =====  
 SFO1 150.9178962 MHz  
 NUC1 <sup>13</sup>C  
 P1 11.80 usec  
 P13 2000.00 usec  
 PLW0 0 W  
 PLW1 85.00000000 W  
 SPNAM[5] Crp60comp.4  
 SPOAL5 0.500  
 SPOFFS5 0 Hz  
 SPW5 18.08300018 W

===== CHANNEL f2 =====  
 SFO2 600.1324005 MHz  
 NUC2 <sup>1</sup>H  
 CPDPRG[2] waltz64  
 P3 10.20 usec  
 P4 20.40 usec  
 PCPD2 80.00 usec  
 PLW2 27.00000000 W  
 PLW12 0.43891999 W

F2 - Processing parameters  
 SI 131072  
 SF 150.9028188 MHz  
 WDW EM  
 SSB 0  
 LB 1.00 Hz  
 GB 0  
 PC 1.40

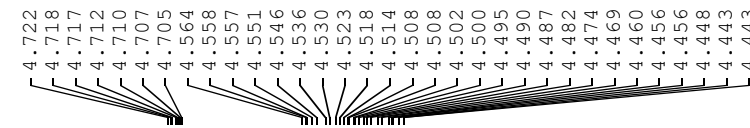


Current Data Parameters  
 NAME HAW-V-Ph3Sn\_Probe-(1)  
 EXPNO 10  
 PROCNO 1

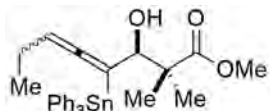
F2 - Acquisition Parameters  
 Date\_ 20181127  
 Time\_ 15.00  
 INSTRUM spect  
 PROBHD 5 mm PABBO BB/  
 PULPROG zg30  
 TD 180286  
 SOLVENT CDCl<sub>3</sub>  
 NS 64  
 DS 0  
 SWH 18028.846 Hz  
 FIDRES 0.100001 Hz  
 AQ 4.9999318 sec  
 RG 25.17  
 DW 27.733 usec  
 DE 7.60 usec  
 TE 300.0 K  
 D1 0.10000000 sec  
 TDO 1

===== CHANNEL f1 ======  
 SF01 600.1337060 MHz  
 NUC1 1H  
 P1 10.00 usec  
 PLW1 26.60000038 W

F2 - Processing parameters  
 SI 262144  
 SF 600.1300463 MHz  
 WDW EM  
 SSB 0  
 LB 0.10 Hz  
 GB 0  
 PC 1.00



Hamish Watson  
HAW-V-043  
Proton  
Ref: 0.00ppm (CDCl<sub>3</sub>-TMS)

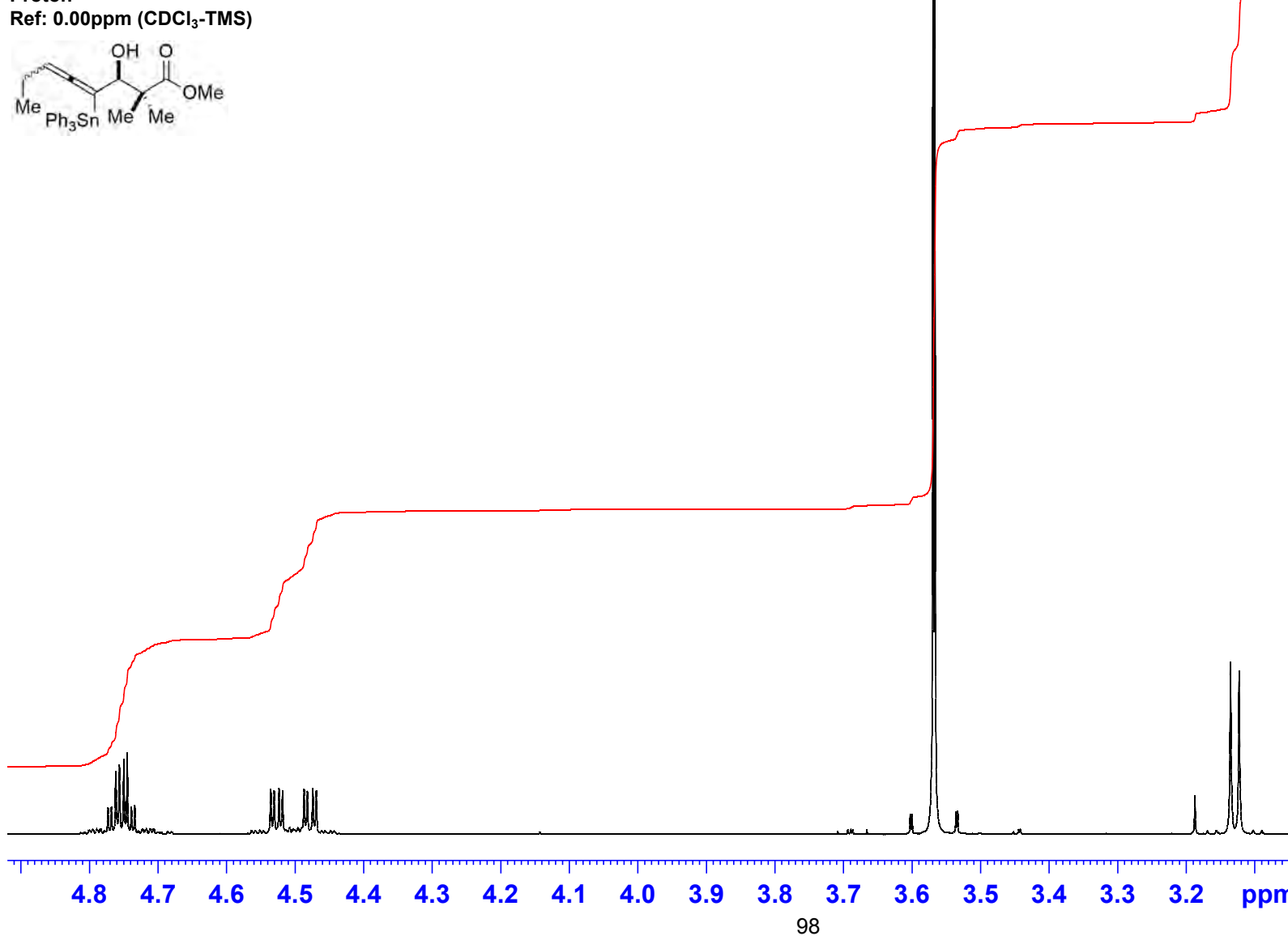


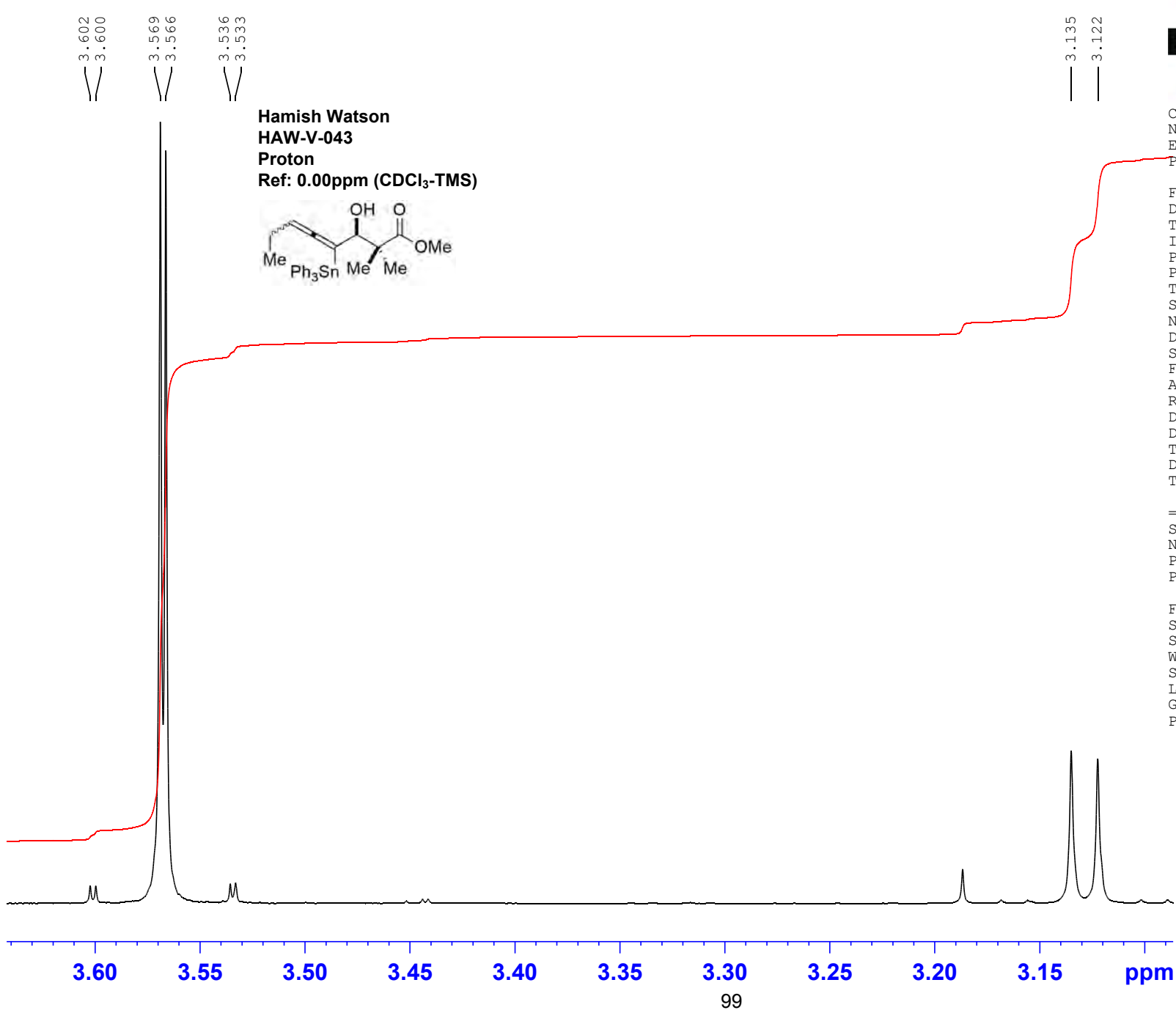
Current Data Parameters  
NAME HAW-V-Ph3Sn\_Probe-(1)  
EXPNO 10  
PROCNO 1

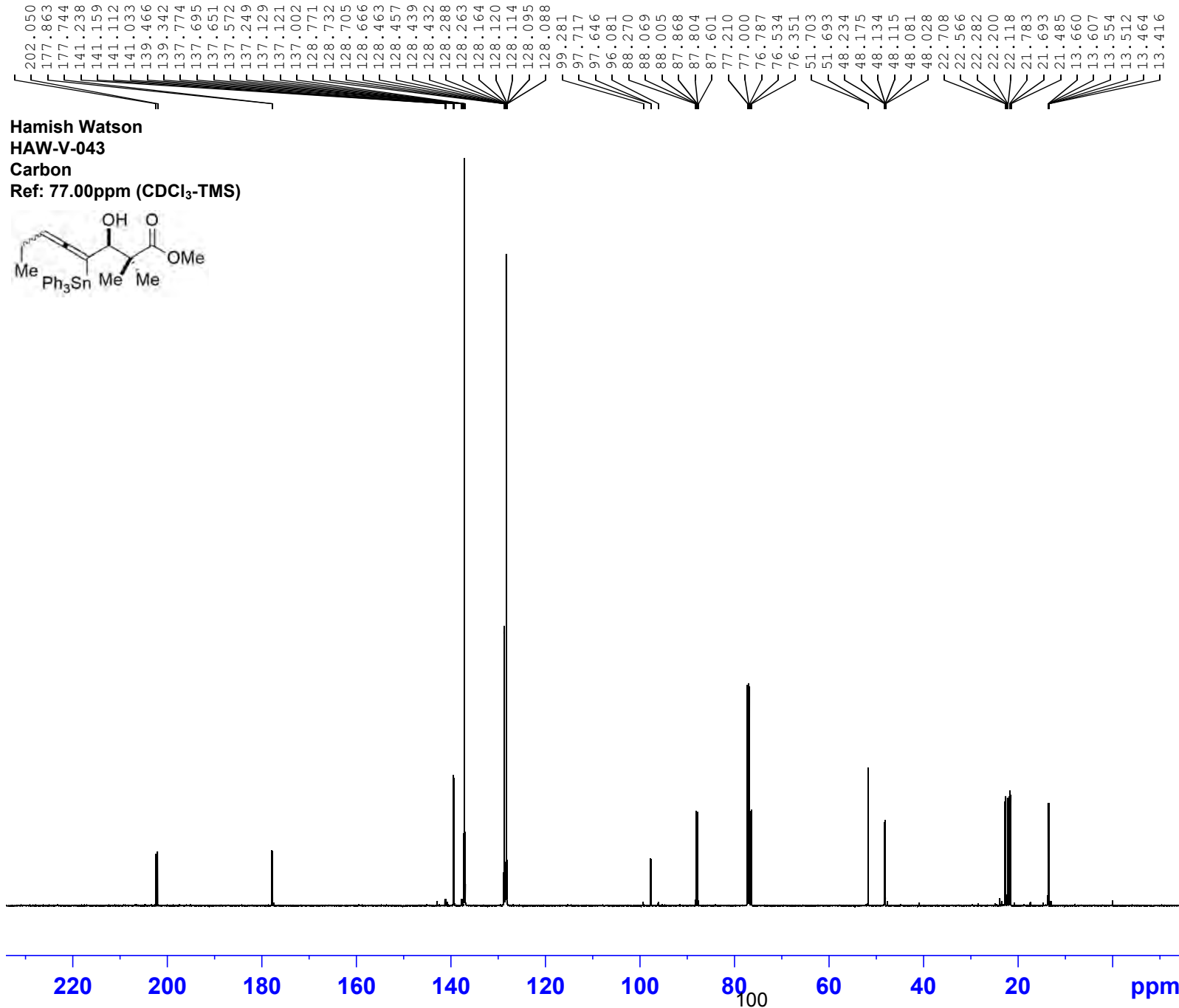
F2 - Acquisition Parameters  
Date\_ 20181127  
Time\_ 15.00  
INSTRUM spect  
PROBHD 5 mm PABBO BB/  
PULPROG zg30  
TD 180286  
SOLVENT CDCl<sub>3</sub>  
NS 64  
DS 0  
SWH 18028.846 Hz  
FIDRES 0.100001 Hz  
AQ 4.9999318 sec  
RG 25.17  
DW 27.733 usec  
DE 7.60 usec  
TE 300.0 K  
D1 0.10000000 sec  
TD0 1

===== CHANNEL f1 =====  
SF01 600.1337060 MHz  
NUC1 1H  
P1 10.00 usec  
PLW1 26.60000038 W

F2 - Processing parameters  
SI 262144  
SF 600.1300463 MHz  
WDW EM  
SSB 0  
LB 0.10 Hz  
GB 0  
PC 1.00







Current Data Parameters  
 NAME HAW-V-Ph3Sn\_Probe-(1)  
 EXPNO 11  
 PROCNO 1

F2 - Acquisition Parameters  
 Date 20181127  
 Time 15.46  
 INSTRUM spect  
 PROBHD 5 mm PABBO BB/  
 PULPROG zpgpg30  
 TD 119044  
 SOLVENT CDCl<sub>3</sub>  
 NS 1024  
 DS 4  
 SWH 37500.000 Hz  
 FIDRES 0.315010 Hz  
 AQ 1.5872533 sec  
 RG 186.92  
 DW 13.333 usec  
 DE 7.73 usec  
 TE 300.0 K  
 D1 1.00000000 sec  
 D11 0.03000000 sec  
 TD0 1

===== CHANNEL f1 ======  
 SFO1 150.9194058 MHz  
 NUC1 <sup>13</sup>C  
 P1 11.80 usec  
 PLW1 85.00000000 W

===== CHANNEL f2 ======  
 SFO2 600.1324005 MHz  
 NUC2 <sup>1</sup>H  
 CPDPRG[2] waltz64  
 PCPD2 80.00 usec  
 PLW2 27.00000000 W  
 PLW12 0.43891999 W  
 PLW13 0.28090999 W

F2 - Processing parameters  
 SI 131072  
 SF 150.9028244 MHz  
 WDW EM  
 SSB 0  
 LB 1.00 Hz  
 GB 0  
 PC 1.40



Current Data Parameters  
NAME HAW-V-Ph3Sn\_Probe-(1)  
EXPNO 12  
PROCNO 1

F2 - Acquisition Parameters  
Date\_ 20181127  
Time 15.58  
INSTRUM spect  
PROBHD 5 mm PABBO BB/  
PULPROG deptsp135.b  
TD 119044  
SOLVENT CDCl<sub>3</sub>  
NS 256  
DS 4  
SWH 35714.285 Hz  
FIDRES 0.300009 Hz  
AQ 1.6666160 sec  
RG 186.92  
DW 14.000 usec  
DE 7.44 usec  
TE 300.0 K  
CNST2 145.0000000  
D1 1.0000000 sec  
D2 0.00344828 sec  
D12 0.00002000 sec  
TD0 1

===== CHANNEL f1 =====  
SFO1 150.9178962 MHz  
NUC1 <sup>13</sup>C  
P1 11.80 usec  
P13 2000.00 usec  
PLW0 0 W  
PLW1 85.00000000 W  
SPNAM[5] Crp60comp.4  
SPOAL5 0.500  
SPOFFS5 0 Hz  
SPW5 18.08300018 W

===== CHANNEL f2 =====  
SFO2 600.1324005 MHz  
NUC2 <sup>1</sup>H  
CPDPRG[2] waltz64  
P3 10.20 usec  
P4 20.40 usec  
PCPD2 80.00 usec  
PLW2 27.00000000 W  
PLW12 0.43891999 W

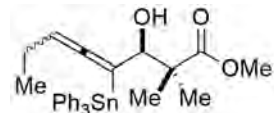
F2 - Processing parameters  
SI 131072  
SF 150.9028246 MHz  
WDW EM  
SSB 0  
LB 1.00 Hz  
GB 0  
PC 1.40

Hamish Watson

HAW-V-043

Dept135

Ref: 77.00ppm (CDCl<sub>3</sub>-TMS)





Current Data Parameters  
 NAME HAW-V-Ph3Sn\_Probe-(1)  
 EXPNO 12  
 PROCNO 1

F2 - Acquisition Parameters  
 Date\_ 20181127  
 Time 15.58  
 INSTRUM spect  
 PROBHD 5 mm PABBO BB/  
 PULPROG deptsp135.b  
 TD 119044  
 SOLVENT CDCl3  
 NS 256  
 DS 4  
 SWH 35714.285 Hz  
 FIDRES 0.300009 Hz  
 AQ 1.6666160 sec  
 RG 186.92  
 DW 14.000 usec  
 DE 7.44 usec  
 TE 300.0 K  
 CNST2 145.0000000  
 D1 1.0000000 sec  
 D2 0.00344828 sec  
 D12 0.00002000 sec  
 TDO 1

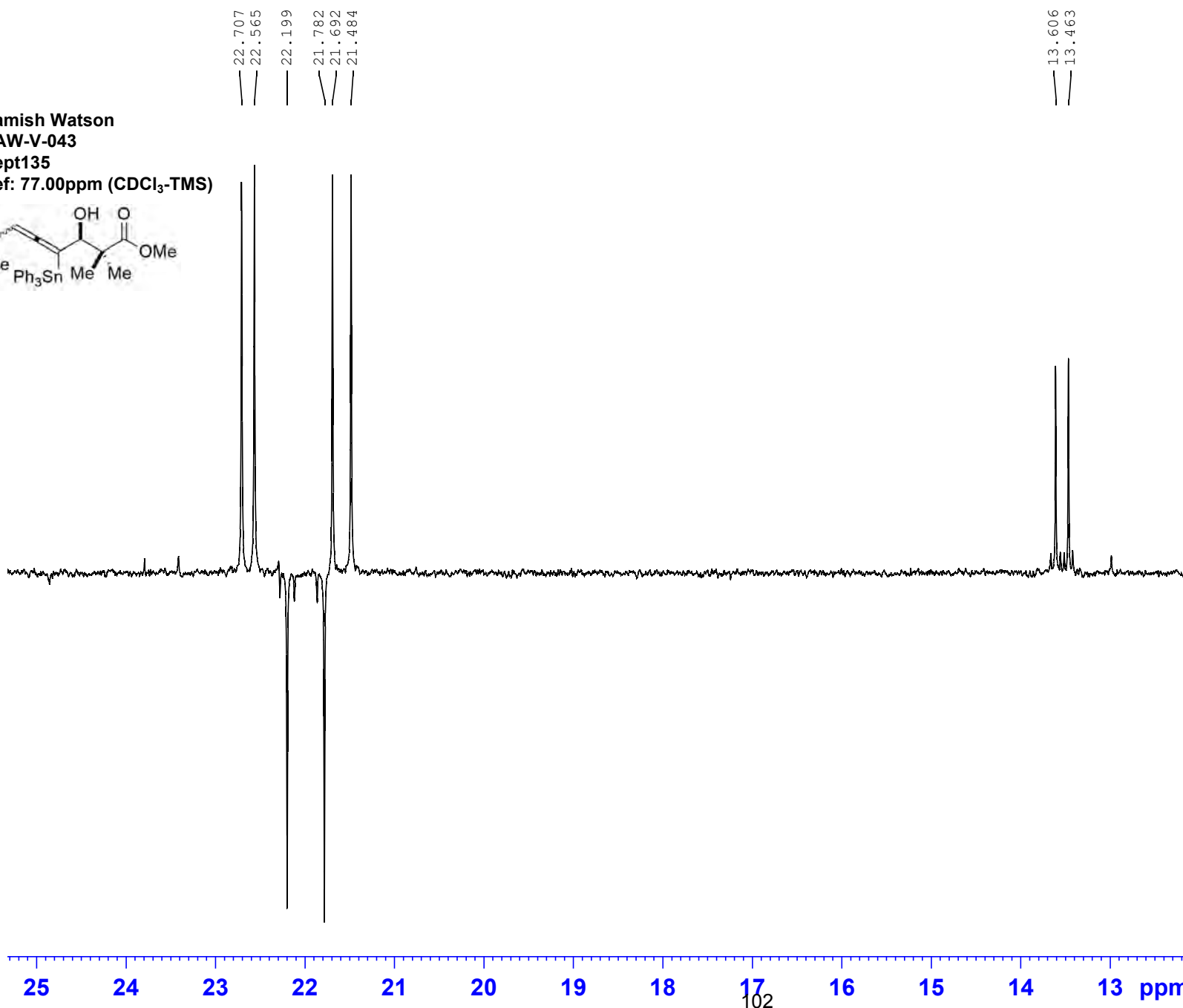
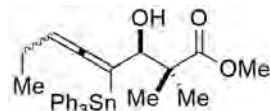
===== CHANNEL f1 =====  
 SFO1 150.9178962 MHz  
 NUC1 13C  
 P1 11.80 usec  
 P13 2000.00 usec  
 PLW0 0 W  
 PLW1 85.00000000 W  
 SPNAM[5] Crp60comp.4  
 SPOAL5 0.500  
 SPOFFS5 0 Hz  
 SPW5 18.08300018 W

===== CHANNEL f2 =====  
 SFO2 600.1324005 MHz  
 NUC2 1H  
 CPDPRG[2] waltz64  
 P3 10.20 usec  
 P4 20.40 usec  
 PCPD2 80.00 usec  
 PLW2 27.00000000 W  
 PLW12 0.43891999 W

F2 - Processing parameters  
 SI 131072  
 SF 150.9028246 MHz  
 WDW EM  
 SSB 0  
 LB 1.00 Hz  
 GB 0  
 PC 1.40

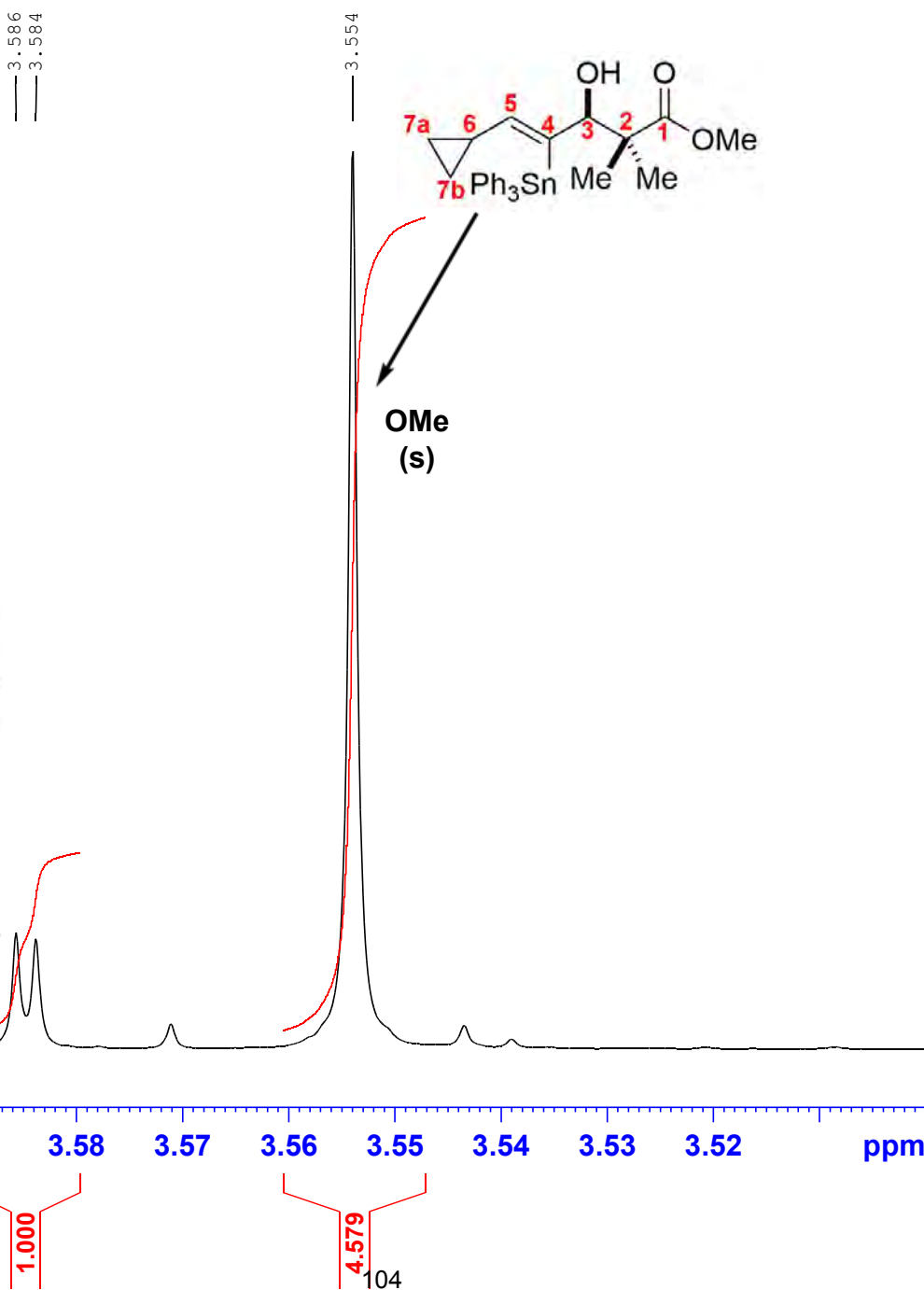
Hamish Watson  
 HAW-V-043  
 Dept135

Ref: 77.00ppm (CDCl<sub>3</sub>-TMS)



**Part E. The 600.13 MHz  $^1\text{H}$  NMR Ratio Determinations For  
the Triphenylstannylallene 4b and Triphenylstannylvinyltin  
5b in  $\text{CDCl}_3$**

HAW-VII-069  
 $\text{Ph}_3\text{SnH}$  (2 equiv),  
 $\text{Et}_3\text{B}$  (0.1 equiv),  
 $\text{PhMe}$  (c of sm = 0.1M),  
20 °C, 24 h



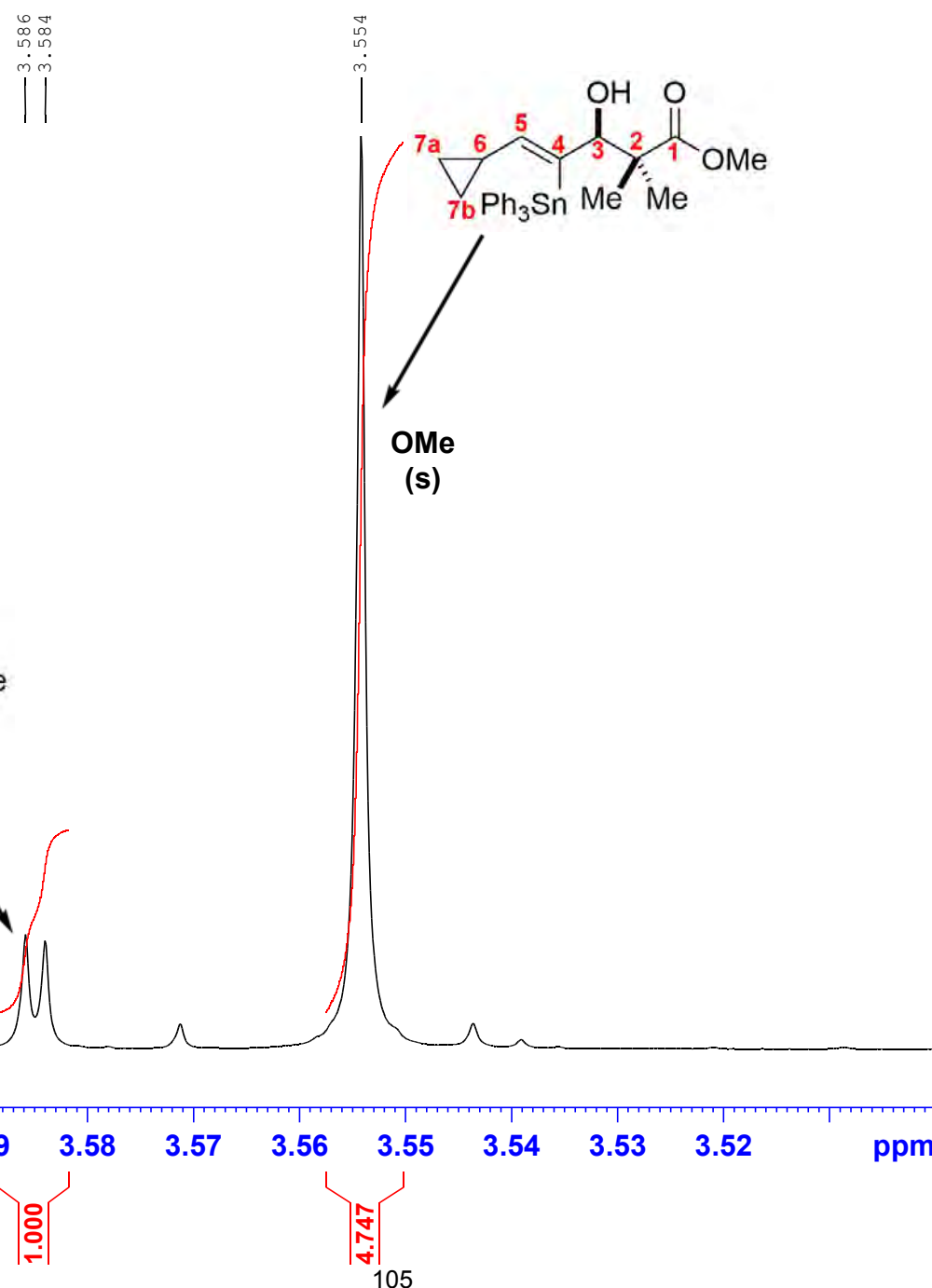
Current Data Parameters  
NAME HAW-VII-069-C  
EXPNO 10  
PROCNO 1

F2 - Acquisition Parameters  
Date 20191218  
Time 4.07  
INSTRUM spect  
PROBHD 5 mm PABBO BB/  
PULPROG zg30  
TD 180286  
SOLVENT CDCl3  
NS 64  
DS 0  
SWH 18028.846 Hz  
FIDRES 0.100001 Hz  
AQ 4.9999318 sec  
RG 97.5  
DW 27.733 usec  
DE 7.60 usec  
TE 300.0 K  
D1 0.10000000 sec  
TD0 1

===== CHANNEL f1 =====  
SFO1 600.1337060 MHz  
NUC1 1H  
P1 10.00 usec  
PLW1 26.60000038 W

F2 - Processing parameters  
SI 262144  
SF 600.1300218 MHz  
WDW EM  
SSB 0  
LB 0.10 Hz  
GB 0  
PC 1.00

HAW-VII-070  
 $\text{Ph}_3\text{SnH}$  (2 equiv),  
 $\text{Et}_3\text{B}$  (0.1 equiv),  
 $\text{PhMe}$  (c of sm = 0.1M),  
20 °C, 24 h



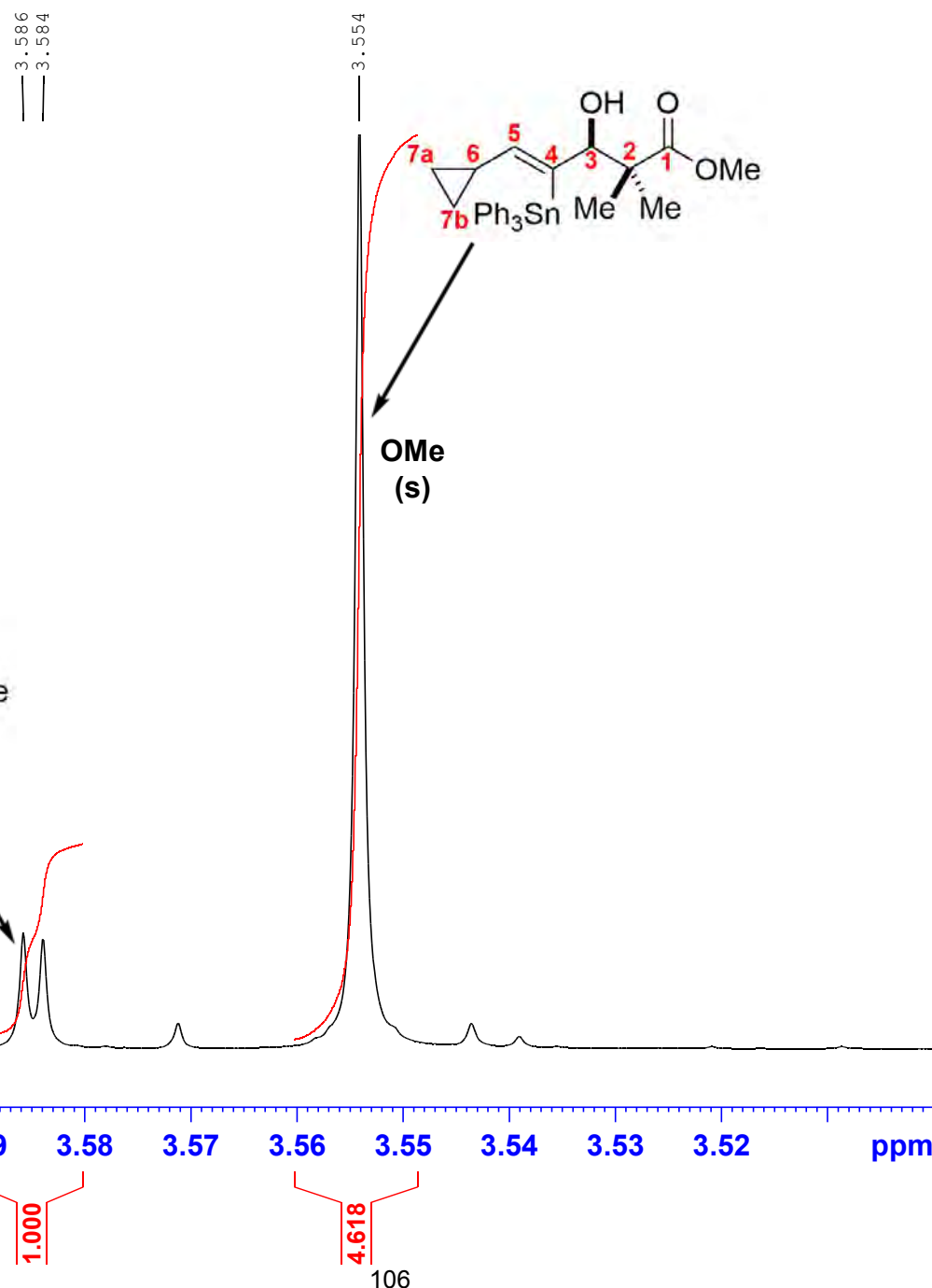
Current Data Parameters  
NAME HAW-VII-070-C  
EXPNO 20  
PROCNO 1

F2 - Acquisition Parameters  
Date 20191218  
Time 4.15  
INSTRUM spect  
PROBHD 5 mm PABBO BB/  
PULPROG zg30  
TD 180286  
SOLVENT CDCl<sub>3</sub>  
NS 64  
DS 0  
SWH 18028.846 Hz  
FIDRES 0.100001 Hz  
AQ 4.9999318 sec  
RG 97.5  
DW 27.733 usec  
DE 7.60 usec  
TE 300.0 K  
D1 0.10000000 sec  
TD0 1

===== CHANNEL f1 =====  
SFO1 600.1337060 MHz  
NUC1 1H  
P1 10.00 usec  
PLW1 26.60000038 W

F2 - Processing parameters  
SI 262144  
SF 600.1300214 MHz  
WDW EM  
SSB 0  
LB 0.10 Hz  
GB 0  
PC 1.00

HAW-VII-071  
 $\text{Ph}_3\text{SnH}$  (2 equiv),  
 $\text{Et}_3\text{B}$  (0.1 equiv),  
 $\text{PhMe}$  ( $c$  of sm = 0.1M),  
20 °C, 24 h



Current Data Parameters  
NAME HAW-VII-071-C  
EXPNO 30  
PROCNO 1

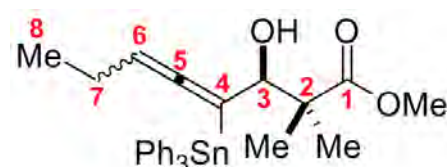
F2 - Acquisition Parameters  
Date 20191218  
Time 4.23  
INSTRUM spect  
PROBHD 5 mm PABBO BB/  
PULPROG zg30  
TD 180286  
SOLVENT CDCl<sub>3</sub>  
NS 64  
DS 0  
SWH 18028.846 Hz  
FIDRES 0.100001 Hz  
AQ 4.9999318 sec  
RG 97.5  
DW 27.733 usec  
DE 7.60 usec  
TE 300.0 K  
D1 0.10000000 sec  
TD0 1

===== CHANNEL f1 =====  
SFO1 600.1337060 MHz  
NUC1 1H  
P1 10.00 usec  
PLW1 26.60000038 W

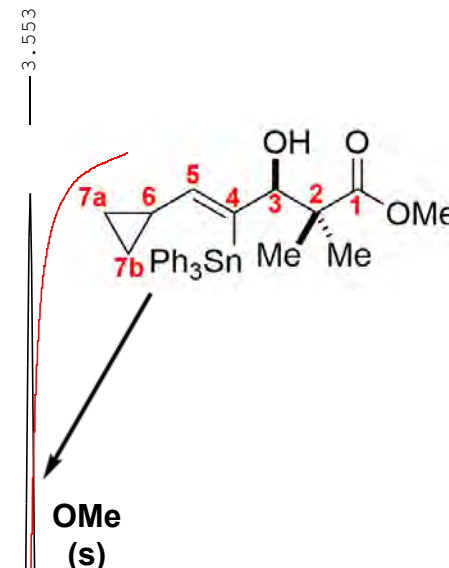
F2 - Processing parameters  
SI 262144  
SF 600.1300215 MHz  
WDW EM  
SSB 0  
LB 0.10 Hz  
GB 0  
PC 1.00

HAW-VII-072  
 $\text{Ph}_3\text{SnH}$  (2 equiv),  
 $\text{Et}_3\text{B}$  (0.1 equiv),  
 $\text{PhMe}$  ( $c$  of  $\text{sm} = 0.1\text{M}$ ),  
20 °C, 24 h

3.585  
3.583



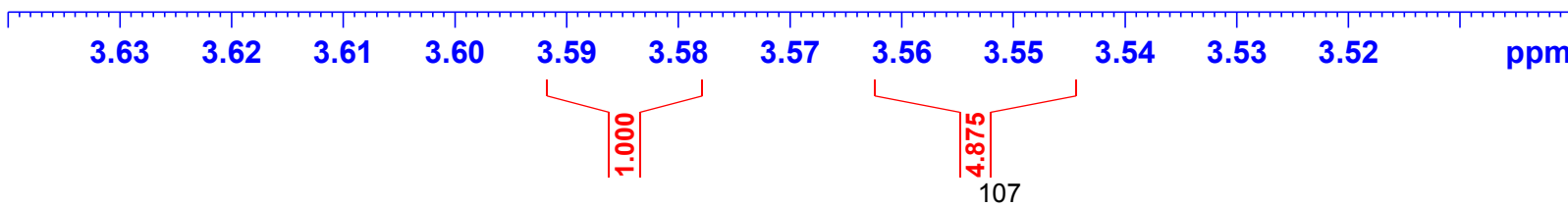
2 x OMe  
(s)  
partially  
overlapped



107

4.875

1.000



Current Data Parameters  
NAME HAW-VII-072-C  
EXPNO 40  
PROCNO 1

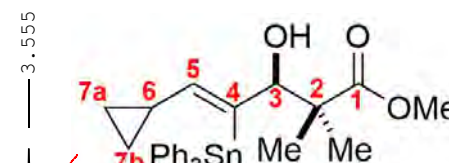
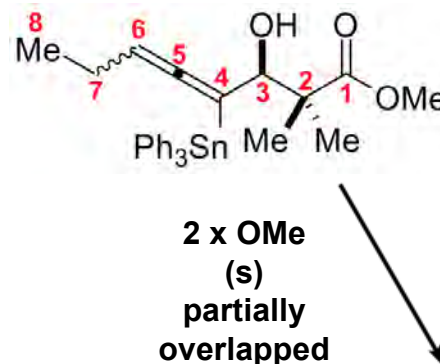
F2 - Acquisition Parameters  
Date 20191218  
Time 4.32  
INSTRUM spect  
PROBHD 5 mm PABBO BB/  
PULPROG zg30  
TD 180286  
SOLVENT CDCl<sub>3</sub>  
NS 64  
DS 0  
SWH 18028.846 Hz  
FIDRES 0.100001 Hz  
AQ 4.9999318 sec  
RG 68  
DW 27.733 usec  
DE 7.60 usec  
TE 300.0 K  
D1 0.10000000 sec  
TD0 1

===== CHANNEL f1 =====  
SFO1 600.1337060 MHz  
NUC1 1H  
P1 10.00 usec  
PLW1 26.60000038 W

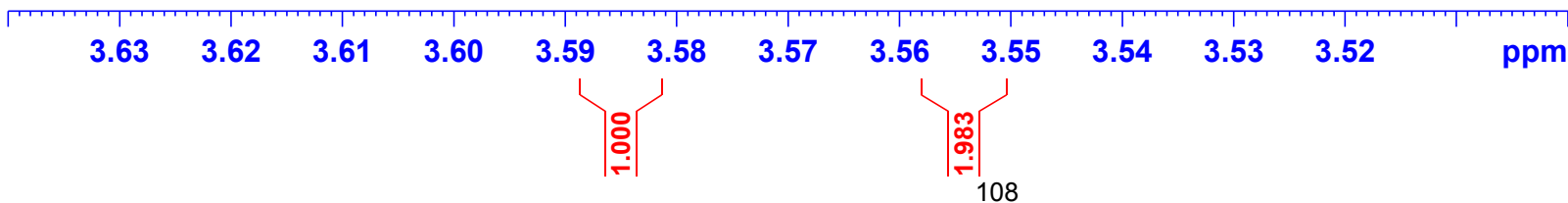
F2 - Processing parameters  
SI 262144  
SF 600.1300236 MHz  
WDW EM  
SSB 0  
LB 0.10 Hz  
GB 0  
PC 1.00

HAW-VII-061  
 $\text{Ph}_3\text{SnH}$  (2 equiv),  
 $\text{Et}_3\text{B}$  (0.1 equiv),  
 $\text{PhMe}$  (*c* of sm = 0.1M),  
40 °C, 24 h

3.586  
3.584



**OMe (s)**



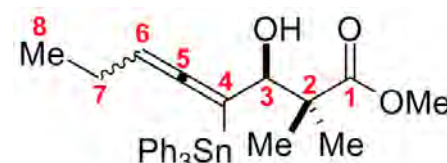
Current Data Parameters  
NAME HAW-VII-061-C  
EXPNO 10  
PROCNO 1

F2 - Acquisition Parameters  
Date 20191218  
Time 3.01  
INSTRUM spect  
PROBHD 5 mm PABBO BB/  
PULPROG zg30  
TD 180286  
SOLVENT CDCl3  
NS 64  
DS 0  
SWH 18028.846 Hz  
FIDRES 0.100001 Hz  
AQ 4.9999318 sec  
RG 97.5  
DW 27.733 usec  
DE 7.60 usec  
TE 300.0 K  
D1 0.10000000 sec  
TD0 1

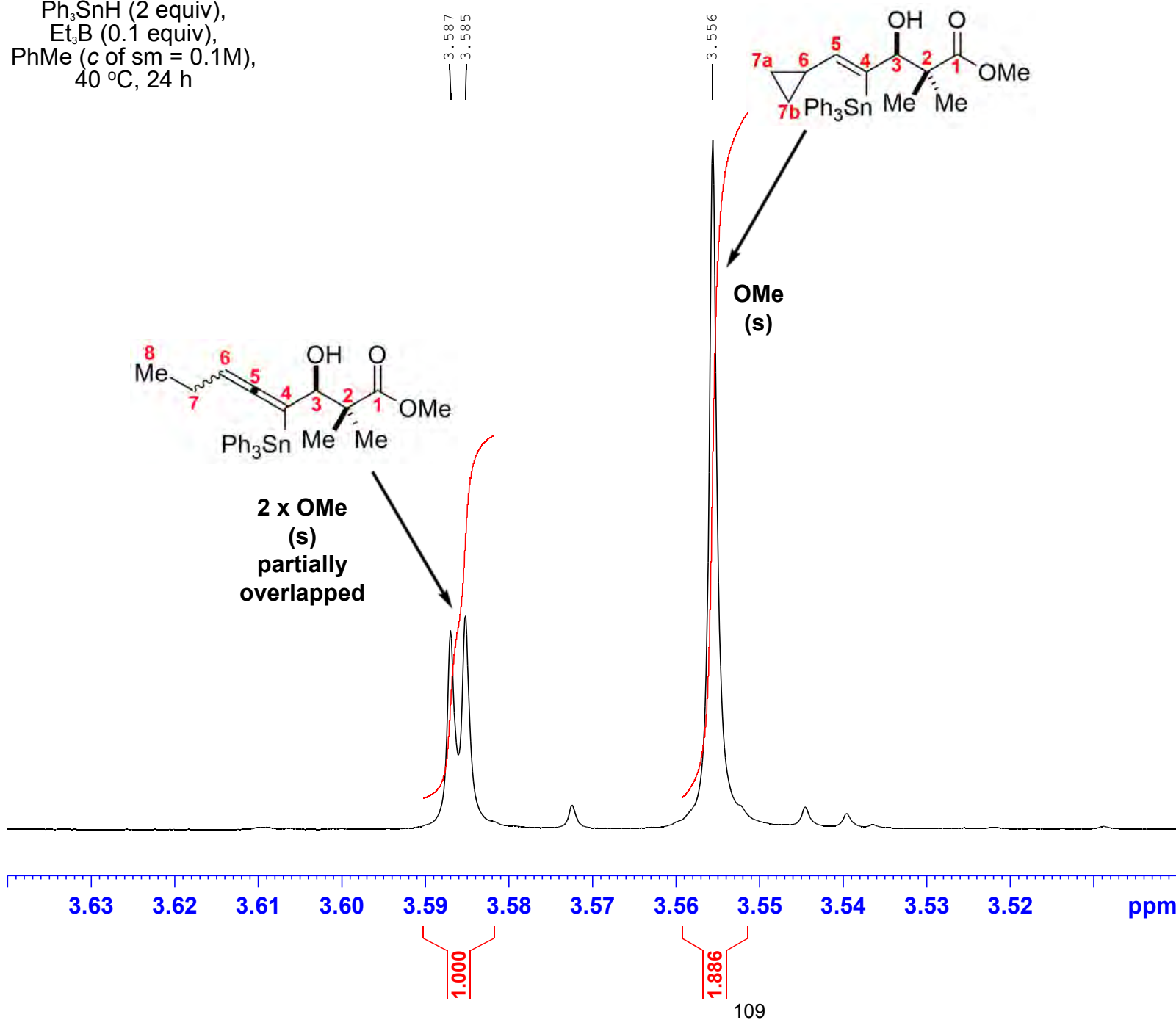
===== CHANNEL f1 =====  
SFO1 600.1337060 MHz  
NUC1 1H  
P1 10.00 usec  
PLW1 26.60000038 W

F2 - Processing parameters  
SI 262144  
SF 600.1300208 MHz  
WDW EM  
SSB 0  
LB 0.10 Hz  
GB 0  
PC 1.00

HAW-VII-062  
 Ph<sub>3</sub>SnH (2 equiv),  
 Et<sub>3</sub>B (0.1 equiv),  
 PhMe (c of sm = 0.1M),  
 40 °C, 24 h



**2 x OMe  
(s)  
partially  
overlapped**



Current Data Parameters  
NAME HAW-VII-062-C  
EXPNO 20  
PROCNO 1

```

F2 - Acquisition Parameters
Date_           20191218
Time_          3.09
INSTRUM        spect
PROBHD        5 mm PABBO BB/
PULPROG       zg30
TD             180286
SOLVENT        CDC13
NS              64
DS                 0
SWH            18028.846 Hz
FIDRES       0.100001 Hz
AQ            4.9999318 sec
RG             97.5
DW             27.733 usec
DE              7.60 usec
TE             300.0 K
D1          0.10000000 sec
TD0                 1

```

===== CHANNEL f1 =====  
SFO1 600.1337060 MHz  
NUC1 1H  
P1 10.00 usec  
PI\_W1 26.60000038 W

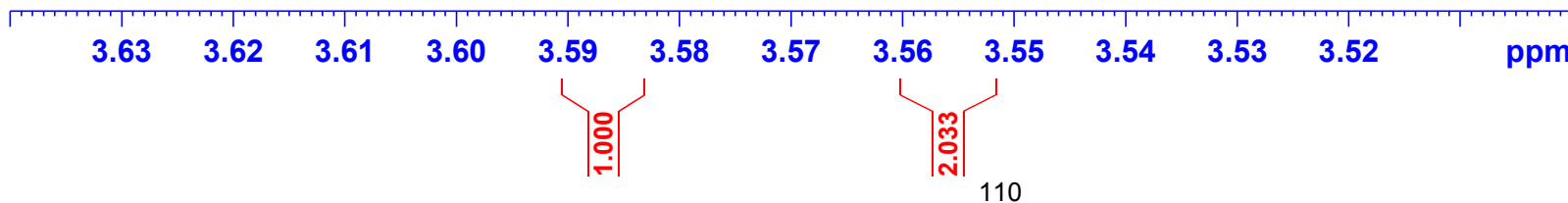
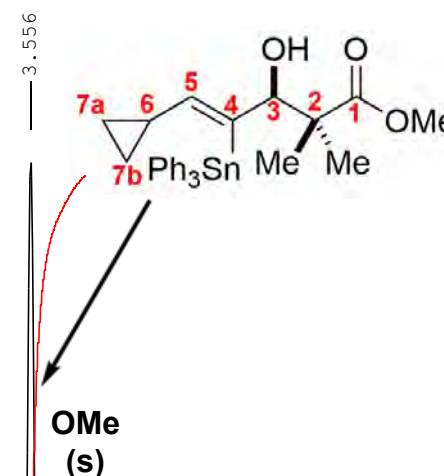
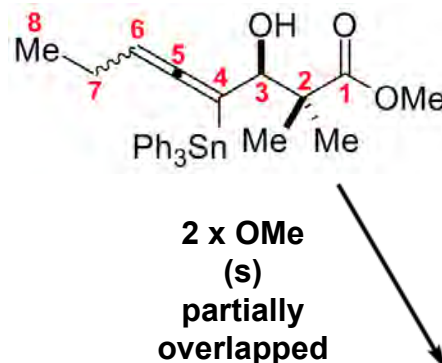
```

F2 - Processing parameters
SI           262144
SF          600.1300192 MHz
WDW          EM
SSB          0
LB           0.10 Hz
GB          0
PC          1.00

```

HAW-VII-063  
 $\text{Ph}_3\text{SnH}$  (2 equiv),  
 $\text{Et}_3\text{B}$  (0.1 equiv),  
 $\text{PhMe}$  (*c* of sm = 0.1M),  
40 °C, 24 h

3.588  
3.586



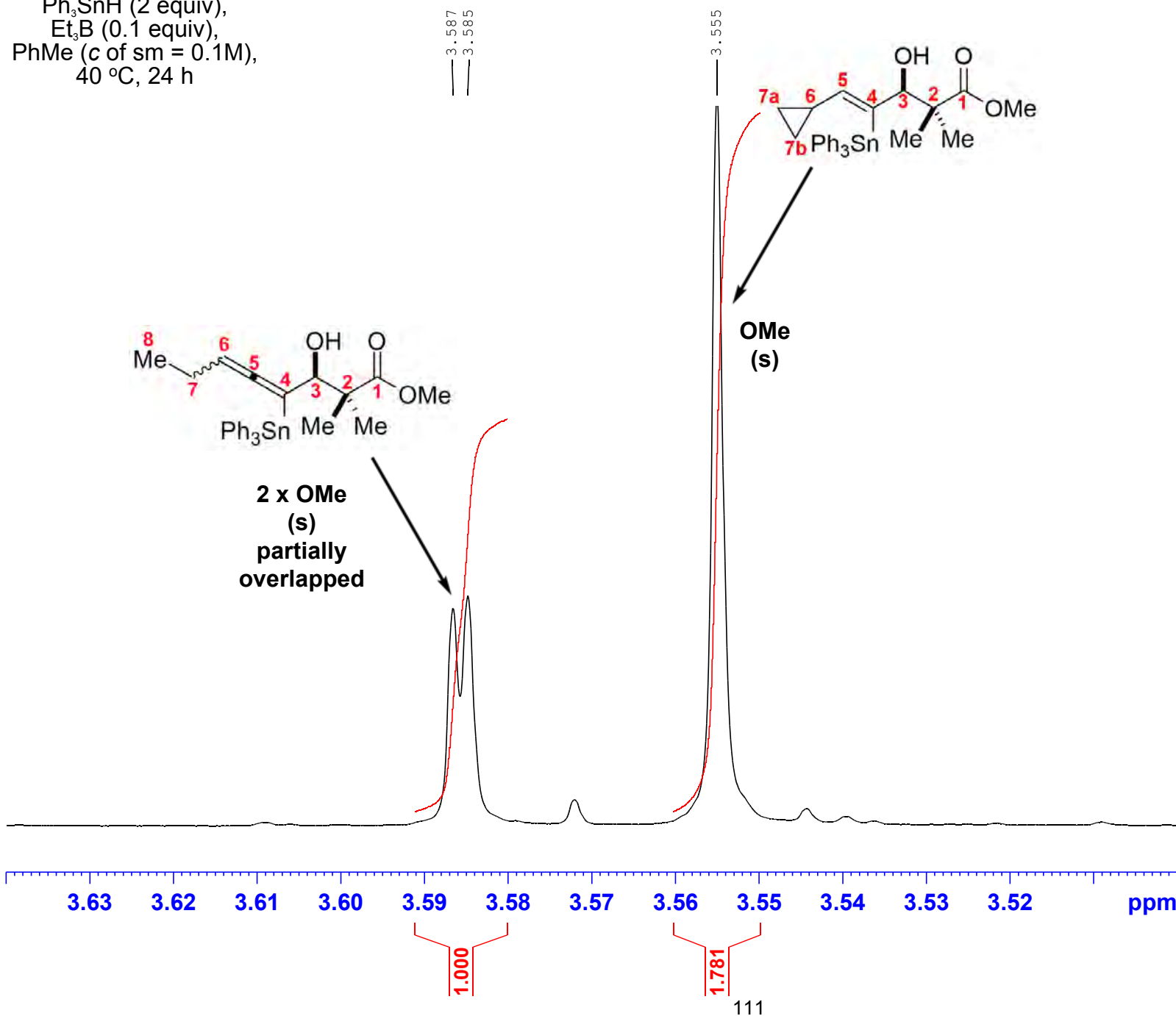
Current Data Parameters  
NAME HAW-VII-063-C  
EXPNO 30  
PROCNO 1

F2 - Acquisition Parameters  
Date 20191218  
Time 3.17  
INSTRUM spect  
PROBHD 5 mm PABBO BB/  
PULPROG zg30  
TD 180286  
SOLVENT CDCl3  
NS 64  
DS 0  
SWH 18028.846 Hz  
FIDRES 0.100001 Hz  
AQ 4.9999318 sec  
RG 97.5  
DW 27.733 usec  
DE 7.60 usec  
TE 300.0 K  
D1 0.10000000 sec  
TD0 1

===== CHANNEL f1 =====  
SFO1 600.1337060 MHz  
NUC1 1H  
P1 10.00 usec  
PLW1 26.60000038 W

F2 - Processing parameters  
SI 262144  
SF 600.1300175 MHz  
WDW EM  
SSB 0  
LB 0.10 Hz  
GB 0  
PC 1.00

HAW-VII-064  
 $\text{Ph}_3\text{SnH}$  (2 equiv),  
 $\text{Et}_3\text{B}$  (0.1 equiv),  
 $\text{PhMe}$  ( $c$  of sm = 0.1M),  
40 °C, 24 h



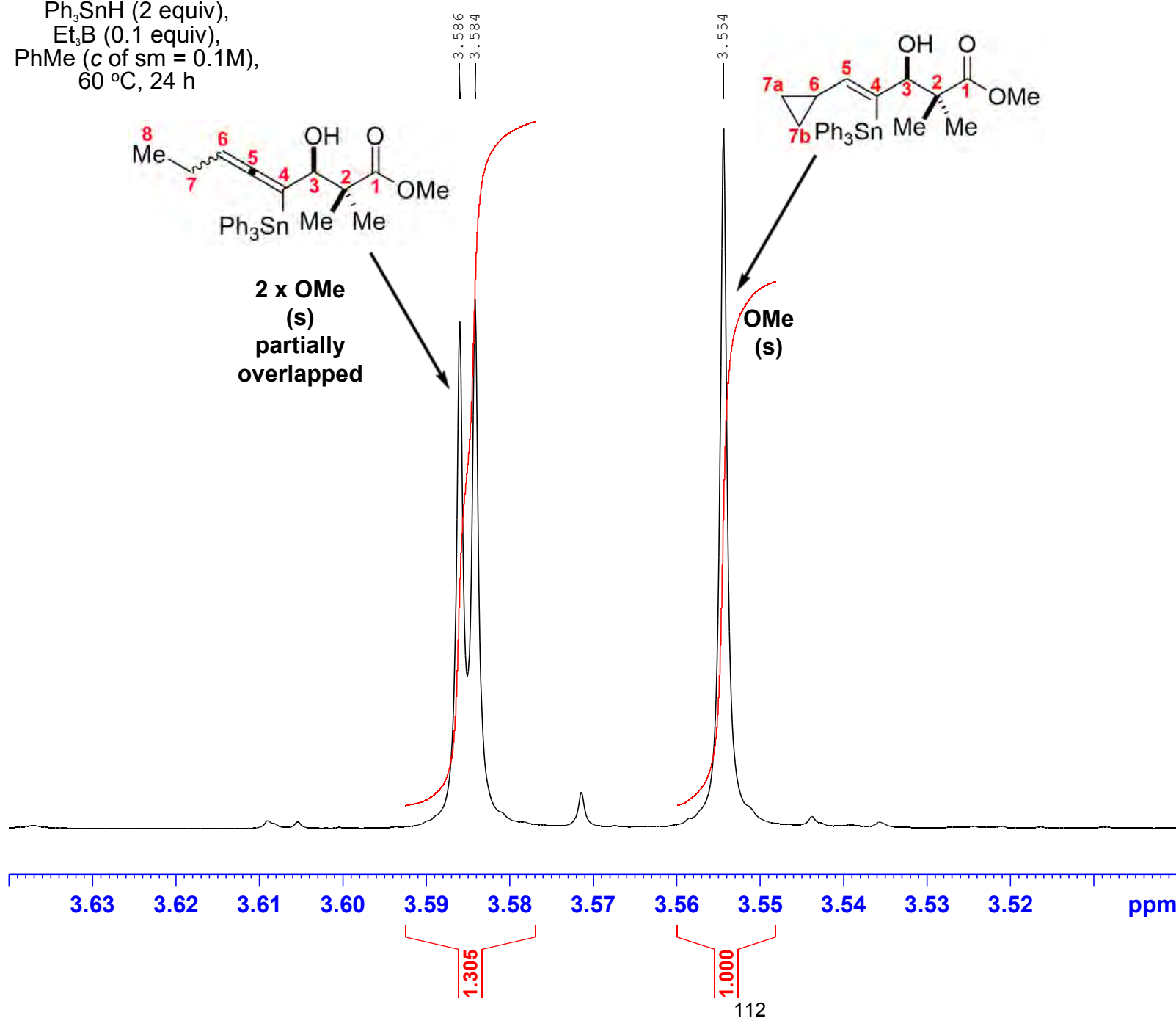
Current Data Parameters  
NAME HAW-VII-064-C  
EXPNO 60  
PROCNO 1

F2 - Acquisition Parameters  
Date 20191219  
Time 2.50  
INSTRUM spect  
PROBHD 5 mm PABBO BB/  
PULPROG zg30  
TD 180286  
SOLVENT CDCl<sub>3</sub>  
NS 64  
DS 0  
SWH 18028.846 Hz  
FIDRES 0.100001 Hz  
AQ 4.9999318 sec  
RG 97.5  
DW 27.733 usec  
DE 7.60 usec  
TE 300.0 K  
D1 0.10000000 sec  
TD0 1

===== CHANNEL f1 =====  
SFO1 600.1337060 MHz  
NUC1 1H  
P1 10.00 usec  
PLW1 26.60000038 W

F2 - Processing parameters  
SI 262144  
SF 600.1300204 MHz  
WDW EM  
SSB 0  
LB 0.10 Hz  
GB 0  
PC 1.00

HAW-VII-065  
 $\text{Ph}_3\text{SnH}$  (2 equiv),  
 $\text{Et}_3\text{B}$  (0.1 equiv),  
 $\text{PhMe}$  ( $c$  of sm = 0.1M),  
60 °C, 24 h



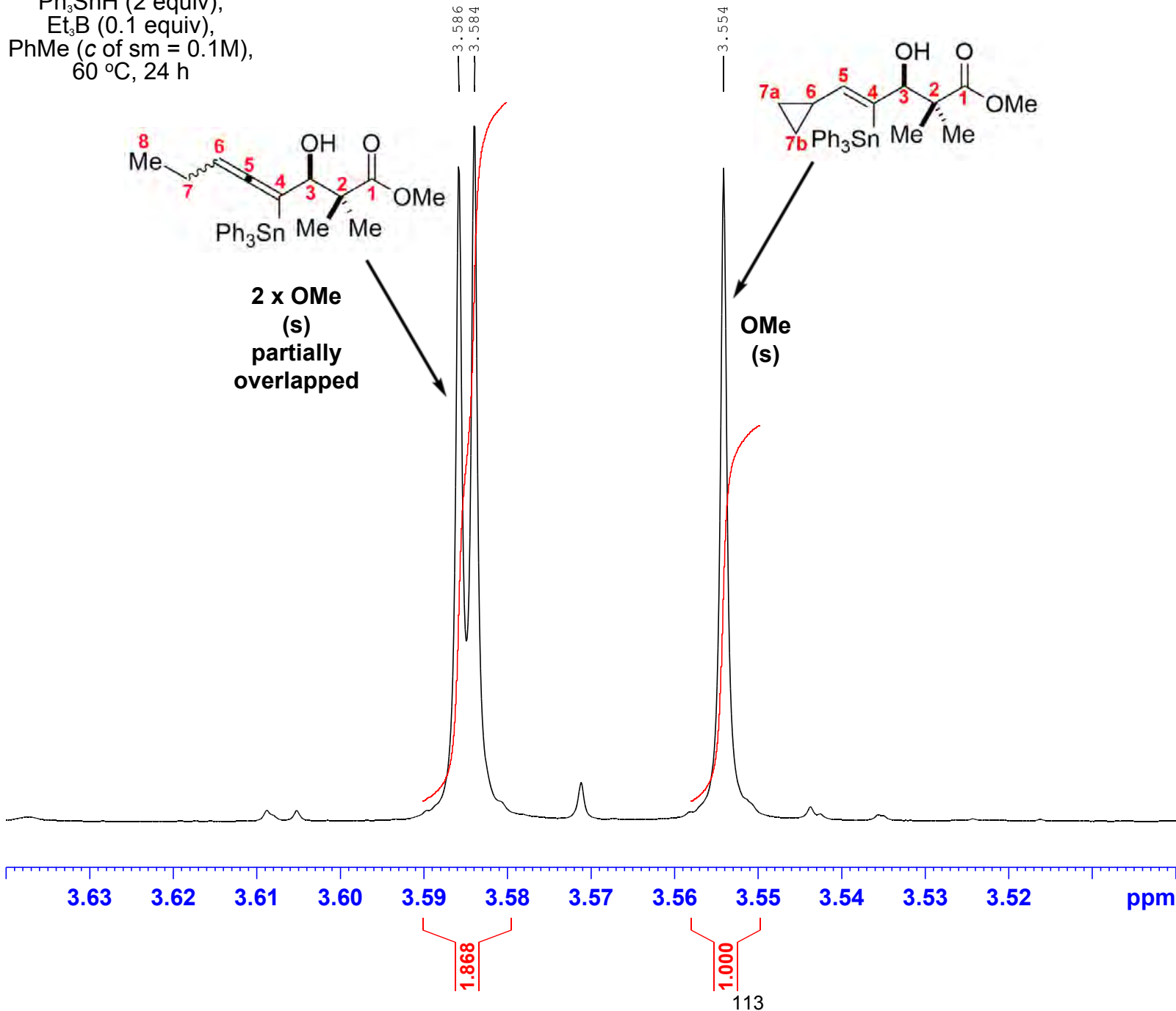
Current Data Parameters  
NAME HAW-VII-065-C  
EXPNO 10  
PROCNO 1

F2 - Acquisition Parameters  
Date 20191218  
Time 3.34  
INSTRUM spect  
PROBHD 5 mm PABBO BB/  
PULPROG zg30  
TD 180286  
SOLVENT CDCl<sub>3</sub>  
NS 64  
DS 0  
SWH 18028.846 Hz  
FIDRES 0.100001 Hz  
AQ 4.9999318 sec  
RG 97.5  
DW 27.733 usec  
DE 7.60 usec  
TE 300.0 K  
D1 0.10000000 sec  
TD0 1

===== CHANNEL f1 =====  
SFO1 600.1337060 MHz  
NUC1 1H  
P1 10.00 usec  
PLW1 26.60000038 W

F2 - Processing parameters  
SI 262144  
SF 600.1300212 MHz  
WDW EM  
SSB 0  
LB 0.10 Hz  
GB 0  
PC 1.00

HAW-VII-066  
 $\text{Ph}_3\text{SnH}$  (2 equiv),  
 $\text{Et}_3\text{B}$  (0.1 equiv),  
 $\text{PhMe}$  ( $c$  of sm = 0.1M),  
60 °C, 24 h



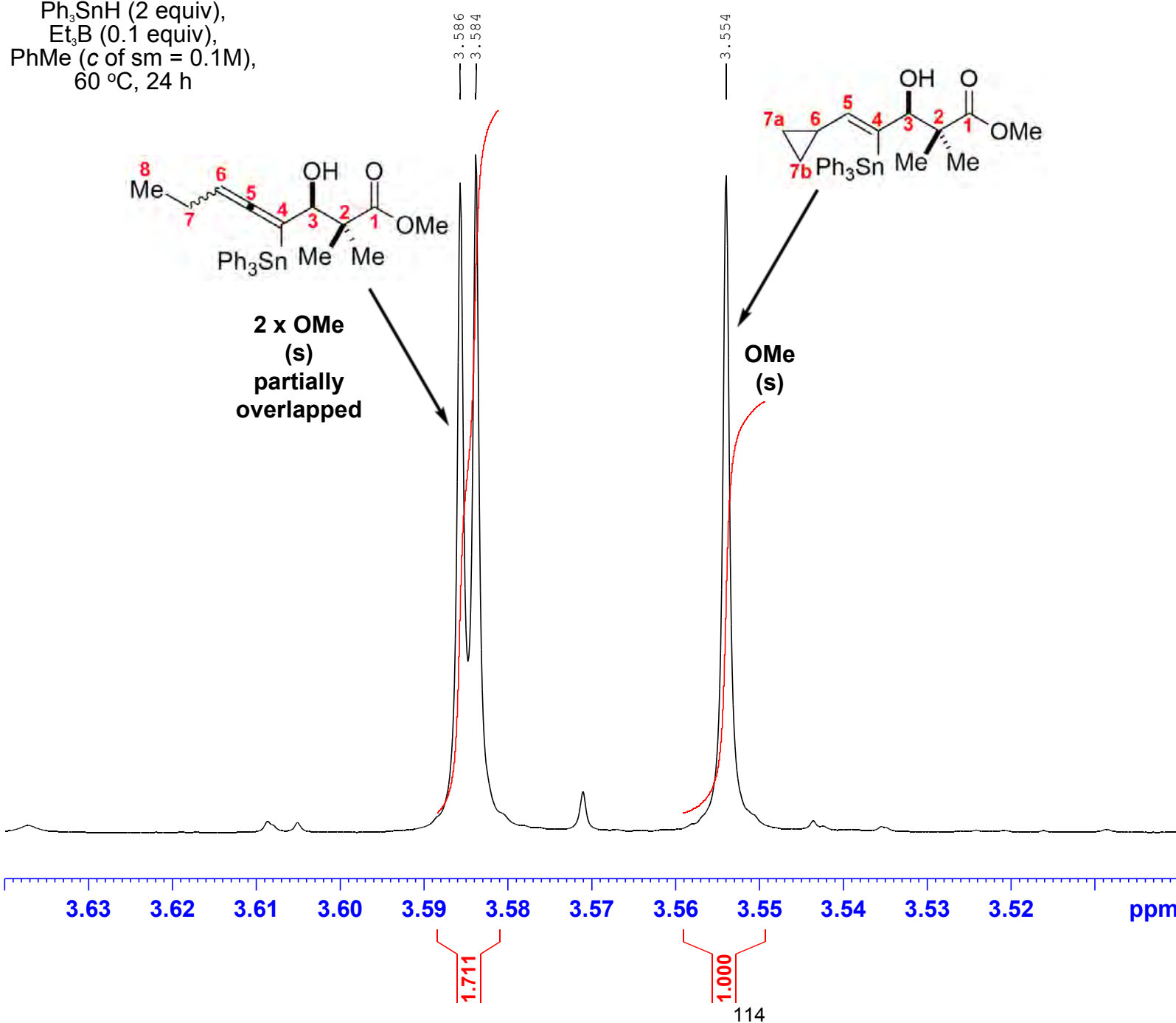
Current Data Parameters  
NAME HAW-VII-066-C  
EXPNO 20  
PROCNO 1

F2 - Acquisition Parameters  
Date 20191218  
Time 3.42  
INSTRUM spect  
PROBHD 5 mm PABBO BB/  
PULPROG zg30  
TD 180286  
SOLVENT CDCl<sub>3</sub>  
NS 64  
DS 0  
SWH 18028.846 Hz  
FIDRES 0.100001 Hz  
AQ 4.9999318 sec  
RG 97.5  
DW 27.733 usec  
DE 7.60 usec  
TE 300.0 K  
D1 0.10000000 sec  
TD0 1

===== CHANNEL f1 =====  
SFO1 600.1337060 MHz  
NUC1 1H  
P1 10.00 usec  
PLW1 26.60000038 W

F2 - Processing parameters  
SI 262144  
SF 600.1300219 MHz  
WDW EM  
SSB 0  
LB 0.10 Hz  
GB 0  
PC 1.00

HAW-VII-067  
 $\text{Ph}_3\text{SnH}$  (2 equiv),  
 $\text{Et}_3\text{B}$  (0.1 equiv),  
 $\text{PhMe}$  ( $c$  of sm = 0.1M),  
60 °C, 24 h



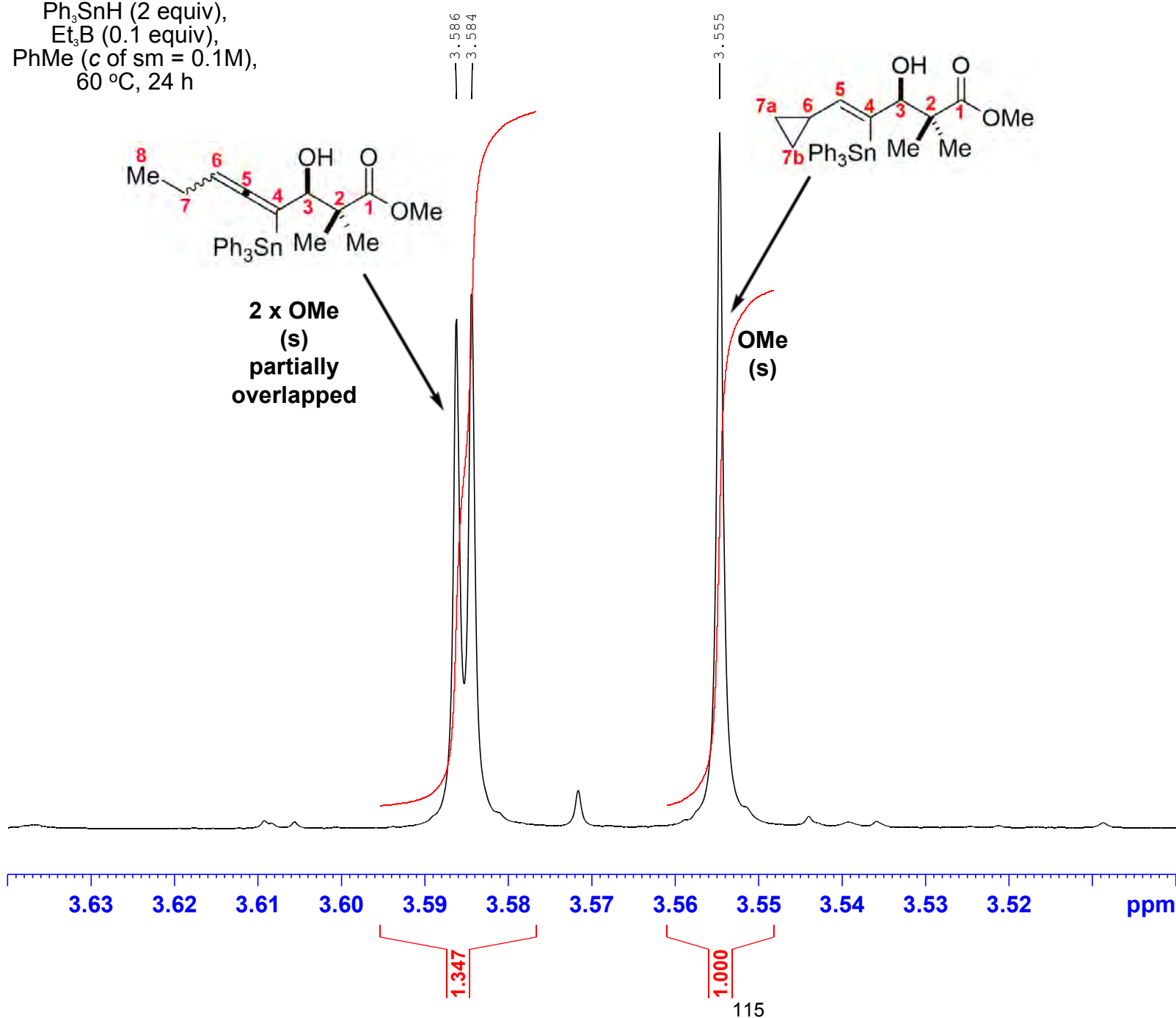
Current Data Parameters  
NAME HAW-VII-067-C  
EXPNO 30  
PROCNO 1

F2 - Acquisition Parameters  
Date 20191218  
Time 3.50  
INSTRUM spect  
PROBHD 5 mm PABBO BB/  
PULPROG zg30  
TD 180286  
SOLVENT CDCl3  
NS 64  
DS 0  
SWH 18028.846 Hz  
FIDRES 0.10001 Hz  
AQ 4.9999318 sec  
RG 97.5  
DW 27.733 usec  
DE 7.60 usec  
TE 300.0 K  
D1 0.1000000 sec  
TD0 1

===== CHANNEL f1 =====  
SFO1 600.1337060 MHz  
NUC1 1H  
P1 10.00 usec  
PLW1 26.60000038 W

F2 - Processing parameters  
SI 262144  
SF 600.1300222 MHz  
WDW EM  
SSB 0  
LB 0.10 Hz  
GB 0  
PC 1.00

HAW-VII-068  
 $\text{Ph}_3\text{SnH}$  (2 equiv),  
 $\text{Et}_3\text{B}$  (0.1 equiv),  
 $\text{PhMe}$  ( $c$  of sm = 0.1M),  
60 °C, 24 h



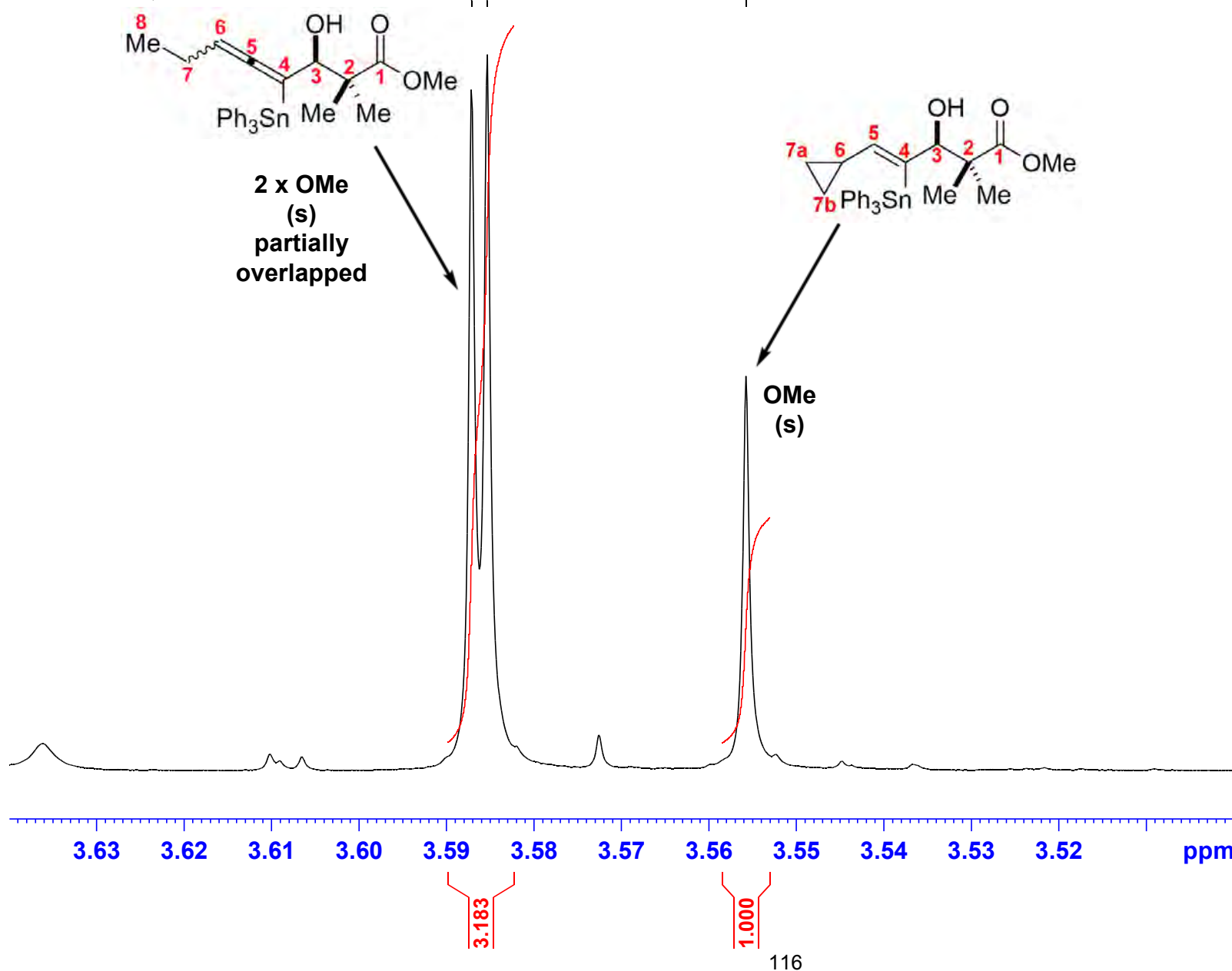
Current Data Parameters  
NAME HAW-VII-068-C  
EXPNO 40  
PROCNO 1

F2 - Acquisition Parameters  
Date 20191218  
Time 3.58  
INSTRUM spect  
PROBHD 5 mm PABBO BB/  
PULPROG zg30  
TD 180286  
SOLVENT CDCl3  
NS 64  
DS 0  
SWH 18028.846 Hz  
FIDRES 0.100001 Hz  
AQ 4.9999318 sec  
RG 97.5  
DW 27.733 usec  
DE 7.60 usec  
TE 300.0 K  
D1 0.10000000 sec  
TD0 1

===== CHANNEL f1 =====  
SFO1 600.1337060 MHz  
NUC1 1H  
P1 10.00 usec  
PLW1 26.60000038 W

F2 - Processing parameters  
SI 262144  
SF 600.1300208 MHz  
WDW EM  
SSB 0  
LB 0.10 Hz  
GB 0  
PC 1.00

HAW-VII-074  
 $\text{Ph}_3\text{SnH}$  (2 equiv),  
 $\text{Et}_3\text{B}$  (0.1 equiv),  
 $\text{PhMe}$  (*c* of *sm* = 0.1M),  
80 °C, 24 h



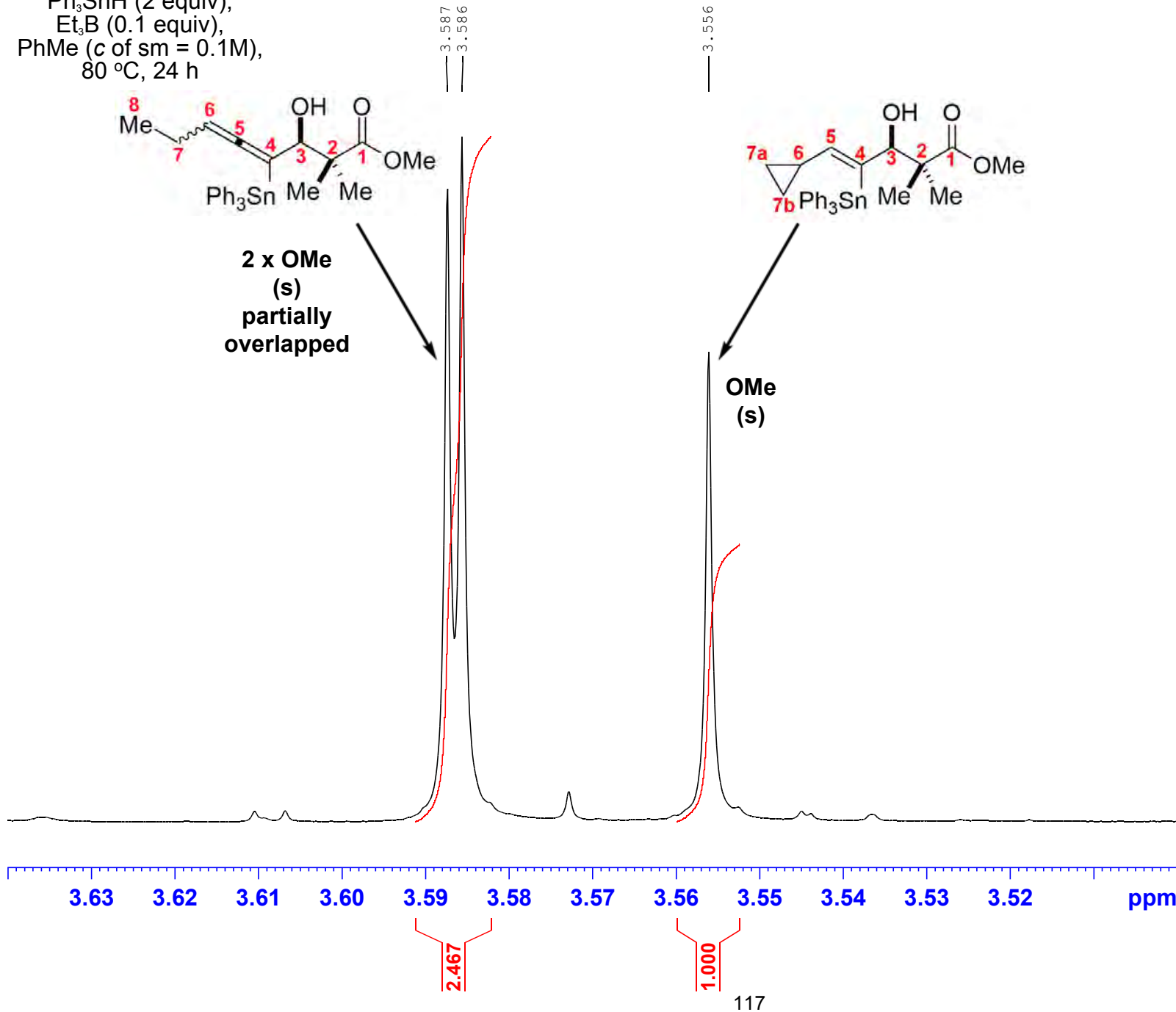
Current Data Parameters  
NAME HAW-VII-074-C  
EXPNO 80  
PROCNO 1

F2 - Acquisition Parameters  
Date 20191219  
Time 3.07  
INSTRUM spect  
PROBHD 5 mm PABBO BB/  
PULPROG zg30  
TD 180286  
SOLVENT CDCl<sub>3</sub>  
NS 64  
DS 0  
SWH 18028.846 Hz  
FIDRES 0.100001 Hz  
AQ 4.9999318 sec  
RG 97.5  
DW 27.733 usec  
DE 7.60 usec  
TE 300.0 K  
D1 0.10000000 sec  
TD0 1

===== CHANNEL f1 =====  
SFO1 600.1337060 MHz  
NUC1 1H  
P1 10.00 usec  
PLW1 26.60000038 W

F2 - Processing parameters  
SI 262144  
SF 600.1300192 MHz  
WDW EM  
SSB 0  
LB 0.10 Hz  
GB 0  
PC 1.00

HAW-VII-075  
 $\text{Ph}_3\text{SnH}$  (2 equiv),  
 $\text{Et}_3\text{B}$  (0.1 equiv),  
 $\text{PhMe}$  (*c* of sm = 0.1M),  
80 °C, 24 h



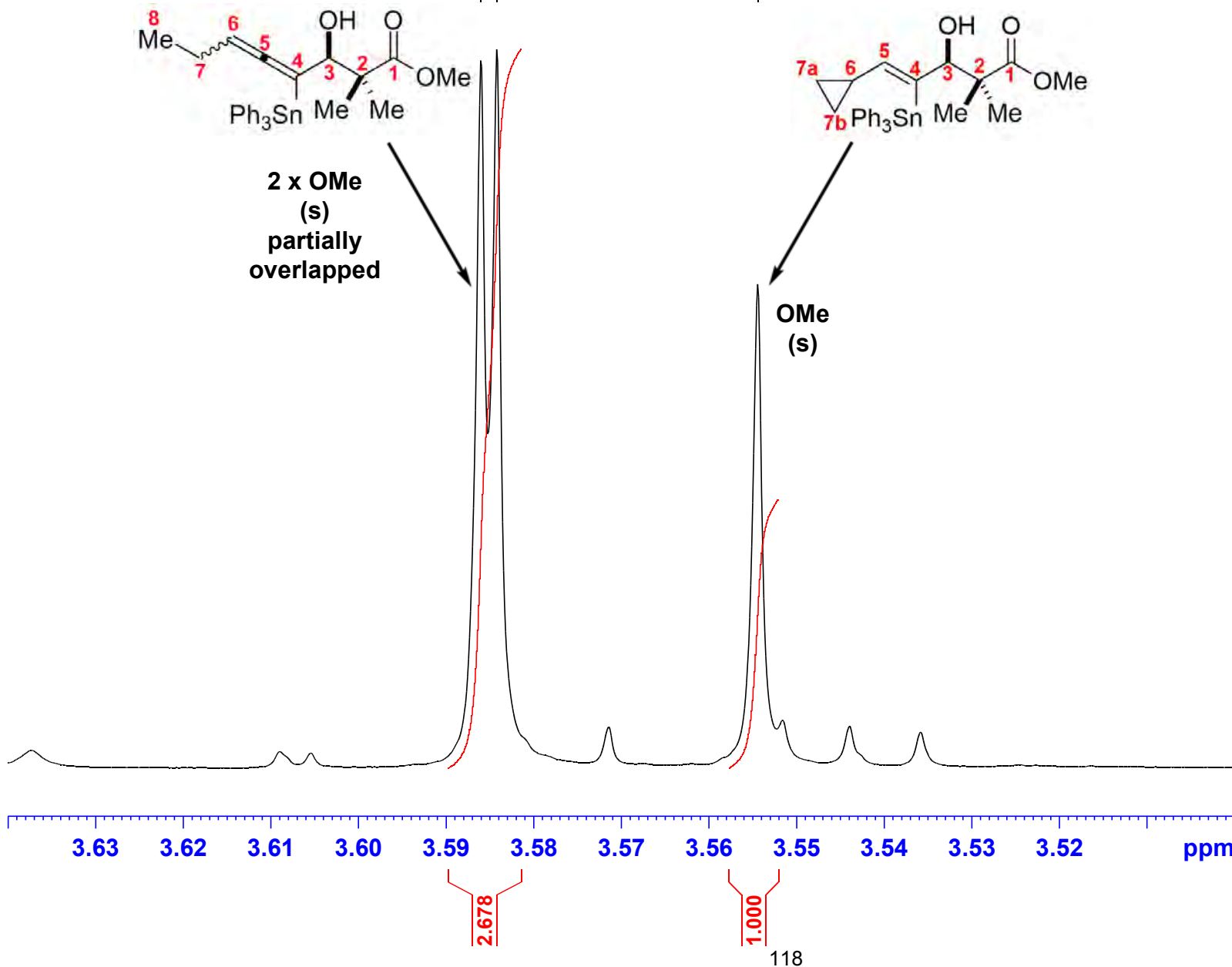
Current Data Parameters  
NAME HAW-VII-075-C  
EXPNO 90  
PROCNO 1

F2 - Acquisition Parameters  
Date 20191219  
Time 3.15  
INSTRUM spect  
PROBHD 5 mm PABBO BB/  
PULPROG zg30  
TD 180286  
SOLVENT CDCl<sub>3</sub>  
NS 64  
DS 0  
SWH 18028.846 Hz  
FIDRES 0.100001 Hz  
AQ 4.9999318 sec  
RG 97.5  
DW 27.733 usec  
DE 7.60 usec  
TE 300.0 K  
D1 0.10000000 sec  
TD0 1

===== CHANNEL f1 =====  
SFO1 600.1337060 MHz  
NUC1 1H  
P1 10.00 usec  
PLW1 26.60000038 W

F2 - Processing parameters  
SI 262144  
SF 600.1300183 MHz  
WDW EM  
SSB 0  
LB 0.10 Hz  
GB 0  
PC 1.00

HAW-VII-079  
 $\text{Ph}_3\text{SnH}$  (2 equiv),  
 $\text{Et}_3\text{B}$  (0.1 equiv),  
 $\text{PhMe}$  (*c* of *sm* = 0.1M),  
80 °C, 24 h



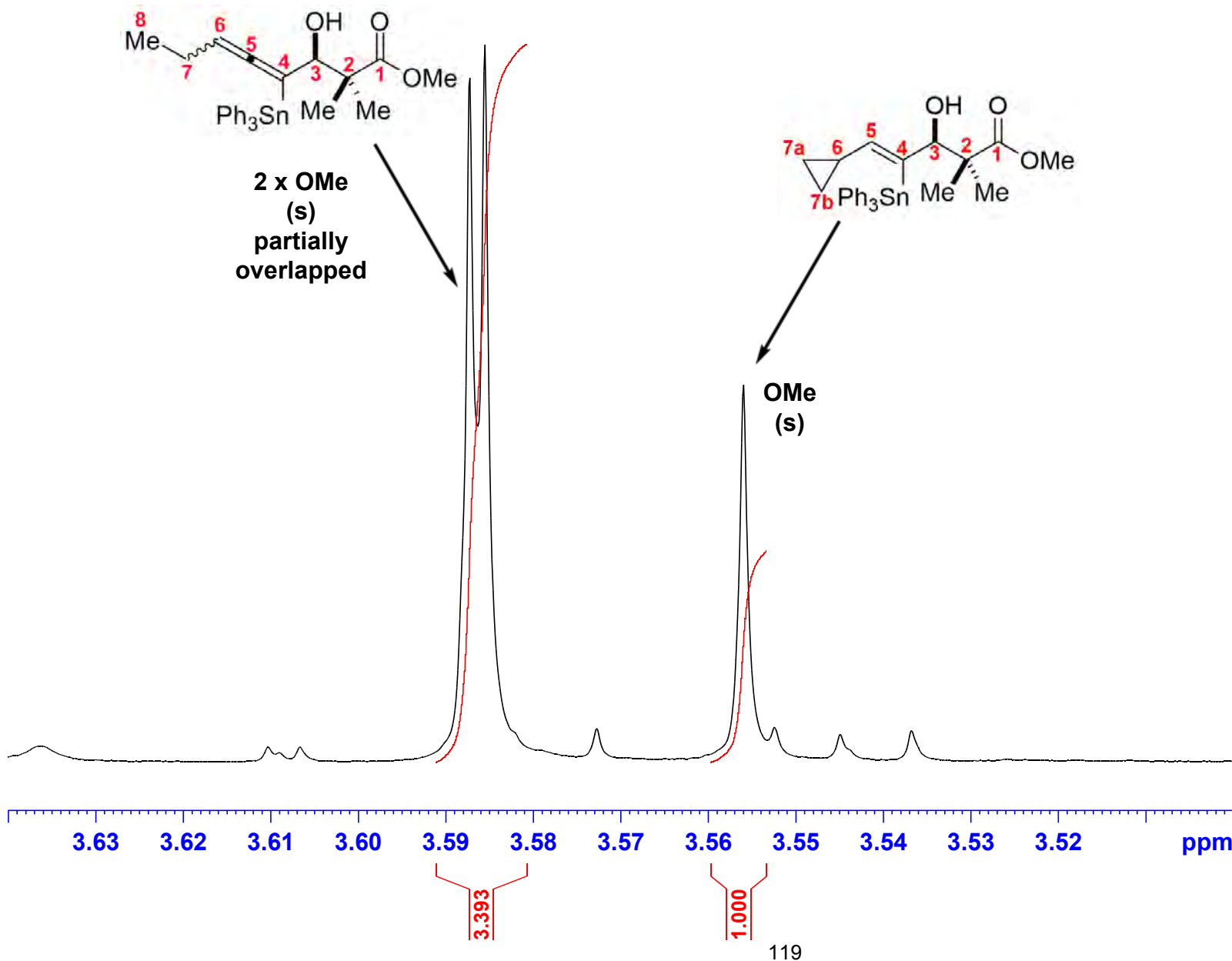
Current Data Parameters  
NAME HAW-VII-079-C  
EXPNO 10  
PROCNO 1

F2 - Acquisition Parameters  
Date 20200115  
Time 11.21  
INSTRUM spect  
PROBHD 5 mm PABBO BB/  
PULPROG zg30  
TD 180286  
SOLVENT CDCl<sub>3</sub>  
NS 64  
DS 0  
SWH 18028.846 Hz  
FIDRES 0.100001 Hz  
AQ 4.9999318 sec  
RG 97.5  
DW 27.733 usec  
DE 7.60 usec  
TE 300.0 K  
D1 0.10000000 sec  
TD0 1

===== CHANNEL f1 =====  
SFO1 600.1337060 MHz  
NUC1 1H  
P1 10.00 usec  
PLW1 26.60000038 W

F2 - Processing parameters  
SI 262144  
SF 600.1300215 MHz  
WDW EM  
SSB 0  
LB 0.10 Hz  
GB 0  
PC 1.00

HAW-VII-080  
 $\text{Ph}_3\text{SnH}$  (2 equiv),  
 $\text{Et}_3\text{B}$  (0.1 equiv),  
 $\text{PhMe}$  (c of sm = 0.1M),  
80 °C, 24 h



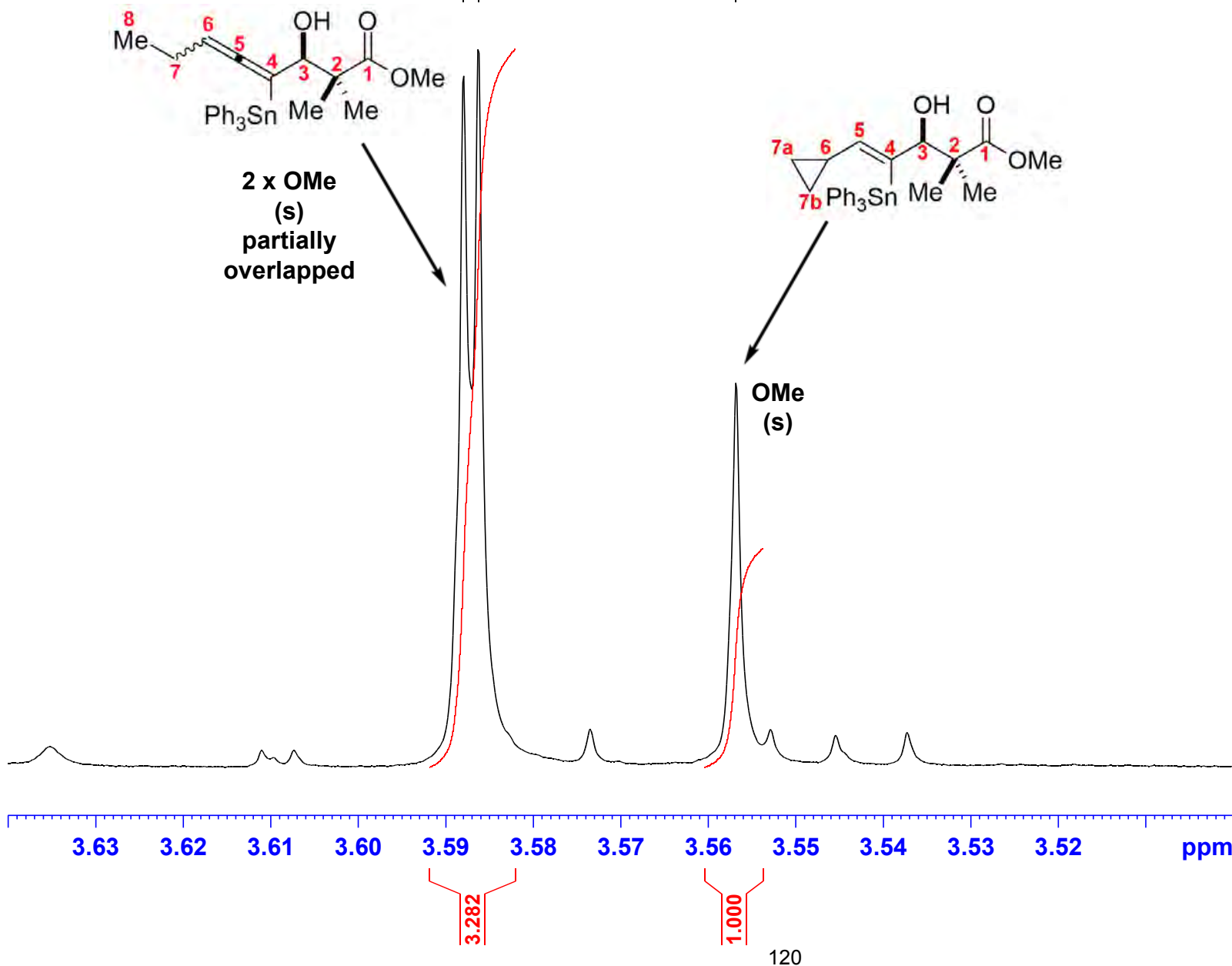
Current Data Parameters  
NAME HAW-VII-080-C  
EXPNO 20  
PROCNO 1

F2 - Acquisition Parameters  
Date 20200115  
Time 11.29  
INSTRUM spect  
PROBHD 5 mm PABBO BB/  
PULPROG zg30  
TD 180286  
SOLVENT CDCl3  
NS 64  
DS 0  
SWH 18028.846 Hz  
FIDRES 0.100001 Hz  
AQ 4.9999318 sec  
RG 97.5  
DW 27.733 usec  
DE 7.60 usec  
TE 300.0 K  
D1 0.10000000 sec  
TD0 1

===== CHANNEL f1 =====  
SFO1 600.1337060 MHz  
NUC1 1H  
P1 10.00 usec  
PLW1 26.60000038 W

F2 - Processing parameters  
SI 262144  
SF 600.1300187 MHz  
WDW EM  
SSB 0  
LB 0.10 Hz  
GB 0  
PC 1.00

HAW-VII-081  
 $\text{Ph}_3\text{SnH}$  (2 equiv),  
 $\text{Et}_3\text{B}$  (0.1 equiv),  
 $\text{PhMe}$  (c of sm = 0.1M),  
80 °C, 24 h



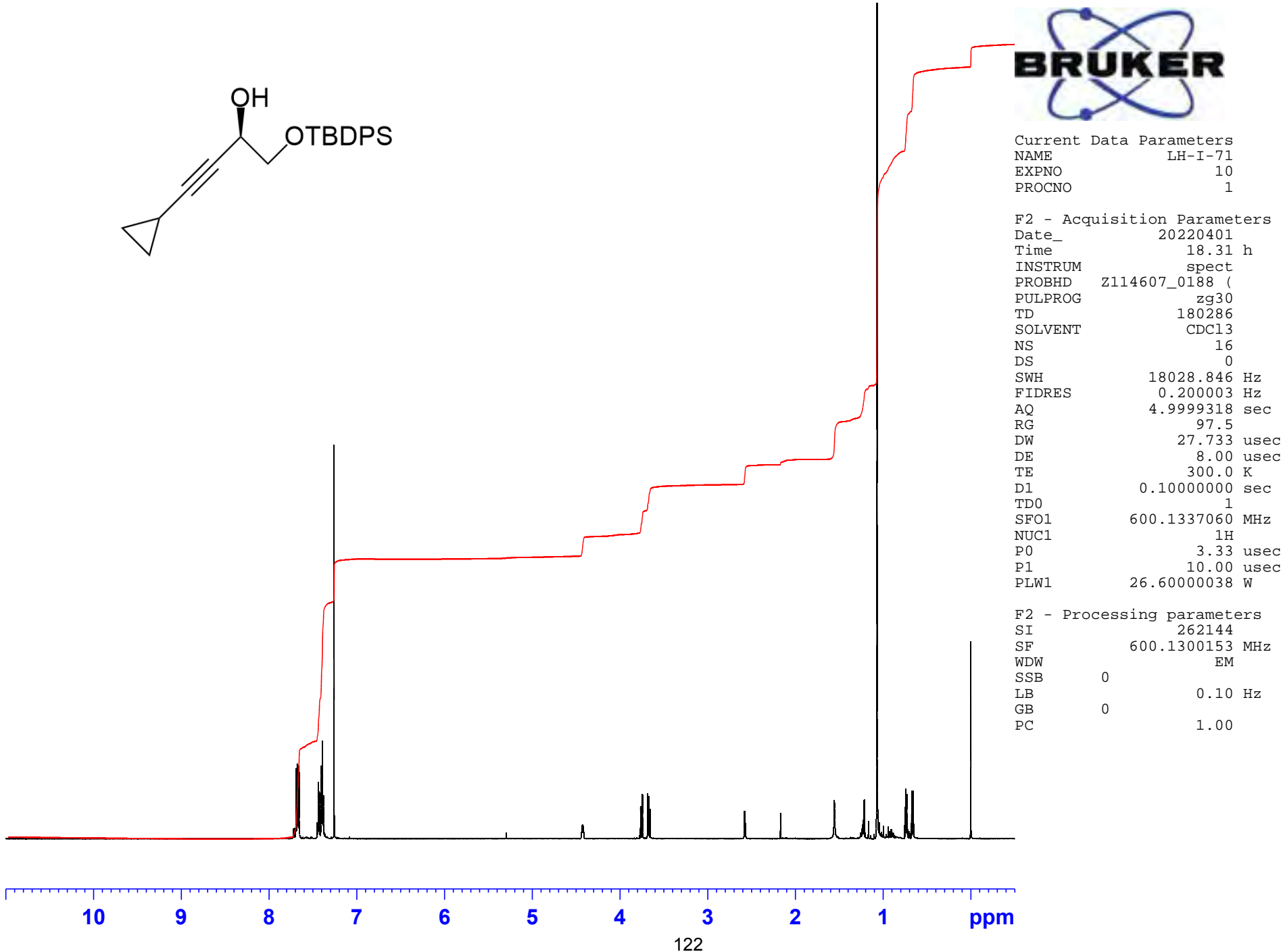
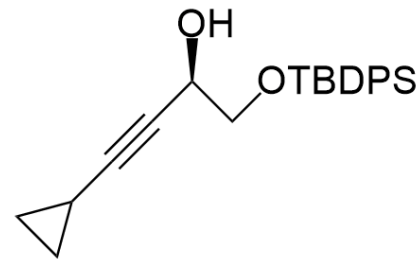
Current Data Parameters  
NAME HAW-VII-081-C  
EXPNO 30  
PROCNO 1

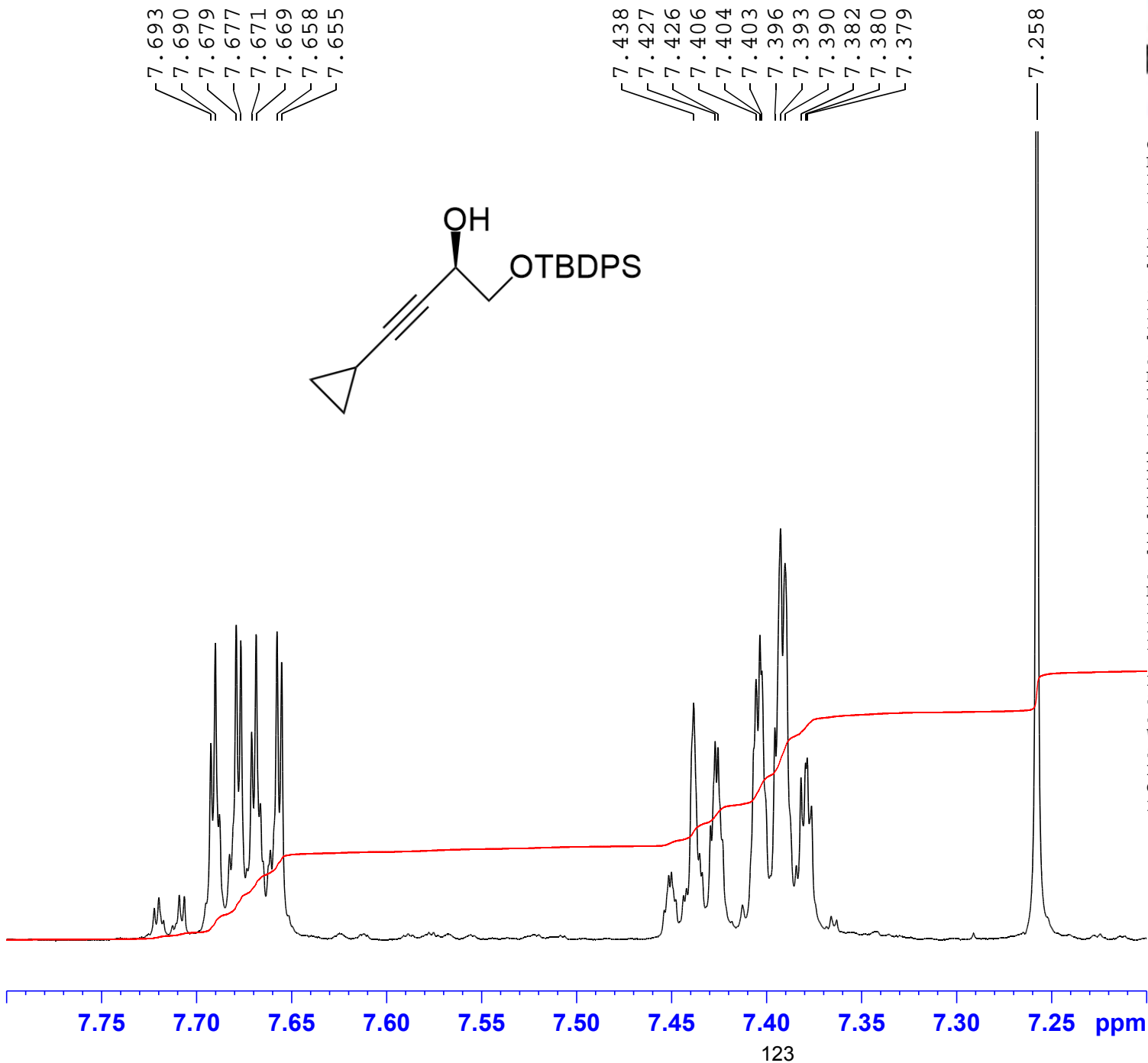
F2 - Acquisition Parameters  
Date 20200115  
Time 11.37  
INSTRUM spect  
PROBHD 5 mm PABBO BB/  
PULPROG zg30  
TD 180286  
SOLVENT CDCl<sub>3</sub>  
NS 64  
DS 0  
SWH 18028.846 Hz  
FIDRES 0.100001 Hz  
AQ 4.9999318 sec  
RG 97.5  
DW 27.733 usec  
DE 7.60 usec  
TE 300.0 K  
D1 0.10000000 sec  
TD0 1

===== CHANNEL f1 =====  
SFO1 600.1337060 MHz  
NUC1 1H  
P1 10.00 usec  
PLW1 26.60000038 W

F2 - Processing parameters  
SI 262144  
SF 600.1300170 MHz  
WDW EM  
SSB 0  
LB 0.10 Hz  
GB 0  
PC 1.00

**Part F. The 600.13 MHz  $^1\text{H}$  NMR and 150.90 MHz  $^{13}\text{C}$  NMR Spectra of the Cyclopropylpropargylic Alcohol 12 and the Tributylstannylallene 15 in  $\text{CDCl}_3$**

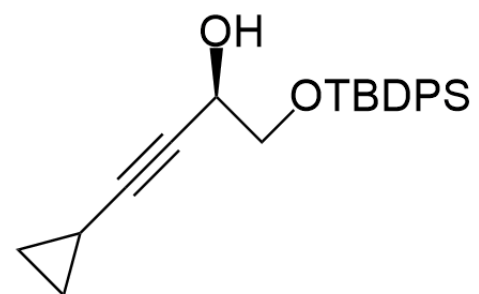




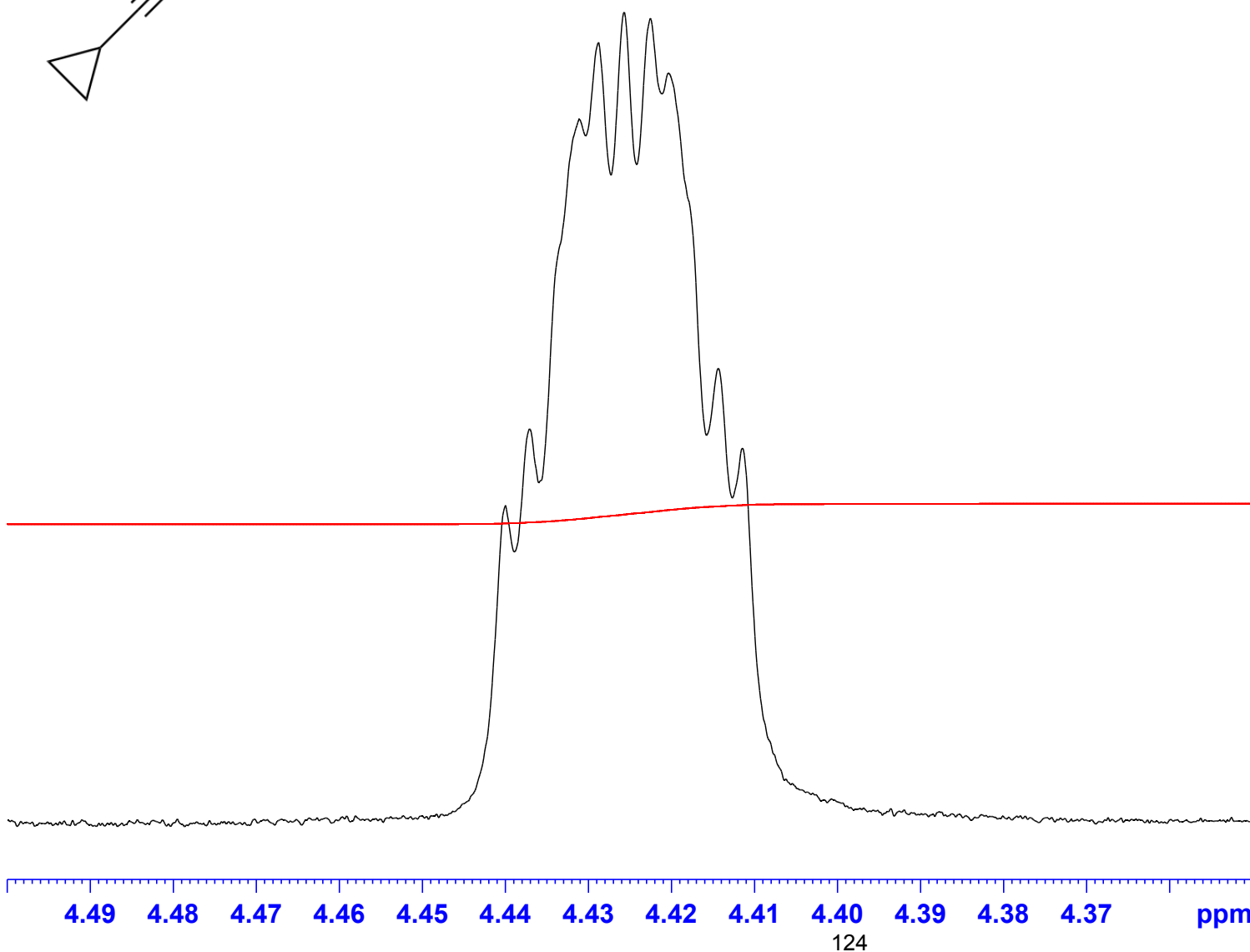
Current Data Parameters  
 NAME LH-I-71  
 EXPNO 10  
 PROCNO 1

F2 - Acquisition Parameters  
 Date\_ 20220401  
 Time 18.31 h  
 INSTRUM spect  
 PROBHD Z114607\_0188 (   
 PULPROG zg30  
 TD 180286  
 SOLVENT CDCl3  
 NS 16  
 DS 0  
 SWH 18028.846 Hz  
 FIDRES 0.200003 Hz  
 AQ 4.9999318 sec  
 RG 97.5  
 DW 27.733 usec  
 DE 8.00 usec  
 TE 300.0 K  
 D1 0.10000000 sec  
 TD0 1  
 SFO1 600.1337060 MHz  
 NUC1 1H  
 P0 3.33 usec  
 P1 10.00 usec  
 PLW1 26.60000038 W

F2 - Processing parameters  
 SI 262144  
 SF 600.1300153 MHz  
 WDW EM  
 SSB 0  
 LB 0.10 Hz  
 GB 0  
 PC 1.00



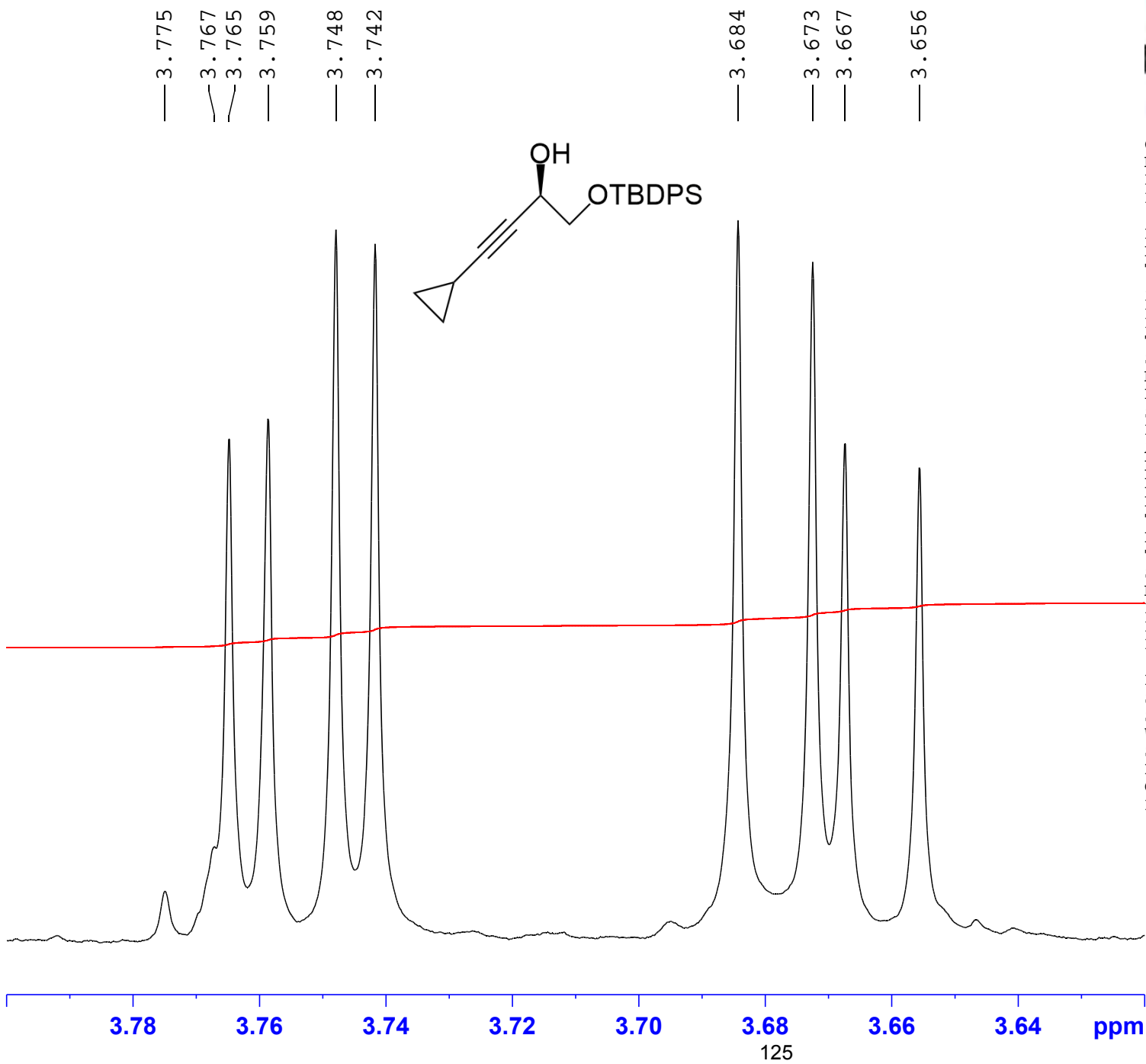
4.440  
4.437  
4.431  
4.429  
4.426  
4.423  
4.420  
4.414  
4.411



Current Data Parameters  
NAME LH-I-71  
EXPNO 10  
PROCNO 1

F2 - Acquisition Parameters  
Date\_ 20220401  
Time 18.31 h  
INSTRUM spect  
PROBHD Z114607\_0188 (   
PULPROG zg30  
TD 180286  
SOLVENT CDCl<sub>3</sub>  
NS 16  
DS 0  
SWH 18028.846 Hz  
FIDRES 0.200003 Hz  
AQ 4.9999318 sec  
RG 97.5  
DW 27.733 usec  
DE 8.00 usec  
TE 300.0 K  
D1 0.10000000 sec  
TD0 1  
SFO1 600.1337060 MHz  
NUC1 <sup>1</sup>H  
P0 3.33 usec  
P1 10.00 usec  
PLW1 26.60000038 W

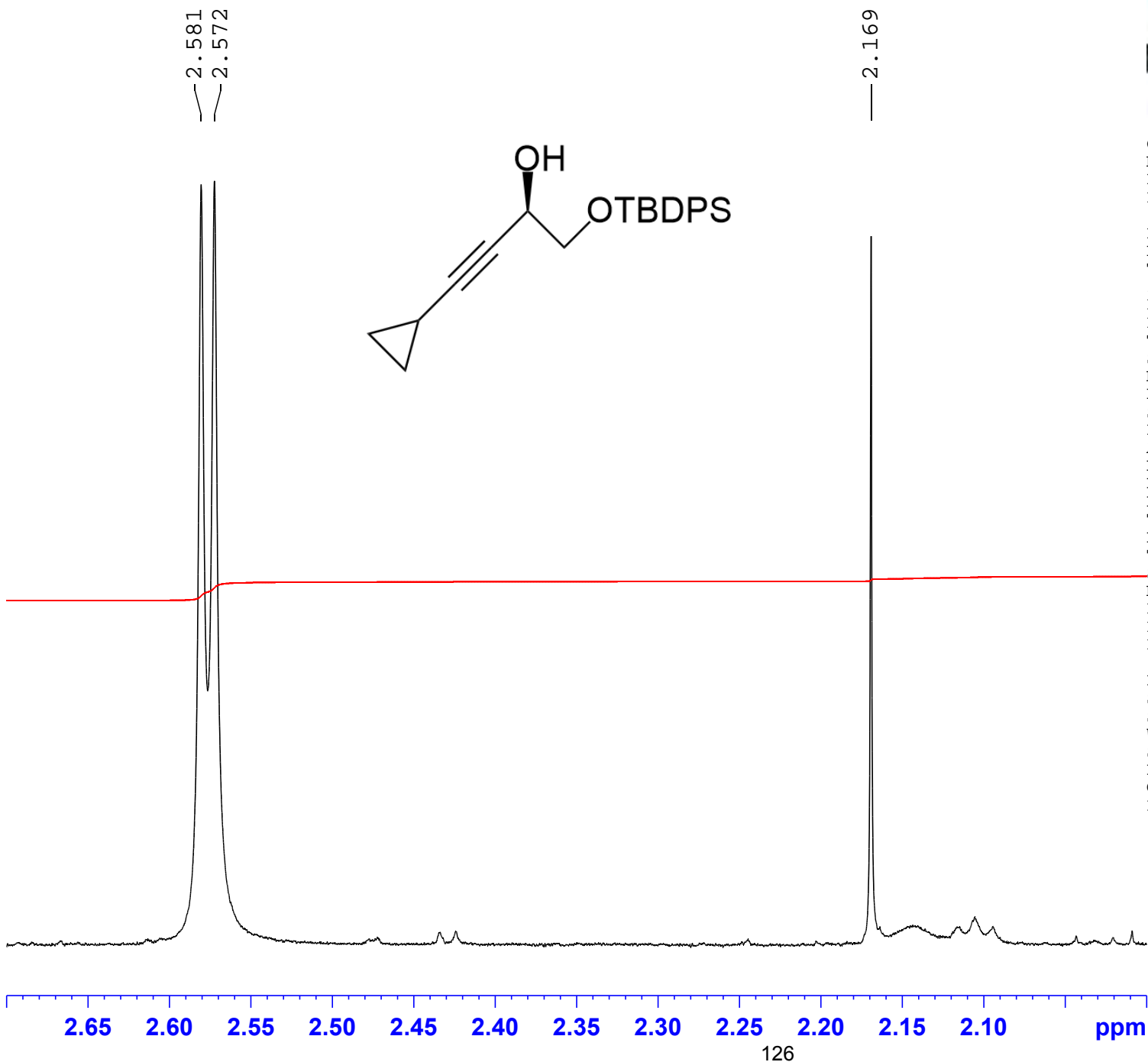
F2 - Processing parameters  
SI 262144  
SF 600.1300153 MHz  
WDW EM  
SSB 0  
LB 0.10 Hz  
GB 0  
PC 1.00



Current Data Parameters  
 NAME LH-I-71  
 EXPNO 10  
 PROCNO 1

F2 - Acquisition Parameters  
 Date\_ 20220401  
 Time 18.31 h  
 INSTRUM spect  
 PROBHD Z114607\_0188 (   
 PULPROG zg30  
 TD 180286  
 SOLVENT CDCl3  
 NS 16  
 DS 0  
 SWH 18028.846 Hz  
 FIDRES 0.200003 Hz  
 AQ 4.9999318 sec  
 RG 97.5  
 DW 27.733 usec  
 DE 8.00 usec  
 TE 300.0 K  
 D1 0.1000000 sec  
 TD0 1  
 SFO1 600.1337060 MHz  
 NUC1 1H  
 P0 3.33 usec  
 P1 10.00 usec  
 PLW1 26.60000038 W

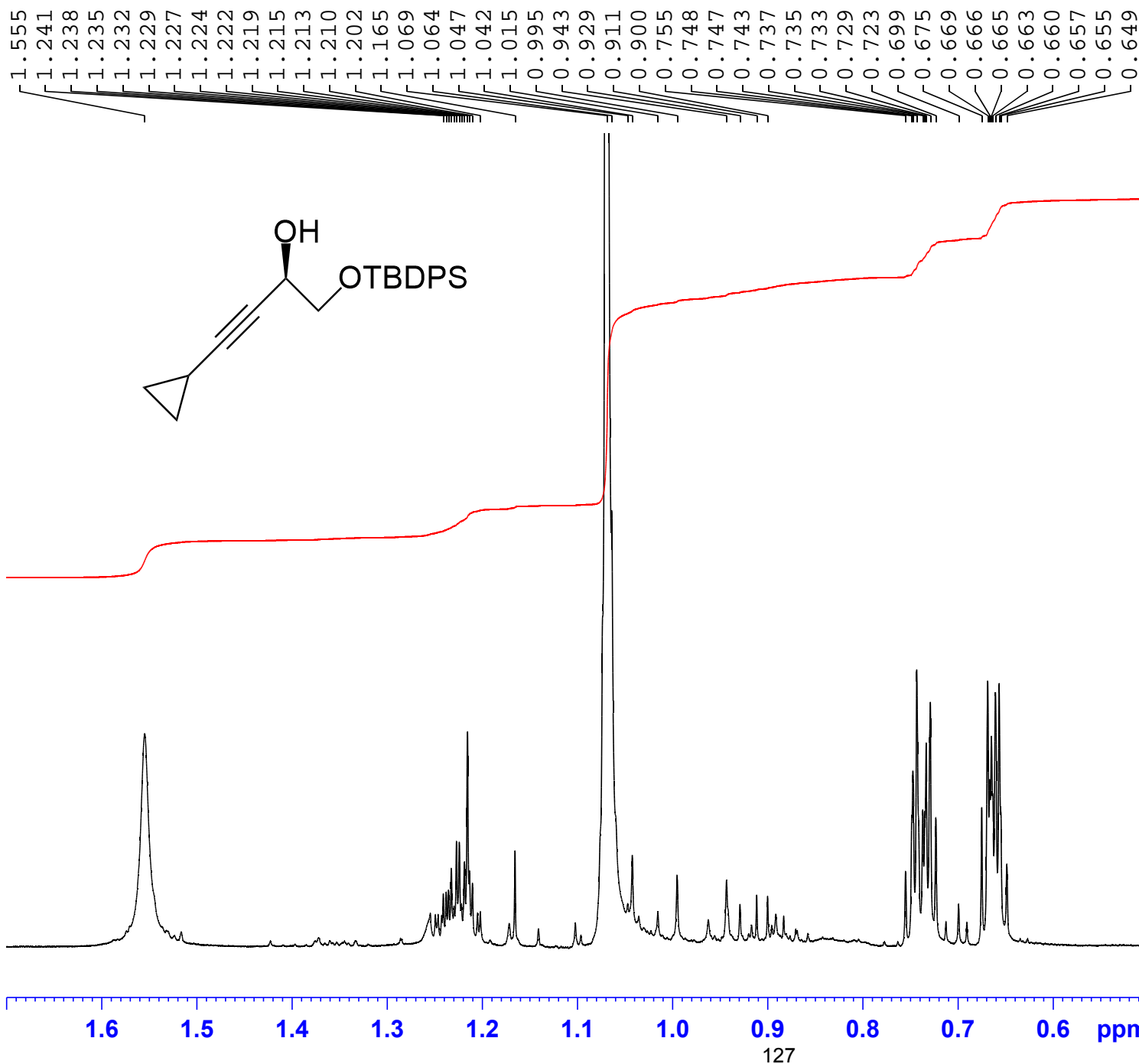
F2 - Processing parameters  
 SI 262144  
 SF 600.1300153 MHz  
 WDW EM  
 SSB 0  
 LB 0.10 Hz  
 GB 0  
 PC 1.00



Current Data Parameters  
 NAME LH-I-71  
 EXPNO 10  
 PROCNO 1

F2 - Acquisition Parameters  
 Date\_ 20220401  
 Time 18.31 h  
 INSTRUM spect  
 PROBHD Z114607\_0188 (   
 PULPROG zg30  
 TD 180286  
 SOLVENT CDCl<sub>3</sub>  
 NS 16  
 DS 0  
 SWH 18028.846 Hz  
 FIDRES 0.200003 Hz  
 AQ 4.9999318 sec  
 RG 97.5  
 DW 27.733 usec  
 DE 8.00 usec  
 TE 300.0 K  
 D1 0.10000000 sec  
 TD0 1  
 SFO1 600.1337060 MHz  
 NUC1 1H  
 P0 3.33 usec  
 P1 10.00 usec  
 PLW1 26.60000038 W

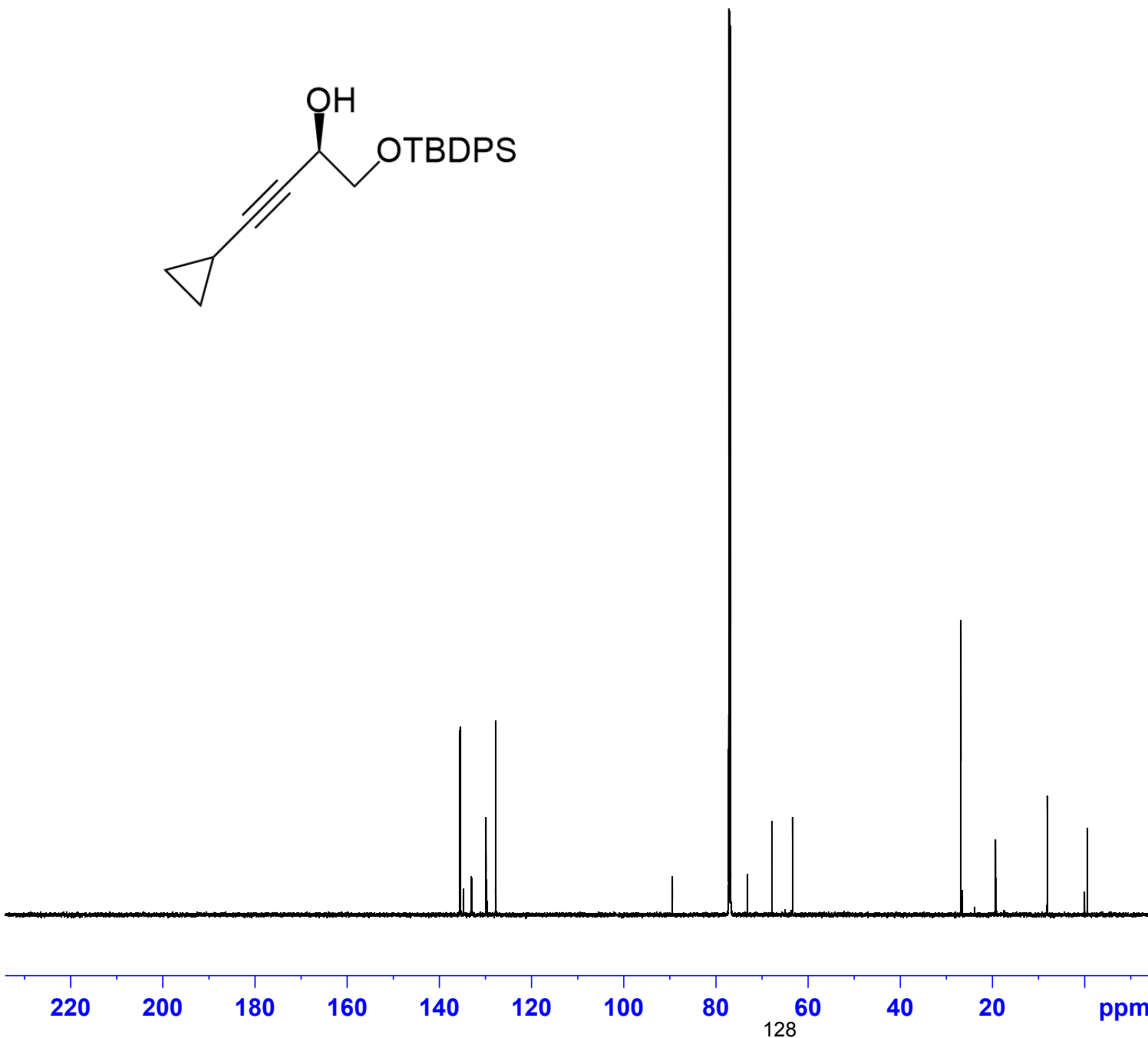
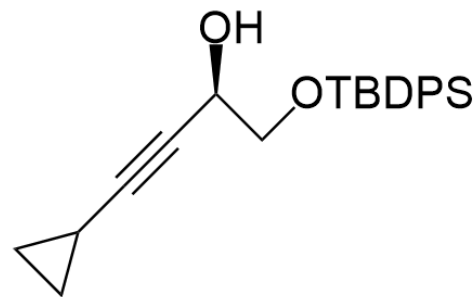
F2 - Processing parameters  
 SI 262144  
 SF 600.1300153 MHz  
 WDW EM  
 SSB 0  
 LB 0.10 Hz  
 GB 0  
 PC 1.00



Current Data Parameters  
 NAME LH-I-71  
 EXPNO 10  
 PROCNO 1

F2 - Acquisition Parameters  
 Date\_ 20220401  
 Time 18.31 h  
 INSTRUM spect  
 PROBHD Z114607\_0188 (zg30  
 PULPROG zg30  
 TD 180286  
 SOLVENT CDCl<sub>3</sub>  
 NS 16  
 DS 0  
 SWH 18028.846 Hz  
 FIDRES 0.200003 Hz  
 AQ 4.9999318 sec  
 RG 97.5  
 DW 27.733 usec  
 DE 8.00 usec  
 TE 300.0 K  
 D1 0.10000000 sec  
 TD0 1  
 SFO1 600.1337060 MHz  
 NUC1 <sup>1</sup>H  
 P0 3.33 usec  
 P1 10.00 usec  
 PLW1 26.60000038 W

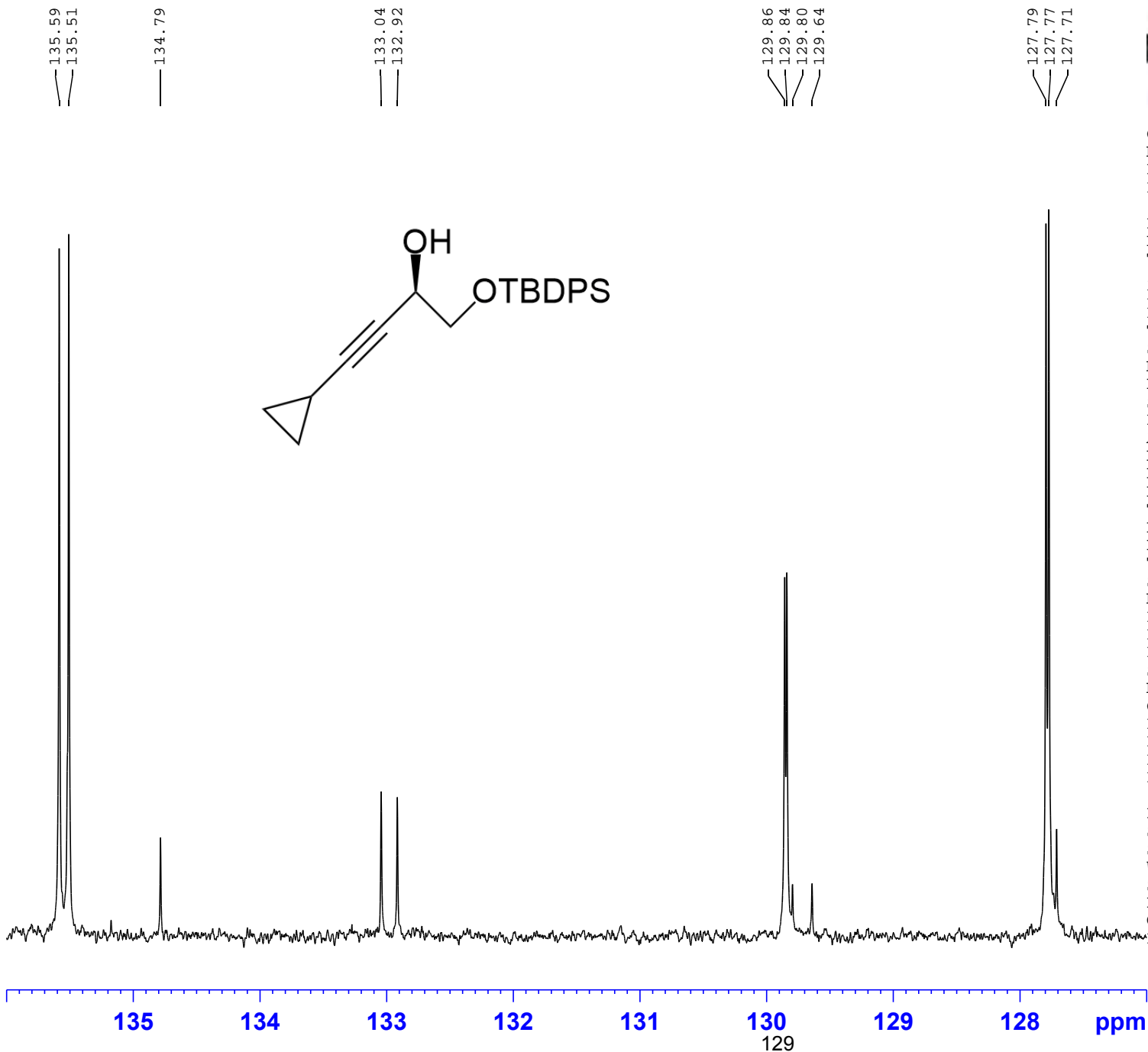
F2 - Processing parameters  
 SI 262144  
 SF 600.1300153 MHz  
 WDW EM  
 SSB 0  
 LB 0.10 Hz  
 GB 0  
 PC 1.00



Current Data Parameters  
 NAME LH-I-71  
 EXPNO 11  
 PROCNO 1

F2 - Acquisition Parameters  
 Date\_ 20220401  
 Time 20.00 h  
 INSTRUM spect  
 PROBHD Z114607\_0188 (   
 PULPROG zgpg30  
 TD 119044  
 SOLVENT CDCl3  
 NS 2000  
 DS 4  
 SWH 37500.000 Hz  
 FIDRES 0.630019 Hz  
 AQ 1.5872533 sec  
 RG 186.92  
 DW 13.333 usec  
 DE 6.53 usec  
 TE 300.0 K  
 D1 1.00000000 sec  
 D11 0.03000000 sec  
 TD0 1  
 SFO1 150.9194058 MHz  
 NUC1 13C  
 P0 3.93 usec  
 P1 11.80 usec  
 PLW1 85.00000000 W  
 SFO2 600.1324005 MHz  
 NUC2 1H  
 CPDPRG[ 2 waltz64  
 PCPD2 70.00 usec  
 PLW2 27.00000000 W  
 PLW12 0.57327998 W  
 PLW13 0.28836000 W

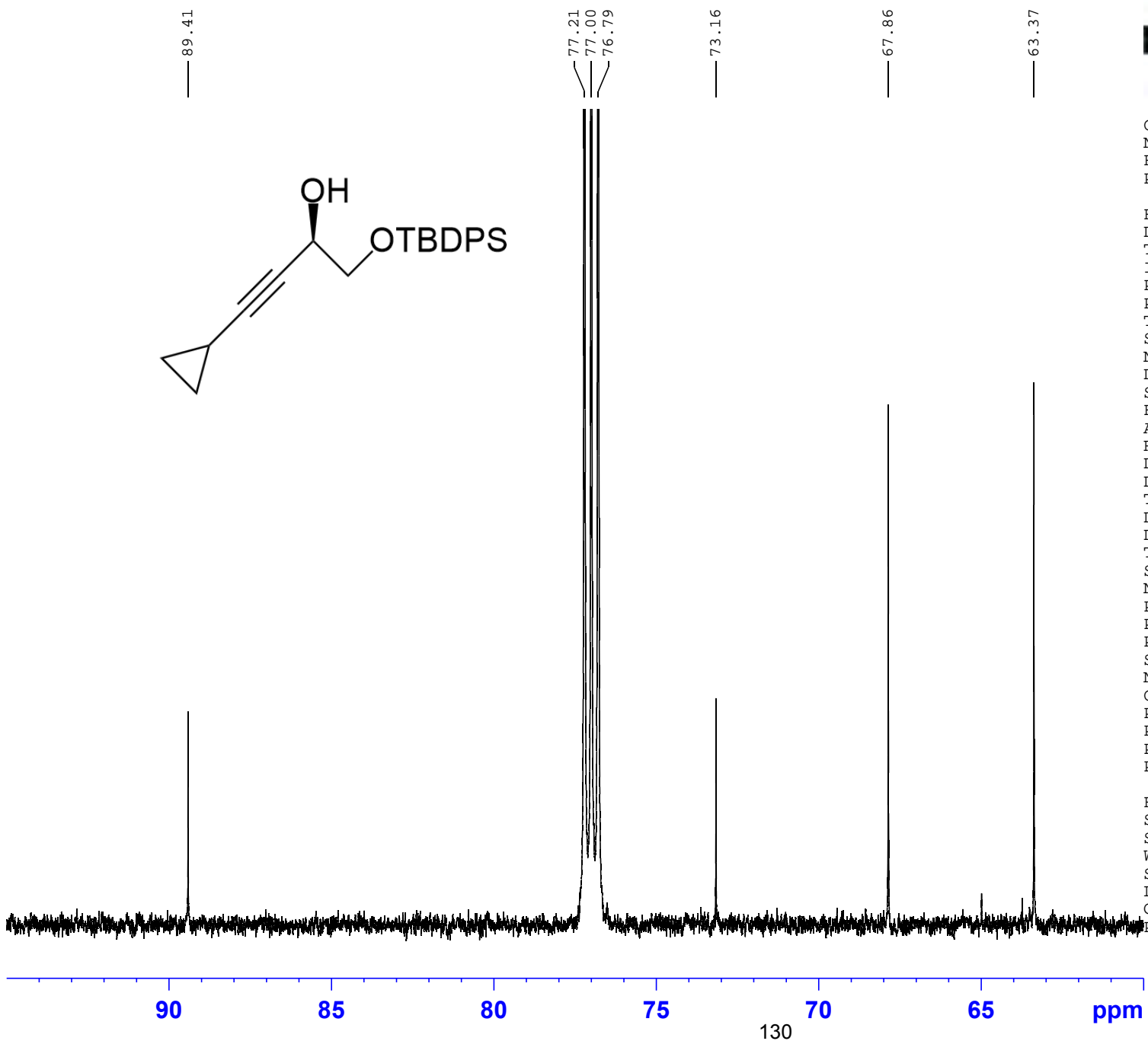
F2 - Processing parameters  
 SI 131072  
 SF 150.9028116 MHz  
 WDW EM  
 SSB 0  
 LB 1.00 Hz  
 GB 0  
 PC 1.40



Current Data Parameters  
 NAME LH-I-71  
 EXPNO 11  
 PROCNO 1

F2 - Acquisition Parameters  
 Date\_ 20220401  
 Time 20.00 h  
 INSTRUM spect  
 PROBHD Z114607\_0188 (   
 PULPROG zgpg30  
 TD 119044  
 SOLVENT CDCl3  
 NS 2000  
 DS 4  
 SWH 37500.000 Hz  
 FIDRES 0.630019 Hz  
 AQ 1.5872533 sec  
 RG 186.92  
 DW 13.333 usec  
 DE 6.53 usec  
 TE 300.0 K  
 D1 1.00000000 sec  
 D11 0.03000000 sec  
 TD0 1  
 SFO1 150.9194058 MHz  
 NUC1 13C  
 P0 3.93 usec  
 P1 11.80 usec  
 PLW1 85.00000000 W  
 SFO2 600.1324005 MHz  
 NUC2 1H  
 CPDPRG[ 2 waltz64  
 PCPD2 70.00 usec  
 PLW2 27.00000000 W  
 PLW12 0.57327998 W  
 PLW13 0.28836000 W

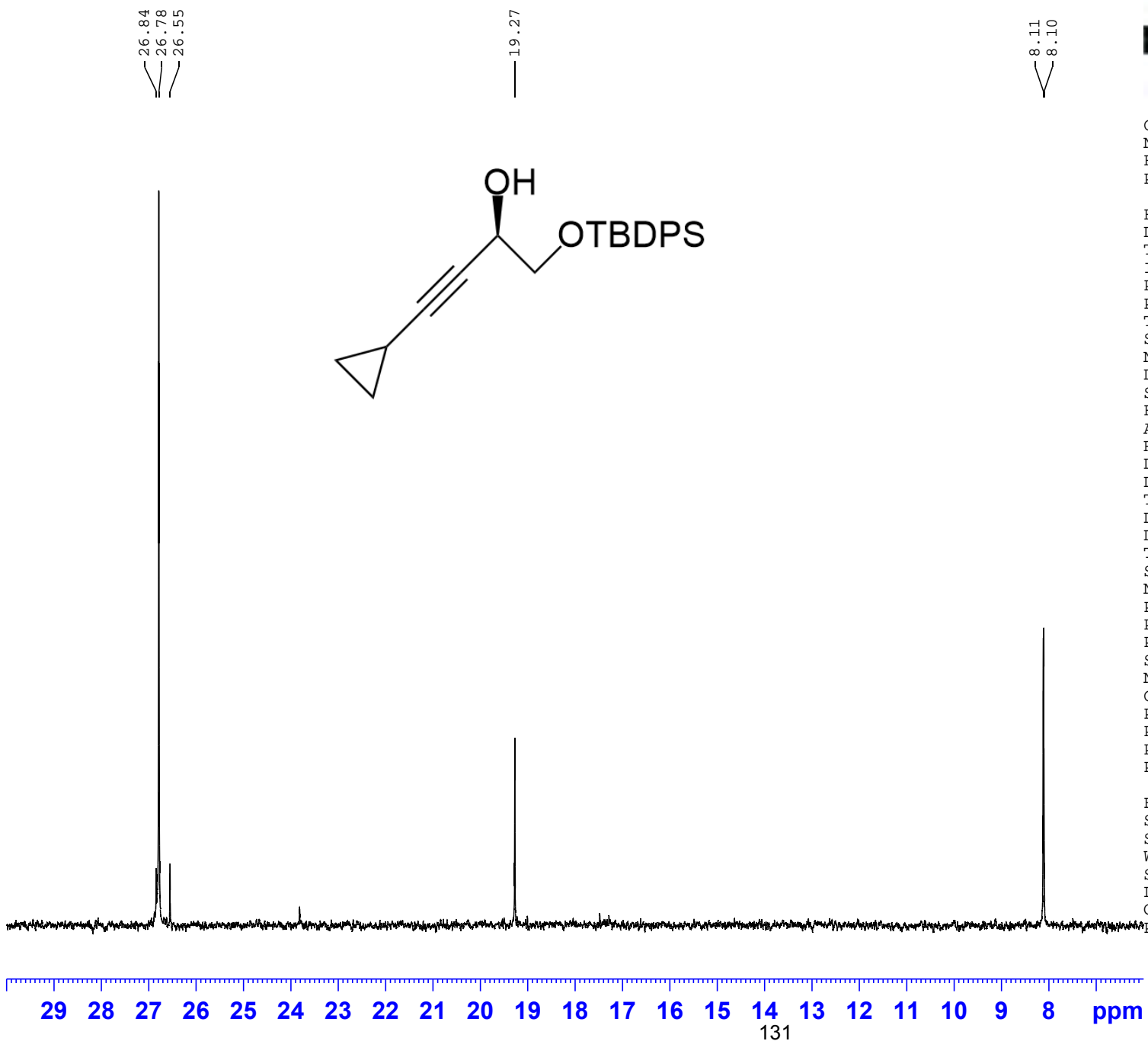
F2 - Processing parameters  
 SI 131072  
 SF 150.9028116 MHz  
 WDW EM  
 SSB 0  
 LB 1.00 Hz  
 GB 0  
 PC 1.40



Current Data Parameters  
 NAME LH-I-71  
 EXPNO 11  
 PROCNO 1

F2 - Acquisition Parameters  
 Date\_ 20220401  
 Time 20.00 h  
 INSTRUM spect  
 PROBHD Z114607\_0188 (   
 PULPROG zgpg30  
 TD 119044  
 SOLVENT CDCl<sub>3</sub>  
 NS 2000  
 DS 4  
 SWH 37500.000 Hz  
 FIDRES 0.630019 Hz  
 AQ 1.5872533 sec  
 RG 186.92  
 DW 13.333 usec  
 DE 6.53 usec  
 TE 300.0 K  
 D1 1.00000000 sec  
 D11 0.03000000 sec  
 TD0 1  
 SFO1 150.9194058 MHz  
 NUC1 <sup>13</sup>C  
 P0 3.93 usec  
 P1 11.80 usec  
 PLW1 85.00000000 W  
 SFO2 600.1324005 MHz  
 NUC2 <sup>1</sup>H  
 CPDPRG[ 2 waltz64  
 PCPD2 70.00 usec  
 PLW2 27.00000000 W  
 PLW12 0.57327998 W  
 PLW13 0.28836000 W

F2 - Processing parameters  
 SI 131072  
 SF 150.9028116 MHz  
 WDW EM  
 SSB 0  
 LB 1.00 Hz  
 GB 0  
 PC 1.40

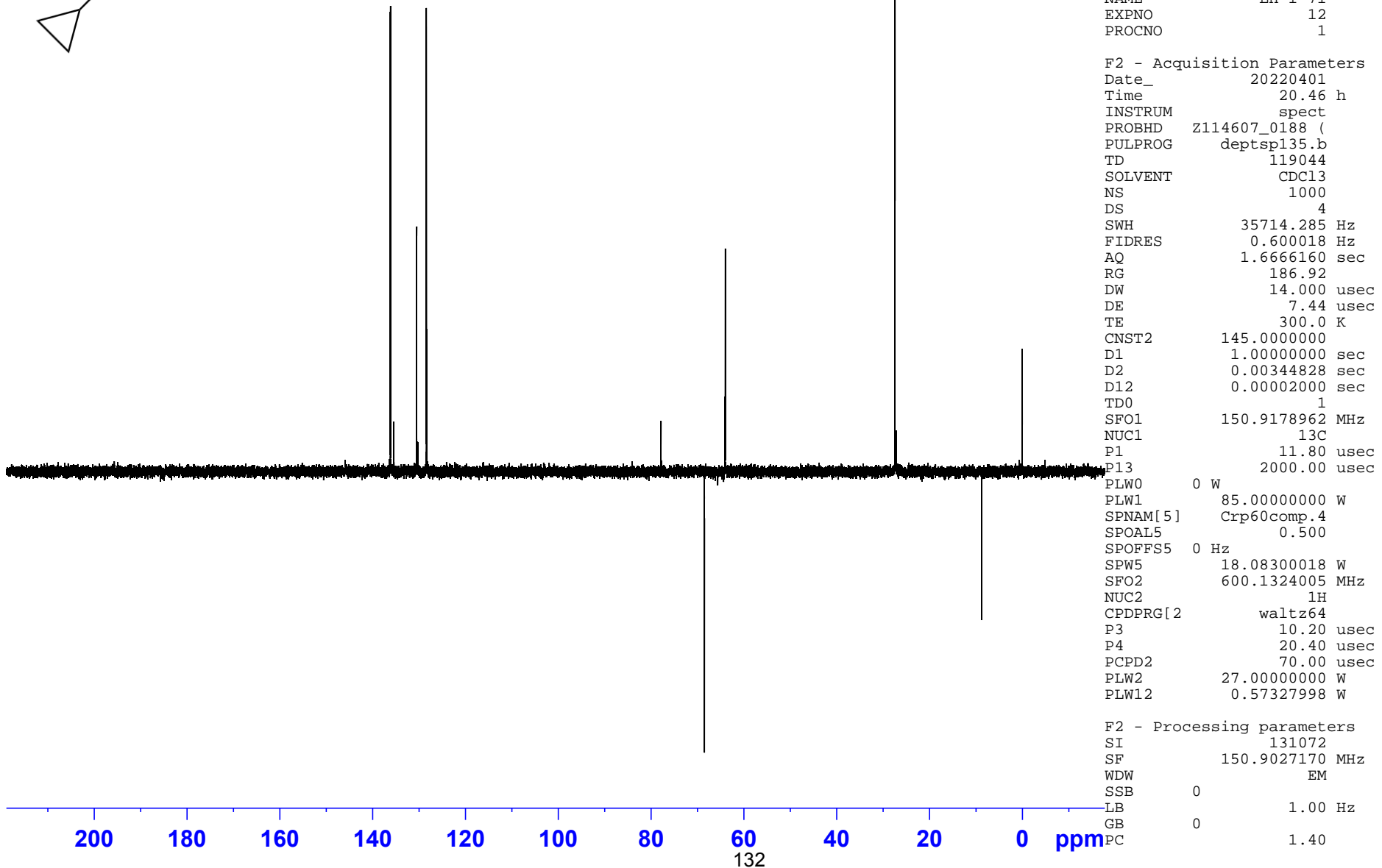
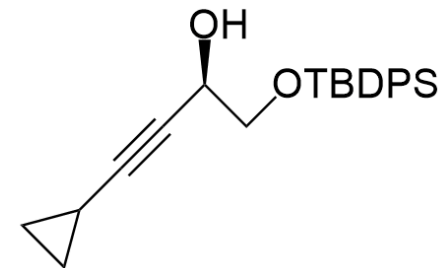


Current Data Parameters  
 NAME LH-I-71  
 EXPNO 11  
 PROCNO 1

F2 - Acquisition Parameters  
 Date\_ 20220401  
 Time 20.00 h  
 INSTRUM spect  
 PROBHD Z114607\_0188 (   
 PULPROG zgpg30  
 TD 119044  
 SOLVENT CDCl3  
 NS 2000  
 DS 4  
 SWH 37500.000 Hz  
 FIDRES 0.630019 Hz  
 AQ 1.5872533 sec  
 RG 186.92  
 DW 13.333 usec  
 DE 6.53 usec  
 TE 300.0 K  
 D1 1.00000000 sec  
 D11 0.03000000 sec  
 TD0 1  
 SFO1 150.9194058 MHz  
 NUC1 <sup>13</sup>C  
 P0 3.93 usec  
 P1 11.80 usec  
 PLW1 85.00000000 W  
 SFO2 600.1324005 MHz  
 NUC2 <sup>1H</sup>  
 CPDPRG[2] waltz64  
 PCPD2 70.00 usec  
 PLW2 27.00000000 W  
 PLW12 0.57327998 W  
 PLW13 0.28836000 W

F2 - Processing parameters  
 SI 131072  
 SF 150.9028116 MHz  
 WDW EM  
 SSB 0  
 LB 1.00 Hz  
 GB 0  
 DPC 1.40

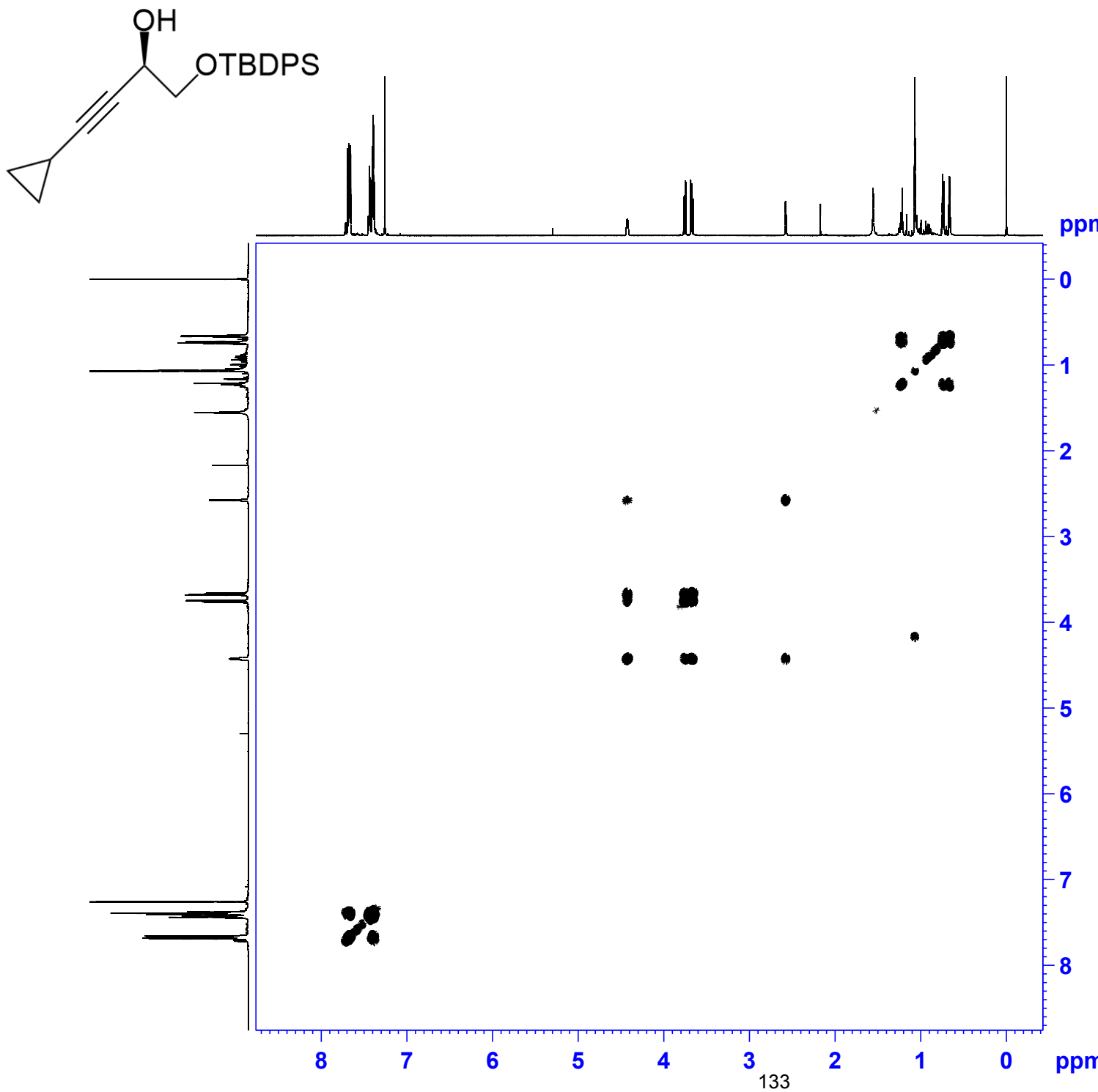
29 28 27 26 25 24 23 22 21 20 19 18 17 16 15 14 13 12 11 10 9 8 ppm  
 131



Current Data Parameters  
 NAME LH-I-71  
 EXPNO 12  
 PROCNO 1

F2 - Acquisition Parameters  
 Date\_ 20220401  
 Time 20.46 h  
 INSTRUM spect  
 PROBHD Z114607\_0188 (   
 PULPROG deptsp135.b  
 TD 119044  
 SOLVENT CDCl3  
 NS 1000  
 DS 4  
 SWH 35714.285 Hz  
 FIDRES 0.600018 Hz  
 AQ 1.6666160 sec  
 RG 186.92  
 DW 14.000 usec  
 DE 7.44 usec  
 TE 300.0 K  
 CNST2 145.0000000  
 D1 1.0000000 sec  
 D2 0.00344828 sec  
 D12 0.00002000 sec  
 TD0 1  
 SFO1 150.9178962 MHz  
 NUC1 13C  
 P1 11.80 usec  
 P13 2000.00 usec  
 PLW0 0 W  
 PLW1 85.00000000 W  
 SPNAM[5] Crp60comp.4  
 SPOAL5 0.500  
 SPOFFSS5 0 Hz  
 SPW5 18.08300018 W  
 SFO2 600.1324005 MHz  
 NUC2 1H  
 CPDPRG[2] waltz64  
 P3 10.20 usec  
 P4 20.40 usec  
 PCPD2 70.00 usec  
 PLW2 27.00000000 W  
 PLW12 0.57327998 W

F2 - Processing parameters  
 SI 131072  
 SF 150.9027170 MHz  
 WDW EM  
 SSB 0  
 LB 0 1.00 Hz  
 GB 0 1.40  
 PC



Current Data Parameters  
 NAME LH-I-71  
 EXPNO 13  
 PROCNO 1

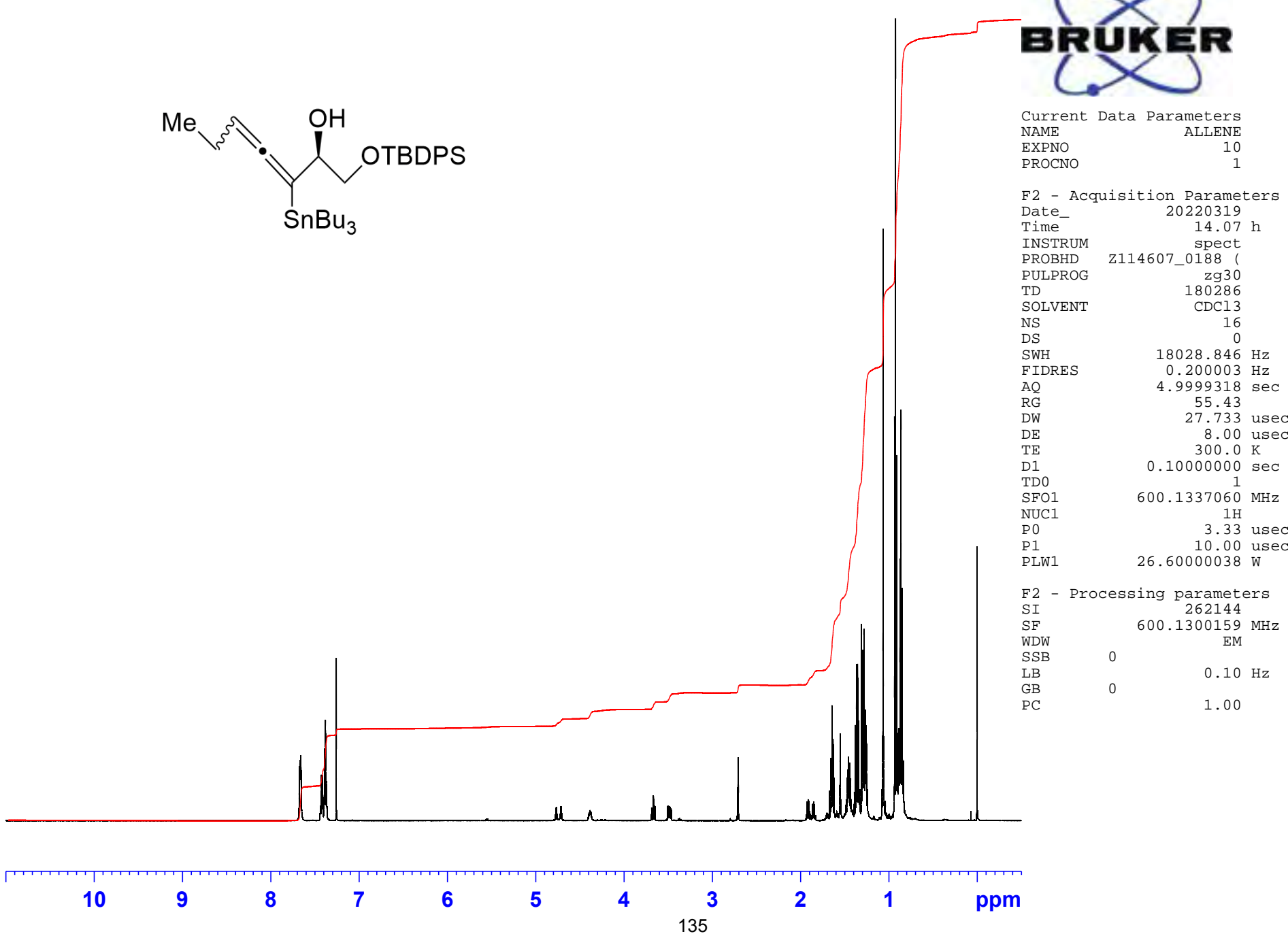
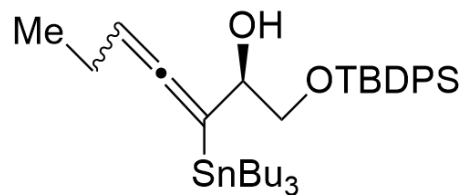
F2 - Acquisition Parameters  
 Date\_ 2020401  
 Time 20.57 h  
 INSTRUM spect  
 PROBHD Z114607\_0188 (PULPROG cosygpmfppqf  
 TD 2048  
 SOLVENT CDCl3  
 NS 2  
 DS 8  
 SWH 5514.706 Hz  
 FIDRES 5.385455 Hz  
 AQ 0.1856853 sec  
 RG 186.92  
 DW 90.667 usec  
 DE 6.50 usec  
 TE 300.0 K  
 D0 0.00000300 sec  
 D1 0.87302327 sec  
 D11 0.03000000 sec  
 D12 0.00002000 sec  
 D13 0.00000400 sec  
 D16 0.00020000 sec  
 IN0 0.00018160 sec  
 TDav 1  
 SFO1 600.1325168 MHz  
 NUC1 1H  
 P1 10.00 usec  
 P17 2500.00 usec  
 PLW1 26.60000038 W  
 PLW10 4.25600004 W  
 GPNAM[1] SMSQ10.100  
 GPZ1 16.00 %  
 GPNAM[2] SMSQ10.100  
 GPZ2 12.00 %  
 GPNAM[3] SMSQ10.100  
 GPZ3 40.00 %  
 P16 1000.00 usec

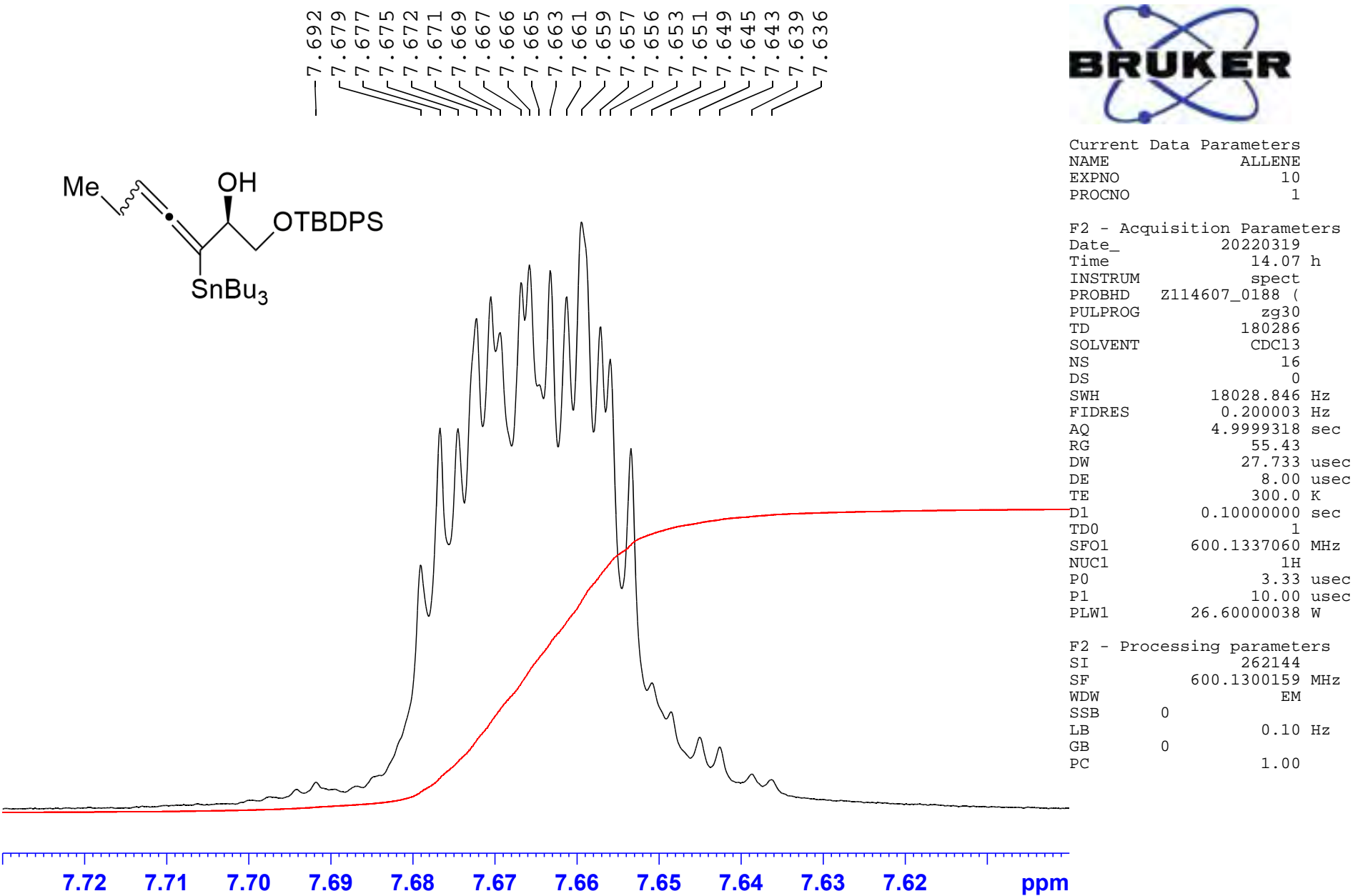
F1 - Acquisition parameters  
 TD 256  
 SFO1 600.1325 MHz  
 FIDRES 43.020374 Hz  
 SW 9.176 ppm  
 FnMODE QF

F2 - Processing parameters  
 SI 1024  
 SF 600.1300153 MHz  
 WDW SINE  
 SSB 0  
 LB 0 Hz  
 GB 0  
 PC 1.40

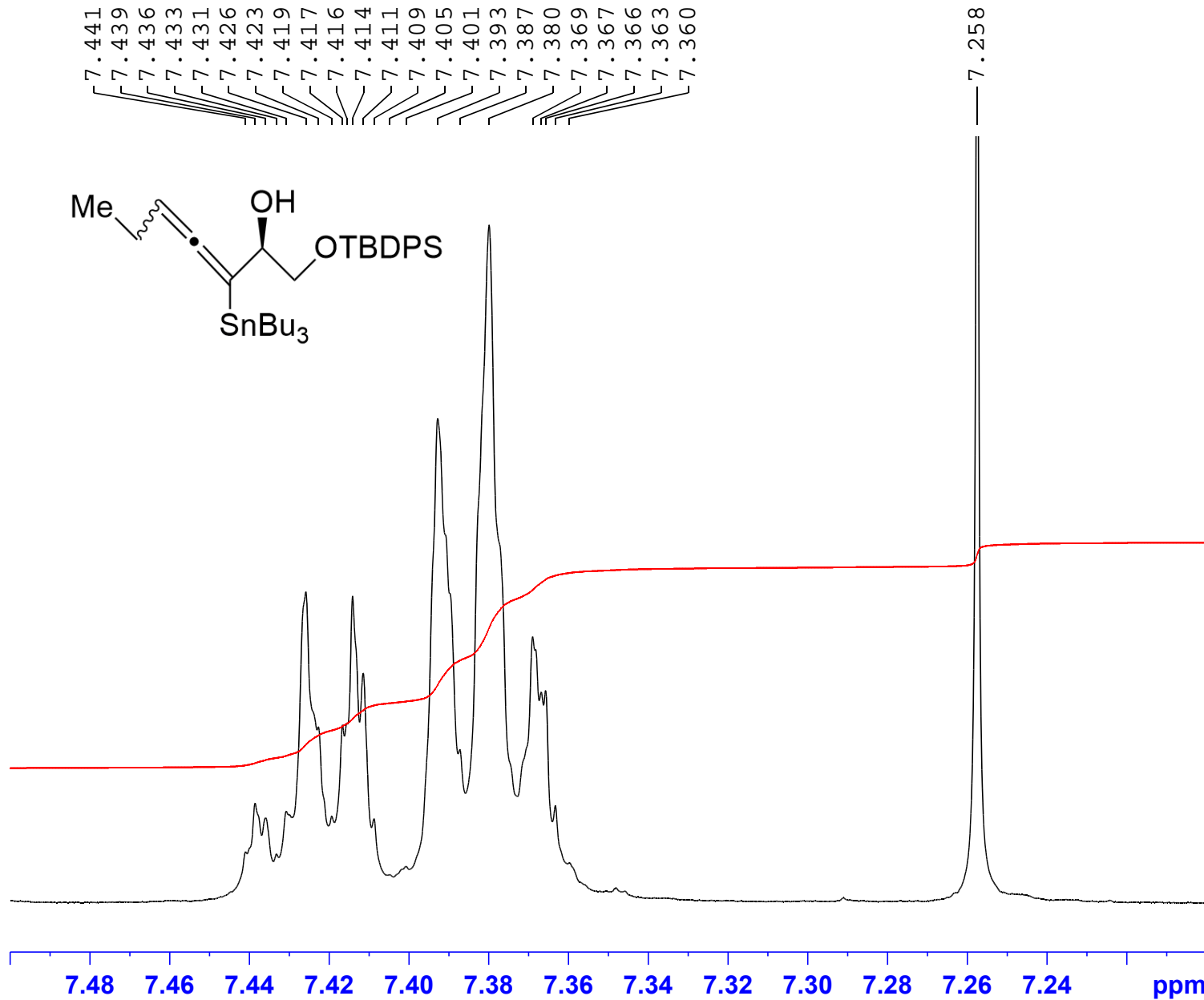
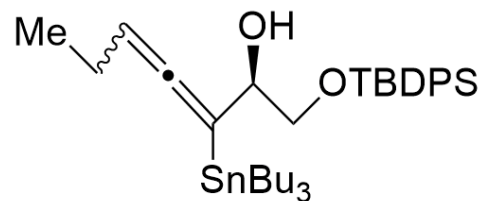
F1 - Processing parameters  
 SI 1024  
 MC2 QF  
 SF 600.1300153 MHz  
 WDW SINE  
 SSB 0  
 LB 0 Hz  
 GB 0







7.441  
7.439  
7.436  
7.433  
7.426  
7.423  
7.419  
7.417  
7.416  
7.414  
7.409  
7.405  
7.401  
7.393  
7.387  
7.380  
7.369  
7.367  
7.366  
7.363  
7.360



#### Current Data Parameters

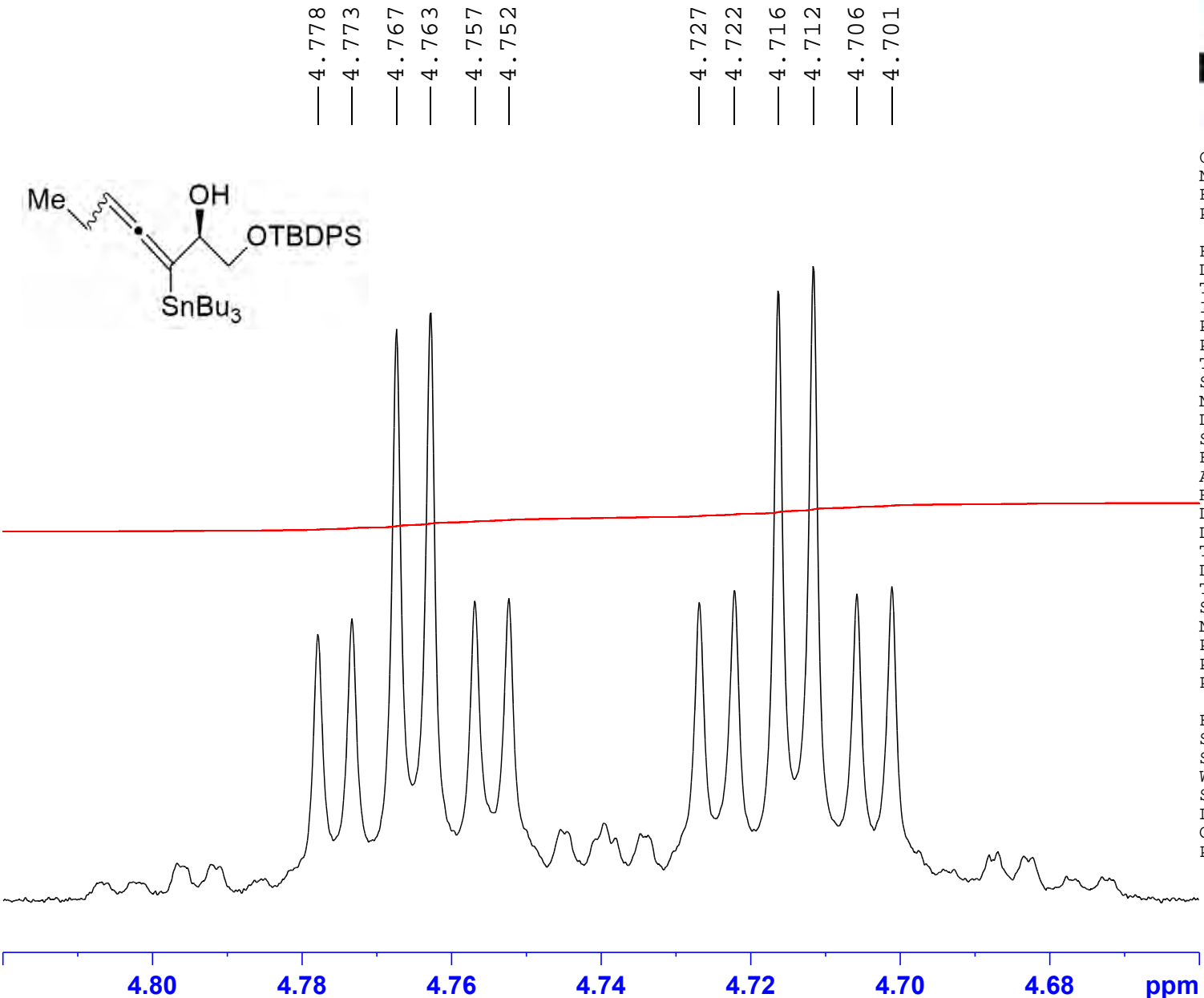
NAME ALLENE  
EXPNO 10  
PROCNO 1

#### F2 - Acquisition Parameters

Date\_ 20220319  
Time 14.07 h  
INSTRUM spect  
PROBHD Z114607\_0188 (   
PULPROG zg30  
TD 180286  
SOLVENT CDCl3  
NS 16  
DS 0  
SWH 18028.846 Hz  
FIDRES 0.200003 Hz  
AQ 4.9999318 sec  
RG 55.43  
DW 27.733 usec  
DE 8.00 usec  
TE 300.0 K  
D1 0.10000000 sec  
TD0 1  
SFO1 600.1337060 MHz  
NUC1 1H  
P0 3.33 usec  
P1 10.00 usec  
PLW1 26.60000038 W

#### F2 - Processing parameters

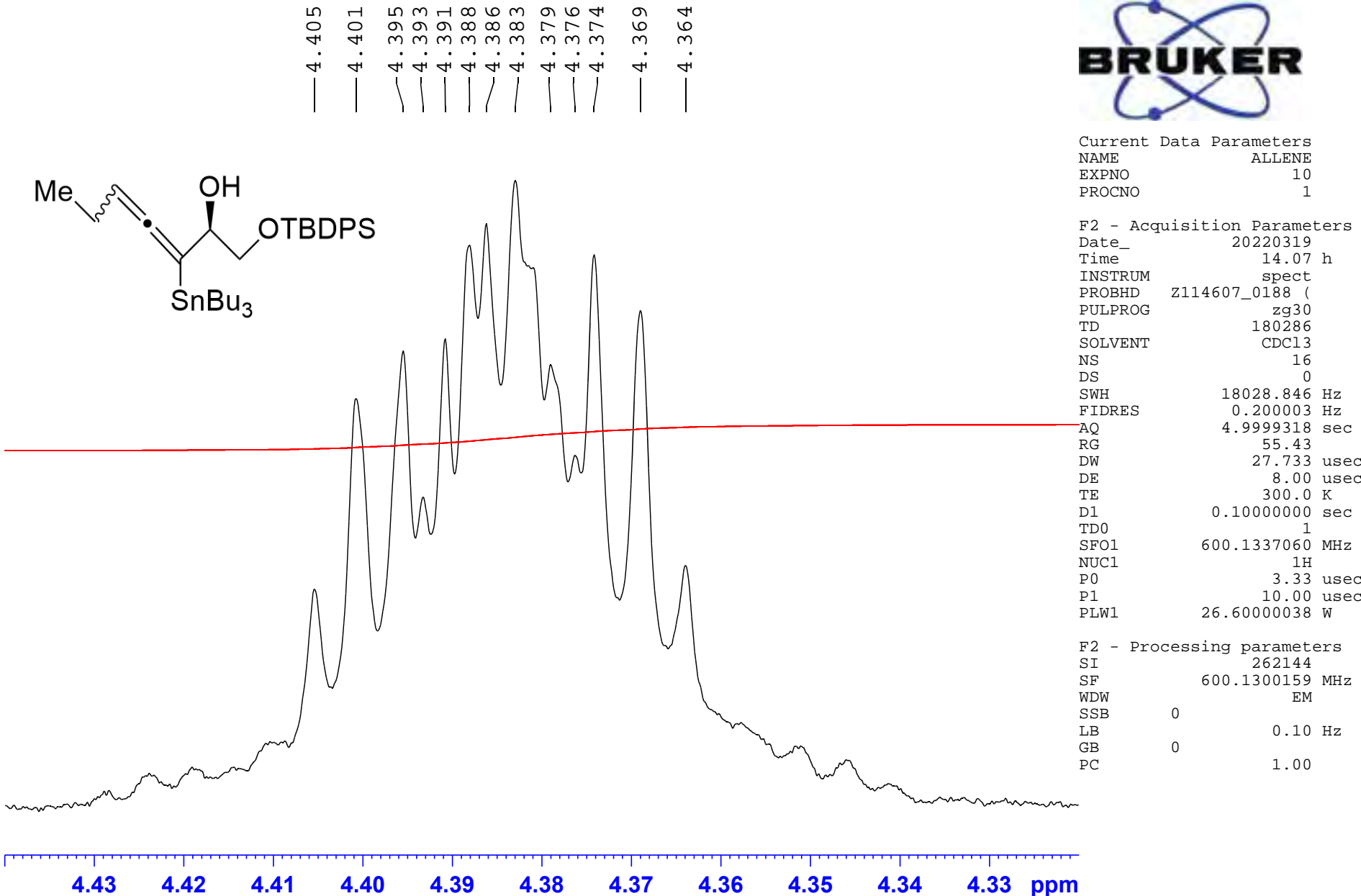
SI 262144  
SF 600.1300159 MHz  
WDW EM  
SSB 0  
LB 0.10 Hz  
GB 0  
PC 1.00

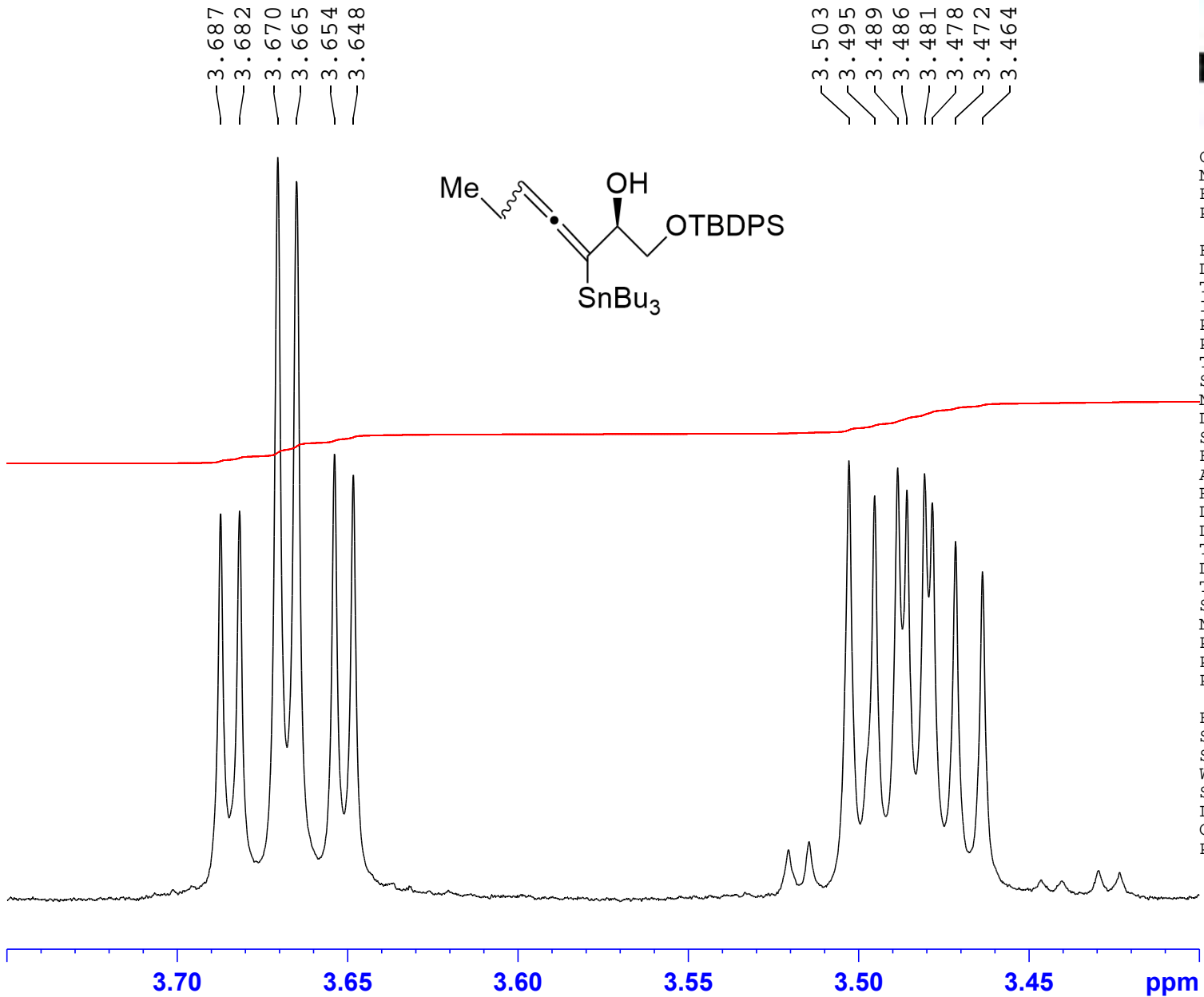


Current Data Parameters  
 NAME ALLENE  
 EXPNO 10  
 PROCNO 1

F2 - Acquisition Parameters  
 Date\_ 20220319  
 Time 14.07 h  
 INSTRUM spect  
 PROBHD Z114607\_0188 (   
 PULPROG zg30  
 TD 180286  
 SOLVENT CDCl3  
 NS 16  
 DS 0  
 SWH 18028.846 Hz  
 FIDRES 0.200003 Hz  
 AQ 4.9999318 sec  
 RG 55.43  
 DW 27.733 usec  
 DE 8.00 usec  
 TE 300.0 K  
 D1 0.10000000 sec  
 TD0 1  
 SFO1 600.1337060 MHz  
 NUC1 1H  
 P0 3.33 usec  
 P1 10.00 usec  
 PLW1 26.60000038 W

F2 - Processing parameters  
 SI 262144  
 SF 600.1300159 MHz  
 WDW EM  
 SSB 0  
 LB 0  
 GB 0  
 PC 1.00

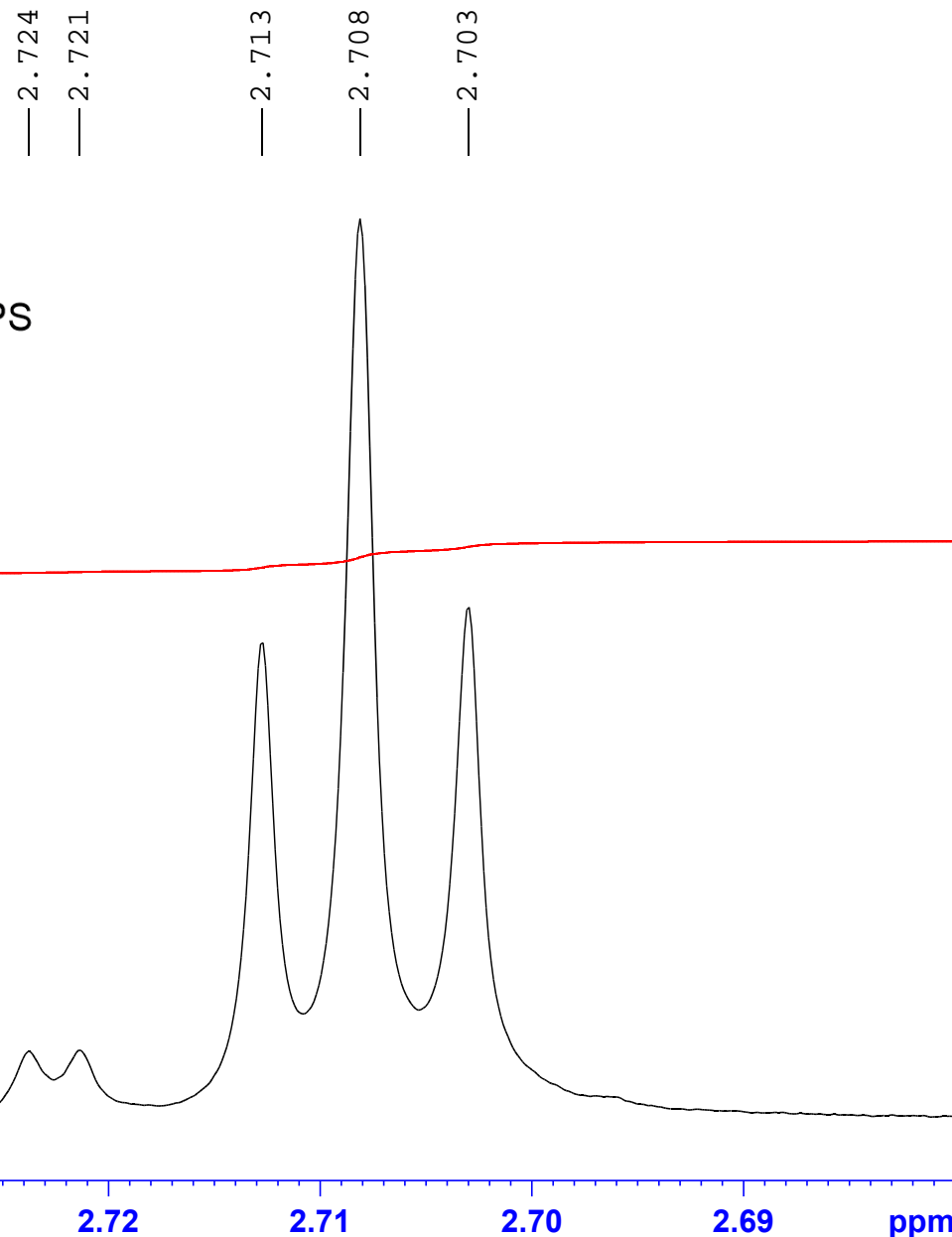
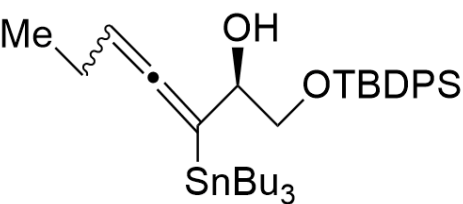




Current Data Parameters  
 NAME ALLENE  
 EXPNO 10  
 PROCNO 1

F2 - Acquisition Parameters  
 Date\_ 20220319  
 Time 14.07 h  
 INSTRUM spect  
 PROBHD Z114607\_0188 (zg30  
 PULPROG zg30  
 TD 180286  
 SOLVENT CDCl<sub>3</sub>  
 NS 16  
 DS 0  
 SWH 18028.846 Hz  
 FIDRES 0.200003 Hz  
 AQ 4.9999318 sec  
 RG 55.43  
 DW 27.733 usec  
 DE 8.00 usec  
 TE 300.0 K  
 D1 0.1000000 sec  
 TD0 1  
 SFO1 600.1337060 MHz  
 NUC1 <sup>1</sup>H  
 P0 3.33 usec  
 P1 10.00 usec  
 PLW1 26.60000038 W

F2 - Processing parameters  
 SI 262144  
 SF 600.1300159 MHz  
 WDW EM  
 SSB 0  
 LB 0.10 Hz  
 GB 0  
 PC 1.00



#### Current Data Parameters

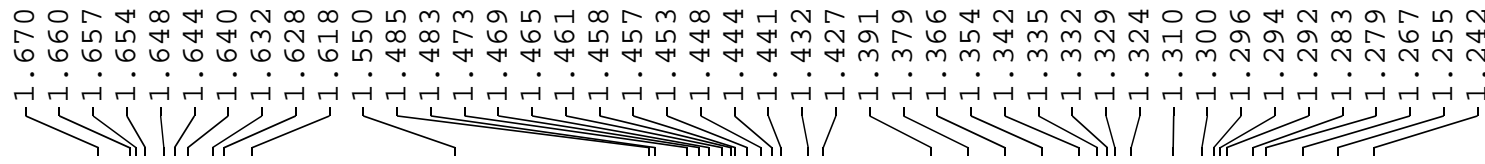
NAME ALLENE  
EXPNO 10  
PROCNO 1

#### F2 - Acquisition Parameters

Date\_ 20220319  
Time 14.07 h  
INSTRUM spect  
PROBHD Z114607\_0188 (   
PULPROG zg30  
TD 180286  
SOLVENT CDCl3  
NS 16  
DS 0  
SWH 18028.846 Hz  
FIDRES 0.200003 Hz  
AQ 4.9999318 sec  
RG 55.43  
DW 27.733 usec  
DE 8.00 usec  
TE 300.0 K  
D1 0.10000000 sec  
TD0 1  
SFO1 600.1337060 MHz  
NUC1 1H  
P0 3.33 usec  
P1 10.00 usec  
PLW1 26.60000038 W

#### F2 - Processing parameters

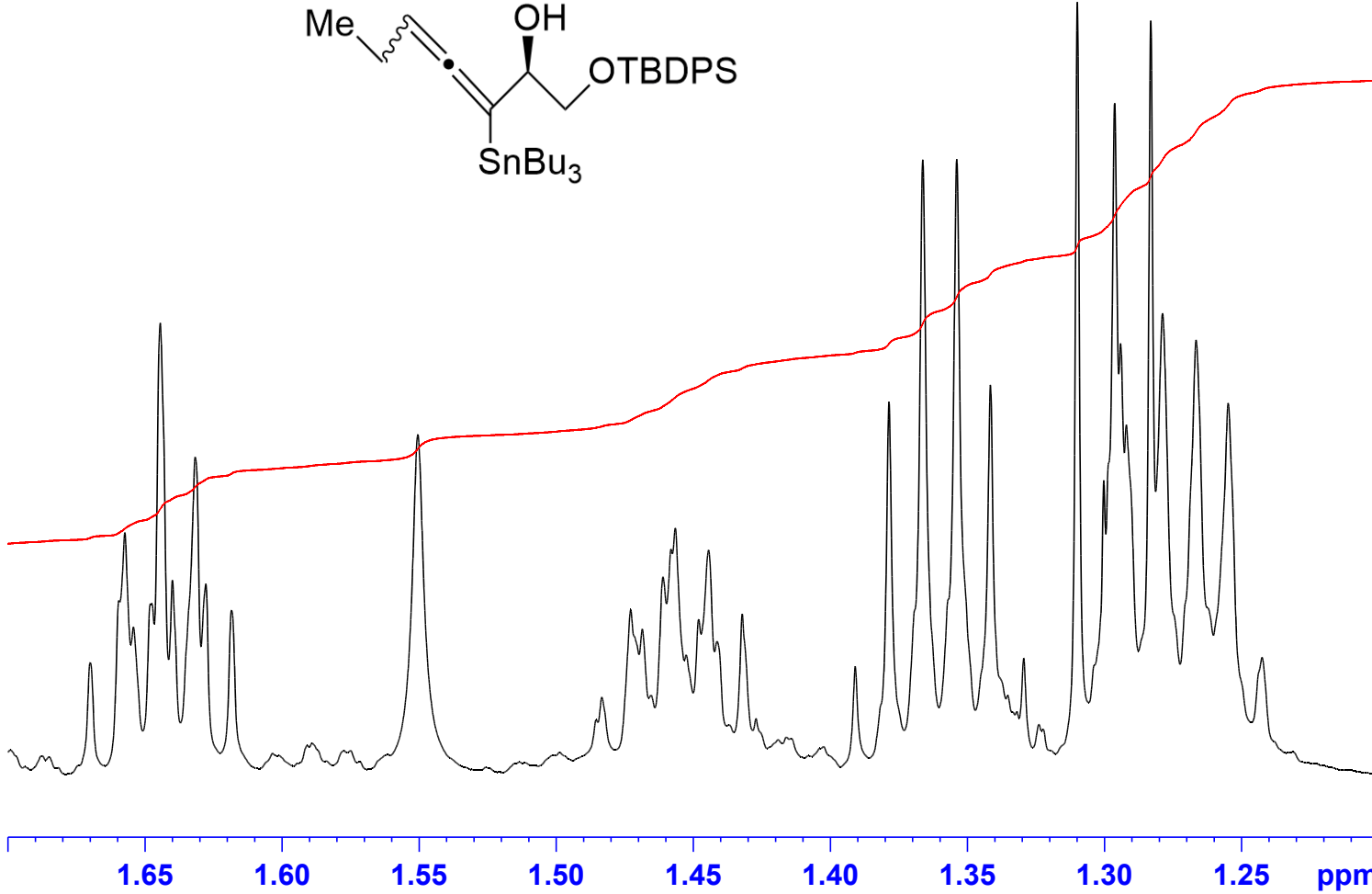
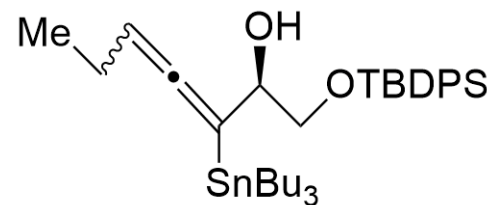
SI 262144  
SF 600.1300159 MHz  
WDW EM  
SSB 0  
LB 0.10 Hz  
GB 0  
PC 1.00

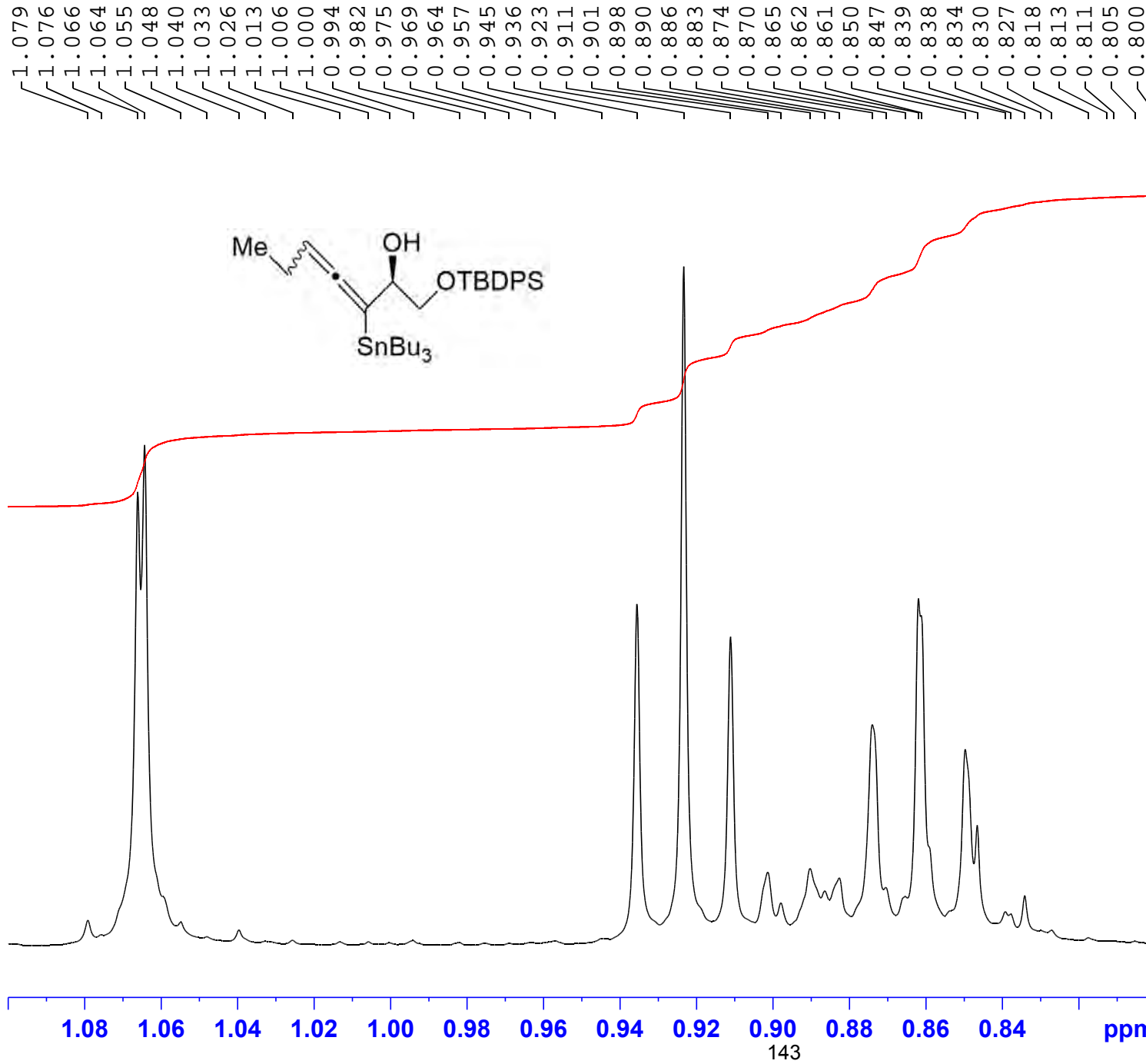


Current Data Parameters  
 NAME ALLENE  
 EXPNO 10  
 PROCNO 1

F2 - Acquisition Parameters  
 Date\_ 20220319  
 Time 14.07 h  
 INSTRUM spect  
 PROBHD Z114607\_0188 (zg30  
 PULPROG zg30  
 TD 180286  
 SOLVENT CDCl3  
 NS 16  
 DS 0  
 SWH 18028.846 Hz  
 FIDRES 0.200003 Hz  
 AQ 4.9999318 sec  
 RG 55.43  
 DW 27.733 usec  
 DE 8.00 usec  
 TE 300.0 K  
 D1 0.10000000 sec  
 TD0 1  
 SFO1 600.1337060 MHz  
 NUC1 1H  
 P0 3.33 usec  
 P1 10.00 usec  
 PLW1 26.60000038 W

F2 - Processing parameters  
 SI 262144  
 SF 600.1300159 MHz  
 WDW EM  
 SSB 0  
 LB 0.10 Hz  
 GB 0  
 PC 1.00

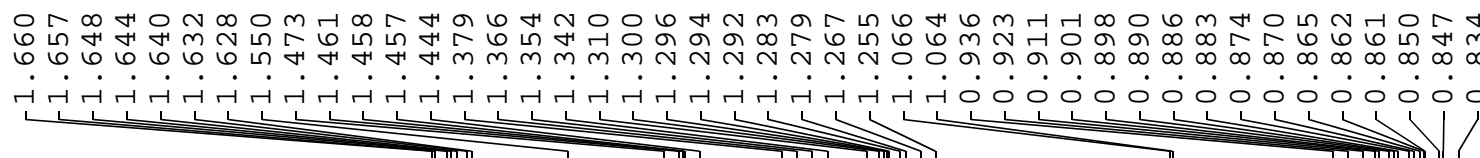




Current Data Parameters  
 NAME ALLENE  
 EXPNO 10  
 PROCNO 1

F2 - Acquisition Parameters  
 Date\_ 20220319  
 Time 14.07 h  
 INSTRUM spect  
 PROBHD Z114607\_0188 (zg30  
 PULPROG zg30  
 TD 180286  
 SOLVENT CDCl3  
 NS 16  
 DS 0  
 SWH 18028.846 Hz  
 FIDRES 0.200003 Hz  
 AQ 4.9999318 sec  
 RG 55.43  
 DW 27.733 usec  
 DE 8.00 usec  
 TE 300.0 K  
 D1 0.10000000 sec  
 TD0 1  
 SFO1 600.1337060 MHz  
 NUC1 1H  
 P0 3.33 usec  
 P1 10.00 usec  
 PLW1 26.60000038 W

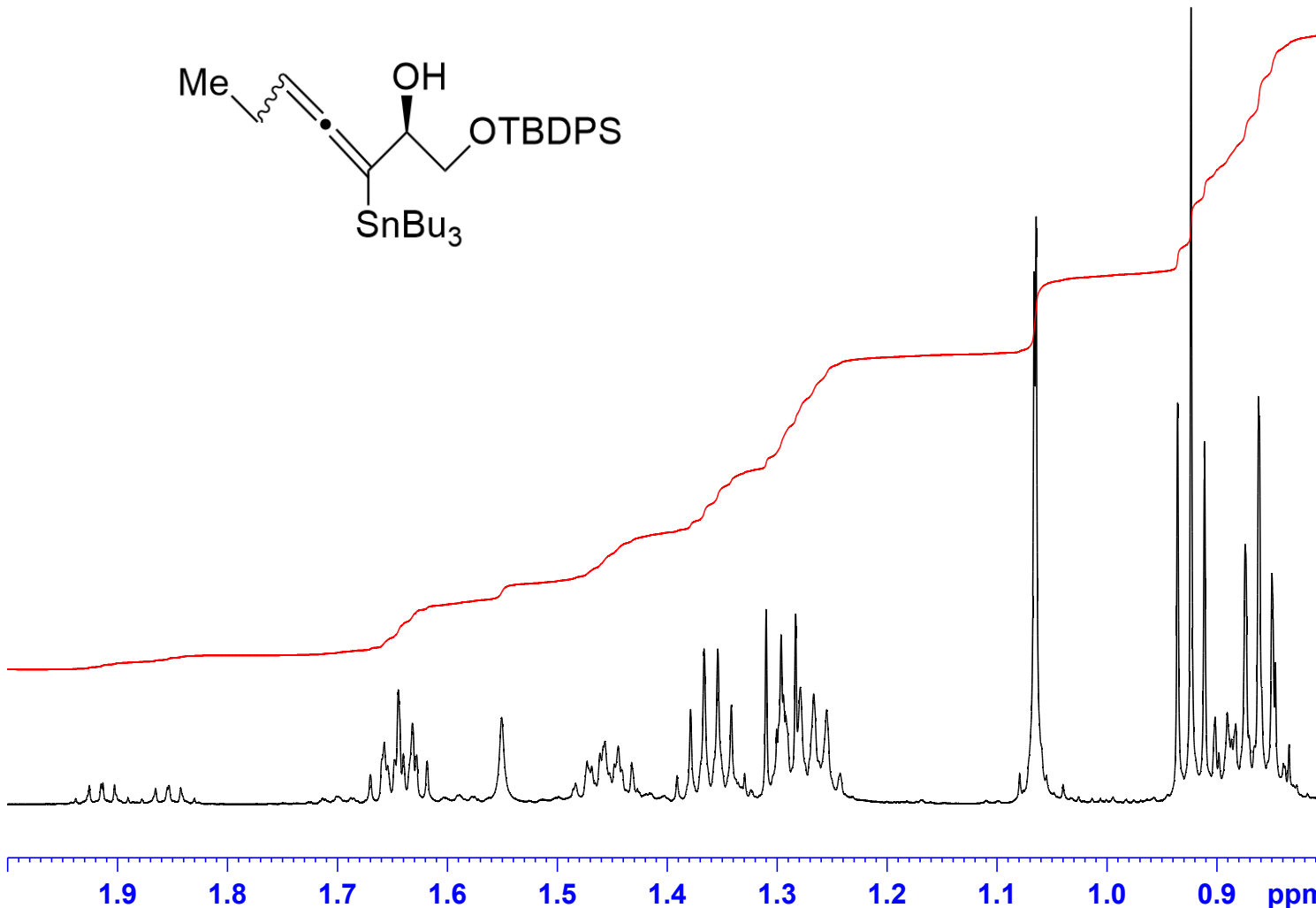
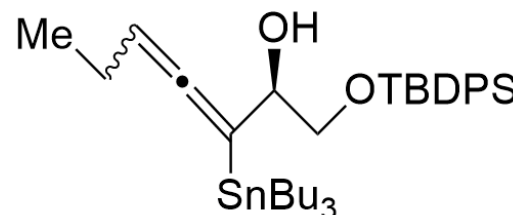
F2 - Processing parameters  
 SI 262144  
 SF 600.1300159 MHz  
 WDW EM  
 SSB 0  
 LB 0.10 Hz  
 GB 0  
 PC 1.00

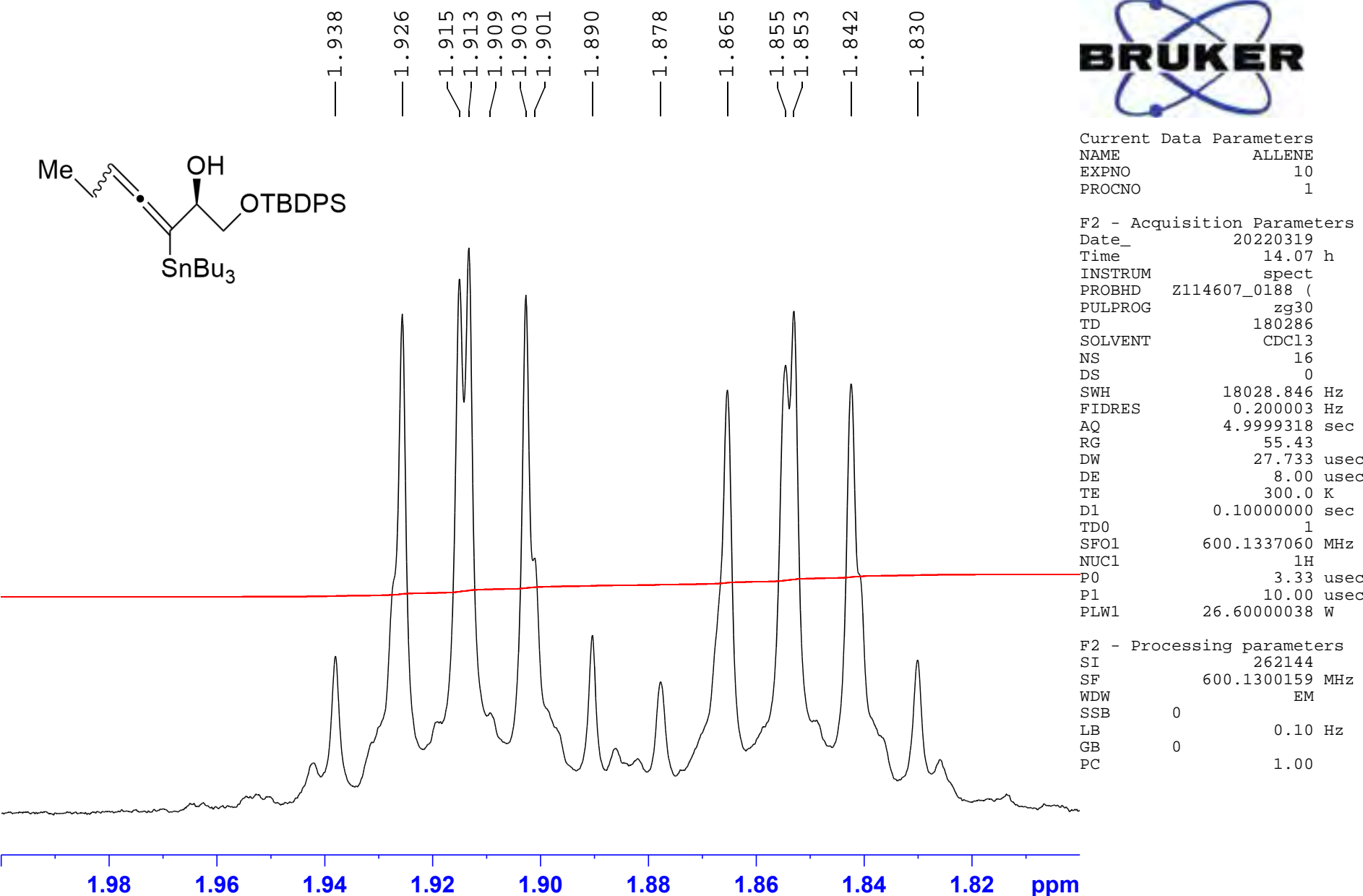


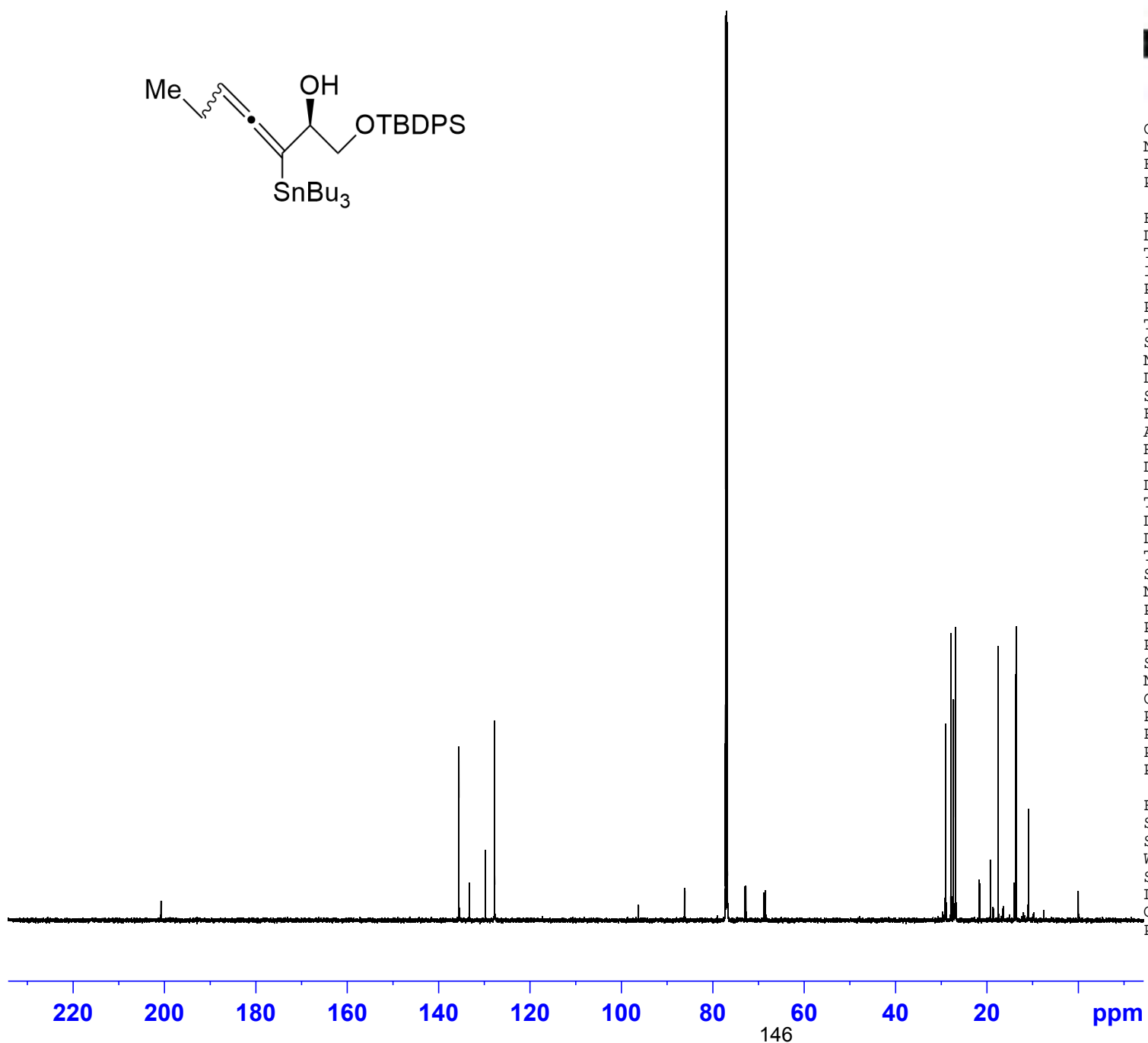
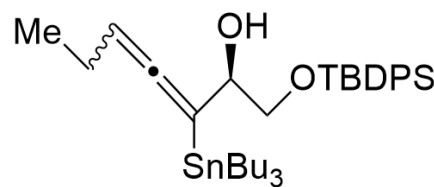
Current Data Parameters  
 NAME ALLENE  
 EXPNO 10  
 PROCNO 1

F2 - Acquisition Parameters  
 Date\_ 20220319  
 Time 14.07 h  
 INSTRUM spect  
 PROBHD Z114607\_0188 (zg30  
 PULPROG 180286  
 SOLVENT CDCl3  
 NS 16  
 DS 0  
 SWH 18028.846 Hz  
 FIDRES 0.200003 Hz  
 AQ 4.9999318 sec  
 RG 55.43  
 DW 27.733 usec  
 DE 8.00 usec  
 TE 300.0 K  
 D1 0.10000000 sec  
 TD0 1  
 SFO1 600.1337060 MHz  
 NUC1 1H  
 P0 3.33 usec  
 P1 10.00 usec  
 PLW1 26.60000038 W

F2 - Processing parameters  
 SI 262144  
 SF 600.1300159 MHz  
 WDW EM  
 SSB 0  
 LB 0.10 Hz  
 GB 0  
 PC 1.00







Current Data Parameters  
NAME ALLENE  
EXPNO 11  
PROCNO 1

## F2 - Acquisition Parameters

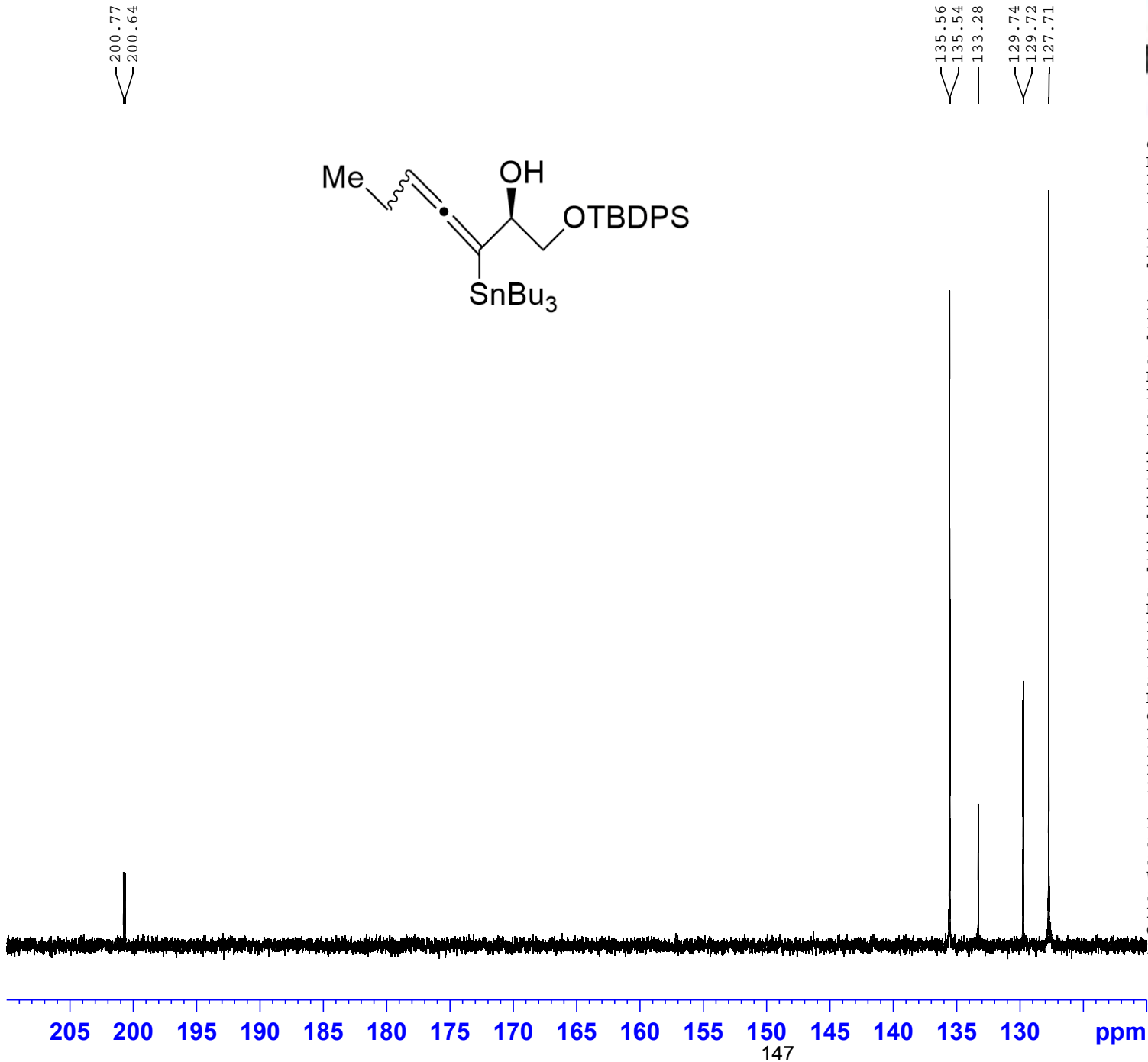
```

Date_          20220319
Time          15.36 h
INSTRUM       spect
PROBHD        Z114607_0188 (
PULPROG      zgpg30
TD            119044
SOLVENT       CDC13
NS            2000
DS             4
SWH           37500.000 Hz
FIDRES       0.630019 Hz
AQ            1.5872533 sec
RG            186.92
DW            13.333 usec
DE            6.53  usec
TE            300.0  K
D1            1.0000000 sec
D11           0.03000000 sec
TD0           1
SFO1          150.9194058 MHz
NUC1          13C
P0            3.93  usec
P1            11.80  usec
PLW1          85.00000000 W
SFO2          600.1324005 MHz
NUC2          1H
CPDPRG[2]    waltz64
PCPD2         70.00  usec
PLW2          27.00000000 W
PLW12         0.57327998 W
PLW13         0.28836000 W

```

## F2 - Processing parameters

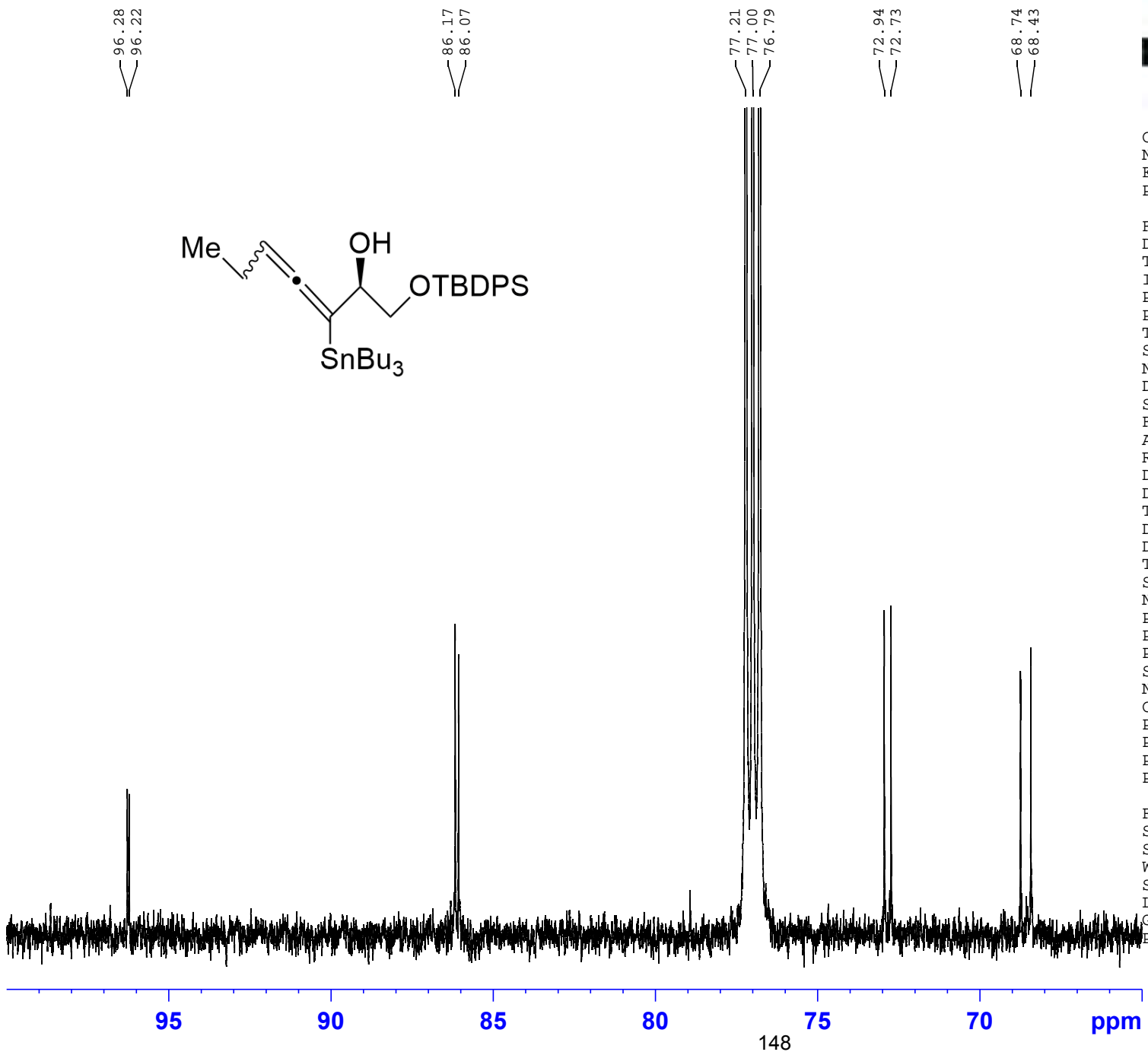
SI	131072
SF	150.9028116 MHz
WDW	EM
SSB	0
LB	1.00 Hz
GB	0
PC	1.40



Current Data Parameters  
 NAME ALLENE  
 EXPNO 11  
 PROCNO 1

F2 - Acquisition Parameters  
 Date\_ 20220319  
 Time 15.36 h  
 INSTRUM spect  
 PROBHD z114607\_0188 (   
 PULPROG zgpg30  
 TD 119044  
 SOLVENT CDCl3  
 NS 2000  
 DS 4  
 SWH 37500.000 Hz  
 FIDRES 0.630019 Hz  
 AQ 1.5872533 sec  
 RG 186.92  
 DW 13.333 usec  
 DE 6.53 usec  
 TE 300.0 K  
 D1 1.00000000 sec  
 D11 0.03000000 sec  
 TD0 1  
 SFO1 150.9194058 MHz  
 NUC1 13C  
 P0 3.93 usec  
 P1 11.80 usec  
 PLW1 85.00000000 W  
 SFO2 600.1324005 MHz  
 NUC2 1H  
 CPDPRG[ 2 waltz64  
 PCPD2 70.00 usec  
 PLW2 27.00000000 W  
 PLW12 0.57327998 W  
 PLW13 0.28836000 W

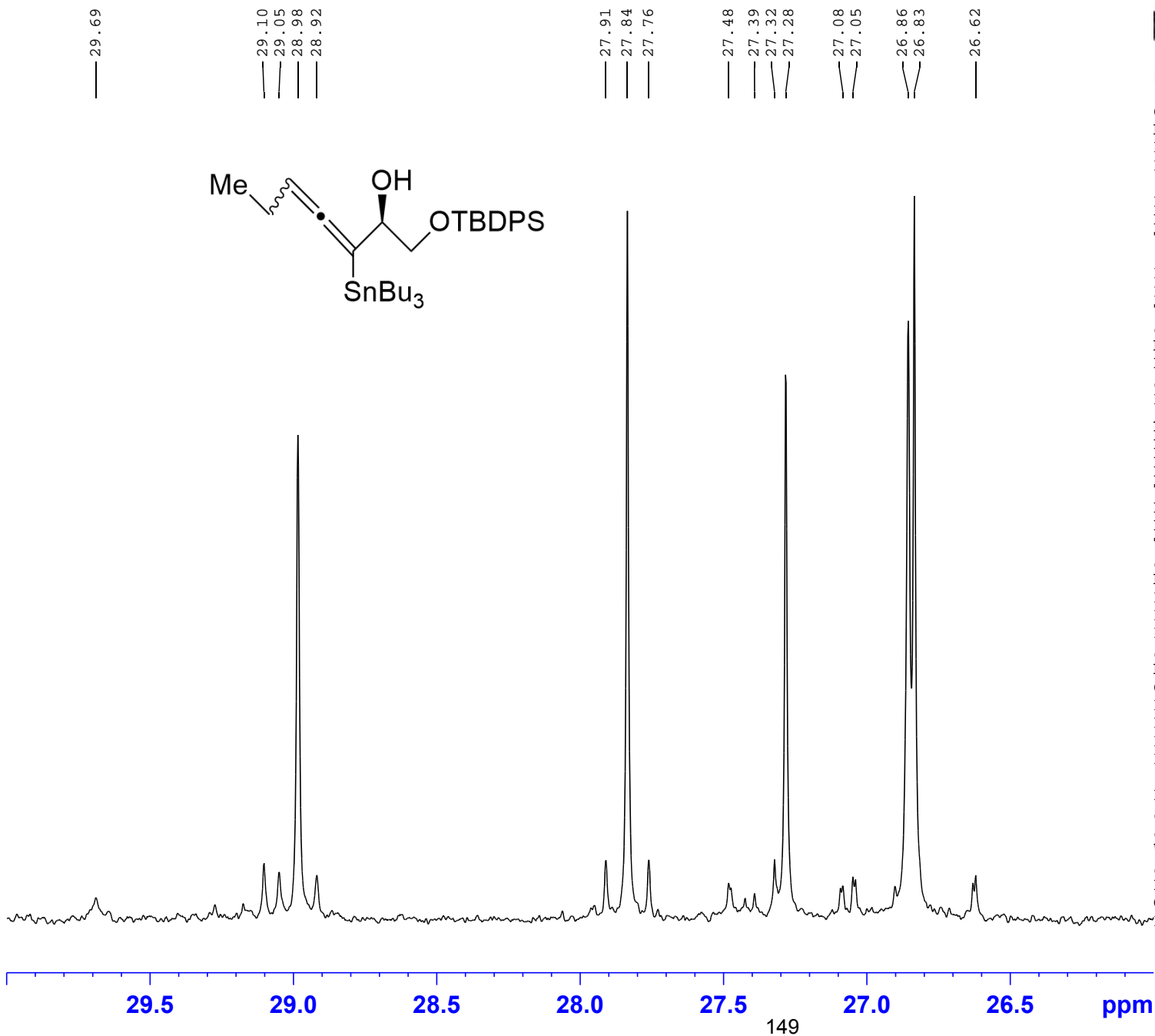
F2 - Processing parameters  
 SI 131072  
 SF 150.9028116 MHz  
 WDW EM  
 SSB 0  
 LB 1.00 Hz  
 GB 0  
 PC 1.40



Current Data Parameters  
 NAME ALLENE  
 EXPNO 11  
 PROCNO 1

F2 - Acquisition Parameters  
 Date\_ 20220319  
 Time 15.36 h  
 INSTRUM spect  
 PROBHD Z114607\_0188 (   
 PULPROG zgpg30  
 TD 119044  
 SOLVENT CDCl3  
 NS 2000  
 DS 4  
 SWH 37500.000 Hz  
 FIDRES 0.630019 Hz  
 AQ 1.5872533 sec  
 RG 186.92  
 DW 13.333 usec  
 DE 6.53 usec  
 TE 300.0 K  
 D1 1.00000000 sec  
 D11 0.03000000 sec  
 TD0 1  
 SFO1 150.9194058 MHz  
 NUC1  $^{13}\text{C}$   
 P0 3.93 usec  
 P1 11.80 usec  
 PLW1 85.00000000 W  
 SFO2 600.1324005 MHz  
 NUC2  $^1\text{H}$   
 CPDPRG[ 2 waltz64  
 PCPD2 70.00 usec  
 PLW2 27.00000000 W  
 PLW12 0.57327998 W  
 PLW13 0.28836000 W

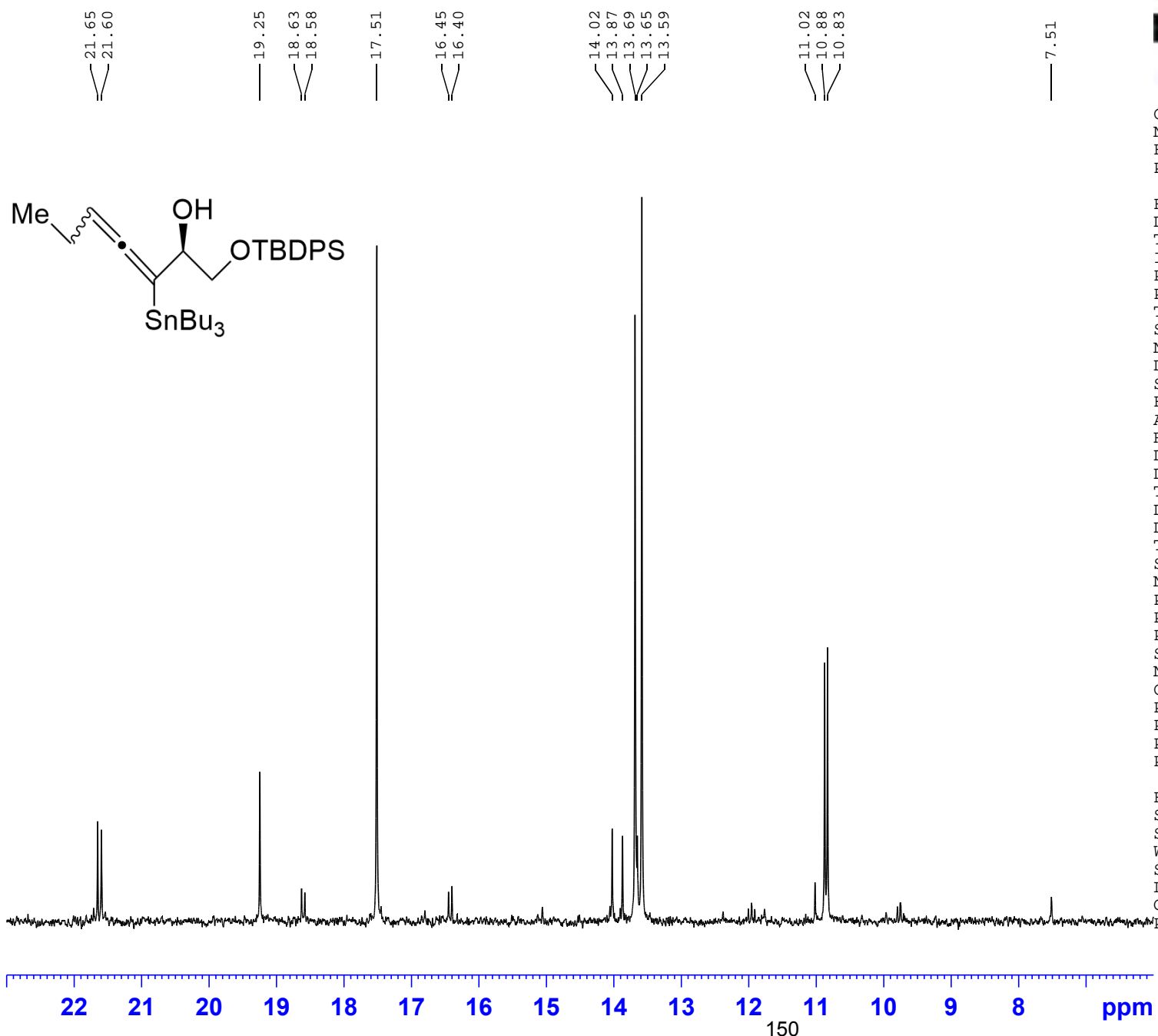
F2 - Processing parameters  
 SI 131072  
 SF 150.9028116 MHz  
 WDW EM  
 SSB 0  
 LB 1.00 Hz  
 GB 0  
 PC 1.40



Current Data Parameters  
 NAME ALLENE  
 EXPNO 11  
 PROCNO 1

F2 - Acquisition Parameters  
 Date\_ 20220319  
 Time 15.36 h  
 INSTRUM spect  
 PROBHD Z114607\_0188 (   
 PULPROG zgpg30  
 TD 119044  
 SOLVENT CDCl3  
 NS 2000  
 DS 4  
 SWH 37500.000 Hz  
 FIDRES 0.630019 Hz  
 AQ 1.5872533 sec  
 RG 186.92  
 DW 13.333 usec  
 DE 6.53 usec  
 TE 300.0 K  
 D1 1.00000000 sec  
 D11 0.03000000 sec  
 TD0 1  
 SFO1 150.9194058 MHz  
 NUC1 13C  
 P0 3.93 usec  
 P1 11.80 usec  
 PLW1 85.00000000 W  
 SFO2 600.1324005 MHz  
 NUC2 1H  
 CPDPRG[ 2 waltz64  
 PCPD2 70.00 usec  
 PLW2 27.00000000 W  
 PLW12 0.57327998 W  
 PLW13 0.28836000 W

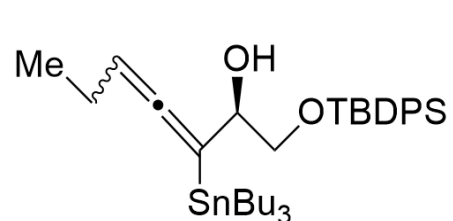
F2 - Processing parameters  
 SI 131072  
 SF 150.9028116 MHz  
 WDW EM  
 SSB 0  
 LB 1.00 Hz  
 GB 0  
 PC 1.40



Current Data Parameters  
 NAME ALLENE  
 EXPNO 11  
 PROCNO 1

F2 - Acquisition Parameters  
 Date\_ 20220319  
 Time 15.36 h  
 INSTRUM spect  
 PROBHD Z114607\_0188 (   
 PULPROG zgpg30  
 TD 119044  
 SOLVENT CDCl3  
 NS 2000  
 DS 4  
 SWH 37500.000 Hz  
 FIDRES 0.630019 Hz  
 AQ 1.5872533 sec  
 RG 186.92  
 DW 13.333 usec  
 DE 6.53 usec  
 TE 300.0 K  
 D1 1.00000000 sec  
 D11 0.03000000 sec  
 TD0 1  
 SFO1 150.9194058 MHz  
 NUC1 <sup>13</sup>C  
 P0 3.93 usec  
 P1 11.80 usec  
 PLW1 85.00000000 W  
 SFO2 600.1324005 MHz  
 NUC2 <sup>1</sup>H  
 CPDPRG[ 2 waltz64  
 PCPD2 70.00 usec  
 PLW2 27.00000000 W  
 PLW12 0.57327998 W  
 PLW13 0.28836000 W

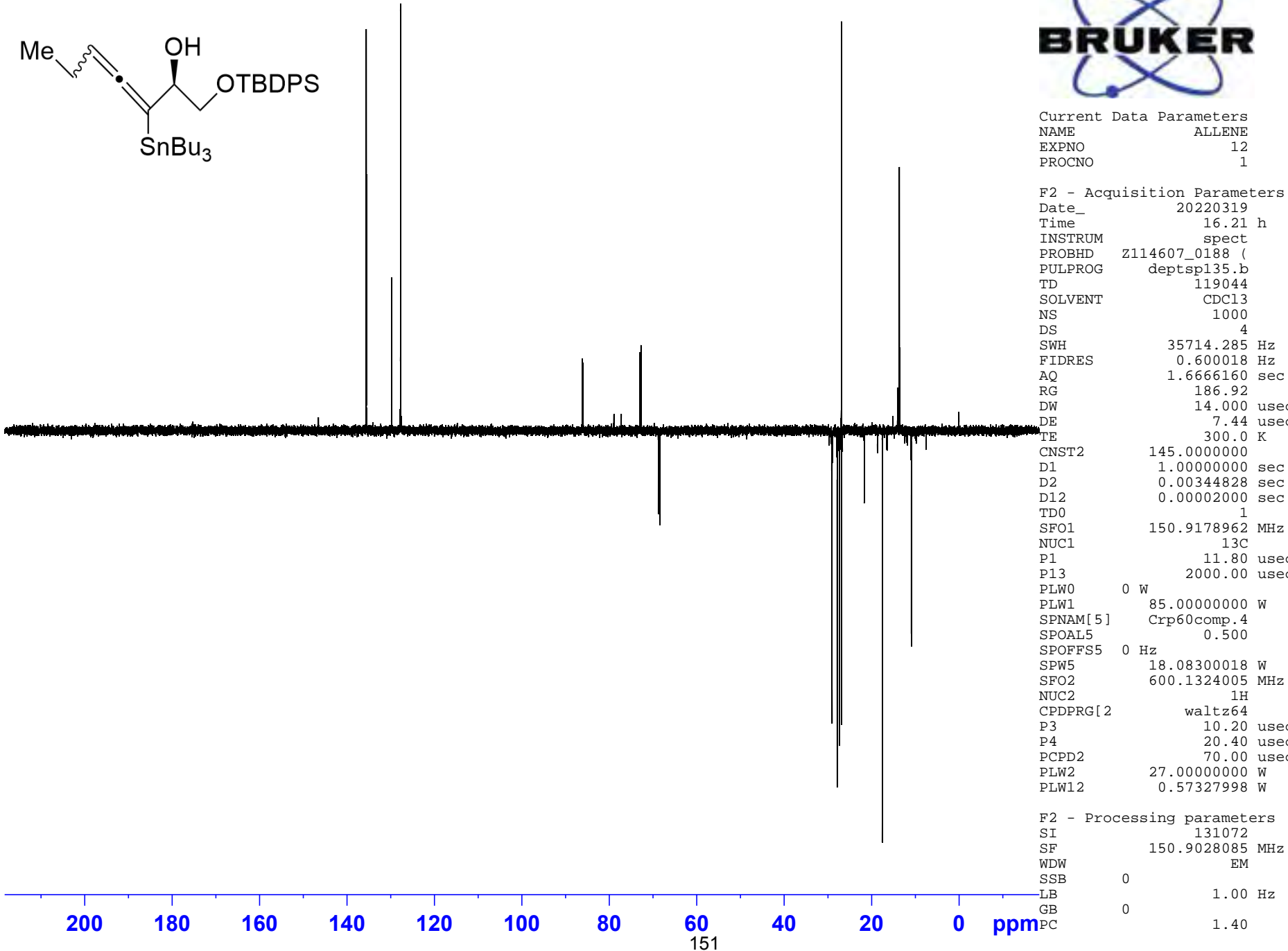
F2 - Processing parameters  
 SI 131072  
 SF 150.9028116 MHz  
 WDW EM  
 SSB 0  
 LB 1.00 Hz  
 GB 0  
 PC 1.40

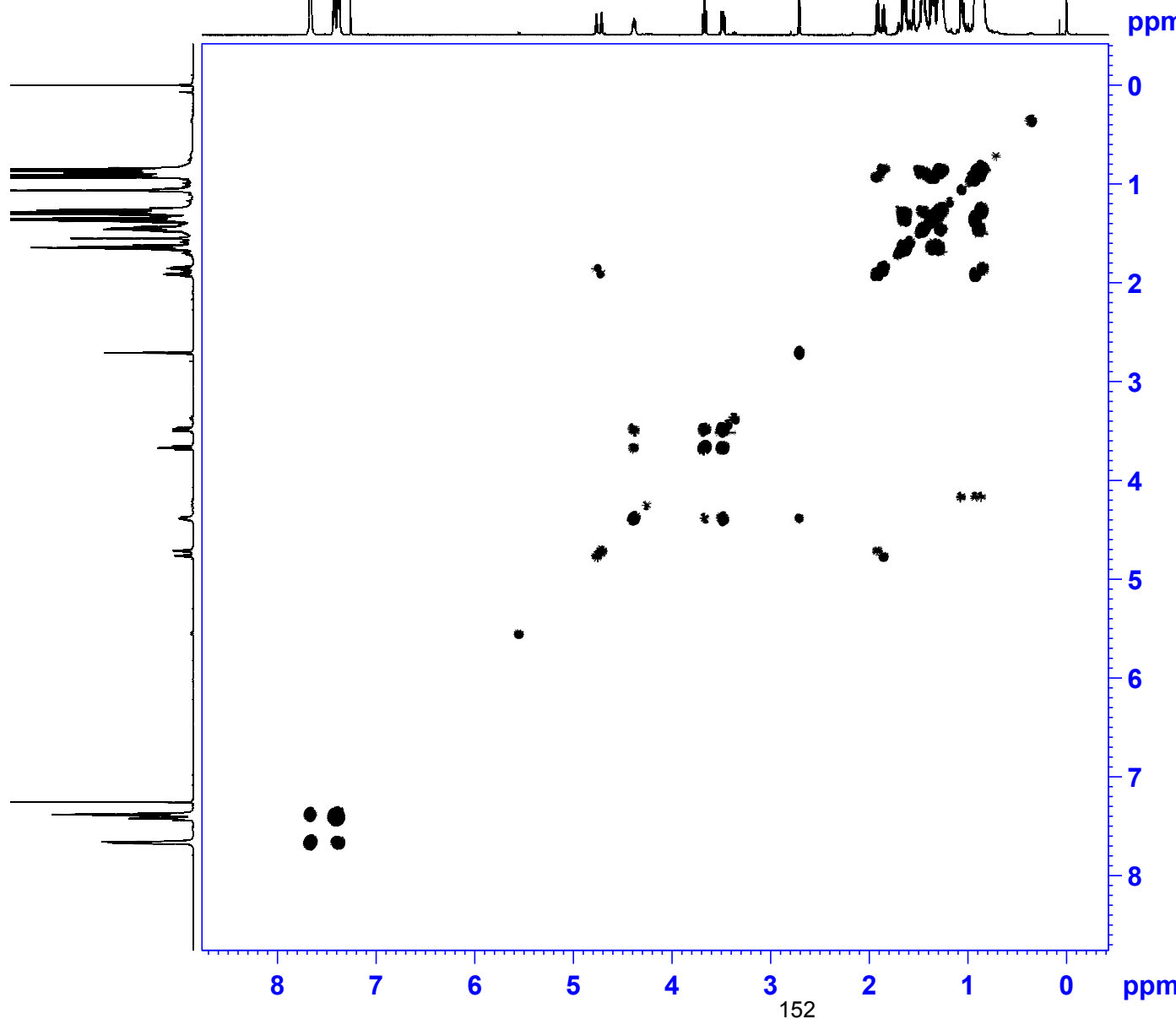
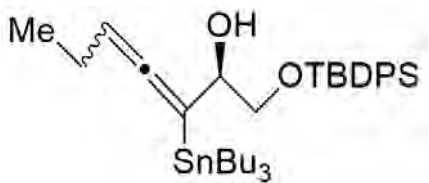


Current Data Parameters  
 NAME ALLENE  
 EXPNO 12  
 PROCNO 1

F2 - Acquisition Parameters  
 Date\_ 20220319  
 Time 16.21 h  
 INSTRUM spect  
 PROBHD Z114607\_0188 (   
 PULPROG deptsp135.b  
 TD 119044  
 SOLVENT CDCl3  
 NS 1000  
 DS 4  
 SWH 35714.285 Hz  
 FIDRES 0.600018 Hz  
 AQ 1.6666160 sec  
 RG 186.92  
 DW 14.000 usec  
 DE 7.44 usec  
 TE 300.0 K  
 CNST2 145.0000000  
 D1 1.00000000 sec  
 D2 0.00344828 sec  
 D12 0.00002000 sec  
 TD0 1  
 SFO1 150.9178962 MHz  
 NUC1 13C  
 P1 11.80 usec  
 P13 2000.00 usec  
 PLW0 0 W  
 PLW1 85.00000000 W  
 SPNAM[5] Crp60comp.4  
 SPOAL5 0.500  
 SPOFFSS5 0 Hz  
 SPW5 18.08300018 W  
 SFO2 600.1324005 MHz  
 NUC2 1H  
 CPDPRG[2] waltz64  
 P3 10.20 usec  
 P4 20.40 usec  
 PCPD2 70.00 usec  
 PLW2 27.00000000 W  
 PLW12 0.57327998 W

F2 - Processing parameters  
 SI 131072  
 SF 150.9028085 MHz  
 WDW EM  
 SSB 0  
 LB 1.00 Hz  
 GB 0  
 PC 1.40





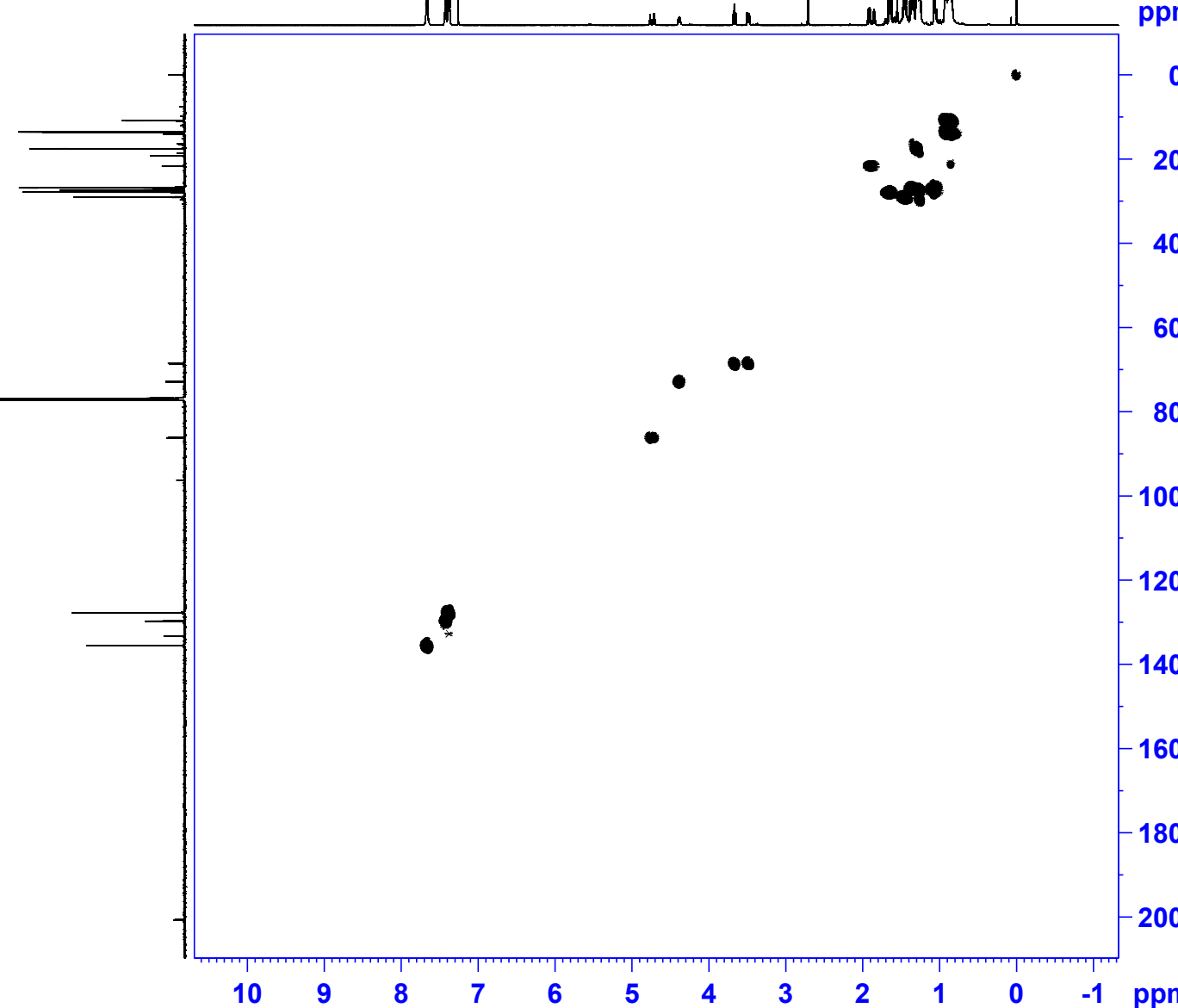
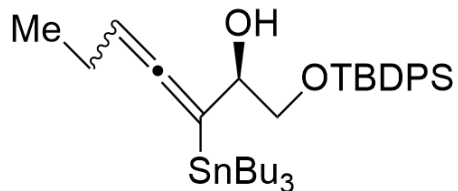
Current Data Parameters  
NAME ALLENE  
EXPNO 13  
PROCNO 1

F2 - Acquisition Parameters  
Date\_ 20220319  
Time 16.32 h  
INSTRUM spect  
PROBHD Z114607\_0188 (   
PULPROG cosygpmfppqf  
TD 2048  
SOLVENT CDCl<sub>3</sub>  
NS 2  
DS 8  
SWH 5514.706 Hz  
FIDRES 5.385455 Hz  
AQ 0.1856853 sec  
RG 186.92  
DW 90.667 usec  
DE 6.50 usec  
TE 300.0 K  
D0 0.00000300 sec  
D1 0.87302327 sec  
D11 0.03000000 sec  
D12 0.000002000 sec  
D13 0.00000400 sec  
D16 0.000020000 sec  
IN0 0.00018160 sec  
TDav 1  
SF01 600.1325169 MHz  
NUC1 1H  
P1 10.00 usec  
P17 2500.00 usec  
PLW1 26.60000038 W  
PLW10 4.25600004 W  
GPNAM[1] SMSQ10.100  
GPZ1 16.00 %  
GPNAM[2] SMSQ10.100  
GPZ2 12.00 %  
GPNAM[3] SMSQ10.100  
GPZ3 40.00 %  
P16 1000.00 usec

F1 - Acquisition parameters  
TD 256  
SF01 600.1325 MHz  
FIDRES 43.020374 Hz  
SW 9.176 ppm  
FnMODE QF

F2 - Processing parameters  
SI 1024  
SF 600.1300139 MHz  
WDW SINE  
SSB 0  
LB 0 Hz  
GB 0  
PC 1.40

F1 - Processing parameters  
SI 1024  
MC2 QF  
SF 600.1300151 MHz  
WDW SINE  
SSB 0  
LB 0 Hz  
GB 0



Current Data Parameters  
NAME ALLENE  
EXPNO 14  
PROCNO 1

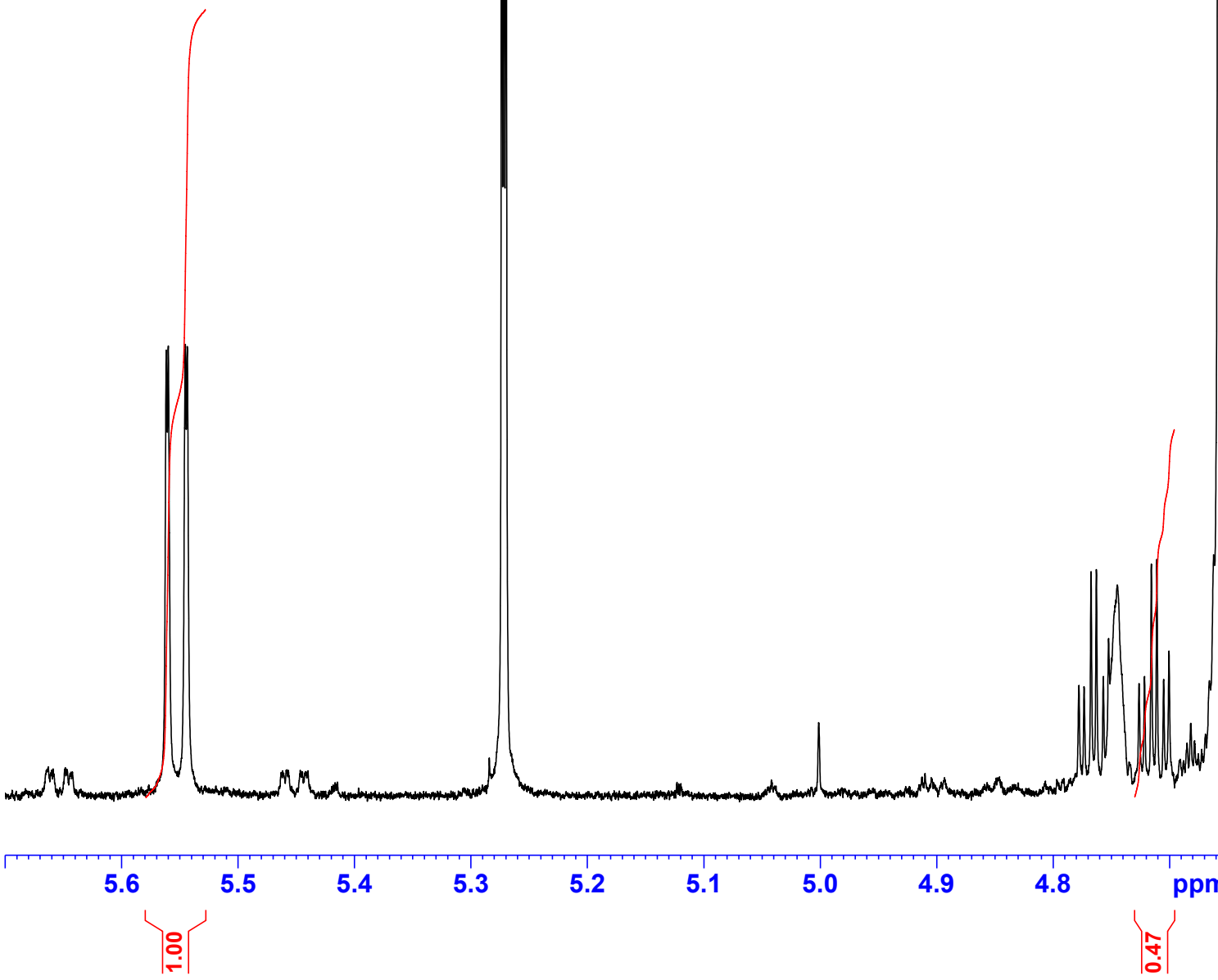
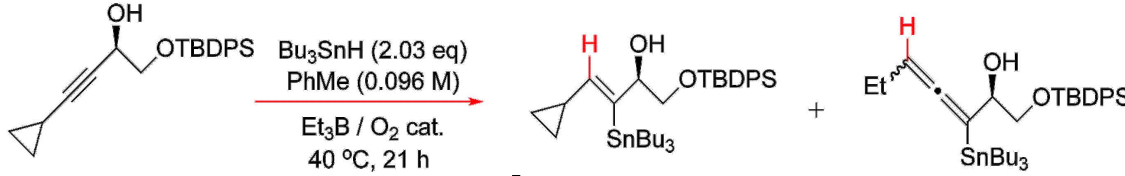
F2 - Acquisition Parameters  
Date\_ 20220319  
Time 16.41 h  
INSTRUM spect  
PROBHD Z114607\_0188 (   
PULPROG hsqcetgpsp.3  
TD 1024  
SOLVENT CDCl3  
NS 2  
DS 32  
SWH 7211.539 Hz  
FIDRES 14.085036 Hz  
AQ 0.0709973 sec  
RG 186.92  
DW 69.333 usec  
DE 6.50 usec  
TE 300.3 K  
CNUST2 145.0000000  
D0 0.00000300 sec  
D1 0.8000001 sec  
D4 0.00172414 sec  
D11 0.0300000 sec  
D16 0.00020000 sec  
D21 0.00360000 sec  
IN0 0.00001510 sec  
TDav 1  
ZGOPTNS 600.1328223 MHz  
SFO1 1H  
P1 10.00 usec  
P2 20.00 usec  
PLW1 26.6000038 W  
SFO2 150.9178984 MHz  
NUC2 13C  
CPDPRG[2] garp4  
P3 11.80 usec  
P14 500.00 usec  
P31 1730.00 usec  
PCPD2 60.00 usec  
PLW0 0 W  
PLW2 85.0000000 W  
PLW12 3.28760004 W  
SPNAM[3] Crp60,0.5,20.1  
SPOAL3 0.500  
SPOFFS3 0 Hz  
SPW3 18.08300018 W  
SPNAM[18] Crp60\_xfilt.2  
SPOAL18 0.500  
SPOFFS18 0 Hz  
SPW18 5.22629976 W  
GPNAME[1] SMSQ10.100  
GPZ1 80.00 %  
GPNAME[2] SMSQ10.100  
GPZ2 20.10 %  
P16 1000.00 usec

F1 - Acquisition parameters  
TD 256  
SFO1 150.9179 MHz  
FIDRES 258.692047 Hz  
SW 219.408 ppm  
FnMODE Echo-Antiecho

F2 - Processing parameters  
SI 1024  
SF 600.1300128 MHz  
WDW QSINE  
SSB 2  
LB 0 Hz  
GB 0  
PC 1.40

F1 - Processing parameters  
SI 1024  
MC2 echo-antiecho  
SF 150.9028016 MHz  
WDW QSINE  
SSB 2  
LB 0 Hz  
GB 0

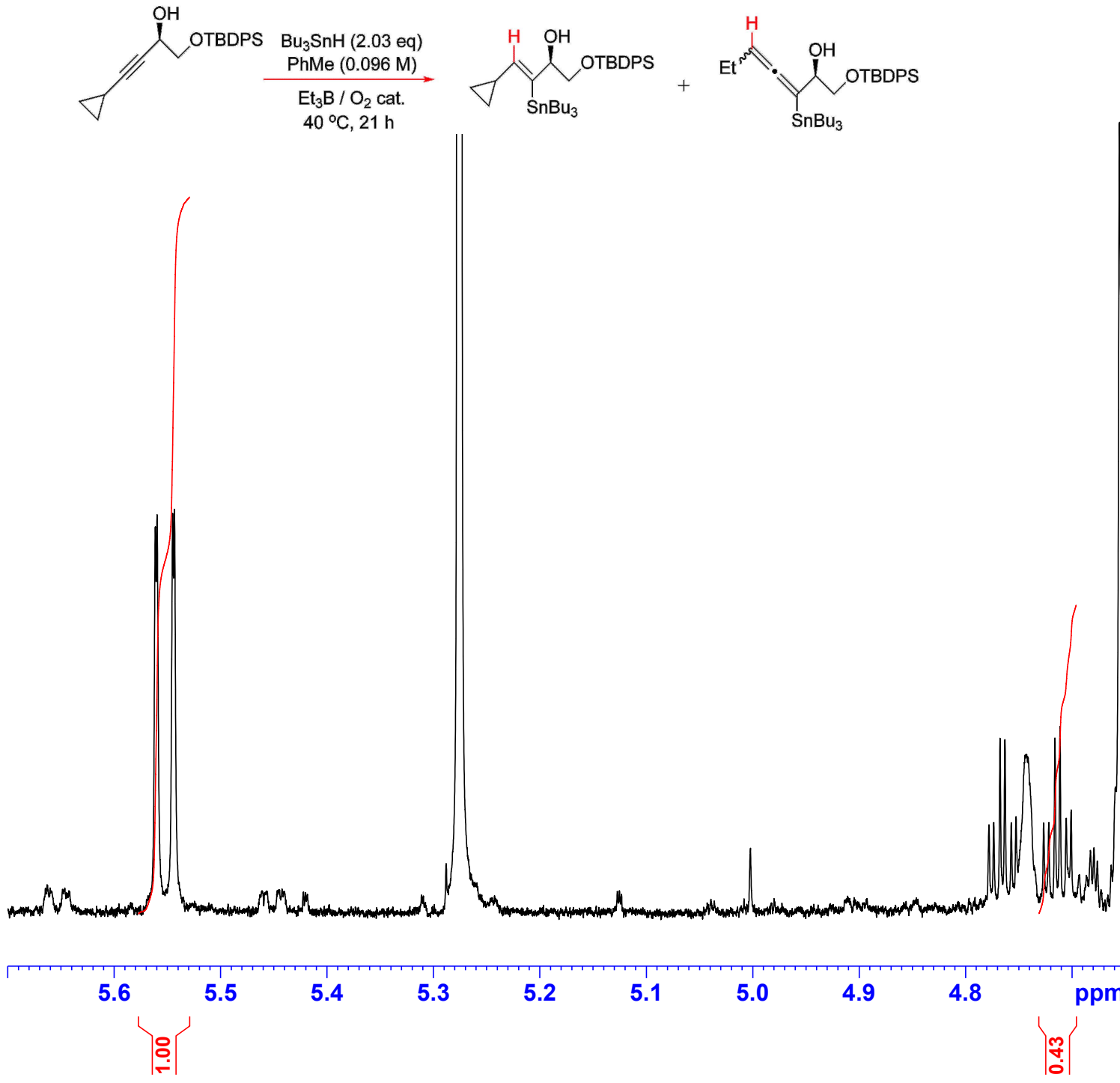
**Part G. The 600.13 MHz  $^1\text{H}$  NMR Ratio Determinations For  
the Tributylstannylallene 15 and Tributylstannylvinyltin 16  
in  $\text{CDCl}_3$  Over the 313 K-353 K Temperature Range**



Current Data Parameters  
 NAME LH-I-89 CRUDE  
 EXPNO 10  
 PROCNO 1

F2 - Acquisition Parameters  
 Date 20220504  
 Time 12.07 h  
 INSTRUM spect  
 PROBHD Z114607\_0188 (zg30  
 PULPROG zg30  
 TD 180286  
 SOLVENT CDCl3  
 NS 16  
 DS 0  
 SWH 18028.846 Hz  
 FIDRES 0.200003 Hz  
 AQ 4.9999318 sec  
 RG 22.13  
 DW 27.733 usec  
 DE 8.00 usec  
 TE 300.0 K  
 D1 0.10000000 sec  
 TD0 1  
 SFO1 600.1337060 MHz  
 NUC1 1H  
 P0 3.33 usec  
 P1 10.00 usec  
 PLW1 26.60000038 W

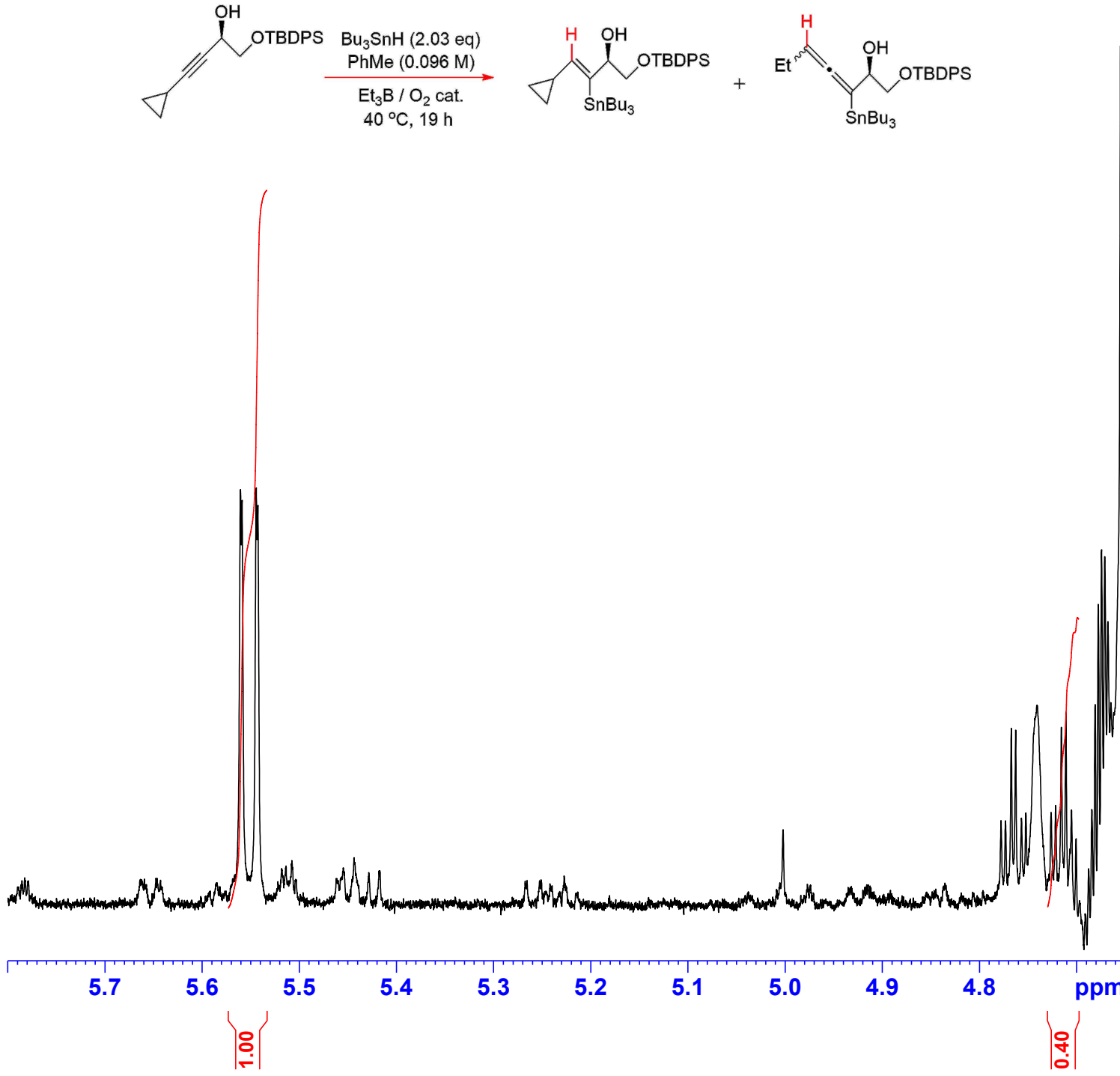
F2 - Processing parameters  
 SI 262144  
 SF 600.1300205 MHz  
 WDW EM  
 SSB 0  
 LB 0.10 Hz  
 GB 0  
 PC 1.00



Current Data Parameters  
 NAME LH-I-90 CRUDE  
 EXPNO 10  
 PROCNO 1

F2 - Acquisition Parameters  
 Date 20220504  
 Time 12.15 h  
 INSTRUM spect  
 PROBHD Z114607\_0188 (zg30  
 PULPROG zg30  
 TD 180286  
 SOLVENT CDCl3  
 NS 16  
 DS 0  
 SWH 18028.846 Hz  
 FIDRES 0.200003 Hz  
 AQ 4.9999318 sec  
 RG 27.87  
 DW 27.733 usec  
 DE 8.00 usec  
 TE 300.0 K  
 D1 0.10000000 sec  
 TD0 1  
 SFO1 600.1337060 MHz  
 NUC1 1H  
 P0 3.33 usec  
 P1 10.00 usec  
 PLW1 26.60000038 W

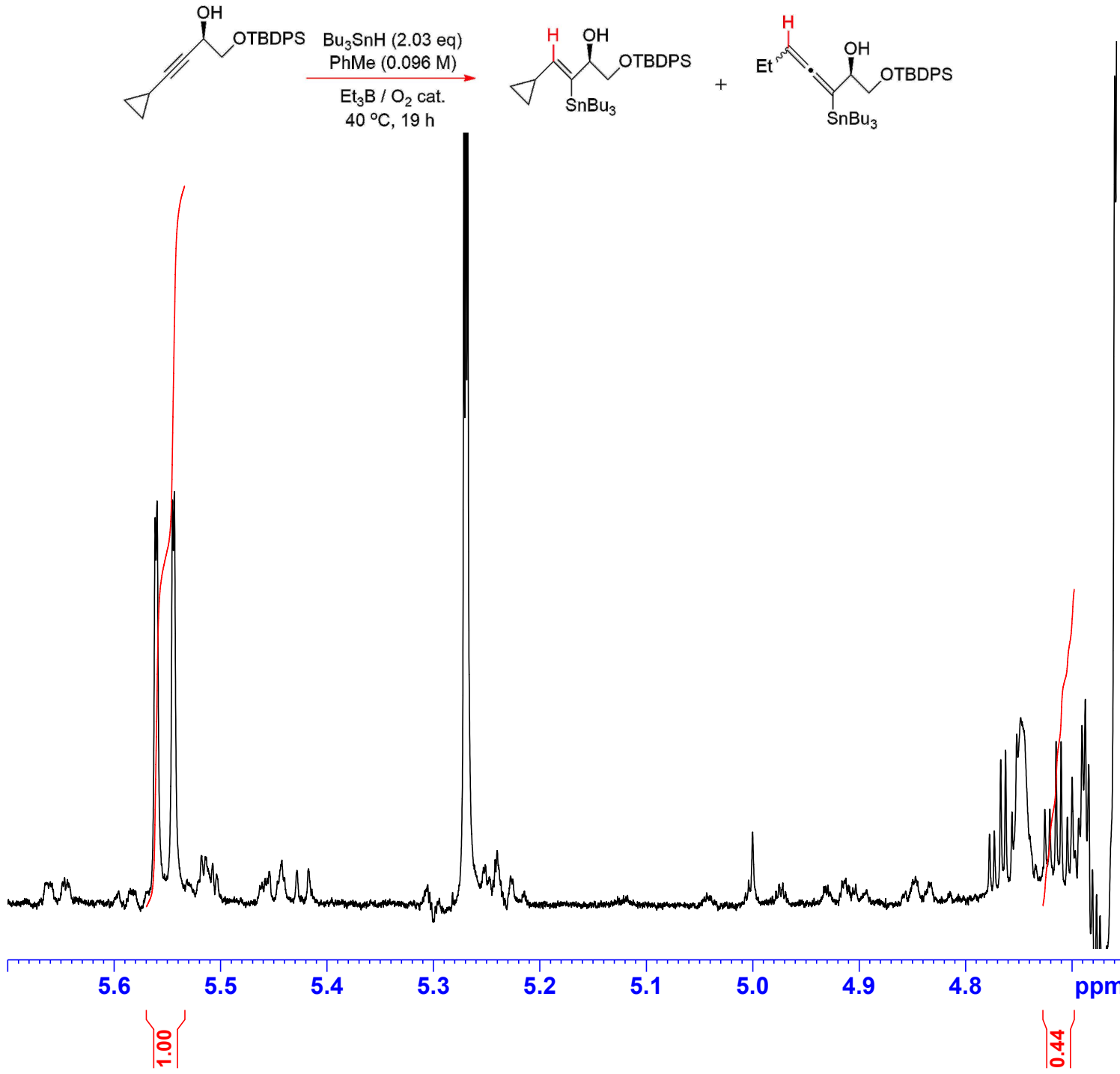
F2 - Processing parameters  
 SI 262144  
 SF 600.1300186 MHz  
 WDW EM  
 SSB 0  
 LB 0.10 Hz  
 GB 0  
 PC 1.00

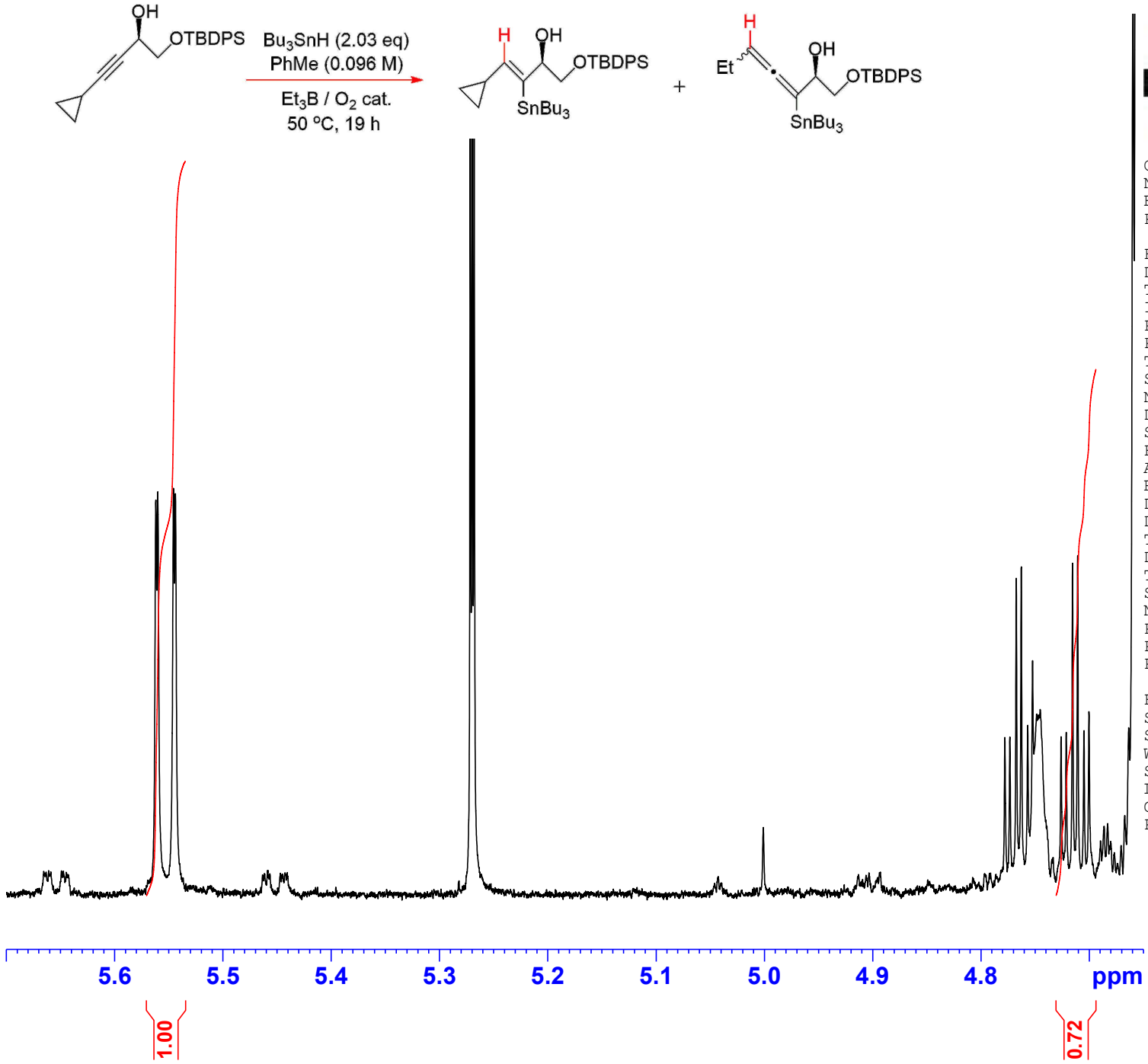


Current Data Parameters  
 NAME LH-I-93 CRUDE  
 EXPNO 10  
 PROCNO 1

F2 - Acquisition Parameters  
 Date 20220519  
 Time 15.05 h  
 INSTRUM spect  
 PROBHD Z114607\_0188 (zg30  
 PULPROG zg30  
 TD 180286  
 SOLVENT CDCl<sub>3</sub>  
 NS 16  
 DS 0  
 SWH 18028.846 Hz  
 FIDRES 0.200003 Hz  
 AQ 4.9999318 sec  
 RG 31.58  
 DW 27.733 usec  
 DE 8.00 usec  
 TE 300.0 K  
 D1 0.10000000 sec  
 TD0 1  
 SFO1 600.1337060 MHz  
 NUC1 1H  
 P0 3.33 usec  
 P1 10.00 usec  
 PLW1 26.60000038 W

F2 - Processing parameters  
 SI 262144  
 SF 600.1300178 MHz  
 WDW EM  
 SSB 0  
 LB 0.10 Hz  
 GB 0  
 PC 1.00

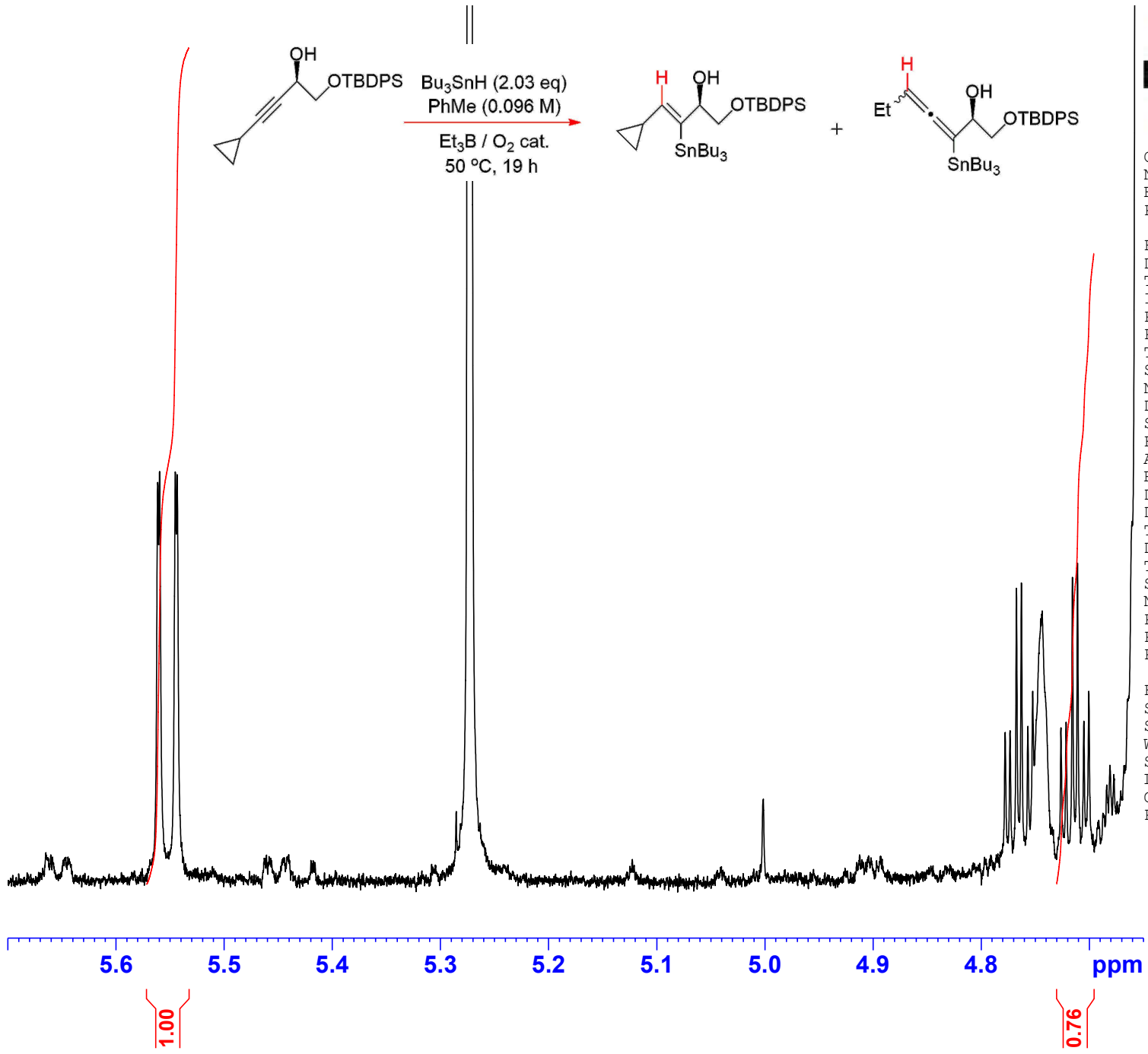




Current Data Parameters  
 NAME LH-I-91 CRUDE  
 EXPNO 10  
 PROCNO 1

F2 - Acquisition Parameters  
 Date 20220504  
 Time 11.31 h  
 INSTRUM spect  
 PROBHD Z114607\_0188 (zg30  
 PULPROG zg30  
 TD 180286  
 SOLVENT CDCl<sub>3</sub>  
 NS 16  
 DS 0  
 SWH 18028.846 Hz  
 FIDRES 0.200003 Hz  
 AQ 4.9999318 sec  
 RG 13.75  
 DW 27.733 usec  
 DE 8.00 usec  
 TE 300.0 K  
 D1 0.10000000 sec  
 TD0 1  
 SFO1 600.1337060 MHz  
 NUC1 1H  
 P0 3.33 usec  
 P1 10.00 usec  
 PLW1 26.60000038 W

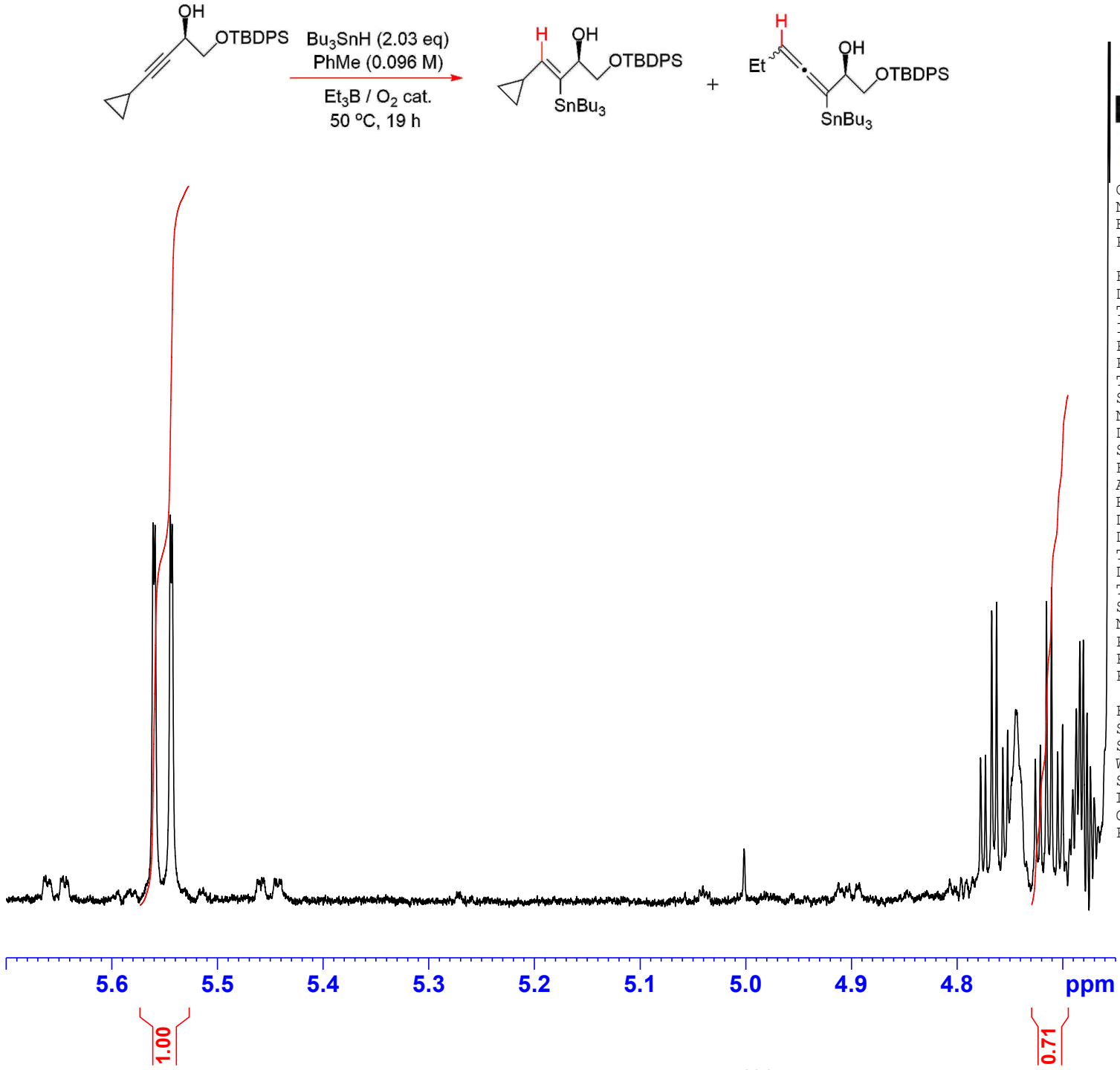
F2 - Processing parameters  
 SI 262144  
 SF 600.1300215 MHz  
 WDW EM  
 SSB 0  
 LB 0.10 Hz  
 GB 0  
 PC 1.00



Current Data Parameters  
NAME LH-I-92 CRUDE  
EXPNO 10  
PROCNO 1

F2 - Acquisition Parameters  
Date 20220504  
Time 11.40 h  
INSTRUM spect  
PROBHD Z114607\_0188 (zg30  
PULPROG zg30  
TD 180286  
SOLVENT CDCl3  
NS 16  
DS 0  
SWH 18028.846 Hz  
FIDRES 0.200003 Hz  
AQ 4.9999318 sec  
RG 25.17  
DW 27.733 usec  
DE 8.00 usec  
TE 300.0 K  
D1 0.10000000 sec  
TD0 1  
SFO1 600.1337060 MHz  
NUC1 1H  
P0 3.33 usec  
P1 10.00 usec  
PLW1 26.60000038 W

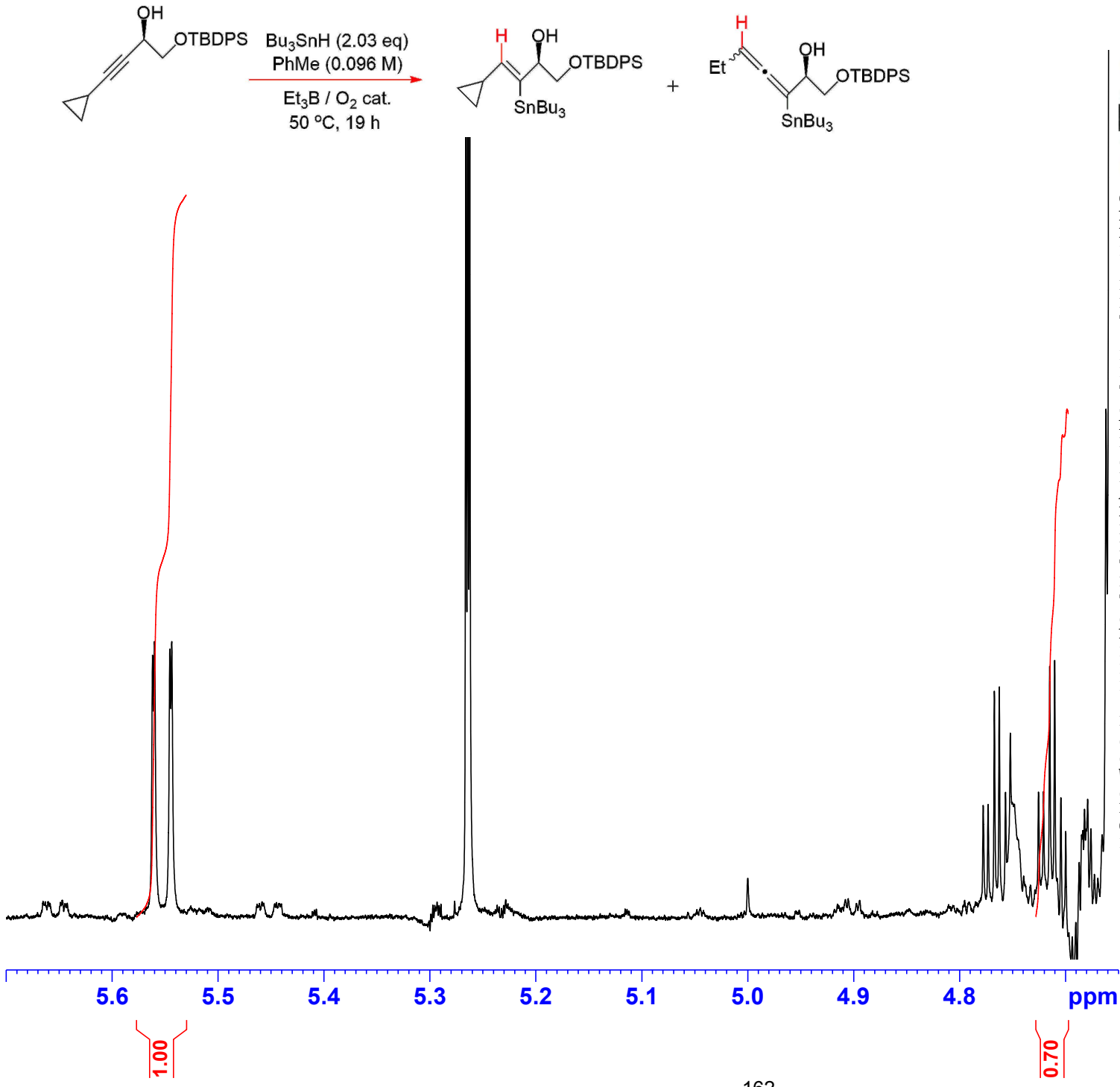
F2 - Processing parameters  
SI 262144  
SF 600.1300198 MHz  
WDW EM  
SSB 0  
LB 0.10 Hz  
GB 0  
PC 1.00



Current Data Parameters  
 NAME LH-I-95 CRUDE  
 EXPNO 10  
 PROCNO 1

F2 - Acquisition Parameters  
 Date 20220519  
 Time 15.19 h  
 INSTRUM spect  
 PROBHD Z114607\_0188 (zg30  
 PULPROG zg30  
 TD 180286  
 SOLVENT CDCl3  
 NS 16  
 DS 0  
 SWH 18028.846 Hz  
 FIDRES 0.200003 Hz  
 AQ 4.9999318 sec  
 RG 27.87  
 DW 27.733 usec  
 DE 8.00 usec  
 TE 300.0 K  
 D1 0.10000000 sec  
 TD0 1  
 SFO1 600.1337060 MHz  
 NUC1 1H  
 P0 3.33 usec  
 P1 10.00 usec  
 PLW1 26.60000038 W

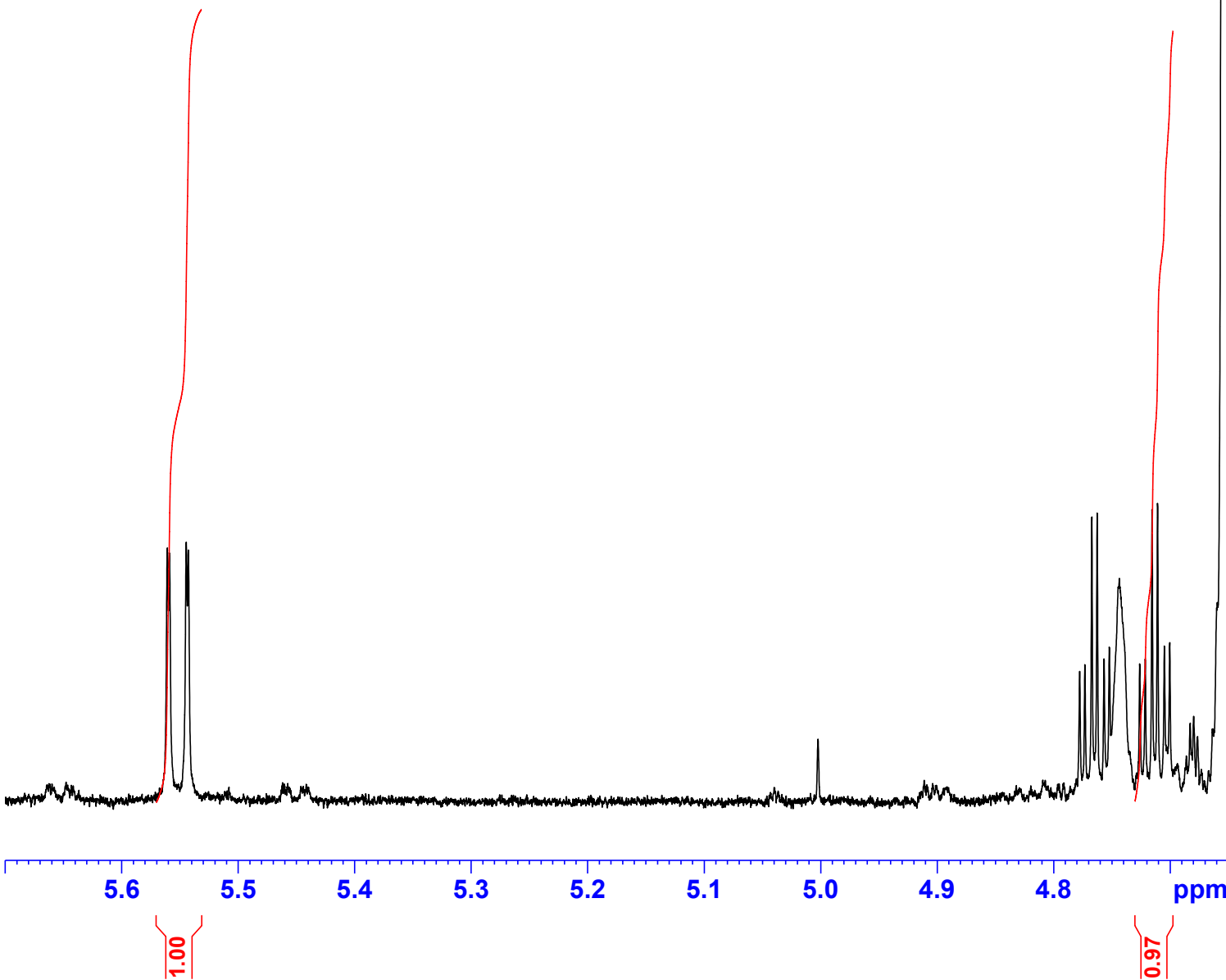
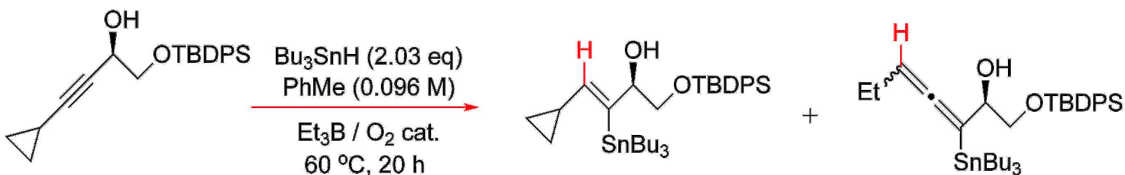
F2 - Processing parameters  
 SI 262144  
 SF 600.1300215 MHz  
 WDW EM  
 SSB 0  
 LB 0.10 Hz  
 GB 0  
 PC 1.00



Current Data Parameters  
 NAME LH-I-96 CRUDE  
 EXPNO 10  
 PROCNO 1

F2 - Acquisition Parameters  
 Date 20220519  
 Time 15.25 h  
 INSTRUM spect  
 PROBHD Z114607\_0188 (zg30  
 PULPROG zg30  
 TD 180286  
 SOLVENT CDCl<sub>3</sub>  
 NS 16  
 DS 0  
 SWH 18028.846 Hz  
 FIDRES 0.200003 Hz  
 AQ 4.9999318 sec  
 RG 12.81  
 DW 27.733 usec  
 DE 8.00 usec  
 TE 300.0 K  
 D1 0.10000000 sec  
 TD0 1  
 SFO1 600.1337060 MHz  
 NUC1 <sup>1</sup>H  
 P0 3.33 usec  
 P1 10.00 usec  
 PLW1 26.60000038 W

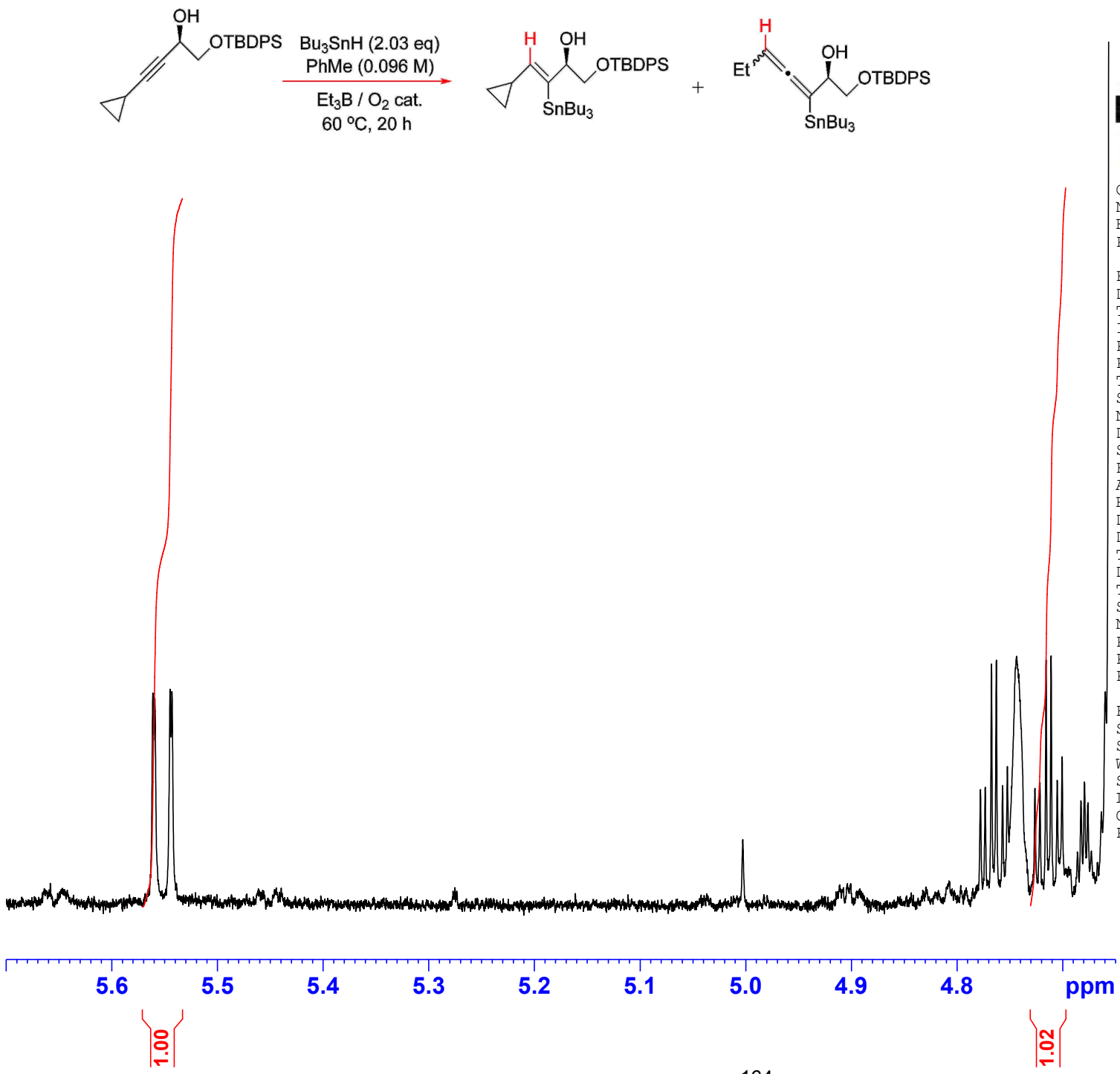
F2 - Processing parameters  
 SI 262144  
 SF 600.1300248 MHz  
 WDW EM  
 SSB 0  
 LB 0.10 Hz  
 GB 0  
 PC 1.00

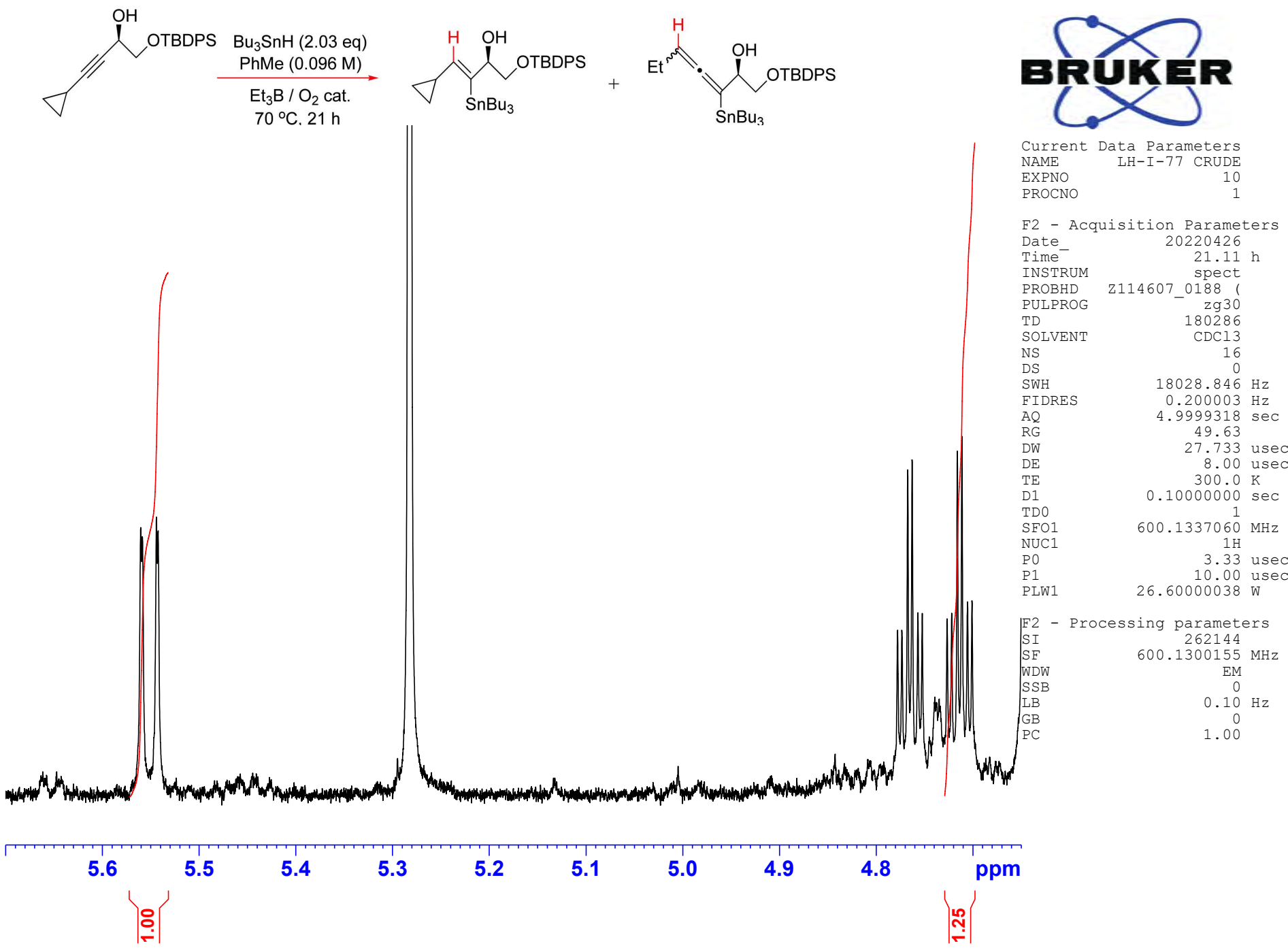


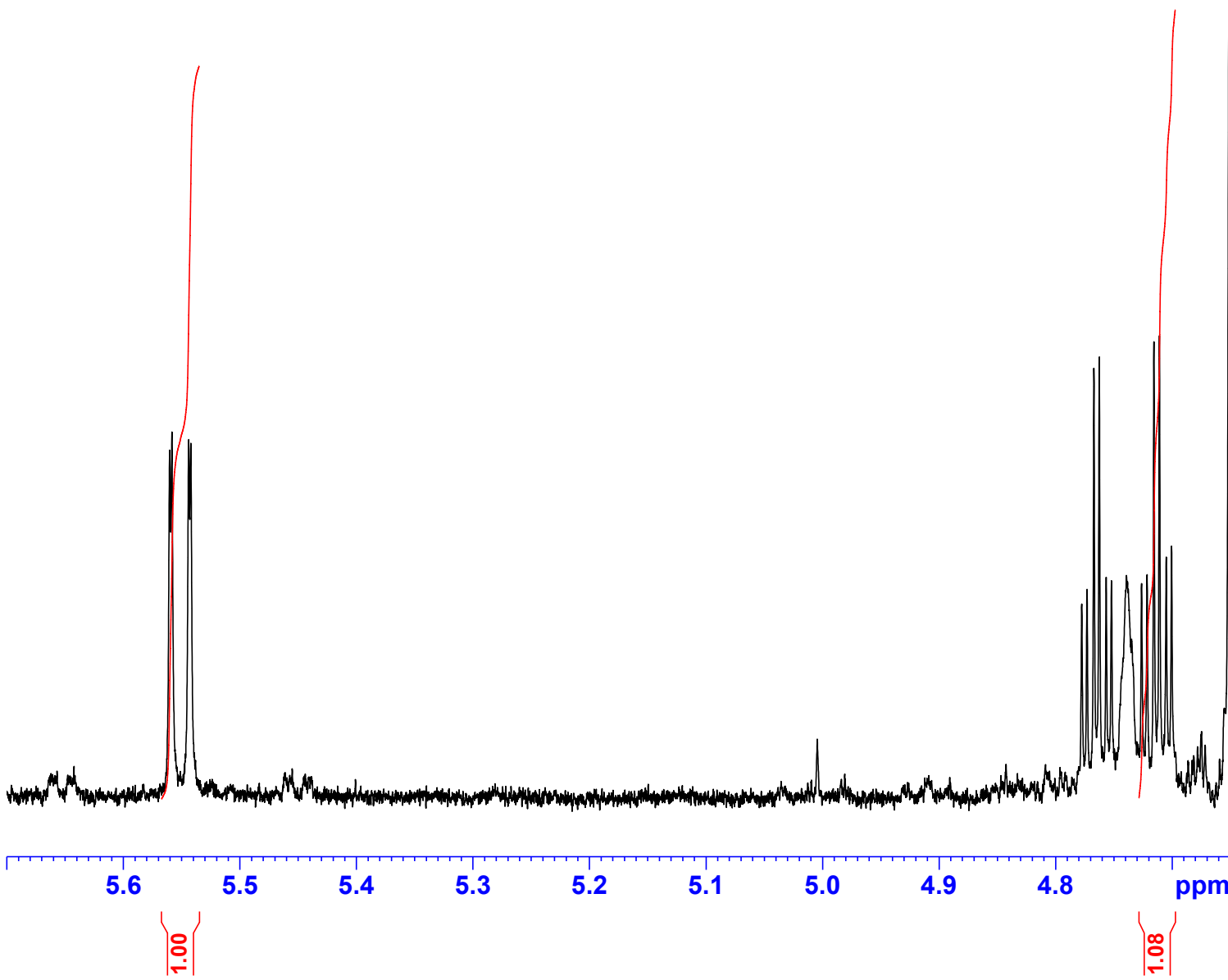
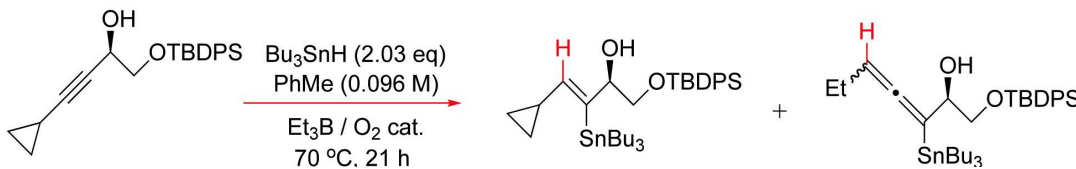
Current Data Parameters  
 NAME LH-I-85 CRUDE  
 EXPNO 10  
 PROCNO 1

F2 - Acquisition Parameters  
 Date 20220502  
 Time 13.59 h  
 INSTRUM spect  
 PROBHD Z114607\_0188 (zg30  
 PULPROG zg30  
 TD 180286  
 SOLVENT CDCl3  
 NS 16  
 DS 0  
 SWH 18028.846 Hz  
 FIDRES 0.200003 Hz  
 AQ 4.9999318 sec  
 RG 27.87  
 DW 27.733 usec  
 DE 8.00 usec  
 TE 300.0 K  
 D1 0.10000000 sec  
 TD0 1  
 SFO1 600.1337060 MHz  
 NUC1 1H  
 P0 3.33 usec  
 P1 10.00 usec  
 PLW1 26.60000038 W

F2 - Processing parameters  
 SI 262144  
 SF 600.1300190 MHz  
 WDW EM  
 SSB 0  
 LB 0.10 Hz  
 GB 0  
 PC 1.00



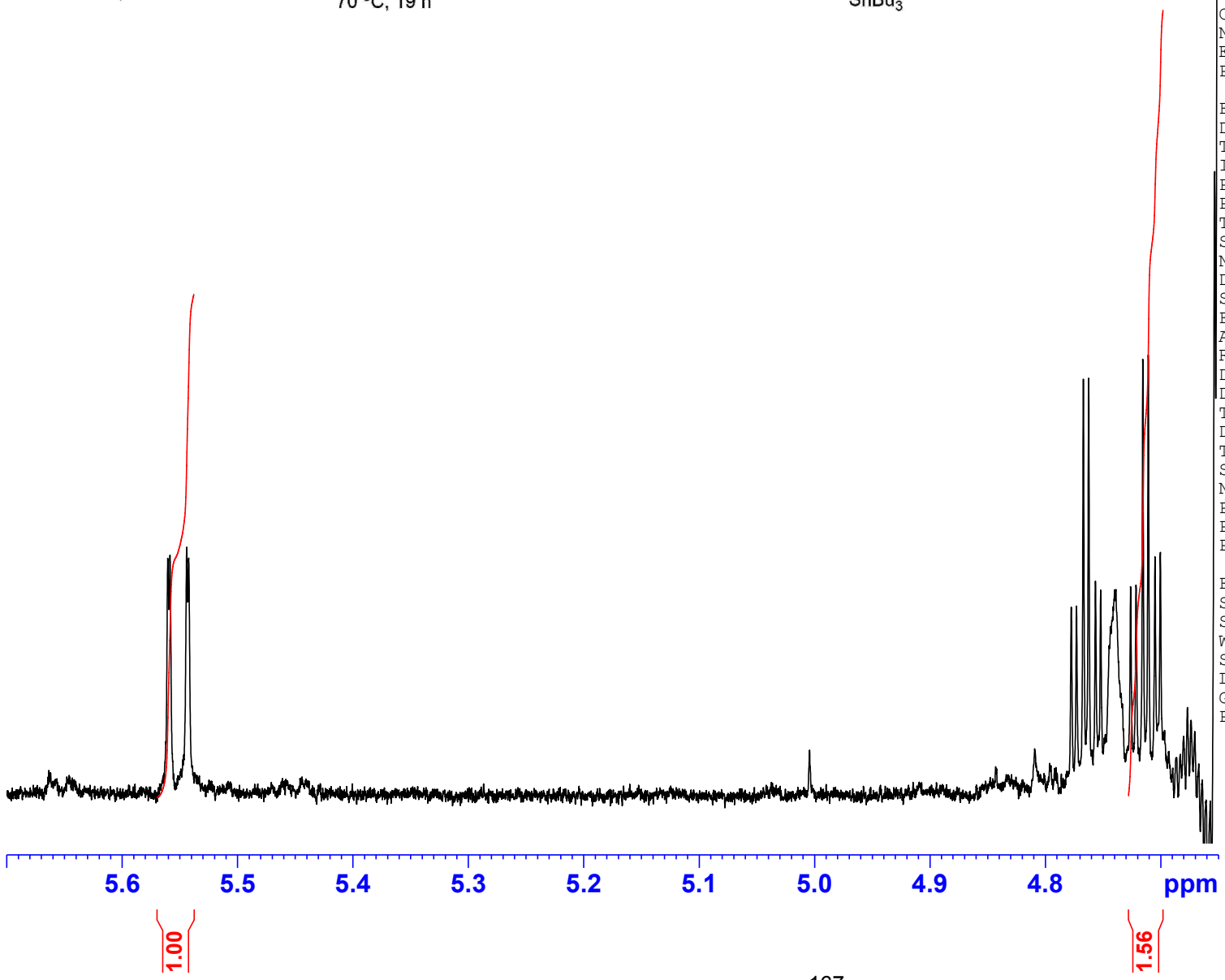




Current Data Parameters  
 NAME LH-I-78 CRUDE  
 EXPNO 10  
 PROCNO 1

F2 - Acquisition Parameters  
 Date 20220426  
 Time 16.31 h  
 INSTRUM spect  
 PROBHD Z114607\_0188 (zg30  
 PULPROG zg30  
 TD 180286  
 SOLVENT CDCl3  
 NS 16  
 DS 0  
 SWH 18028.846 Hz  
 FIDRES 0.200003 Hz  
 AQ 4.9999318 sec  
 RG 43.25  
 DW 27.733 usec  
 DE 8.00 usec  
 TE 300.0 K  
 D1 0.10000000 sec  
 TD0 1  
 SFO1 600.1337060 MHz  
 NUC1 1H  
 P0 3.33 usec  
 P1 10.00 usec  
 PLW1 26.60000038 W

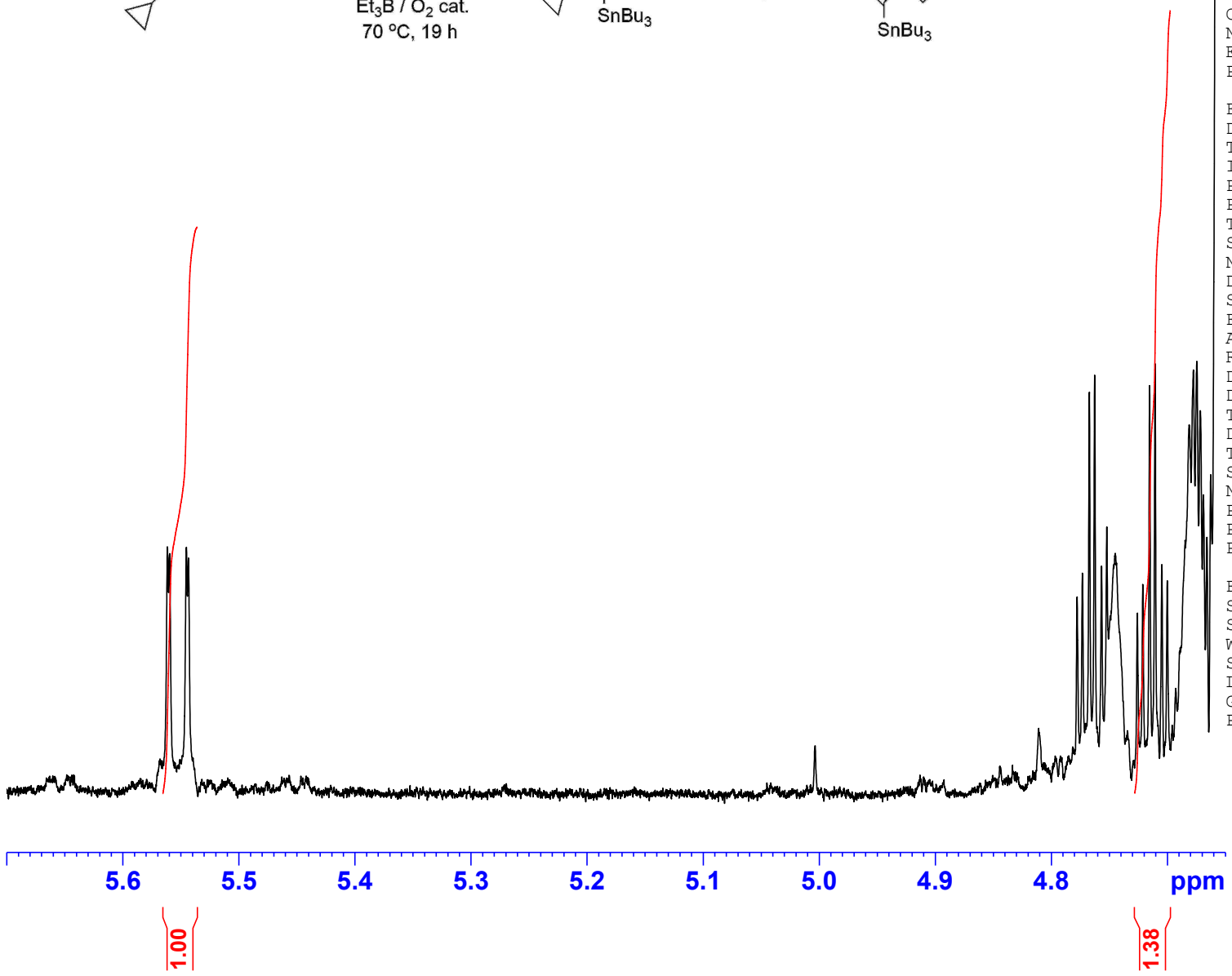
F2 - Processing parameters  
 SI 262144  
 SF 600.1300164 MHz  
 WDW EM  
 SSB 0  
 LB 0.10 Hz  
 GB 0  
 PC 1.00



Current Data Parameters  
 NAME LH-I-87 CRUDE  
 EXPNO 10  
 PROCNO 1

F2 - Acquisition Parameters  
 Date 20220502  
 Time 14.16 h  
 INSTRUM spect  
 PROBHD Z114607\_0188 (zg30  
 PULPROG zg30  
 TD 180286  
 SOLVENT CDCl<sub>3</sub>  
 NS 16  
 DS 0  
 SWH 18028.846 Hz  
 FIDRES 0.200003 Hz  
 AQ 4.9999318 sec  
 RG 34.91  
 DW 27.733 usec  
 DE 8.00 usec  
 TE 300.0 K  
 D1 0.10000000 sec  
 TD0 1  
 SFO1 600.1337060 MHz  
 NUC1 <sup>1</sup>H  
 P0 3.33 usec  
 P1 10.00 usec  
 PLW1 26.60000038 W

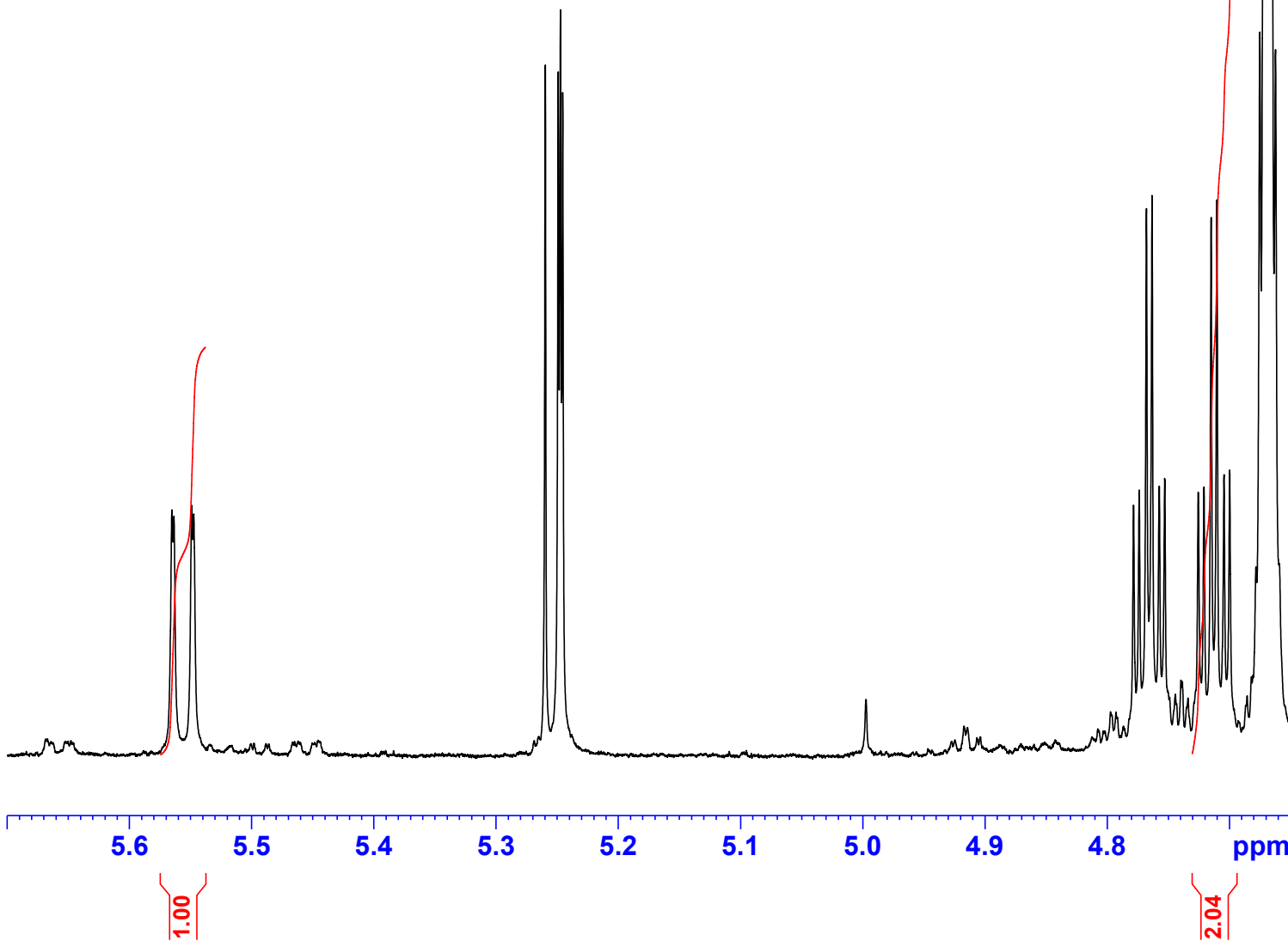
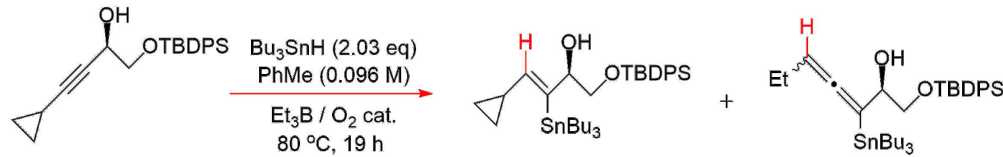
F2 - Processing parameters  
 SI 262144  
 SF 600.1300173 MHz  
 WDW EM  
 SSB 0  
 LB 0.10 Hz  
 GB 0  
 PC 1.00



Current Data Parameters  
 NAME LH-I-88 CRUDE  
 EXPNO 10  
 PROCNO 1

F2 - Acquisition Parameters  
 Date 20220502  
 Time 14.25 h  
 INSTRUM spect  
 PROBHD Z114607\_0188 (zg30  
 PULPROG zg30  
 TD 180286  
 SOLVENT CDCl<sub>3</sub>  
 NS 16  
 DS 0  
 SWH 18028.846 Hz  
 FIDRES 0.200003 Hz  
 AQ 4.9999318 sec  
 RG 25.17  
 DW 27.733 usec  
 DE 8.00 usec  
 TE 300.0 K  
 D1 0.10000000 sec  
 TD0 1  
 SFO1 600.1337060 MHz  
 NUC1 1H  
 P0 3.33 usec  
 P1 10.00 usec  
 PLW1 26.60000038 W

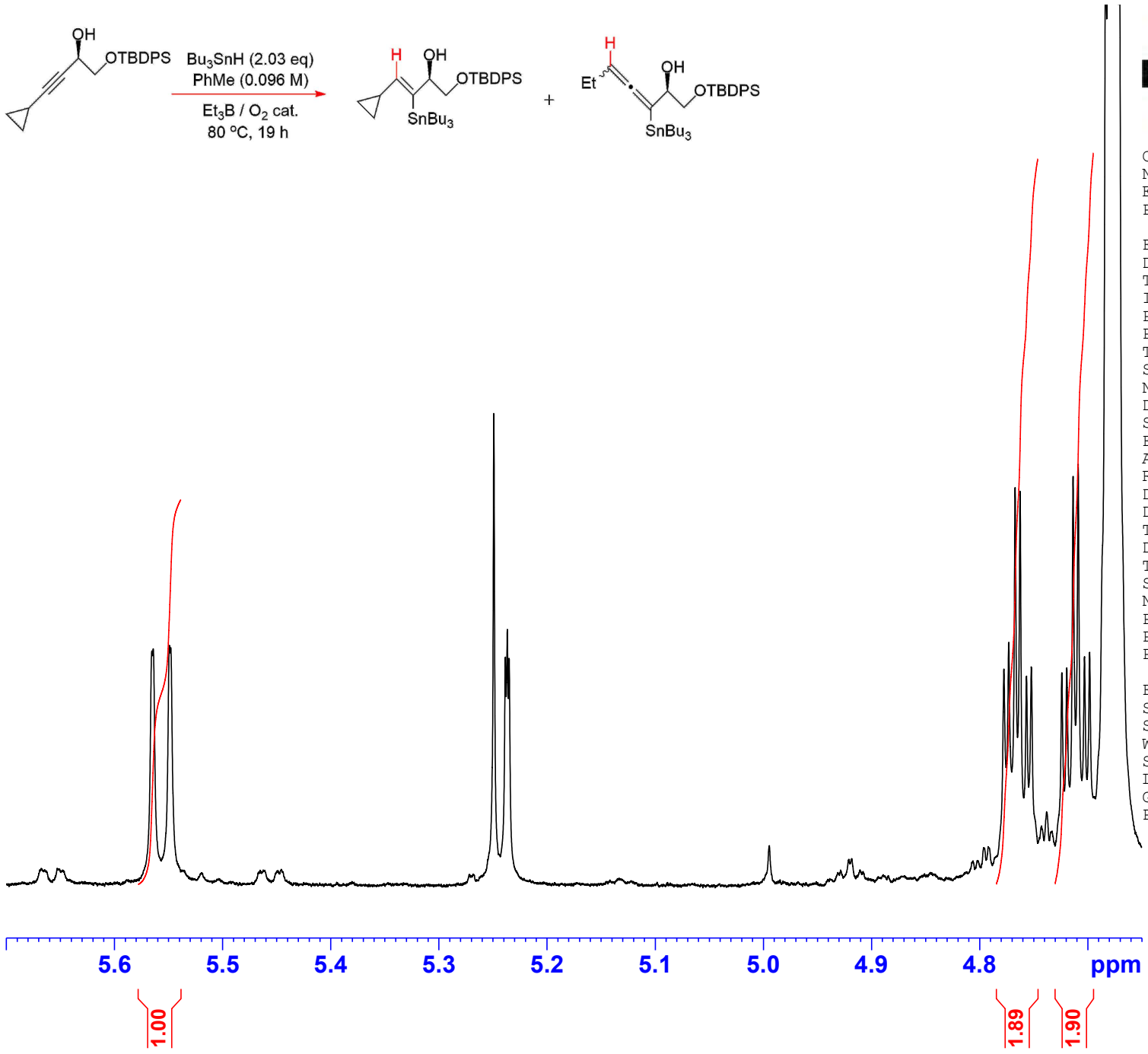
F2 - Processing parameters  
 SI 262144  
 SF 600.1300202 MHz  
 WDW EM  
 SSB 0  
 LB 0.10 Hz  
 GB 0  
 PC 1.00



Current Data Parameters  
 NAME LH-I-73  
 EXPNO 10  
 PROCNO 1

F2 - Acquisition Parameters  
 Date 20220407  
 Time 18.07 h  
 INSTRUM spect  
 PROBHD Z114607\_0188 (zg30  
 PULPROG zg30  
 TD 180286  
 SOLVENT CDCl3  
 NS 16  
 DS 0  
 SWH 18028.846 Hz  
 FIDRES 0.200003 Hz  
 AQ 4.9999318 sec  
 RG 7.97  
 DW 27.733 usec  
 DE 8.00 usec  
 TE 300.0 K  
 D1 0.10000000 sec  
 TD0 1  
 SFO1 600.1337060 MHz  
 NUC1 1H  
 P0 3.33 usec  
 P1 10.00 usec  
 PLW1 26.60000038 W

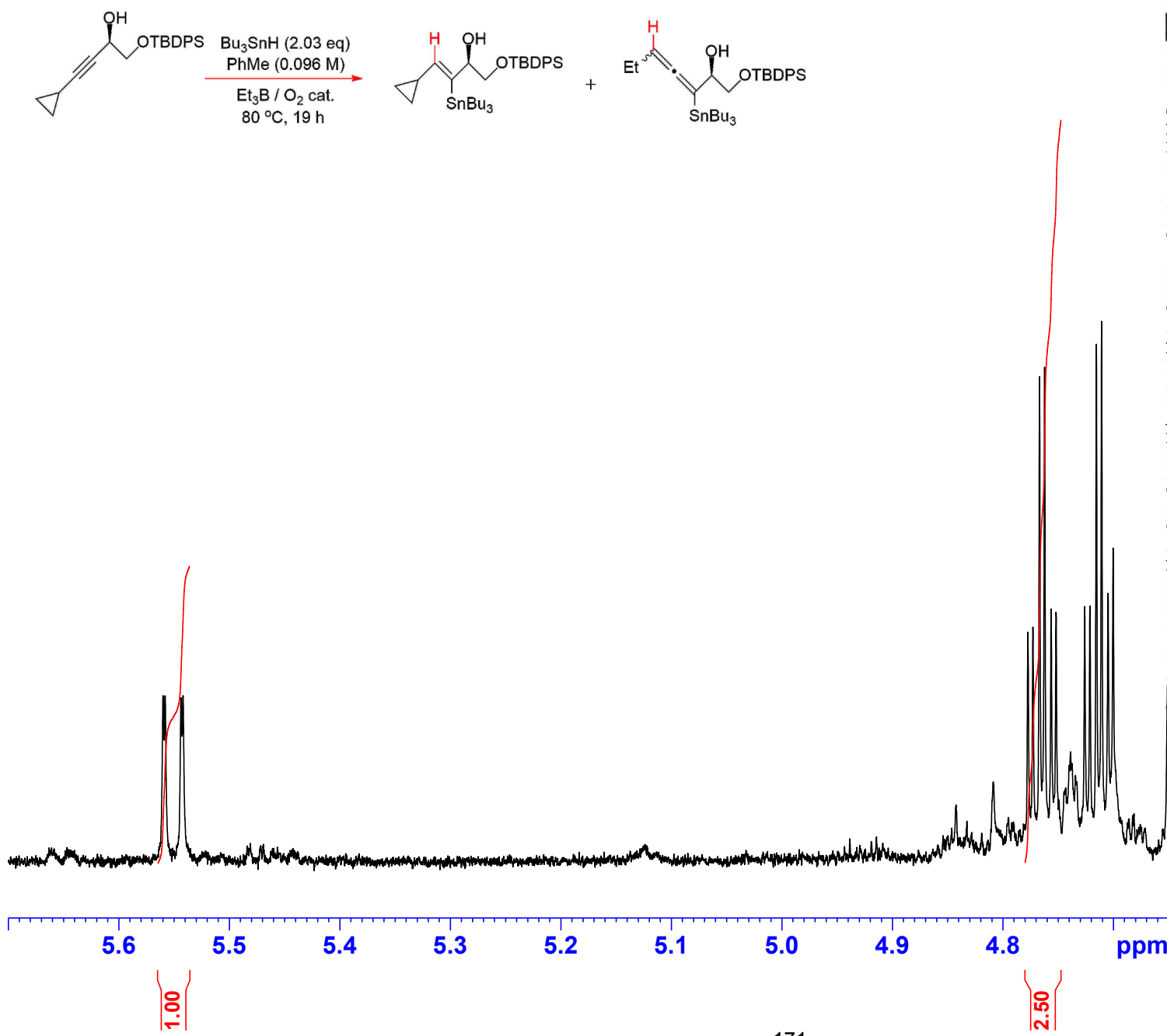
F2 - Processing parameters  
 SI 262144  
 SF 600.1300252 MHz  
 WDW EM  
 SSB 0  
 LB 0.10 Hz  
 GB 0  
 PC 1.00



Current Data Parameters  
 NAME LH-I-74  
 EXPNO 10  
 PROCNO 1

F2 - Acquisition Parameters  
 Date 20220407  
 Time 18.15 h  
 INSTRUM spect  
 PROBHD Z114607\_0188 (zg30  
 PULPROG zg30  
 TD 180286  
 SOLVENT CDCl3  
 NS 16  
 DS 0  
 SWH 18028.846 Hz  
 FIDRES 0.200003 Hz  
 AQ 4.9999318 sec  
 RG 6.18  
 DW 27.733 usec  
 DE 8.00 usec  
 TE 300.0 K  
 D1 0.10000000 sec  
 TD0 1  
 SFO1 600.1337060 MHz  
 NUC1 1H  
 P0 3.33 usec  
 P1 10.00 usec  
 PLW1 26.60000038 W

F2 - Processing parameters  
 SI 262144  
 SF 600.1300288 MHz  
 WDW EM  
 SSB 0  
 LB 0.10 Hz  
 GB 0  
 PC 1.00



Current Data Parameters  
 NAME LH-I-83 CRUDE  
 EXPNO 10  
 PROCNO 1

F2 - Acquisition Parameters  
 Date 20220428  
 Time 20.33 h  
 INSTRUM spect  
 PROBHD Z114607\_0188 (zg30  
 PULPROG zg30  
 TD 180286  
 SOLVENT CDCl3  
 NS 16  
 DS 0  
 SWH 18028.846 Hz  
 FIDRES 0.200003 Hz  
 AQ 4.9999318 sec  
 RG 49.63  
 DW 27.733 usec  
 DE 8.00 usec  
 TE 300.0 K  
 D1 0.10000000 sec  
 TD0 1  
 SFO1 600.1337060 MHz  
 NUC1 1H  
 P0 3.33 usec  
 P1 10.00 usec  
 PLW1 26.60000038 W

F2 - Processing parameters  
 SI 262144  
 SF 600.1300168 MHz  
 WDW EM  
 SSB 0  
 LB 0.10 Hz  
 GB 0  
 PC 1.00